

**Kansas Aviation Research and Technology (KART) Program  
KART R51827**

**Experimental Identification of  
Lightning Conducted-Current  
Fastener Sparking Thresholds  
(25.981 Project) – Test Results**

**Metal Test Report**

**Document Number: ENV-RP-2016-003– Rev A**

*Last Revised: 1/21/2021*

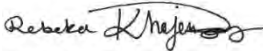

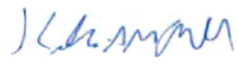
*Original Issue Date: 12/18/2017*

**Electromagnetic Effects Test Laboratory  
National Institute for Aviation Research (NIAR)  
Wichita State University**



## Revisions

Rev	Date	Prepared By:	Checked By:	Approved By:
-	12/18/2017	Michelle Cronkleton	Yulia Kostogorova-Beller	Billy Martin
Section		Description		
All		Initial Release of Document		

Rev	Date	Prepared By:	Checked By:	Approved By:
A	1/21/2021			
Section		Description		
All		Updated wording to clarify between the nominal fastener text and the faulted fasteners text.		
All		Expanded each report section to include results from faulted fastener testing.		
All		Updated formatting for readability.		
Table of Contents		Updated page numbers and sections to include changes throughout document.		
List of Figures		Updated to include new figures for faults data.		
List of Tables		Updated to include new tables for faults data.		
2		Added Testing Article Naming Convention Table.		
3		Added section for DEL generator.		
5.1		Updated nominal paint thickness plots for consistency.		
5.3		Removed section discussing joint sparking bias due to lack of relevance to test setup.		
6.1		Corrected figure reference.		
7.6		Removed Figure 32: Thickness of HI-KOTE 1 coating.		
7		Added sections to account for added factors. Removed table 7, summarized in section 8.1.		



7.1	Removed and updated charts for clarity and corrected the text to match.
7.14	Re-named section from Test Article Anomalies to Anomalies Discovered During and After Testing.
7.4.1	Reworded for clarity.
7.5.1	Reworded for clarity.
7.6.1	Expanded on internal sparking definition for clarity
Appendices	Removed appendices containing check-in sheets and full data listing for brevity.
Appendix A	Added appendix containing EMA Wing Simulation Report.
Appendix D	Added appendix for faulted fastener joint drawings.
Appendix H	Added appendix for nominal and faulted test article data.

## TABLE OF CONTENTS

<b>1.0</b>	<b>PURPOSE AND SCOPE OF TEST .....</b>	<b>1</b>
1.1	Detection and Definitions of Ignition Sources .....	1
<b>2.0</b>	<b>TEST ARTICLES.....</b>	<b>3</b>
2.1	Test Articles Received.....	5
<b>3.0</b>	<b>TEST EQUIPMENT.....</b>	<b>7</b>
3.1	Scaled-Down (25.981) Lightning Generator .....	9
3.2	Direct Effects of Lightning Generator .....	12
3.3	Photographic Chamber .....	13
3.4	Digital Cameras.....	13
<b>4.0</b>	<b>TEST SETUP .....</b>	<b>14</b>
<b>5.0</b>	<b>ANALYSIS PLAN.....</b>	<b>16</b>
5.1	Manufacturing Variance Check .....	16
5.2	Energy Delivery Variance Check .....	23
5.3	Test Setup Biases Check .....	31
<b>6.0</b>	<b>DATA AND OBSERVATIONS.....</b>	<b>34</b>
6.1	Nominal Test Articles .....	34
6.2	Faulted Test Articles .....	42
<b>7.0</b>	<b>TEST RESULTS.....</b>	<b>46</b>
7.1	Nominal Test Articles .....	46
7.2	Faulted Test Articles .....	48
7.3	Factor 1 - Type of Fastener .....	49
7.4	Factor 2 - Fastener Head Type .....	52
7.5	Factor 3 - Diameter of Fastener.....	53
7.6	Factor 4 - Fit Type.....	53
7.7	Factor 5 - Fastener Coating .....	54
7.8	Factor 6 - Number of Fasteners.....	56
7.9	Factor 7 - Fastener Fault Type.....	57
7.10	Factor 8 - Manufacturer .....	60
7.11	Fasteners Not Coated in Sealant .....	62
7.12	Pre-test DC Resistance vs Sparking Level .....	62
7.13	Anomalies Discovered During or After Testing .....	64
<b>8.0</b>	<b>CONCLUSIONS.....</b>	<b>66</b>
8.1	Nominal Test Articles .....	66
8.2	Faulted Test Articles .....	67
<b>APPENDIX A - EMA WING SIMULATION REPORT.....</b>		<b>68</b>
<b>APPENDIX B - SINGLE-FASTENER JOINT DRAWING.....</b>		<b>116</b>
<b>APPENDIX C - QUAD-FASTENER JOINT DRAWING.....</b>		<b>117</b>





<b>APPENDIX D - FAULTED FASTENER JOINT DRAWINGS.....</b>	<b>118</b>
<b>APPENDIX F - TEST PHOTOGRAPHS .....</b>	<b>126</b>
<b>APPENDIX G - 200 MJ CAMERA CALIBRATION.....</b>	<b>168</b>
<b>APPENDIX H – TEST ARTICLE DATA.....</b>	<b>187</b>

## LIST OF FIGURES

Figure 1: Test Article MN-1I12, #6, before the test.....	2
Figure 2: Test Article MN-1I12, #6, during test.....	2
Figure 3: Test Article MN-1I12, #6, Voltage Waveforms.....	2
Figure 4: Example of Single Fastener Test Article.....	3
Figure 5: Example of Quadruple Fastener Test Article .....	3
Figure 6: Scaled-Down Current Component A Waveform .....	10
Figure 7: Scaled-Down Current Component B/C* Waveform.....	10
Figure 8: Front View of 25.981 Lightning Generator .....	11
Figure 9: Side View of 25.981 Lightning Generator.....	11
Figure 10: Scaled Current Component A Waveform .....	12
Figure 11: Scaled Current Component B/C* Waveform .....	12
Figure 12: Schematic of the Photographic Chamber .....	13
Figure 13: 25.981 Generator Test Setup.....	14
Figure 14: Right-End View of Test Setup (Left) and Photo Chamber (Right).....	15
Figure 15: DEL Generator Setup .....	15
Figure 16: Nominal DC Resistance at Check-In.....	18
Figure 17: Nominal Paint Thickness at Check-In .....	19
Figure 18: Faulted DC Resistance at Check-In .....	21
Figure 19: Faulted Paint Thickness at Check-In .....	22
Figure 20: Energy Delivery Check - Nominal - Single, Peak Current - Component A.....	24
Figure 21: Energy Delivery Check – Nominal - Quad, Peak Current - Component A .....	24
Figure 22: Energy Delivery Check - Nominal - Single, Action Integral - Component A.....	25
Figure 23: Energy Delivery Check – Nominal Quad, Action Integral - Component A .....	25
Figure 24: Energy Delivery Check – Nominal - Single, Charge Transfer - Component B/C* .....	26
Figure 25: Energy Delivery Check – Nominal - Quad, Charge Transfer - Component B/C* .....	26
Figure 26: Energy Delivery Check – Faults, Peak Current 10 kA – Component A.....	27
Figure 27: Energy Delivery Check – Faults, Peak Current 100 kA – Component A.....	28
Figure 28: Energy Delivery Check – Faults, Action Integral – 10 kA Test Level.....	29
Figure 29: Energy Delivery Check – Faults, Action Integral – 100 kA Test Level.....	29
Figure 30: Energy Delivery Check – Faults, Charge Transfer – 10 kA Test Level .....	30
Figure 31: Energy Delivery Check – Faults, Charge Transfer – 100 kA Test Level .....	31
Figure 32: Peak Current Over Time .....	32
Figure 33: Calibration Peak Current Over Time.....	33
Figure 34: DC Resistance of OEM 1 with sparking – Nominal Single Fasteners.....	35
Figure 35: DC Resistance of OEM 2 with sparking – Nominal Single Fasteners .....	35

Figure 36: DC Resistance of OEM 3 with sparking – Nominal Single Fasteners .....	36
Figure 37: DC Resistance of OEM 4 with sparking – Nominal Single Fasteners .....	36
Figure 38: DC Resistance of OEM 5 with sparking – Nominal Single Fasteners .....	37
Figure 39: DC Resistance with Sparking – Nominal Single Fasteners – All OEMs .....	38
Figure 40: Peak Current with Sparking – Nominal Single Fasteners – All OEMs .....	39
Figure 41: DC Resistance with Sparking – Nominal Quad Fasteners – All OEMs .....	40
Figure 42: Peak Current with Sparking – Nominal Quad Fasteners – All OEMs.....	41
Figure 43: DC Resistance of OEM 1 - Faulted Fasteners.....	43
Figure 44: DC Resistance of OEM 2 - Faulted Fasteners .....	43
Figure 45: DC Resistance of OEM 3 - Faulted Fasteners .....	44
Figure 46: DC Resistance of OEM 5 - Faulted Fasteners .....	44
Figure 47: DC resistances across all OEMs– Faulted Fasteners .....	45
Figure 49: Nominal Single Fastener Sparking Thresholds by OEM .....	47
Figure 51: Nominal Quadruple Fastener Sparking Thresholds by OEM .....	48
Figure 52: Nonsparking Thresholds by Fastener .....	49
Figure 51: Sparking Percent for Fastener Types of Nominal Test Articles.....	50
Figure 54: Sparking Percent for Fastener Types of Faulted Test Articles on 25.981 Generator .....	51
Figure 55: Sparking Percent for Fastener Types of Faulted Test Articles on DEL Generator .....	52
Figure 56: Effect of Fit Type Differences on DC Resistance - Nominal Single Fasteners....	54
Figure 57: Nominal Sparking Count by Coating Type .....	55
Figure 58: Faulted Average Nonsparking Threshold .....	55
Figure 59: HI KOTE 1 coated fastener .....	56
Figure 60: Conductive Nonsparking Thresholds by Faults.....	58
Figure 61: Nonconductive Nonsparking Thresholds by Faults .....	59
Figure 62: Sparking Percent by Each Individual Fastener.....	60
Figure 63: Conductive Fastener Nonsparking Thresholds by OEM .....	61
Figure 64: Nonconductive Fastener Nonsparking Thresholds by OEM .....	61
Figure 65: DC Resistance of Nominal Test Articles by OEM.....	63

## **LIST OF TABLES**

Table 1: Test Article Abbreviation Sequence .....	4
Table 2: Fastener Assemblies for Nominal Metal Testing.....	6
Table 3: Fastener Assemblies for Faulted Metal Testing.....	7
Table 4: List of Test Equipment for DEL Generator.....	7
Table 5: List of Test Equipment for 25.981 Generator .....	8
Table 6: List of Test Equipment for both generators.....	9
Table 7: External Sparking Percentage for Singles vs Quads (by fastener).....	57
Table 8: Sparking percentage by OEM .....	60
Table 9: DC Resistance vs Sparking .....	63
Table 10: Description of Faults .....	125
Table 11: Camera Calibration Parameters.....	168
Table 12: Nominal Test Article Data .....	187
Table 13: Faulted Test Article Data .....	187

## APPLICABLE DOCUMENTS

Document Number	Description
SAE Aerospace ARP 5412B Revised 2013	Aircraft Lightning Environment and Related Test Waveforms
SAE Aerospace ARP 5414A Reaffirmed 2012	Aircraft Lightning Zone
SAE Aerospace ARP 5416A Revised 2013	Aircraft Lightning Test Methods
SAE Aerospace ARP 5577 Reaffirmed 2008	Aircraft Lightning Direct Effects Certification
NIAR Document ENV-WP-2016-001 2015	Test Article Manufacturing and Fastener Installation Requirements in Application to Metal Fuel Tank Lightning Sparking Threshold Identification
NIAR Document ENV-TP-2015-007 Revised 2/29/16	Experimental Identification of Lightning Conducted-Current Fuel-Tank Fastener Ignition Source Thresholds (25.981 Project) Test Plan
ICOLSE Document Kostogorova-Beller, 2015	Lightning Research at NIAR: Development of Fastener Sparking Threshold Database for Metal Fuel Tanks: Inception
Second Edition 2004	Fisher F.A., Plumer J.A., Perala R.A. Lightning Protection of Aircraft, Lightning Technologies, Inc., Pittsfield, MA
DOT/FAA/CT-94/74 1994	Aircraft Fuel System Lightning Protection Design and Qualification Test Procedures Development, Final Report

## **1.0 Purpose and Scope of Test**

The purpose of these tests are experimental identification of the occurrence of a potential ignition source(s) emanated by a fastener(s)-containing joint as a result of induced lightning conducted current within the joint. The data from this test report will be put towards implementation of the NIAR/WSU KART project entitled “Development of Fuel Tank Lightning Protection Design Handbook” (Phase 1), the purpose of which is compiling a fastener ignition source threshold database for metal test article coupons containing nominal and fault fastener installations for the fasteners commonly utilized in aircraft fuel tank structures. The test level, at which no visible light is observed utilizing the photographic test method per ARP 5416A, establishes the ignition source threshold for a particular joint assembly.

In addition to the metal coupon testing, an electromagnetic model of a metal wing was created by Electro Magnetic Applications, Inc. (EMA) to determine the conducted current lightning threat at wing fastener locations as an example of the simulation portion of 25.981 compliance. Multiple lightning strike scenarios are simulated to determine the resulting current densities in various regions of the wing. The current density values are compared with fastener sparking thresholds determined via coupon testing with the intent of showing that the fasteners in each wing location are not capable of acting as an ignition source. Validation testing was performed on a metal wing at NIAR for comparison with the results of the simulation. The full report of the wing evaluation, provided by EMA, can be found in Appendix A.

### **1.1 Detection and Definitions of Ignition Sources**

Laboratory studies involving simulated lightning strikes to fuel tanks have demonstrated two possible ignition mechanisms: thermal and electrical ignition sources. Specifically, the thermal sources include hot spots on the interior surfaces of metal or composite fuel tanks caused by lightning attachment to exterior surfaces. The electrical ignition sources are subdivided into electrical sparks and arcs. The former are ionizations of the air between isolated conductive elements, and formed by potential difference arising from lightning currents in the airframe, or from changing magnetic fields. The latter are the ionized air containing hot gases formed by the melting and vaporization of the contact surfaces [Ref.: Fisher F.A., Plumer J.A., Perala R.A. Lightning Protection of Aircraft, Lightning Technologies, Inc., Pittsfield, MA, 2004].

The current test plan utilizes a combination of the photographic method [Ref.: ARP 5416A, Section 7.7.1] and dynamic voltage measurement across each joint (V-t) for ignition source detection and joint electrical characterization, respectively, during conduction of lightning current. The characterization based on voltage measurements is used complementarily to the photographic method in order to allow distinction between the types of ignition sources defined above. Specifically, the joint's external and/or internal spark source may be observed: the former is represented by light on camera with V-t waveform fluctuations; the latter is manifested as a fluctuating voltage rise detected in the V-t, but absence of detectable light on the camera.

See Figure 1 to Figure 3 for an example of a test article with fluctuating voltage waveforms that represent sparking in a metal test article containing a single HI-LOK™ fastener in each joint. There are external ignition sources in joint 1 and joint 2 and no ignition source in joint 3.

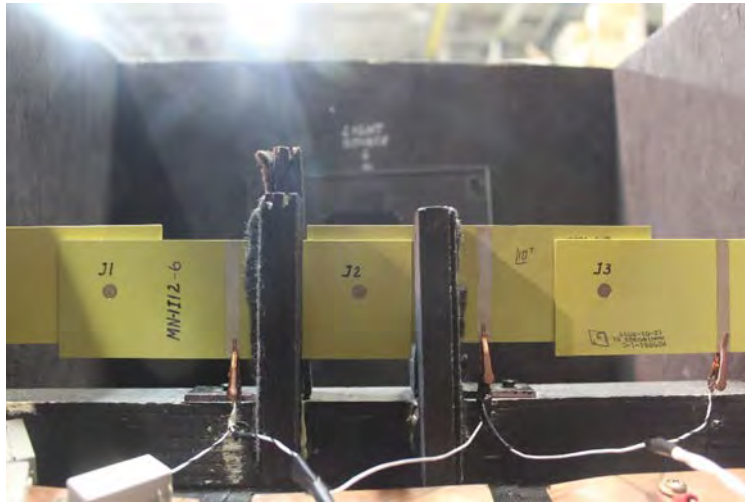


Figure 1: Test Article MN-1I12, #6, before the test



Figure 2: Test Article MN-1I12, #6, during test

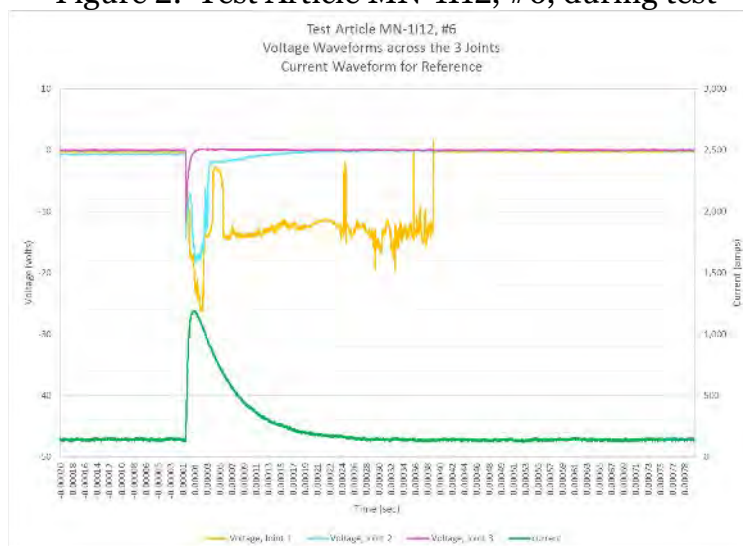


Figure 3: Test Article MN-1I12, #6, Voltage Waveforms



## 2.0 TEST ARTICLES

During the course of the NIAR/WSU KART project, two standardized test article designs, including a single and a quadruple fastener assembly per joint, having three joints in series per test article, have been identified and validated in a collaborative effort by the Federal Aviation Administration (FAA) and Society of Automotive Engineers (SAE) International AE-2 Committee. Examples are shown in Figure 4 and Figure 5.

Test articles containing four fasteners per joint were determined to be the simplest installation to represent current flow through typical aircraft structure. Although there would likely never be a single fastener at any interface in an aircraft installation, single nominal fastener joints were tested in addition to quads to find a worst case sparking threshold. The sparking threshold for the single fastener installations was more likely to be reached, which allowed for a better assessment of relative performance. Only quad fastener joints were tested for the faulted fastener installations. One of the four fasteners at each of the joints was a faulted configuration, intended to represent the low probability that all fasteners in a given location would all contain the same manufacturing fault. The smallest fastener diameter coupled with the thinnest aluminum was selected to simulate the worst case installations for each class of fasteners.

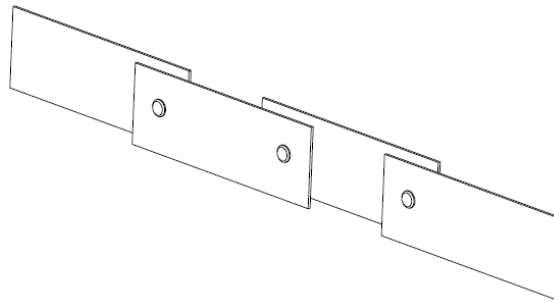


Figure 4: Example of Single Fastener Test Article

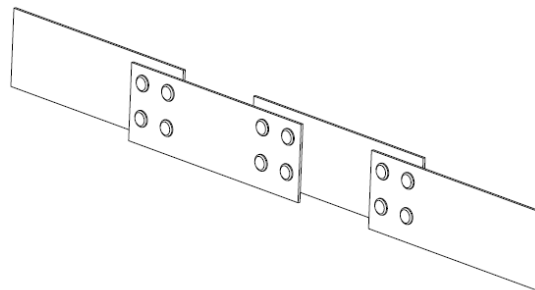


Figure 5: Example of Quadruple Fastener Test Article

Fault-type selection was coordinated with the SAE AE-2 committee, specifically the ARP 6205 task group. The outcome of the fault-type classification developed for this project is expected to be incorporated into ARP 6205 for use in future testing. The 6 faults were specified based



on likelihood of occurrence, ability to be consistently reproduced, and applicability to type of construction and fastener location. Certain faults were eliminated if a worst case alternative fault produced a similar sparking mechanism.

The KART project required the participating original equipment manufacturers (OEMs) to build the test articles in accordance with the NIAR Document ENV-WP-2016-001 “Test Article Manufacturing and Fastener Installation Requirements in Application to Metal Fuel Tank Lightning Ignition Source Threshold Identification.” The test articles contain nominal and faulted fastener installations. Examples of the engineering drawings for metal nominal installations are shown in [Appendices B](#) and [C](#), and drawings for the faulted joints are shown in [Appendix D](#).

The naming convention for the nominal installations follows the AB-CDE-F pattern in Table 1 below while the naming convention for the faulted installations follows the AB#-CDE-F pattern.

Table 1: Test Article Abbreviation Sequence

A	Test article material	M-metal, C-composite
B	Type of fastener installation	N-nominal, F-fault
#	Type of fault	1-straight gap 2-gap under head 3-gap under collar 4-scratch 5-burr 6-under-torqued
C	Number of fasteners per joint	1-single fastener, 4-quadruple fastener
D	Fastener fit type	I-interference, T-transition, o-N/A
E	Unique pin/collar combination	01-HL10VBJ5-3/HL70-5 02- HL10VBJ8-3/HL70-8 03-HL11VBJ5-3/HL70-5 04- HL11VBJ8-3/HL70-8 05- HST10BJ5-3/HST79CY5 06- HST10BJ8-3/HST79CY 8 07- HST11BJ5-3/HST79CY 5 08- HST11BJ8-3/HST79CY 8 09-MS20470AD4 10- MS20470AD6 11-HST11AG5-3/HST79CY5 12-HL11VAZ5-3/HL70-5
F	OEM Identifier	1-XXX, 2-XXX, 3-XXX, 4-XXX, 5-XXX

## **2.1 Test Articles Received**

### **2.1.1 Nominal Test Articles**

Based off the drawings in [Appendix B](#) and [Appendix C](#), the participating OEMs provided a total of 595 nominal test articles. These included rivets and both HI-LOK™ and HI-LITE™ fasteners and HI-LOK™ or HI-LITE™ fasteners with the HI-KOTE coating. A description of the test article assemblies that were provided is shown in Table 2.

Two different skin thicknesses tested:

1. All 0.063" coupons
2. Half 0.063" coupons and half 0.090" coupons

Every fourth test article configuration used two 0.063" coupons on the bottom and two 0.090" coupons on the top. Therefore, MN-1Io4, MN-1Io8, MN-1To4, and MN-1To8 test articles used two of the thicker coupons for the single fastener test articles. MN-4Io4, MN-4Io8, MN-4To4, and MN4To8 used two of the thicker coupons for the quadruple fastener test articles. Test articles with rivets used all 0.063" coupons. See Figure 4 and Figure 5 for examples of the single fastener and quadruple fastener test articles.

Table 2: Fastener Assemblies for Nominal Metal Testing

No. of fasteners	Fastener Type	Head Type	Diameter	Fit Type	OEM 1	OEM 2	OEM 3	OEM 4	OEM 5	
Single-Fastener	HI-LOK™	Protruding	Small	Interference & Transition	4 4	6 6			6 6	
			Large	Interference & Transition	6 6	6 6			6 6	
		Countersunk	Small	Interference & Transition	2 0	6 6			6 6	
			Large	Interference & Transition	4 6	6 6			6 6	
		HI-LITE™	Protruding	Small	Interference & Transition			6 6	6 6	6 6
				Large	Interference & Transition			6 6	6 6	6 6
	Countersunk		Small	Interference & Transition			6 6	6 5	6 6	
			Large	Interference & Transition			6 6	6 6	6 6	
	HI-KOTE/ HI-LOK™	Countersunk	Small	Interference & Transition	6 6	6			6	
	HI-KOTE/ HI-LITE™	Countersunk	Small	Interference				6	6	
	Rivet	Protruding	Small	Rivet	6	6	6	6	6	
			Large	Rivet	6	6	6	6	6	
	Quad-Fastener	HI-LOK™	Protruding	Small	Interference & Transition	4 4	1 1			1 1
				Large	Interference & Transition	6 10	1 1			1 1
			Countersunk	Small	Interference & Transition	4 0	1 1			1 1
				Large	Interference & Transition	4 0	1 1			1 1
HI-LITE™			Protruding	Small	Interference & Transition			6 6	6 6	1 1
				Large	Interference & Transition			6 6	6 5	1 1
		Countersunk	Small	Interference & Transition			6 6	6 6	1 1	
			Large	Interference & Transition			6 6	6 6	1 1	
HI-KOTE/ HI-LOK™		Countersunk	Small	Interference & Transition	4 4	1			1	
HI-KOTE/ HI-LITE™		Countersunk	Small	Interference				6	1	
Rivet		Protruding	Small	Rivet	6	6	6	6	6	
			Large	Rivet	6	6	6	6	6	
Total Number of Test Articles					108	87	120	130	150	

### 2.1.2 Faulted Test Articles

All faulted installations were of the quadruple configuration with only 1 fastener in each joint was faulted while the remaining 3 were nominal installations. Based off the drawings in [Appendix D](#), the participating OEMs provided a total of 335 faulted metal test articles. These included both HI-LOK™ and HI-LITE™ fasteners and HI-LOK™ or HI-LITE™ fasteners with the HI-KOTE coating. A description of the test article assemblies that were provided is shown in Table 3.

Table 3: Fastener Assemblies for Faulted Metal Testing

No. of fasteners	Fastener Type	Head Type	Diameter	Fit Type	OEM 1	OEM 2	OEM 3	OEM 5
Quad-Fastener	HI-LOK™	Protruding	Small	Transition	30	30		30
		Countersunk	Small	Transition	5	5		5
	HI-LITE™	Protruding	Small	Transition			36	30
		Countersunk	Small	Transition			6	5
	HI-KOTE/ HI-LOK™	Countersunk	Small	Transition	22	25		25
	HI-KOTE/ HI-LITE™	Countersunk	Small	Transition				25
	Rivet	Protruding	Small	Rivet	12	15	12	17
Total Number of Test Articles					69	75	54	137

## 3.0 TEST EQUIPMENT

Table 4, Table 5, and Table 6 list the test equipment required for testing.

Table 4: List of Test Equipment for DEL Generator

DEL Generator				
Description	Manufacturer ID	Model Number	Serial Number	Calibration Required
High Current Generator	NIAR	HC1	001	No
Oscilloscope	Yokogawa	DL850E	91P313729	Yes
Analog Voltage Input Module	Yokogawa	701250	91P321170	Yes
Analog Voltage Input Module	Yokogawa	701250	91P321166	Yes
Current Monitor Probe, 1000:1, 500,000A	Pearson	1423	147997	Yes
Current Monitor Probe	Pearson	301X	147836	Yes
HV DC Power Supply	Spellman	SL8PN2000X4874	102151349-A00001	No
HV DC Power Supply	Spellman	STR70N6/200/3PHASE	102186808-A00003	No

Table 5: List of Test Equipment for 25.981 Generator

25.981 Generator				
Description	Manufacturer ID	Model Number	Serial Number	Calibration Required
Scaled-down direct-effects conducted current Generator	NIAR	N/A	N/A	No
Four-channel oscilloscope	Tektronix	DPO5054B	C050190	Yes
Oscilloscope	Tektronix	DPO 2014B	C011290	Yes
Oscilloscope	Agilent	MSO6104A	MY44004620	Yes
Differential voltage probe	Keysight Technologies	N2791A	PH50293663	Yes
Differential voltage probe	Keysight Technologies	N2791A	PH50293779	Yes
Differential voltage probe	Keysight Technologies	N2791A	PH50293863	Yes
Component A current probe	Pearson Electronics	101	157914	Yes
HV DC Power Supply	Glassman	PS/FC10R12.0-11	N207038-01AM080505	No
HV DC Power Supply	Spellman	SL60P300	104757616-A05007	No
Rogowski Current Waveform Transducer	P.E.M.	CWT 6R	44254-31990	Yes
Component B/C* current probe	P.E.M.	CWT 60R	8460-9769	Yes

Table 6: List of Test Equipment for both generators

Used for Both Generators				
Description	Manufacturer ID	Model Number	Serial Number	Calibration Due Date
DC milliohm resistance meter	Hioki	RM3544	150428133	Yes
DC milliohm resistance meter	Keithley	580	0685151	Yes
Resistance Meter	HIOKI	RM3548	160513487	Yes
Light tight box	NIAR	N/A	N/A	No
Reference Lights and Power Source	NIAR	N/A	N/A	No
Barometric Pressure/ Humidity/Temperature Datalogger	Extech Instruments	SD700	Q774074	No
Digital camera 1	Canon	EOS Rebel T5	142073019286	Appendix G - 200 $\mu$ J Camera Calibration
Digital Camera 2	Canon	EOS Rebel T5	122073012940	Appendix G - 200 $\mu$ J Camera Calibration
Digital Camera (#3) and Lens	Canon	EOS Rebel T3i	Body: 402077002849	Appendix G - 200 $\mu$ J Camera Calibration

### 3.1 Scaled-Down (25.981) Lightning Generator

A scaled-down conducted-current lightning generator, purposely constructed for this KART project, is to be utilized during testing. The generator was built having a 1-to-20 target ratio with respect to full-threat generator characteristics per ARP 5412A. The scaled waveforms are shown in Figure 6 and Figure 7. The rationale for the design is based on scaling down the action integral parameter of the full-threat current Component A, while the total charge transferred is scaled to obtain the reduced Component B current (Charge = Current x Time). Finally, the scaled Component B waveform is to be extended beyond its designated 5-ms duration in order to account for the charge transfer contributed by the scaled C\*. The 25.981 generator is shown in Figure 8 and Figure 9.

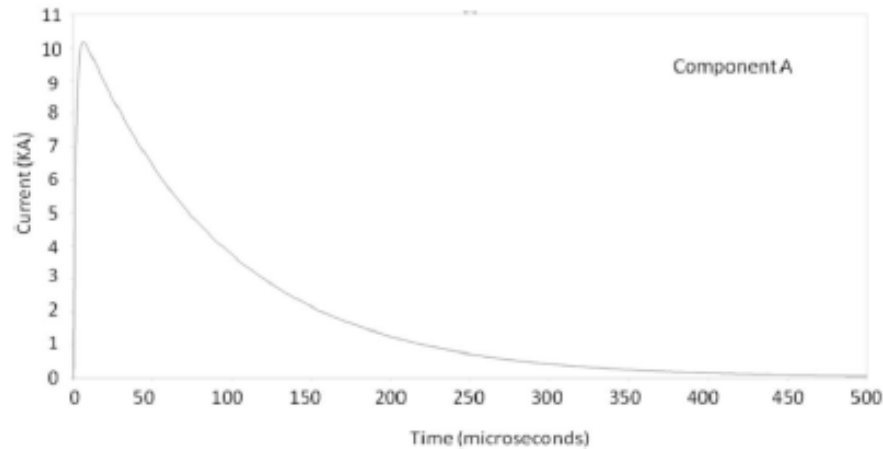


Figure 6: Scaled-Down Current Component A Waveform

The characteristics for the scaled current **Component A** include:

- Unidirectional waveform
- $5.0 \cdot 10^3 \text{ A}^2\text{s}$  ( $\pm 20\%$ ) action integral within 500  $\mu\text{s}$
- 10 kA ( $\pm 10\%$ ) peak current amplitude
- $\leq 50 \mu\text{s}$  rise time between 10% and 90% of peak amplitude
- 70  $\mu\text{s}$  time to 50% decay
- Total time to 1% peak not exceeding 500  $\mu\text{s}$ .

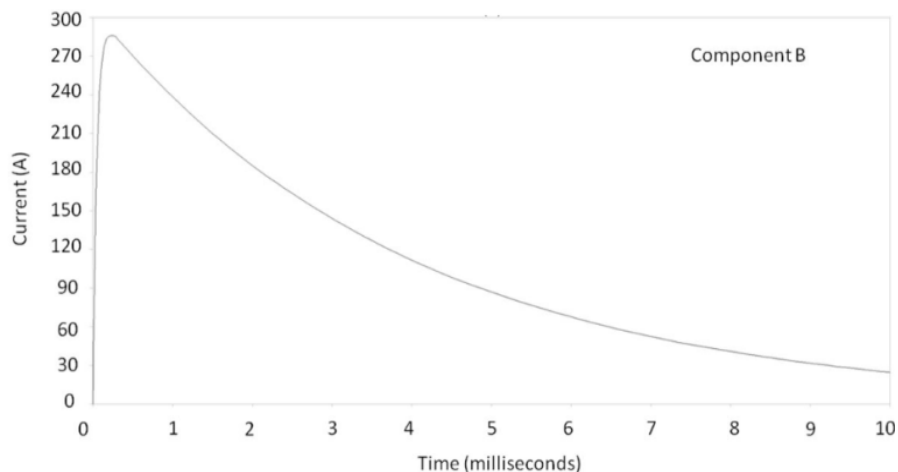


Figure 7: Scaled-Down Current Component B/C\* Waveform

The characteristics for the scaled current **Component B/C\*** include:

- Unidirectional waveform
- 171 A ( $\pm 20\%$ ) average current
- 290 A peak current
- 1.4 C ( $\pm 10\%$ ) total charge transfer.





Figure 8: Front View of 25.981 Lightning Generator



Figure 9: Side View of 25.981 Lightning Generator



### 3.2 Direct Effects of Lightning Generator

A direct effects generator was also used for testing the conductive faulted fasteners. The waveforms and test set up is shown below in Figure 10 and Figure 11.

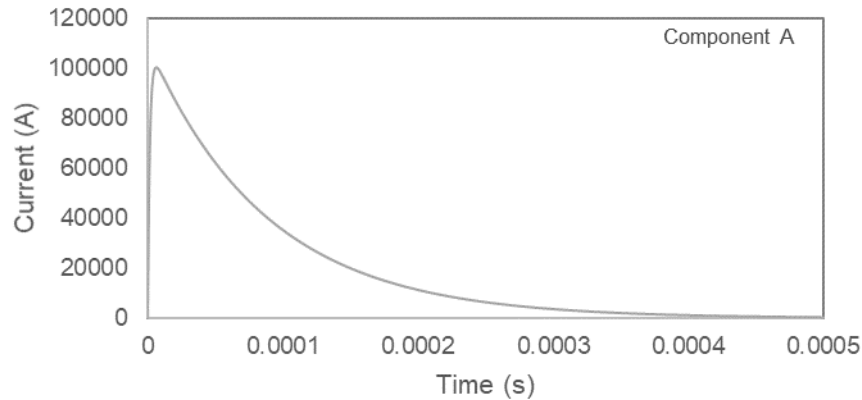


Figure 10: Scaled Current Component A Waveform

The characteristics for the scaled current component A include:

- Unidirectional waveform
- $250 \text{ kA}^2\text{s} \pm 20\%$  action integral in  $500 \mu\text{s}$
- Peak current of 100 kA
- $6.4 \mu\text{s}$  rise time,  $70 \mu\text{s}$  to 50% decay
- Total time  $\leq 500 \mu\text{s}$

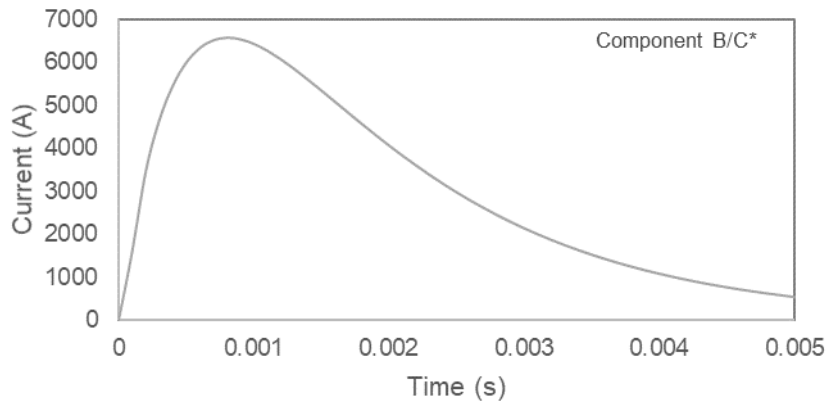


Figure 11: Scaled Current Component B/C\* Waveform

The characteristics for the current component B/C\* include:

- Unidirectional waveform
- 3 kA average current
- 6.5 kA peak current
- 0.8 ms rise time
- 14 C total charge transfer

### 3.3 Photographic Chamber

For the 25.981 generator, the light-tight photographic chamber was constructed in accordance with ARP 5416A, Section 7.7.1, which describes the photographic test method. The chamber contains two reference light sources, one on each side, for verifying the camera shutters proper opening during the test. A schematic of the electrical circuit containing the photographic chamber is shown in Figure 12. The test setups between the two generators were identical, except the voltage probes were not used at the direct effects generator.

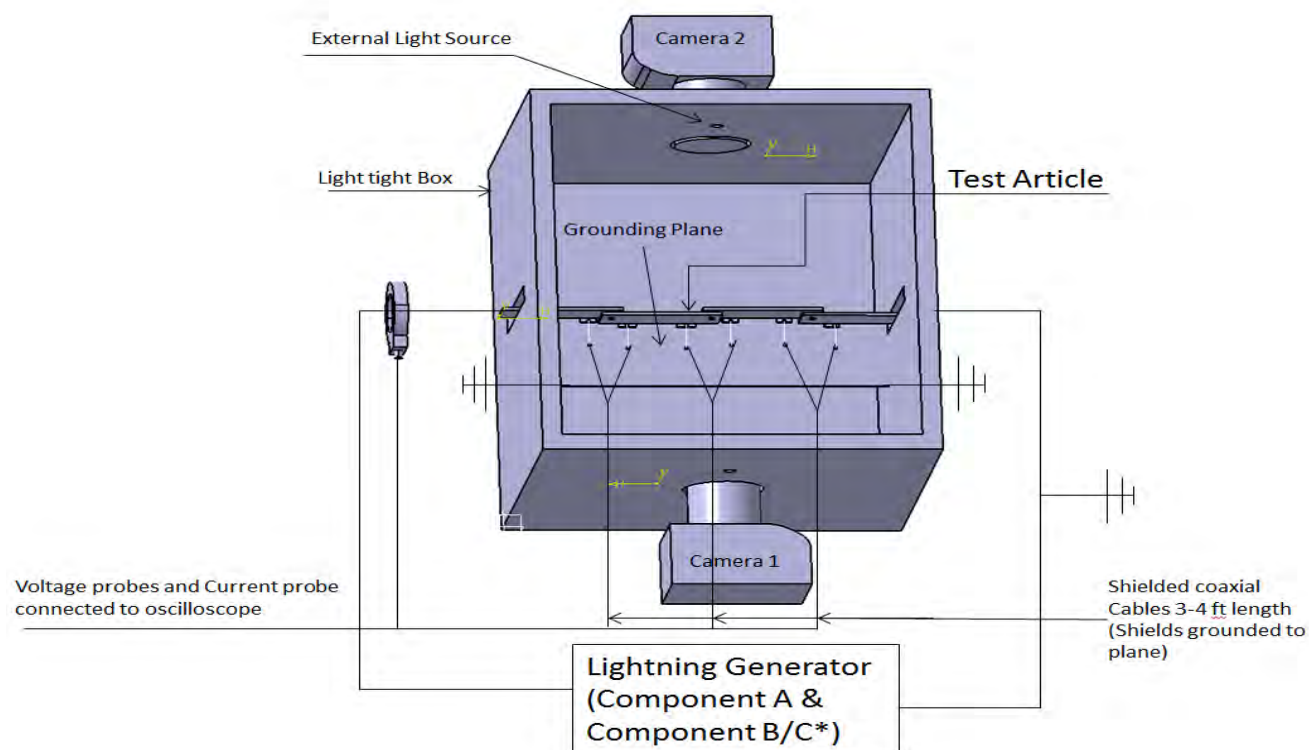


Figure 12: Schematic of the Photographic Chamber

### 3.4 Digital Cameras

The photographic method described in ARP 5416A uses cameras to detect ignition sources of electrical sparks (voltage sparks) or electrical arcs (current sparks) during lightning testing. The test setup for the scaled down generator used in testing the nominal articles utilizes two digital cameras to capture the event of emitted light from the front and back of the test article. The photographic method used must be capable of detecting  $200 \mu\text{J} \pm 10\%$  electrical voltage sparks. For the testing of nominal test articles, the test cameras were calibrated by DNB Engineering, Inc. in accordance with the procedure for the construction and operation of a standard voltage spark ignition source as outlined in the DOT/FAA/CT-94/74 Final Report "Aircraft Fuel System Lightning Protection Design and Qualification Test Procedures Development," U.S. Department of Transportation Federal Aviation Administration (1994). The cameras were recalibrated for testing of the faulted test articles according to the calibration procedure summarized in Appendix G -  $200 \mu\text{J}$  Camera Calibration.

#### 4.0 TEST SETUP

The test setup for the 25.981 generator is shown in Figure 13 and

Figure 14. The test setup for the direct effects generator is shown in Figure 15.

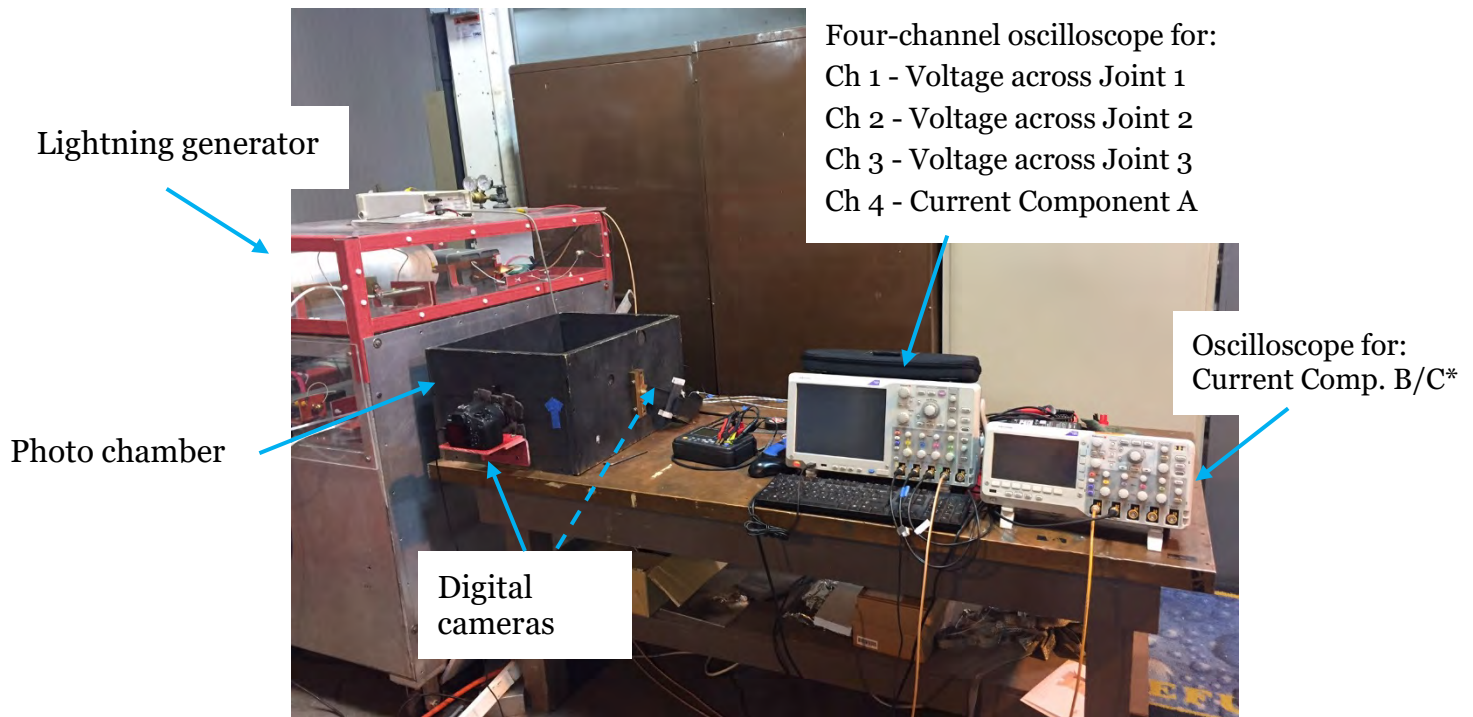


Figure 13: 25.981 Generator Test Setup

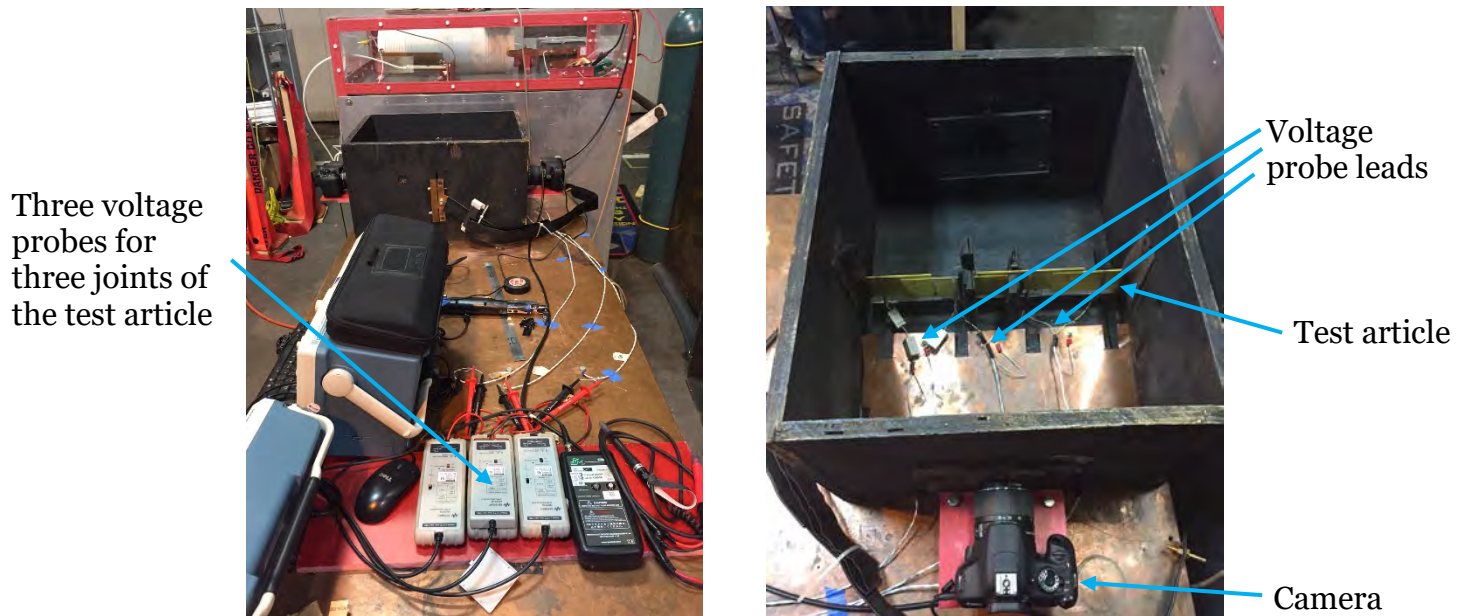


Figure 14: Right-End View of Test Setup (Left) and Photo Chamber (Right)



Figure 15: DEL Generator Setup



## 5.0 ANALYSIS PLAN

The nominal test articles were tested to determine the sparking threshold first at 10 kA, with subsequent tests repeated with decreasing peak current amplitudes until the test article does not spark. The conductive faulted test articles, however, were tested beginning from 10 kA and increasing to 100 kA to determine the nonsparking threshold. Nonconductive faulted fasteners were first tested at 5 kA and the current for the next test was either increased or decreased depending on if the test article sparked the first time or not.

In order to be confident in the value for the sparking and nonsparking threshold, the amount of uncertainty or variance must not be too large. Therefore, the manufacturing variance, the energy delivery variance, and any test setup biases must be controlled or accounted for.

The manufacturing variance should be the largest and the hardest to control because the test articles come from 5 different OEMs with different manufacturing procedures. Anomalies in manufacturing that are not accounted for can lead to misleading thresholds. To understand the manufacturing variance, there is a test articles check-in procedure. The pre-test DC resistance is measured for each joint of each test article. This measurement will help assess manufacturing quality. The coating thickness is also measured in 3 locations for each test article. This measurement will help to determine if there is anything unusual with the test articles.

The energy delivery variance should be easier to control because it is from the same equipment delivered by the same person following the same procedure during testing. The values for the peak current, action integral, and charge transfer are recorded for each test shot. This data can be compiled to ensure that both the requirements for the test are met and the energy delivered is consistent.

Test setup can sometimes be determined if a supposedly constant response is plotted over time. An example of setup specific bias due to test article design could be unequal joint sparking distribution. There were changes in the test setup that could have affected energy distribution. To track both sudden and gradual changes in energy distribution, a Ni-Cr strip was used for a test shot to calibrate the generator at the beginning of each day of the nominal test article testing. All data from the calibration shots was recorded to be used to track changes over time.

### 5.1 Manufacturing Variance Check

All the test articles received from participating OEMs were inspected and validated against the engineering drawings. Check-in sheets were prepared to verify number of test articles, test article identification markings, fasteners, measurements for the thickness of the aluminum coupons, and to note any anomalies.

#### 5.1.1 Nominal Test Articles

##### *DC Resistance*

Part of the check-in procedure was to take measurements of the DC resistance across each joint. A graph of DC resistance by test article for all OEMs is shown in Figure 16.

#### OEM 1

Check-in resistances for OEM 1 were the highest of all the OEMs because of the MN-1To3 and MN-1T12 configurations. Several other configurations for OEM 1 had high check-in resistance values also. The test articles with the highest DC resistance values were all made with the non-conductive coating fasteners (Hi-Lok/Hi-Kote HL11VAZ5-3) which measured high for all OEMs.

#### OEM 2

Check-in resistances for OEM 2 were lower in comparison to the other OEMs. All resistances for OEM 2 were below 10 mΩ. The check-in resistance values for the two configurations with the non-conductive coating were only slightly higher.

#### OEM 3

The check-in resistances of the single fastener test articles were higher than the resistances of the quadruple fastener test articles.

#### OEM 4

The check-in resistances of the transition fit test articles were much higher than the resistances of the interference fit test articles for both quadruple and single fasteners. The check-in resistance values for the two configurations with the non-conductive coating were high. The single fastener configuration resistance was much higher than everything else. In comparison to the other OEMs, the check-in resistance values for OEM 4 are higher. Note: If the check-in resistance value exceeded 1000 mΩ, the value was set to 1000 mΩ.

#### OEM 5

Check-in resistances for OEM 5 were consistent with the other OEMs where most of the resistance measurements were below 10 mΩ. The check-in resistance values for the two configurations with the non-conductive coating were high, measuring around 400 mΩ, but that is also consistent across all OEMs. The one anomaly for OEM 5 is that the check-in resistance measurements for MN-1Io1 were higher than other comparable test articles.

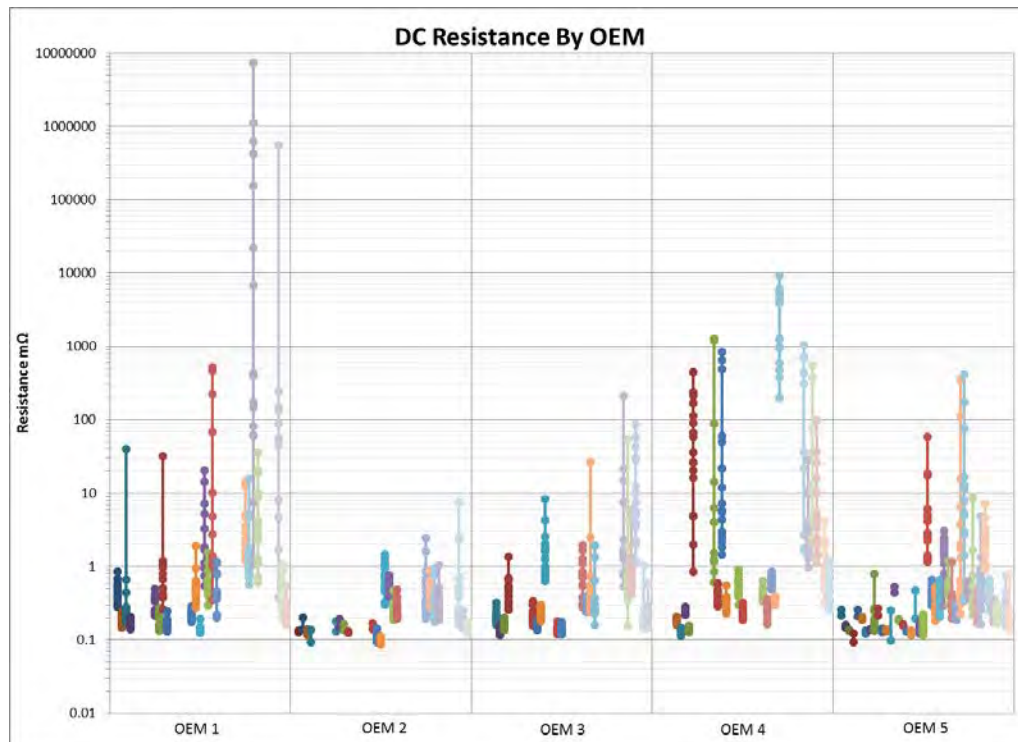


Figure 16: Nominal DC Resistance at Check-In

### *Paint Thickness*

Measurements of coating thickness were taken in three different locations across each test article and averaged. The coating thickness data is shown in a box and whisker plot to include the variation. A graph of the nominal paint thickness by test article for all OEMs is shown in Figure 17. The overall average paint thickness for the nominal installations was 1.58 mils  $\pm$  0.33 mils.

#### OEM 1

Average check-in paint thickness for OEM 1 was around 1.8 mils. This is slightly higher than the average due to an additional thick nonconductive anodized coating that was used by OEM 1.

#### OEM 2

Check-in paint thicknesses for OEM 2 were consistent with the other OEMs where most of the thickness measurements were between 1 and 1.5 mils. The variance difference between the quadruples and the singles is understandable because there were 6 single-fastener test articles and only 1 quad test article, so the single-fastener test articles should have a larger variance.

#### OEM 3

Check-in coating thicknesses for OEM 3 were consistent with the other OEMs and have an overall average thickness around 1.7 mils.

#### OEM 4

Check-in coating thicknesses for nominal OEM 4 coupons were consistent with the other OEMs and having an overall average thickness around 1.78 mils. The variance was a little unusual in that there seemed to be two groups of thicknesses: one at 1.5 mils and one at 2.0 mils which pulled the average up a little.

#### OEM 5

Check-in coating thicknesses for OEM 5 were consistent with the other OEMs where most of the thickness measurements were around 1.5 mils. The variance difference between the quadruples and the singles is understandable because there were 6 single-fastener test articles and only 1 quad test article so the single-fastener test articles would have a much larger variance. The difference in the mean coating thickness between the quadruples and the singles may be due to different painters, different equipment, or different painting times.

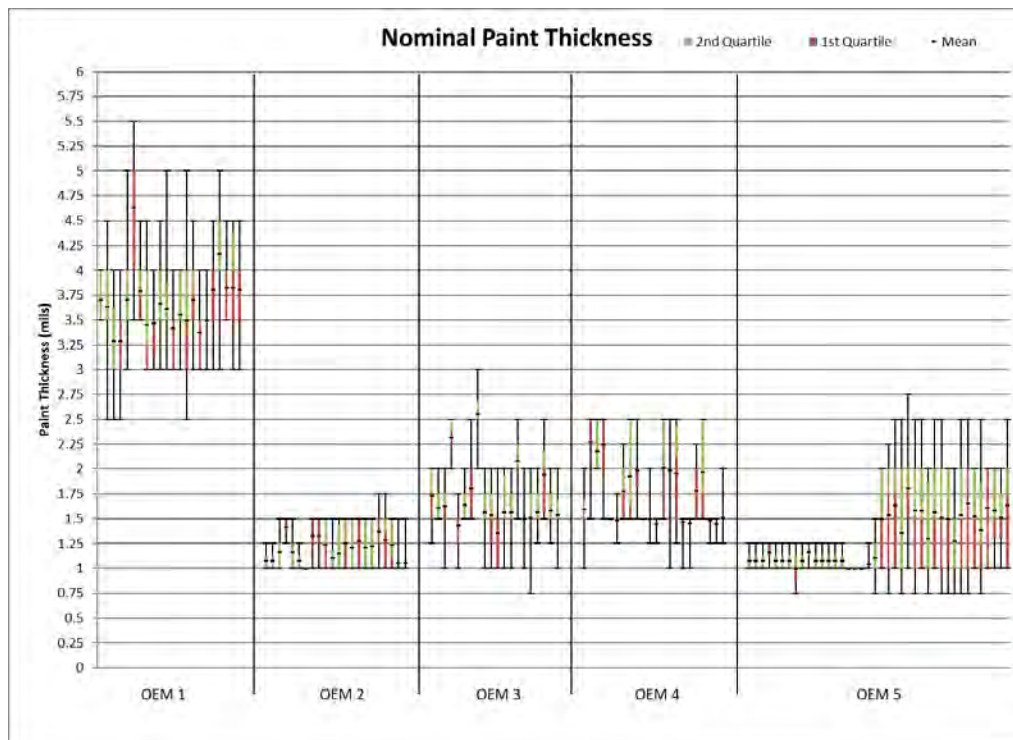


Figure 17: Nominal Paint Thickness at Check-In

### *Manufacturing Anomalies Observed at Check-In*

#### OEM 1

Many of the test articles for OEM 1 substituted the small countersunk head Hi-Kote fasteners for the small countersunk Hi-Lok fasteners. All the fastener substitutions are listed below:

1. MN-4Io3 – Hi-Kote (HL11VAZ5-3) instead of Hi-Lok (HL11VBJ5-3) fasteners,
2. MN-4To3 - Hi-Kote (HL11VAZ5-3) instead of Hi-Lok (HL11VBJ5-3) fasteners,
3. MN-4To4 – Protruding head (HL10VBJ8-3) instead of countersunk (HL11VBJ8-3),
4. MN-4T12 – Hi-Lok (HL11VBJ5-3) instead of Hi-Kote (HL11VAZ5-3) fasteners,
5. MN-1Io3, #1 – Hi-Kote (HL11VAZ5-3) instead of Hi-Lok (HL11VBJ5-3) fasteners,



6. MN-1Io3, #3 - Hi-Kote (HL11VAZ5-3) instead of Hi-Lok (HL11VBJ5-3) for joints 1 & 2,
7. MN-1To3 – Hi-Kote (HL11VAZ5-3) instead of Hi-Lok (HL11VBJ5-3) fasteners.

All the test article configurations listed above were changed to their actual configuration name code for data analysis. For example: all the 4To4 test articles were changed to 4To2 test articles for data analysis.

#### OEM 2

None noted.

#### OEM 3

The nominal collars requested were HST79CY5 and HST79CY8. OEM 3 provided HST79CK5 and HST79CK8 collars. The only difference in these collars is the outer surface finish color.

#### OEM 4

Two of the single fastener test articles had joints that were crooked (MN-1Io5 #3 and MN-1Io10 #2). Test articles MN-4To6 #5 and MN-1To7 #1 were sent unassembled so were not tested. Test article MN-1To7 #6 had a very loose fastener at joint 2. Test article MN-1Io6 #3 still had the masking tape on it. The quadruple fastener test article MN-4To8 #1 was missing one of the fasteners from Joint 3.

#### OEM 5

Several of the single fastener test articles from OEM 5 were found to be loose (MN-1Io3, MN-1To1, and MN-1To3). The nominal collar, HL70-8 was specified for use with the large HI-LOK™ fasteners but an oversized collar, HL79-8 was used instead on several test articles (MN-1Io2 #2-6, MN-1Io4 #1-6, MN-1To4 #1-6, MN-4Io4 joints 1 & 2, and MN-4To4). The test article marked MN-4Io5 used HI-LOK™ pins instead of the HI-LITE™ pins that were specified.

### **5.1.2 Faulted Test Articles**

#### *DC Resistance*

Part of the check-in procedure was to take measurements of the DC resistance across each joint. A graph of DC resistance by test article for all OEMs is shown in Figure 18.

#### OEM 1

Check-in resistances for OEM 1 were the highest of all the OEMs because of the MF-4To3 and MF-4T12 configurations.

#### OEM 2

Check-in resistances for OEM 2 were lower in comparison to the other OEMs. All resistances for OEM 2 were below 1 mΩ.

#### OEM 3

All resistances were below 3 mΩ, no HI-KOTE fasteners were provided

### OEM 5

Check-in resistances for OEM 5 was consistent with the other OEMs where most of the resistance measurements were below 10 mΩ. Some of the test articles of the MF3-4T11, MF4-4T11, and MF6-4T12 configurations had resistances greater than 10 mΩ.

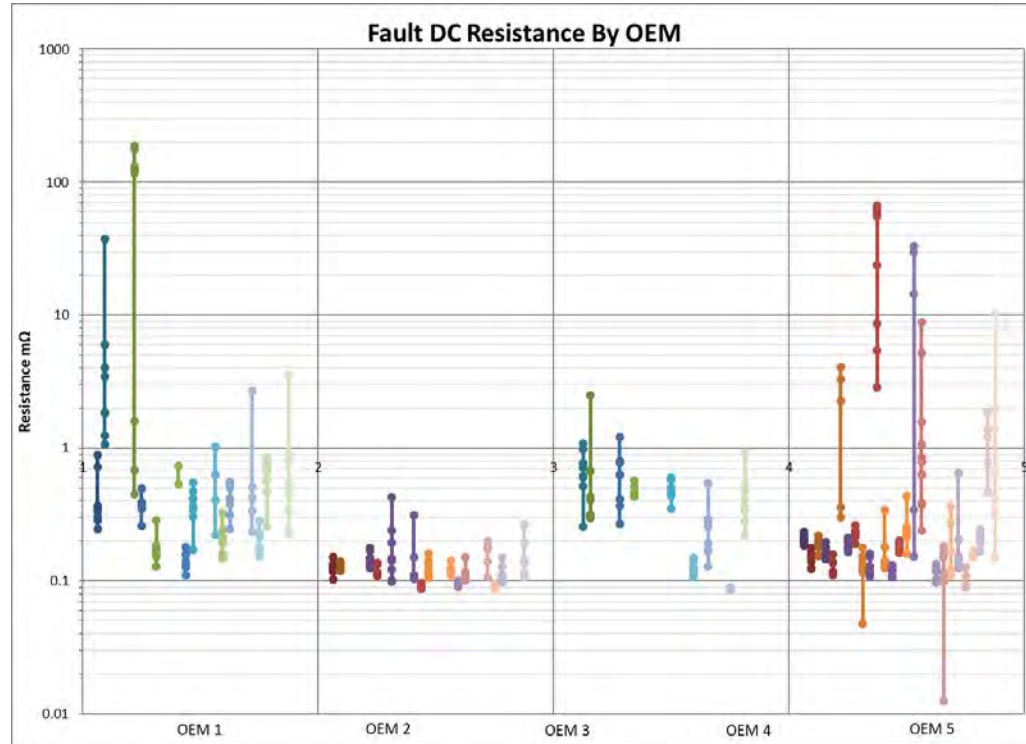


Figure 18: Faulted DC Resistance at Check-In

### *Paint Thickness*

Measurements of coating thickness were also taken in three different locations across each test article and averaged. The coating thickness data is shown in a box and whisker plot to include the variation. A graph of the nominal paint thickness by test article for all OEMs is shown in Figure 19. The overall average paint thickness for the faulted articles on average was 1.03 mils  $\pm 0.44$  mils.

### OEM 1

OEM 1 had the lowest values averaging to 0.89 mils despite having the same anodized coating present in their nominal fasteners.

### OEM 2

The majority check-in paint thickness for the OEM 2 faulted coupons were close to the 1 mil average except the MF5-4T01 coupons which had more variance between articles.

### OEM 3

Check-in coating thicknesses for OEM 3 was consistent with the other OEMs and have an overall average thickness of 0.9 mils.

#### OEM 5

Check-in coating thicknesses for OEM 5 was consistent with the other OEMs where the average thickness measurement was 1.18 mils.

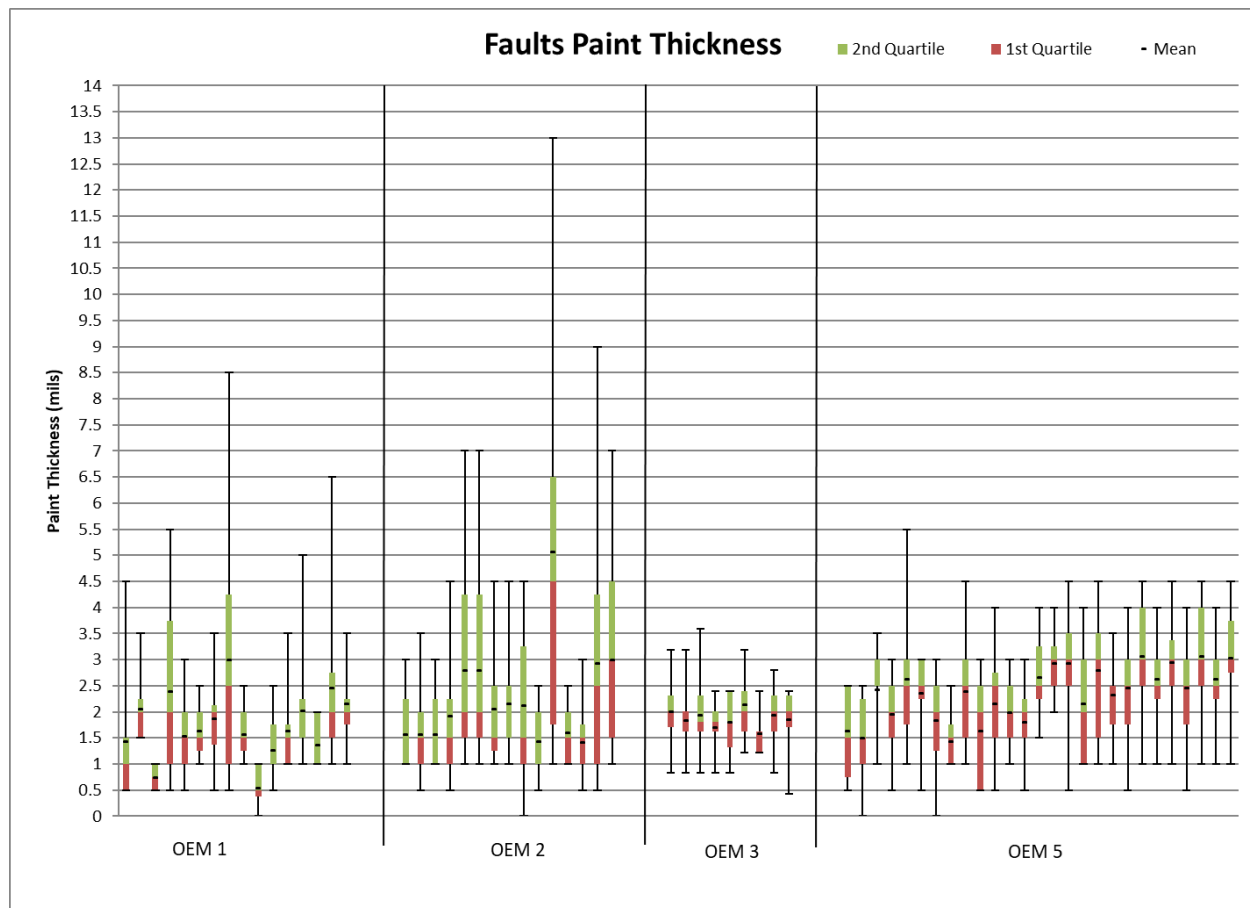


Figure 19: Faulted Paint Thickness at Check-In

### *Manufacturing Anomalies Observed at Check-in*

#### OEM 1

The most notable anomaly in the test articles provided by OEM 1 is the use of sealant which sometimes came through the collar/head of the fasteners. The MF3-4009 test articles did not buck the shop head of the fasteners.

#### OEM 2

Many fasteners had apparent gaps under head despite being specified as nominal installations or in addition to the assigned fault. There was a bend in the bottom coupon of joint 1 on the MF4-4To1-1 test article creating a larger gap between coupons. The bottom coupon of joint 2 of MF3-4009-2 has a deformation in the metal around the fastener. On MF5-4009 the burrs are under the head side of the article instead of the tail side. MF5-4To1 had the scratch under the

head side instead of the tail side. On MF5-4To1-2, two fasteners on joint 3 are flattened on the head side and rounded on the tail side.

### OEM 3

The MF1-4To7 faulted fastener used a protruding head fastener instead of a countersunk one. In the MF2-4To5 coupons, different pins were used on some of the faulted fasteners and on the sixth test article, the whole fastener spins when turned. In MF3-4To5 it appears that there is a gap under head in addition to the assigned gap under collar fault and the whole fastener spins when turned on joint 3. In the MF4-4To5 coupons there was a scratch between the plates, rather than under the fastener head. In MF5-4To5 and MF6-4To5 different fasteners were different lengths. In the MF6-4To5 test articles, the collar wrenching device is not attached, indicating that the controlled preload was met, and the fasteners are likely not under-torqued.

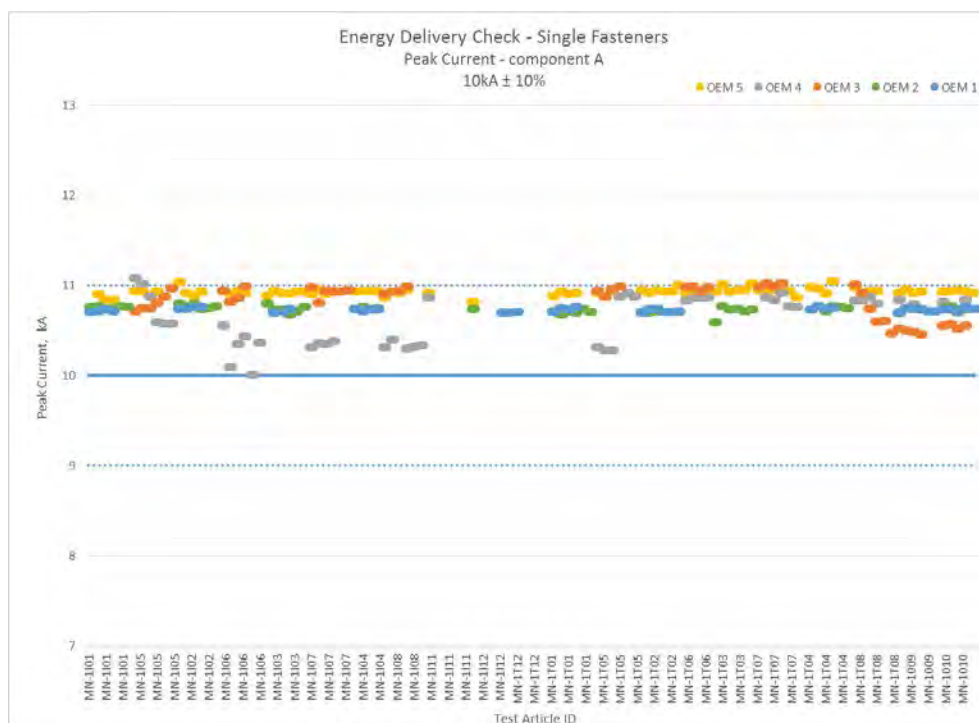
### OEM 5

Many test articles had a slight bend over the length of the coupons, likely due to storage methods, but this should not have impacted the testing. The fourth instance of the MF3-4To1 test article provided by OEM 5 was bent more severely and was not tested.

## 5.2 Energy Delivery Variance Check

### 5.2.1 Nominal Test Articles

Graphs of peak current for single fastener test articles and for quadruple fastener test articles for all OEMs are shown in Figure 20 and Figure 21. The ideal value of 10 kA is shown on the graphs as a solid blue line. The acceptable  $\pm 10\%$  values are shown on the graphs as dashed



blue lines. Most of the data hovers close to 11 kA at the top dashed blue line. There were a few times when the current exceeded the upper limit but none of those times resulted in a spark.  
Figure 20: Energy Delivery Check - Nominal - Single, Peak Current - Component A

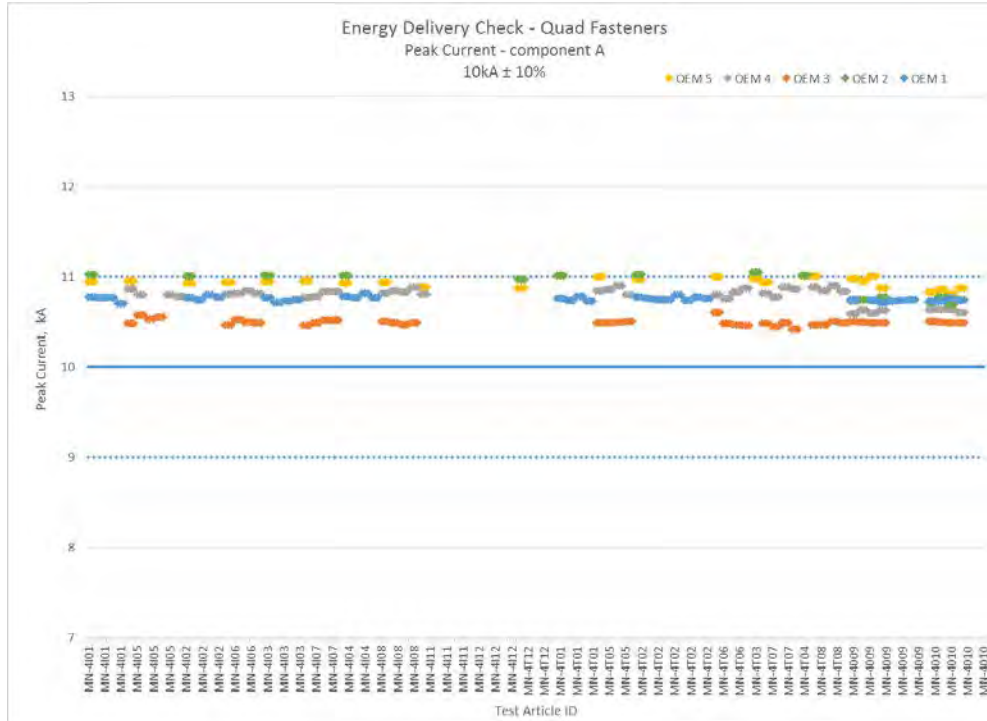


Figure 21: Energy Delivery Check – Nominal - Quad, Peak Current - Component A

Graphs of action integral for single fastener test articles and for quadruple fastener test articles for all OEMs are shown in Figure 22 and Figure 23. The ideal value of  $5.0 \times 10^3 \text{ A}^2\text{s}$  is shown on the graphs as a solid blue line. The acceptable  $\pm 20\%$  values are shown on the graphs as dashed blue lines. Most of the data hovers close to the ideal value at the center blue line.

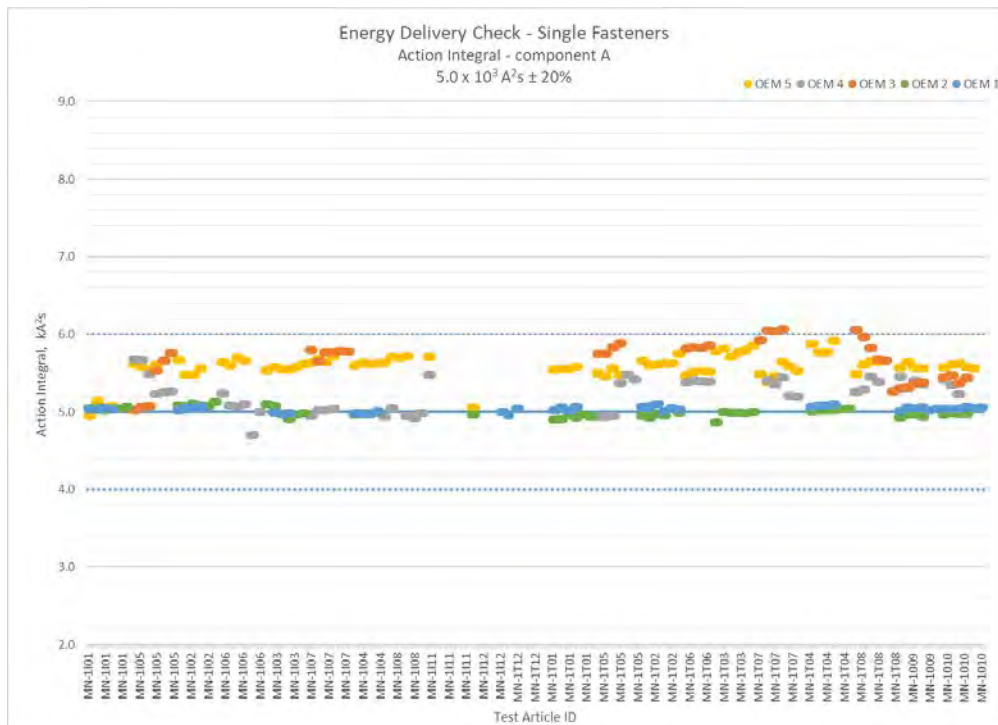


Figure 22: Energy Delivery Check - Nominal - Single, Action Integral - Component A

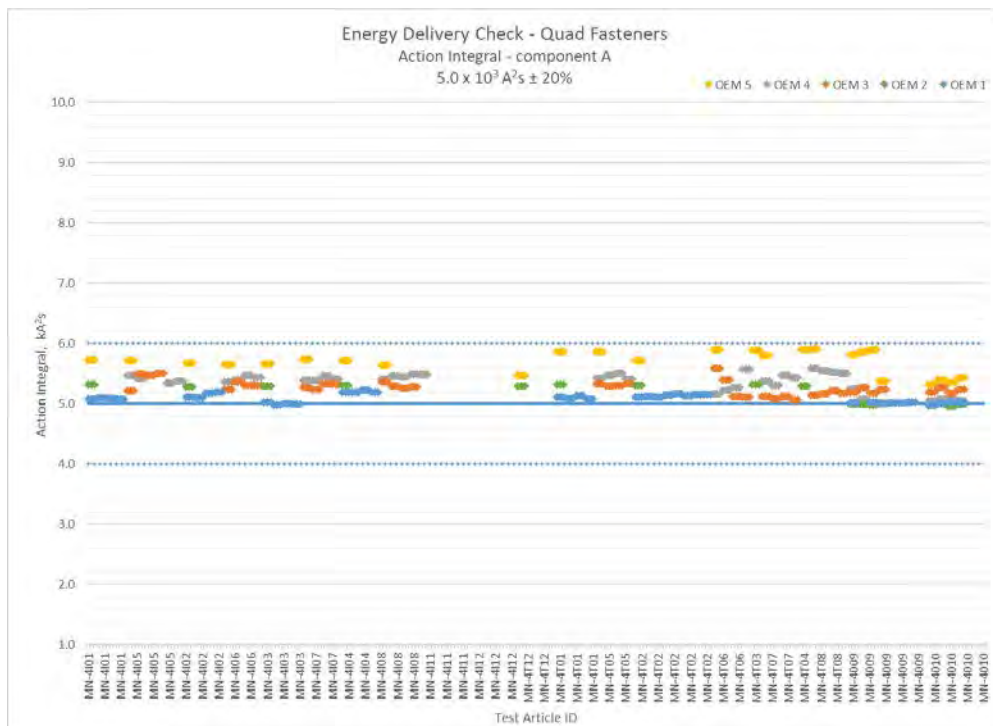


Figure 23: Energy Delivery Check – Nominal Quad, Action Integral - Component A

Graphs of charge transfer for single fastener test articles and for quadruple fastener test articles are shown in Figure 24 and Figure 25. The ideal value of 1.4 C is shown on the graphs as a solid blue line. The acceptable  $\pm 10\%$  values are shown on the graphs as dashed blue lines. Most of the data is below the center blue line but within the lower limit. There are a few times



when the charge transfer for the nominal fasteners exceeded the upper limit but none of those times resulted in a spark.

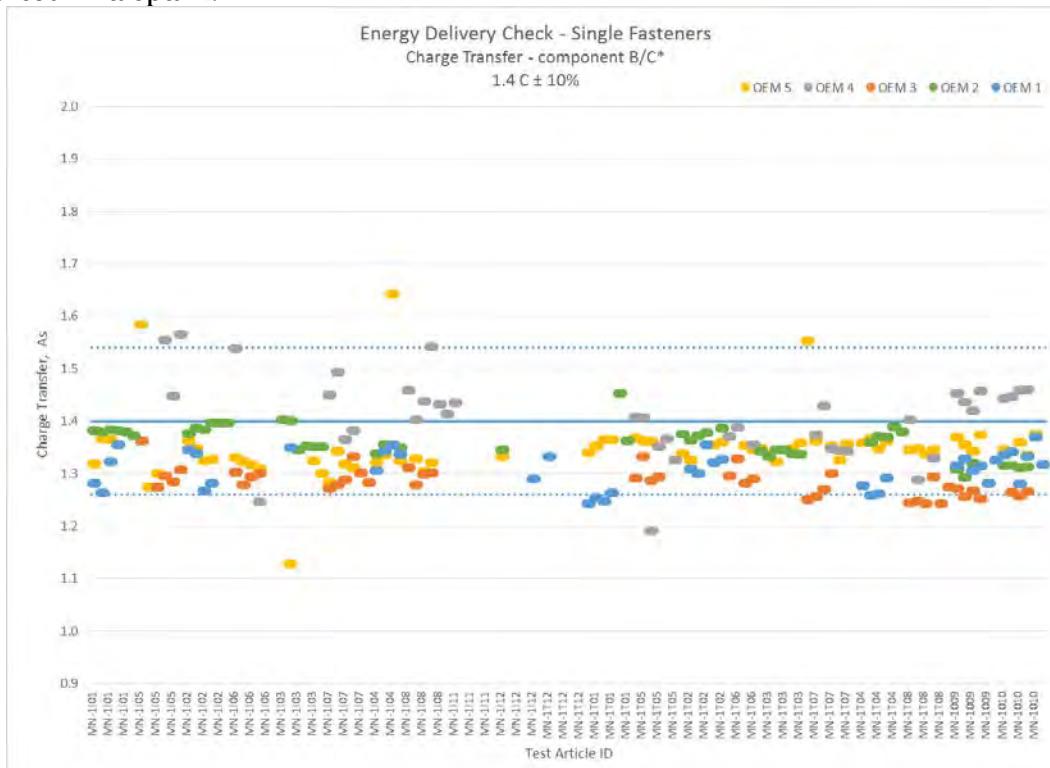


Figure 24: Energy Delivery Check – Nominal - Single, Charge Transfer - Component B/C\*

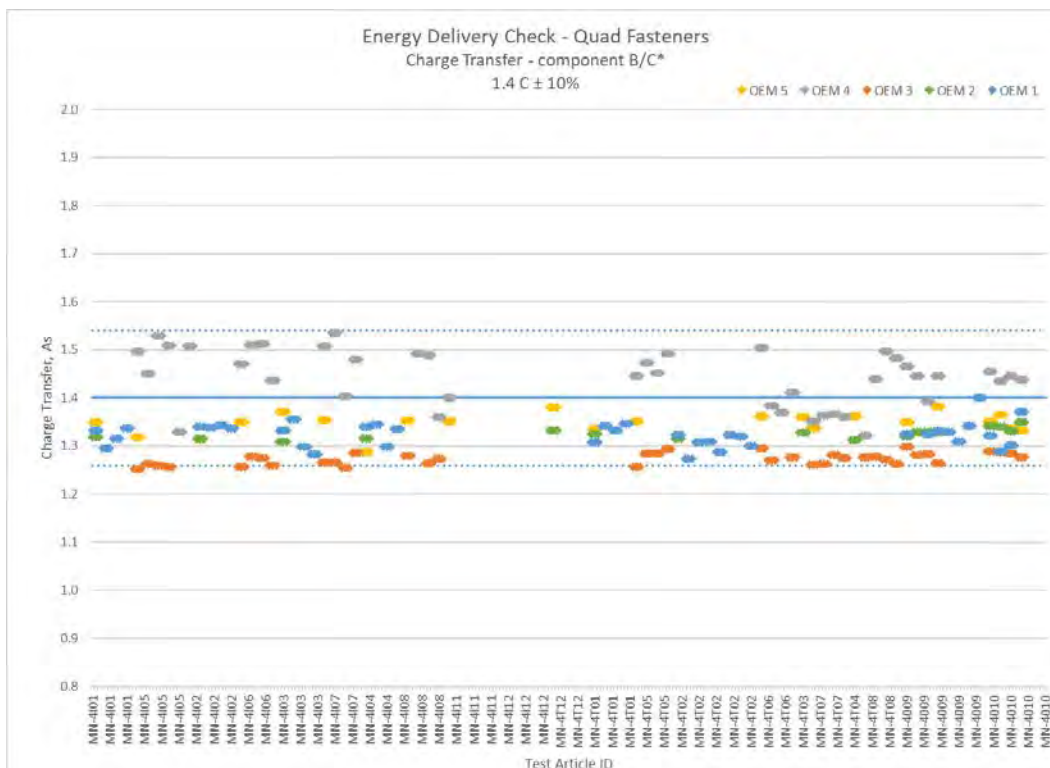


Figure 25: Energy Delivery Check – Nominal - Quad, Charge Transfer - Component B/C\*

It can be seen from the graphs of peak current, action integral, and charge transfer in Figure 20 through Figure 25 that the energy delivery for the nominal testing consistently falls within the acceptable range.

### 5.2.2 Faulted Test Articles

Graphs of the peak current for both test levels of the faulted quadruple fastener test articles are shown in Figure 26 and Figure 27. For the 10 kA test level, the ideal value of 10 kA is shown on the graphs as a solid blue line. The acceptable  $\pm 10\%$  values are shown on the graphs as dashed blue lines. Most of the data hovers close to 11 kA at the top dashed blue line. The conductive faulted fasteners were also tested 100 kA test level. As shown in Figure 27, the ideal value of 100 kA is the solid blue line while the 10% bounds are shown as dashed lines. Most of the data hovers close to the ideal value at the center blue line.

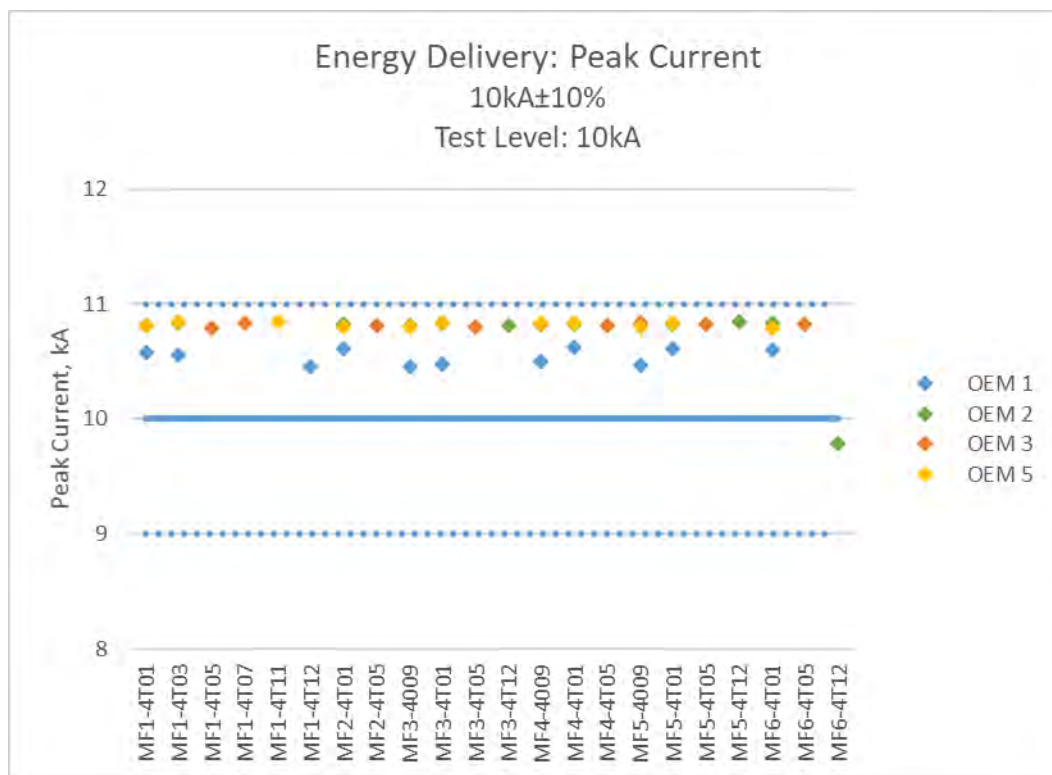


Figure 26: Energy Delivery Check – Faults, Peak Current 10 kA – Component A



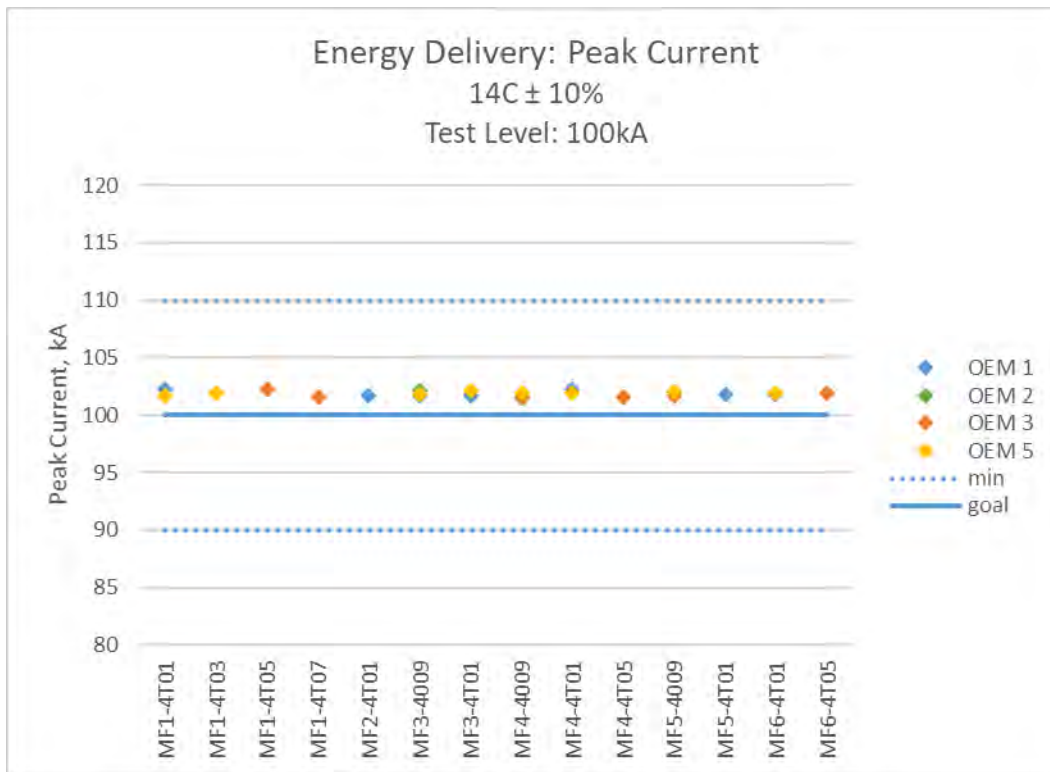


Figure 27: Energy Delivery Check – Faults, Peak Current 100 kA – Component A

Graphs of action integral for the faulted quadruple fasteners tested at 10kA is shown in Figure 28. The ideal value of  $5.0 \times 10^3 \text{ A}^2\text{s}$  is shown on the graphs as a solid blue line. The acceptable  $\pm 20\%$  values are shown on the graphs as dashed blue lines. Most of the data hovers close to the ideal value at the center blue line. The graph of the action integral for the faulted fasteners tested at 100kA is shown in Figure 29. The ideal value of  $500 \text{ kA}^2\text{s}$  is shown on the graphs as a solid blue line. The acceptable  $\pm 20\%$  values are shown on the graphs as dashed blue lines. Most of the data hovers close to the maximum value at the top dashed blue line.

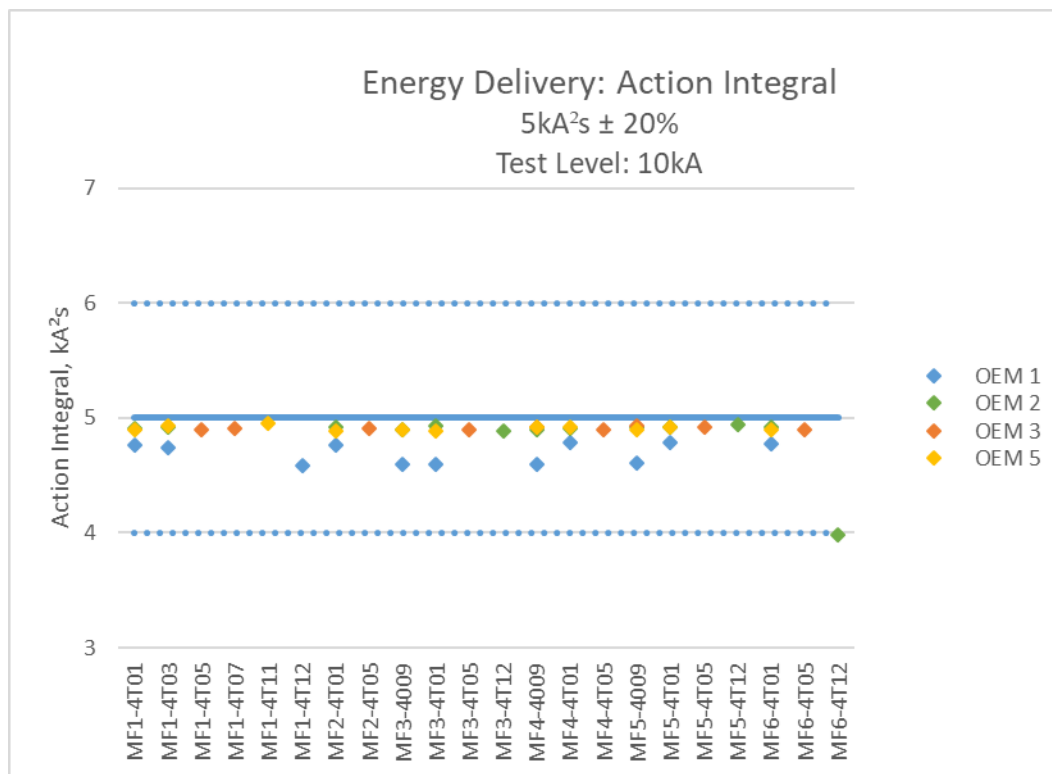


Figure 28: Energy Delivery Check – Faults, Action Integral – 10 kA Test Level

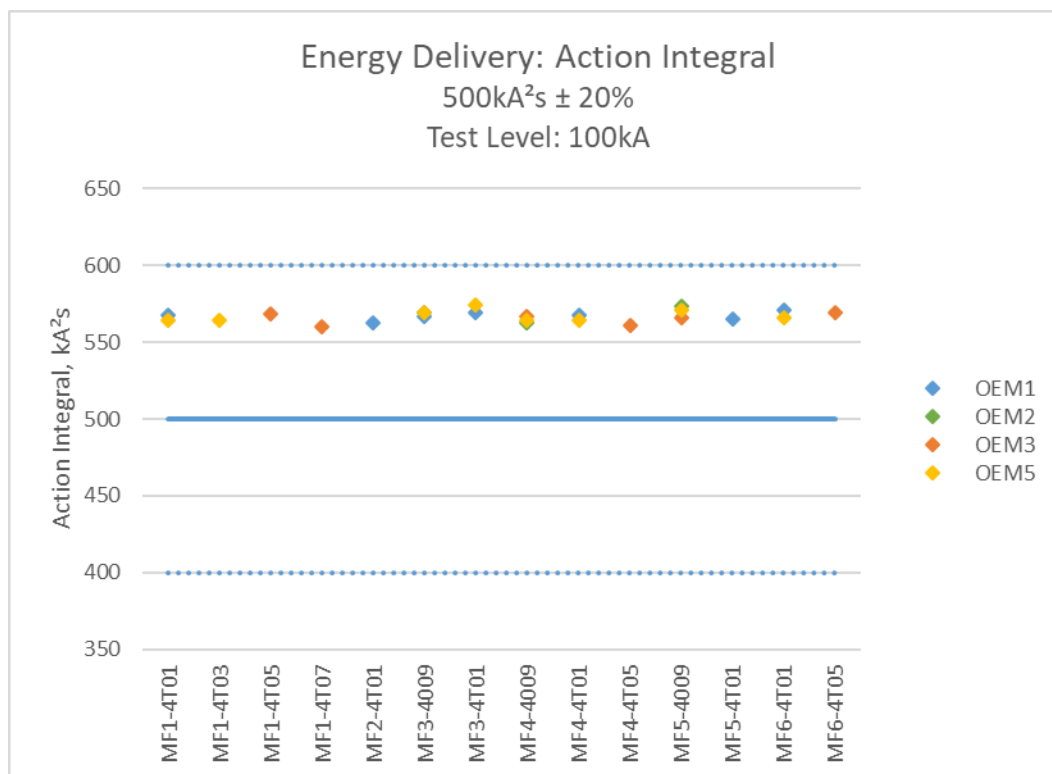


Figure 29: Energy Delivery Check – Faults, Action Integral – 100 kA Test Level

Graphs of charge transfer of the faulted fasteners tested at 10kA is shown in Figure 30. The ideal value of 1.4 C is shown on the graphs as a solid blue line. The acceptable  $\pm 10\%$  values are shown on the graphs as dashed blue lines. Most of the data is below the center blue line but within the lower limit. The graph of the charge transfer for the fasteners tested at 100 kA is shown below in Figure 31. The ideal value of 14 C is shown on the graphs as a solid blue line. The acceptable  $\pm 10\%$  values are shown by the dashed blue lines. Most of the data hovers around the solid blue line at 14 C.

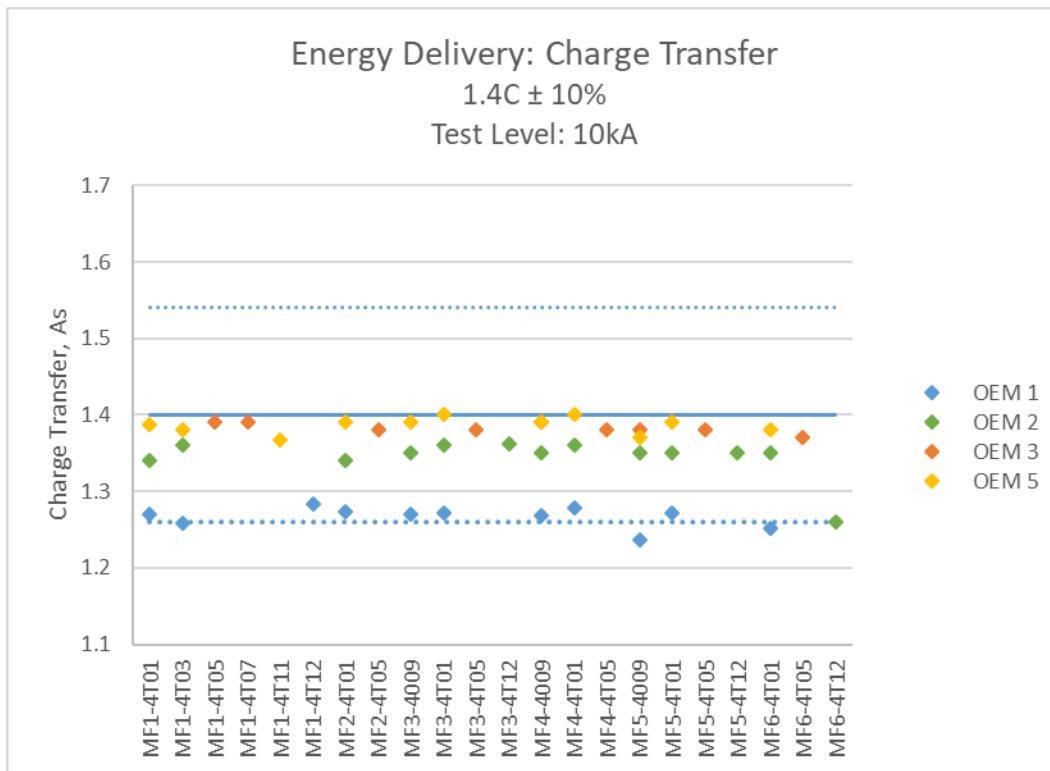


Figure 30: Energy Delivery Check – Faults, Charge Transfer – 10 kA Test Level

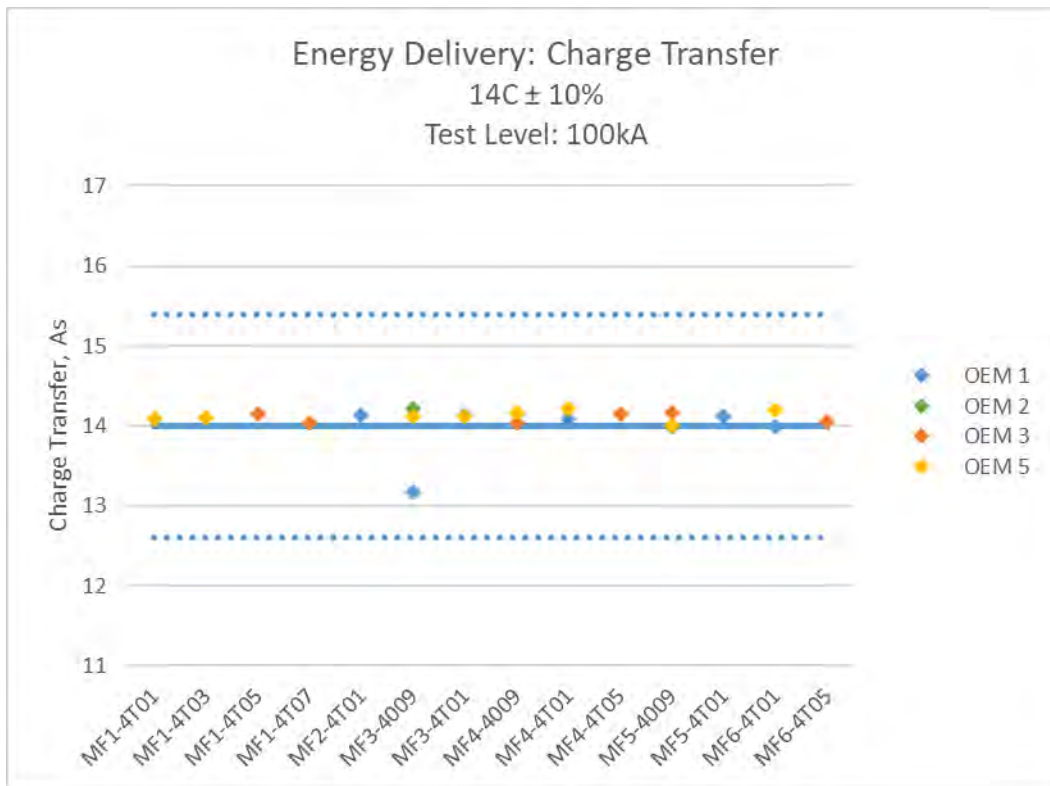


Figure 31: Energy Delivery Check – Faults, Charge Transfer – 100 kA Test Level

It can be seen from the graphs of peak current, action integral, and charge transfer in Figure 26 through Figure 31 that the energy delivery for the faulted fastener testing consistently falls within the acceptable range.

## 5.3 Test Setup Biases Check

### 5.3.1 Nominal Test Articles

A common way to spot a bias is to look at a supposed constant value over time. Figure 32 shows the values of peak current over the entire course of the nominal testing for all OEMs. Events that changed the test setup and might have influenced the data are also recorded with their timeframe.

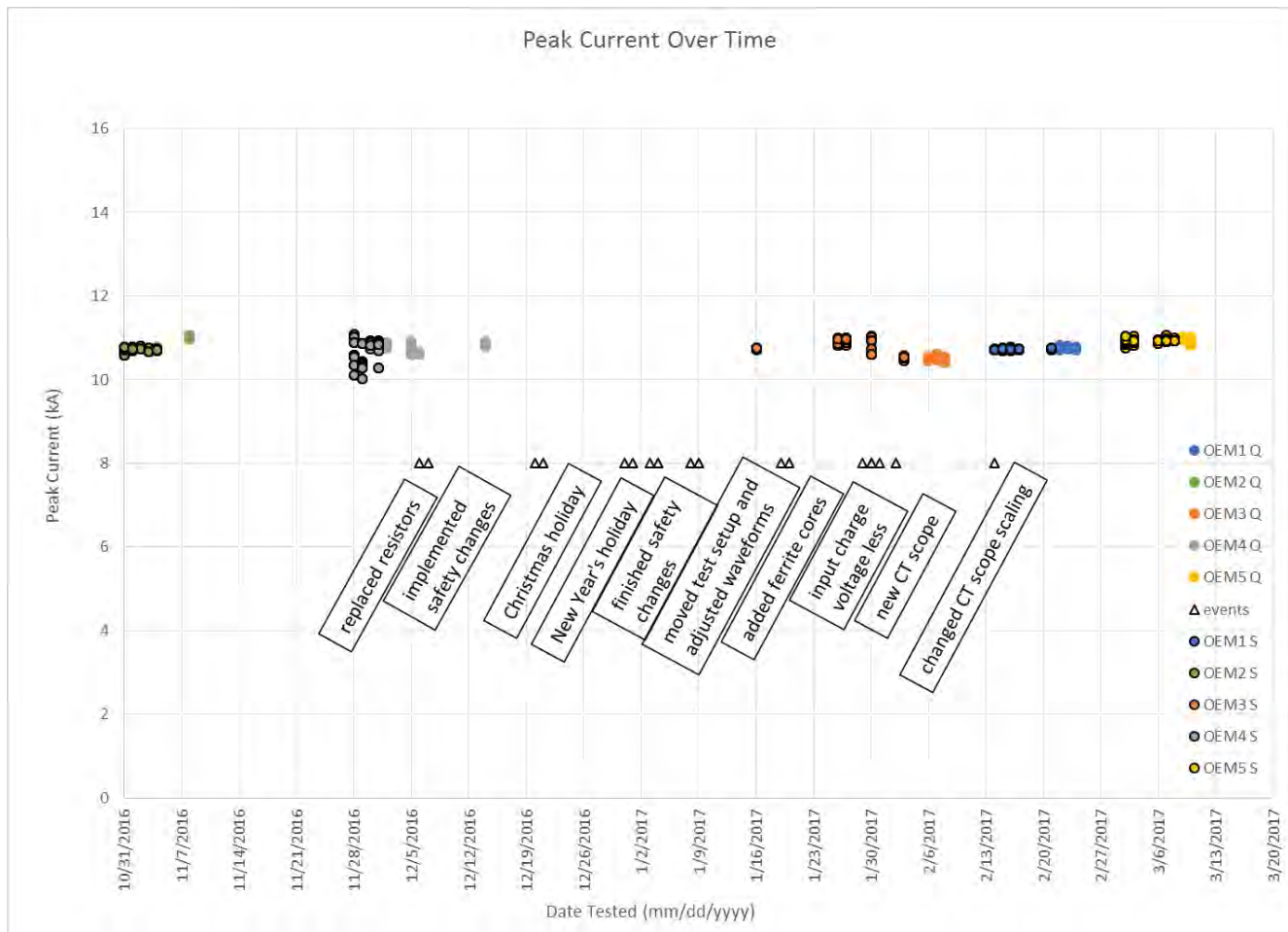


Figure 32: Peak Current Over Time

There is some higher variance within the single fastener test articles of OEM 4 but the majority of the values are within the 10.5 to 11 kA range with the other OEMs.

Shown in Figure 33 are the calibration values taken with the Ni-Cr strip each day before the start of testing. The peak current values are used for comparison purposes. There is a small amount of variance but overall the values are consistent. Therefore, no bias is assumed and no adjustments were made to the data.

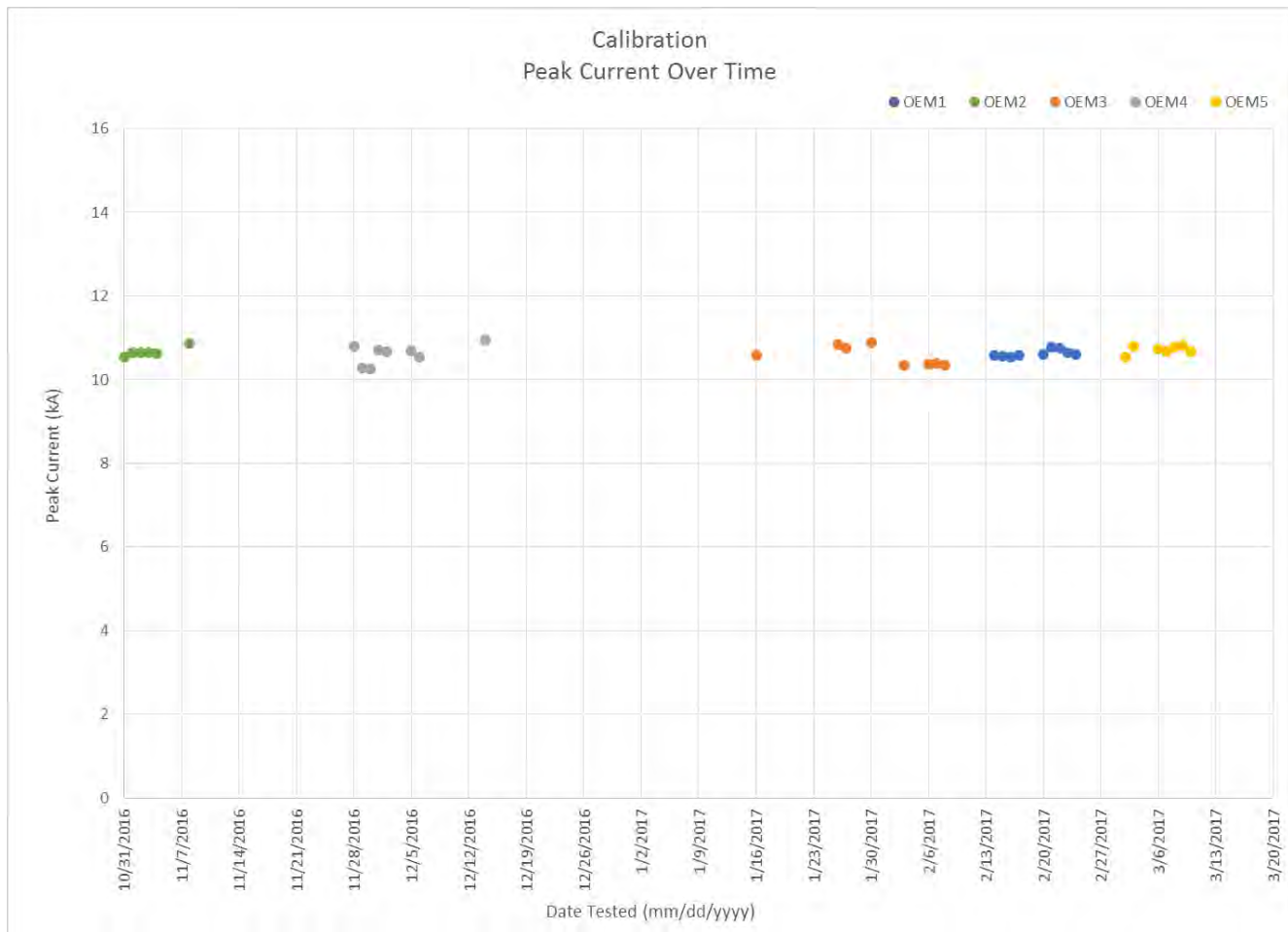


Figure 33: Calibration Peak Current Over Time

### 5.3.2 Faulted Test Articles

The testing of faulted fasteners at the DEL generator was conducted over a much shorter period of time than that of the nominal testing. The test levels varied throughout the DEL testing as well, so there is not a constant test level to measure over the course of the testing. Based on a lack of constant test level data, the calibration plots for nominal testing in Figure 32 and Figure 33 will not be reproduced for the faulted installation testing.

## 6.0 DATA and OBSERVATIONS

The graphical representations of the DC resistance and peak current data for all OEMs combined for the nominal single and quadruple fasteners are shown in Figure 34 - Figure 42 and in Figure 43 - Figure 47 are the faulted fasteners.

The DC resistance measurements across the joints of the test article before the test are shown in the figures by the gray line. The DC resistance measurements across the joints of the test article after the test are shown by the blue line. An external spark (seen by the camera) is shown as a red star on the nominal test articles. An internal spark (voltage waveform disturbance) on the nominal fasteners is shown as a gold star. Internal sparks were not recorded for the faulted fasteners.

It is important to note that the nominal and faults tests were conducted with different approaches. While the test set-ups were the same, the nominal articles were tested to find the point of failure by starting at 10 kA and if sparking occurs, lowering the current to find the level where it no longer sparked. Testing was capped at  $10\text{ kA} \pm 10\%$  whether or not sparking occurred, and regardless of a threshold being obtained. The faulted articles were tested to determine the maximum current they could sustain without sparking, starting at 10 kA for the conductive fastener tests and increasing the current until the coupon sparked. The nonconductive faulted fastener tests began at a level below 10 kA, typically 5 kA, and the current was either increased or decreased depending on if a spark occurred. Note that testing was capped at  $100\text{ kA} \pm 10\%$  regardless of a threshold being obtained. In short, the nominal installations were tested to find the minimum *sparking* threshold and the fault installations were tested to find the maximum *nonsparking* threshold.

### 6.1 Nominal Test Articles

The highest pre-test DC resistance values are for MN-1I11 (Hi-Lite/Hi-Kote) and MN-1I12 (Hi-Lok/Hi-Kote) with the nonconductive coating and for MN-1T05 and MN-1T07 which are the small Hi-Lite transition fit fasteners. The majority of the sparking occurred with MN-1I11 and MN-1I12 (Hi-Lok/Hi-Kote) with the nonconductive coating. As evidence of conditioning the test article, the post test DC resistance (blue line) shown in Figure 39 and Figure 41 is much lower than the pre-test DC resistance for all test articles except the MN-1T12 test articles. All test articles except for the MN-1I11 (Hi-Lite/Hi-Kote) and MN-1I12 (Hi-Lok/Hi-Kote) with the nonconductive coating were tested at the maximum peak current around 11 kA.

The quadruples followed the same trends as the singles as far as the majority of sparks being from the nonconductive coated fastener test articles. Pre-test DC resistance increased from the interference to the transition fit, especially for the small transition fit test articles MN-1T05 and MN-1T07, Figure 39.

Sparking with rivet test articles at low currents is very unexpected. No single fastener installation rivet had an external spark during testing and only 1 (MN-4009) quadruple rivet installation sparked. The nature of the rivet installation process provides good surface contact and bonding, thus they are expected to conduct current effectively.



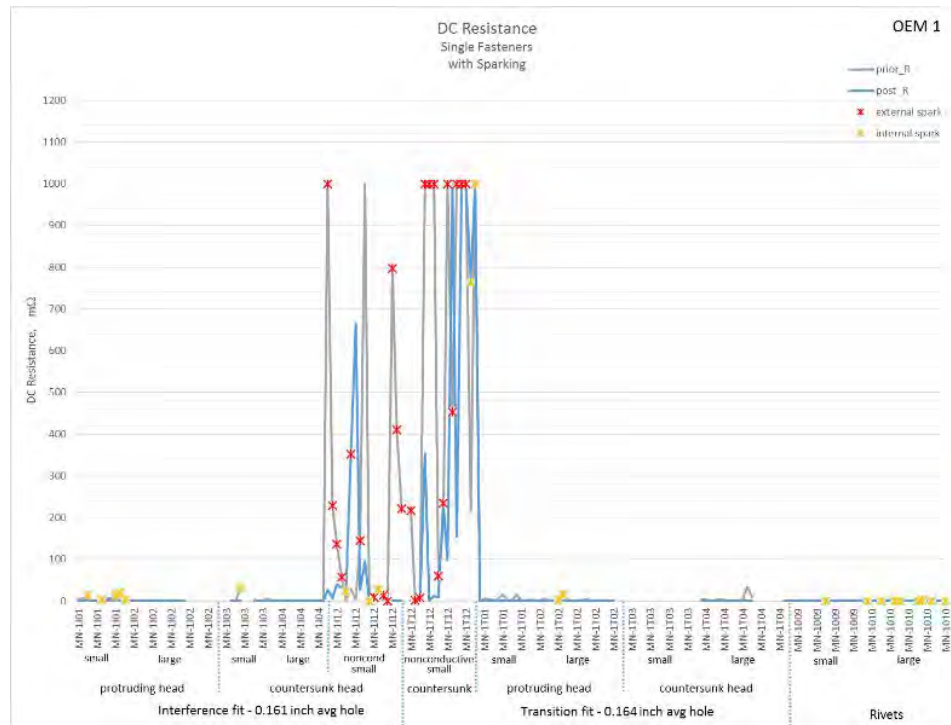


Figure 34: DC Resistance of OEM 1 with sparking – Nominal Single Fasteners

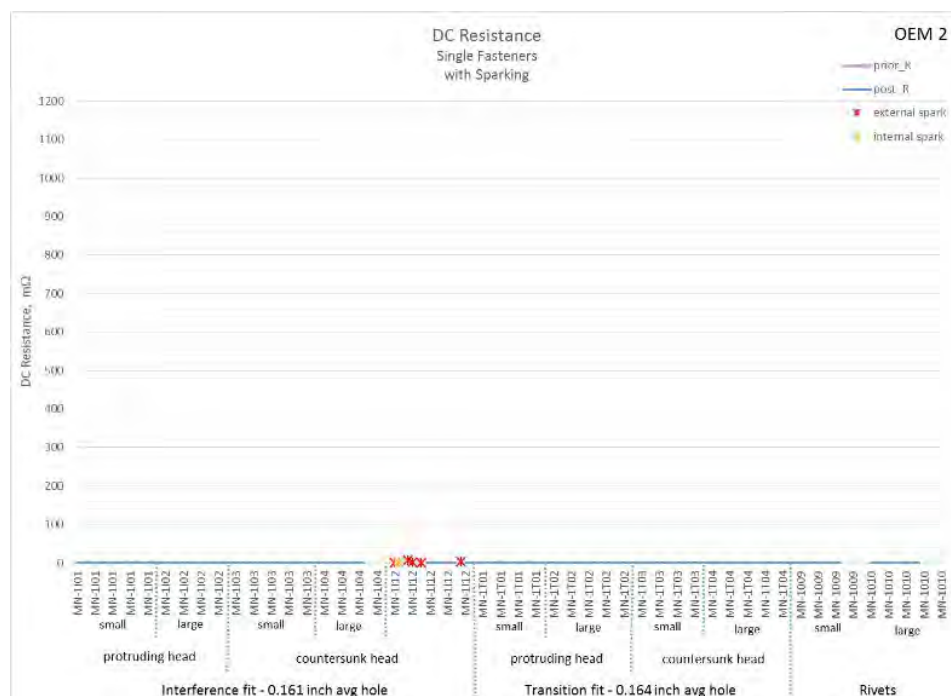


Figure 35: DC Resistance of OEM 2 with sparking – Nominal Single Fasteners

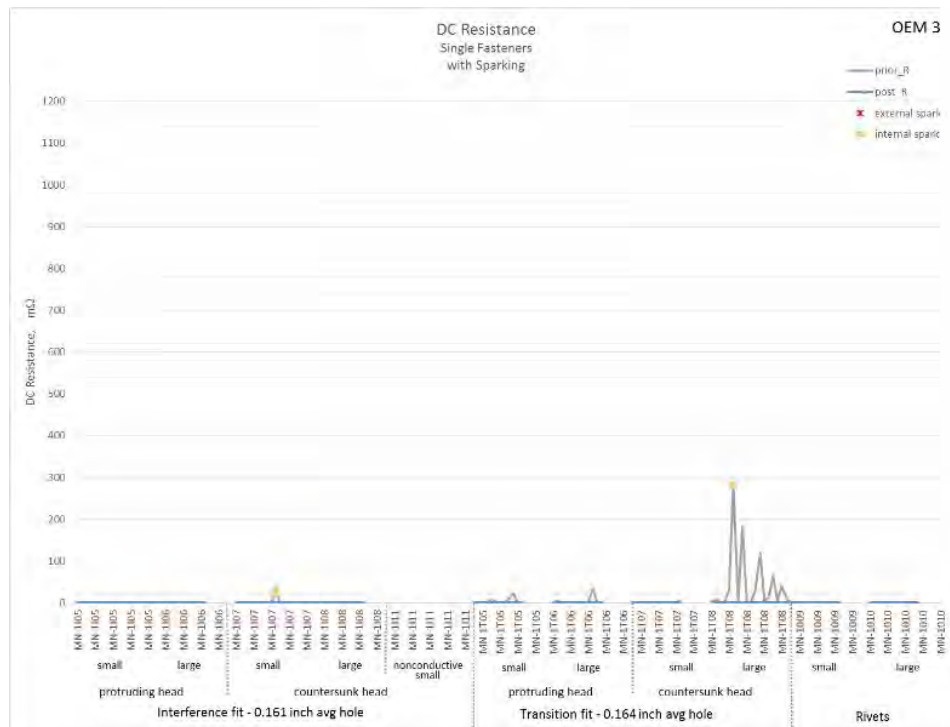


Figure 36: DC Resistance of OEM 3 with sparking – Nominal Single Fasteners

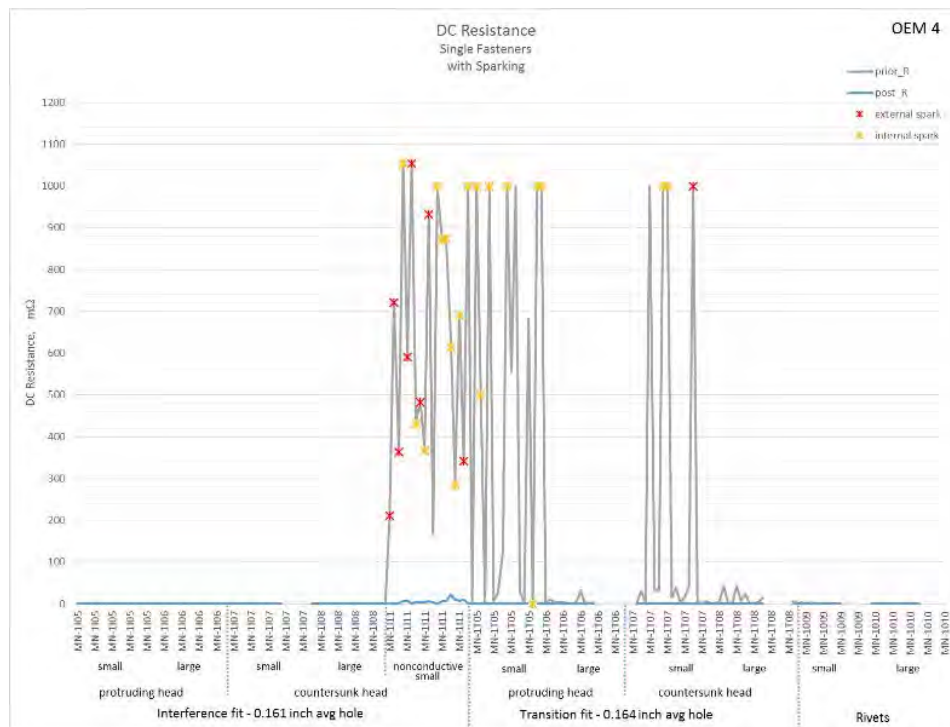


Figure 37: DC Resistance of OEM 4 with sparking – Nominal Single Fasteners

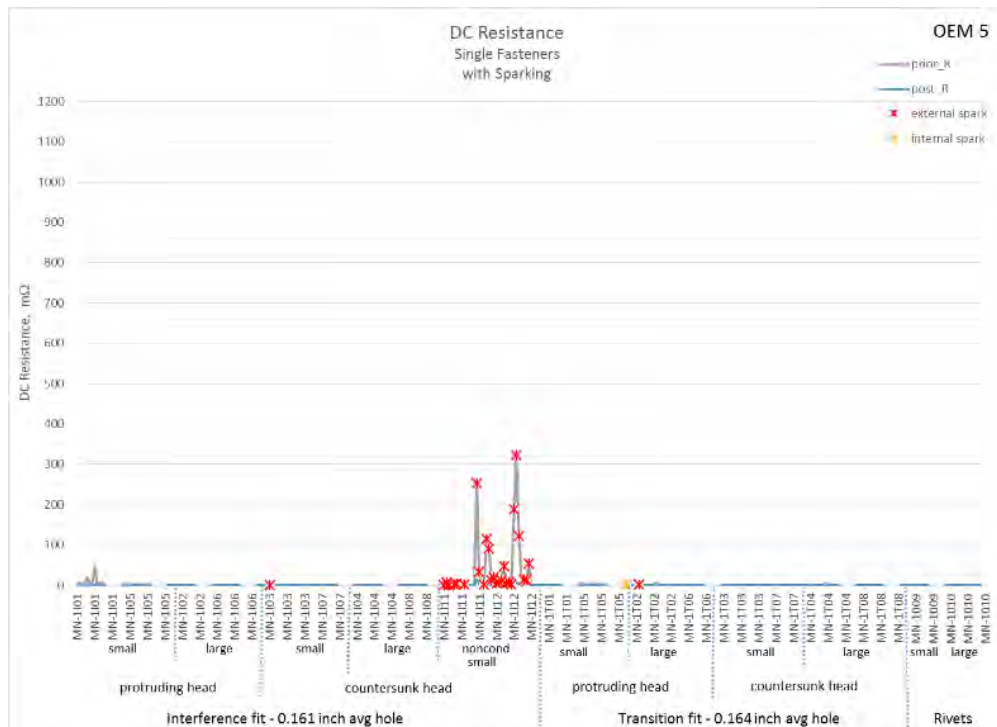
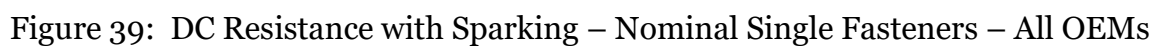
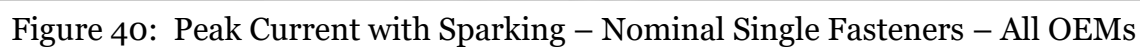
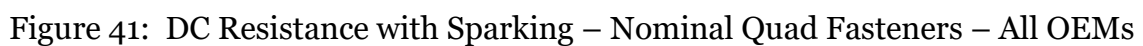


Figure 38: DC Resistance of OEM 5 with sparking – Nominal Single Fasteners











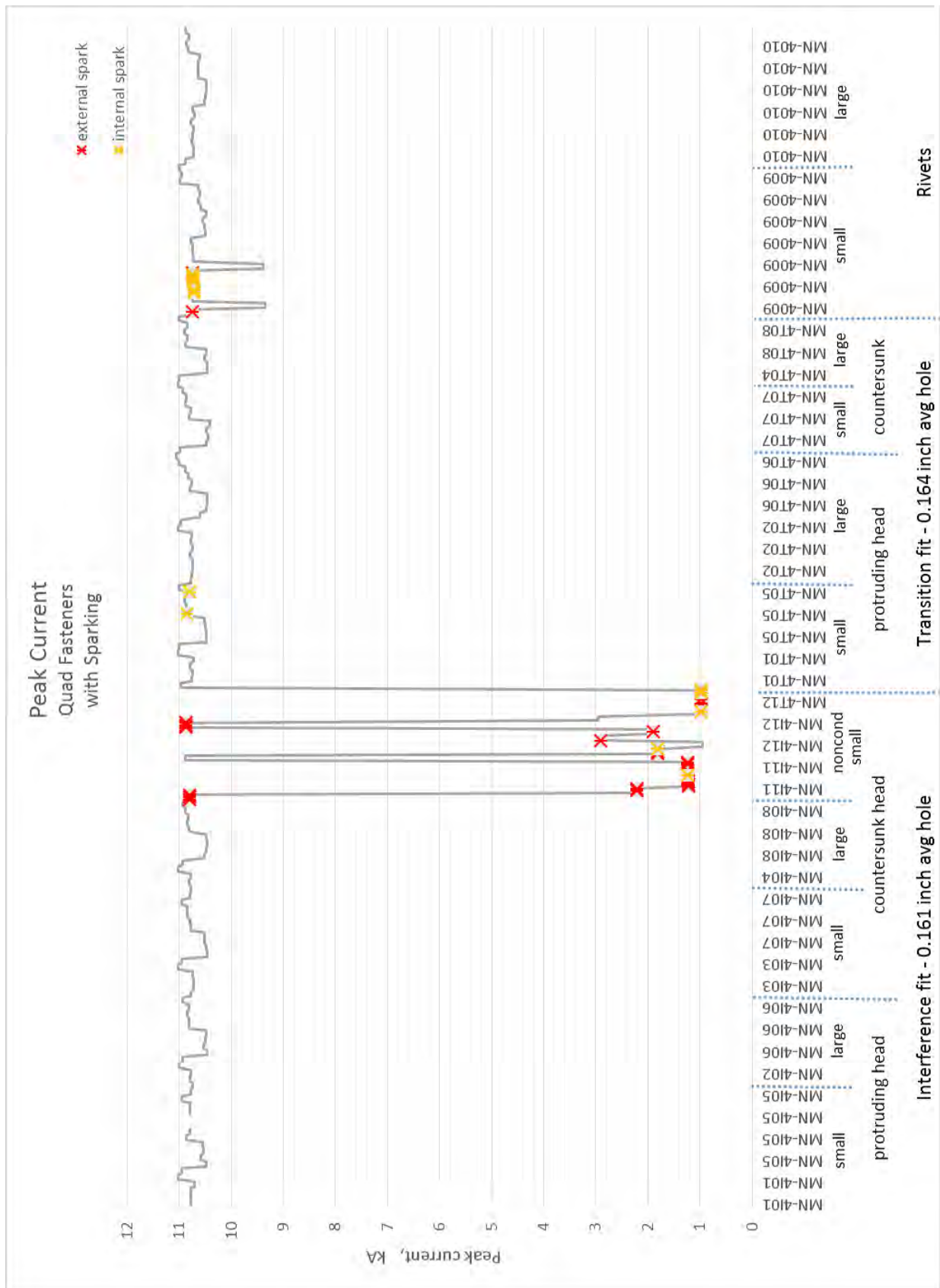


Figure 42: Peak Current with Sparking – Nominal Quad Fasteners – All OEMs

## 6.2 Faulted Test Articles

The highest pre-test DC resistance values are for MF4-4T12 (Hi-Lok/Hi-Kote with oversized hole fault) and MF6-4T01 (Hi-Lok with under-torqued fault). The majority of the sparking occurred with MF-4T11 (Hi-Lite/Hi-Kote) and MF-4T12 (Hi-Lok/Hi-Kote) with the nonconductive coating. As evidence of conditioning the test article, in Figure 47-46, the post test DC resistance (blue line) is much lower than the pre-test DC resistance for all faulted test articles except the MF-4T01 and the MF-4T03 articles from OEM 2. All of the faulted test articles except for the MF-4T11 (Hi-Lite/Hi-Kote) and MF-4T12 (Hi-Lok/Hi-Kote) with the nonconductive coating were tested at 10 kA once to show they would not spark before being tested at higher currents (up to 100 kA) on the DEL generator. The MF-4T11 and MF-4T12 fasteners were only tested up to 10 kA.

Sparking with rivet test articles at low currents is very unexpected and never occurred below 11 kA. MF3-4009, MF4-4009, and MF5-4009 from OEM 1 sparked at 18, 13, and 18 kA respectively but no other rivet sparked throughout the rest of the testing. The nature of the rivet installation processes means that they have more surface contact and better bonding thus they conduct current more effectively.

Shown below are the individual graphs for DC resistance with sparking by OEM for both nominal and faulted fasteners for comparison purposes with the overall combined graphs, as well as graphs for the peak currents for the nominal tests. For the nominal fasteners, only the single fastener data is shown by OEM.

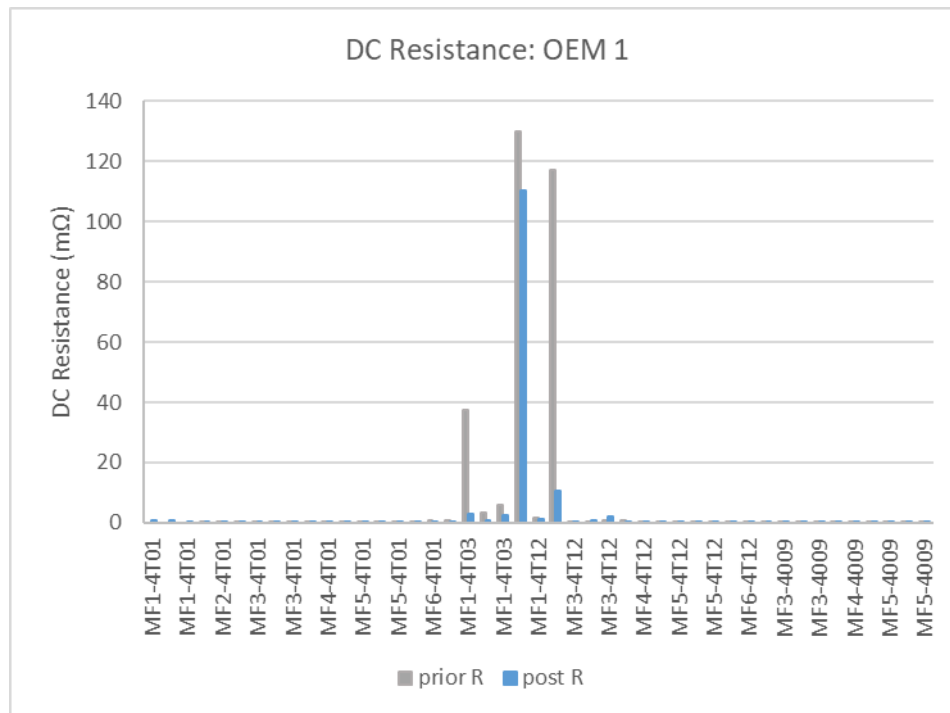


Figure 43: DC Resistance of OEM 1 - Faulted Fasteners

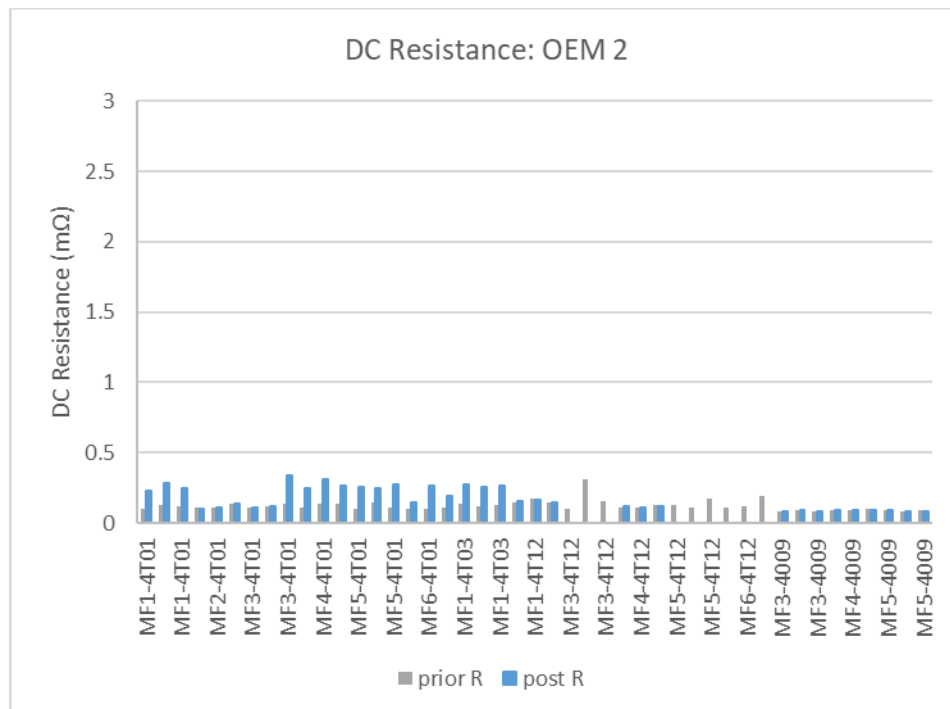


Figure 44: DC Resistance of OEM 2 - Faulted Fasteners

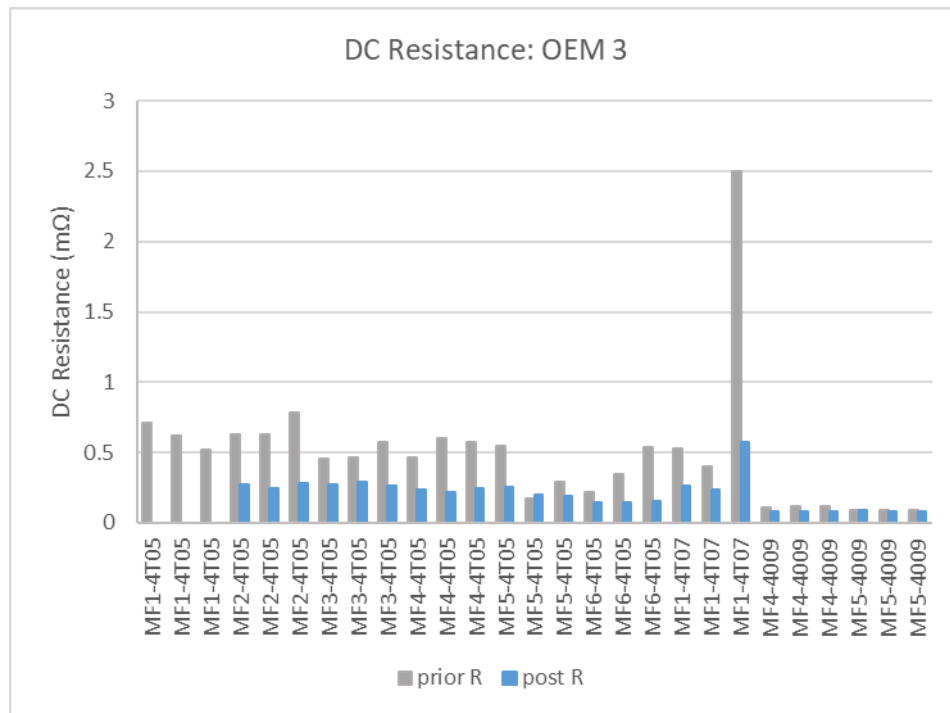


Figure 45: DC Resistance of OEM 3 - Faulted Fasteners

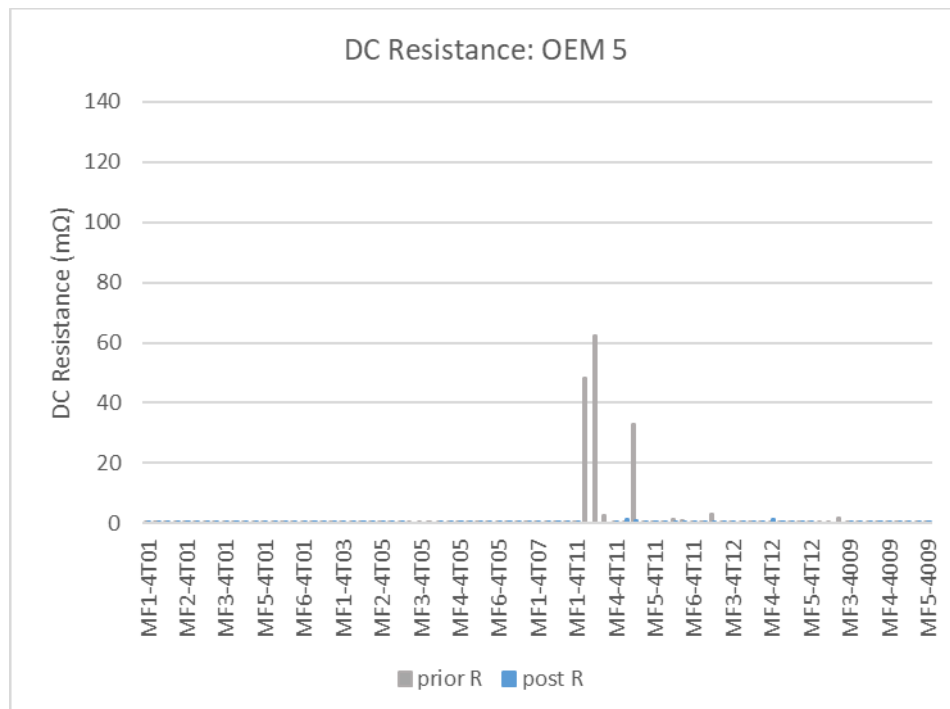


Figure 46: DC Resistance of OEM 5 - Faulted Fasteners



## 7.0 TEST RESULTS

The main result to be expected from this research is the maximum peak current amplitude that can be conducted through the simulated fuel tank test articles to determine the sparking and nonsparking threshold for each fastener configuration. Current levels through the nominal single fastener test articles are shown in Figure 48. **Error! Reference source not found.** Current levels through the nominal quadruple fastener test articles are shown in Figure 49. Current levels through the faulted quadruple fastener test articles are shown in Figure 50.

Another intention of this testing was to test various factors for their influence on sparking:

- 1) Type of fastener – HI-LOK™, HI-LITE™, or rivet
- 2) Fastener head type – protruding or countersunk
- 3) Diameter of fastener – small or large
- 4) Fit type – interference or transition
- 5) Fastener coating – conductive or nonconductive
- 6) Number of fasteners – single or quadruple
- 7) Type of fault – straight gap, gap under head, gap under collar, scratch, burr, or under-torqued
- 8) Manufacturer – OEM 1, OEM 2, OEM3, OEM4, OEM 5

For more information, details on the analysis of each of the factors are listed in the sections below.

### 7.1 Nominal Test Articles

For nominal test articles, there were eight factors tested for sparking influence. In the analysis of the nominal test articles, seven of the factors were included in the model below. The manufacturer factor was not considered.

Factor effects are considered statistically significant if their (Probability > F) is less than or equal to 0.05. The Type III Sum of Squares table must be used for the results because this data is very unbalanced.

Figure 48 and Figure 49 are detailed representations of the current threshold data, showing all the current values by OEM. The sparking percentage for each type of fastener is noted along the X-axis.

Almost all the sparking occurred with the test articles that used the nonconductive coating on the fasteners, HST11AG5-3 and HL11VAZ5-3. The current level was reduced to about 1 kA and the fasteners with the nonconductive coating still produced external sparks. The 25.981 generator was not able to go low enough to discover the sparking threshold for the HL11VAZ5-3 fasteners for the single fasteners or the HST11AG5-3 fasteners for the quadruple fasteners.

The 25.981 generator was not able to go high enough to discover the sparking threshold for most of the fasteners with the conductive coating, however:

- the large protruding head Hi-Loks for singles (HL10VBJ8-3) had 1 external spark,
- the small countersunk head Hi-Loks for singles (HL11VBJ5-3) had 1 external spark,



- the small countersunk head Hi-Lites for singles (HST11BJ5-3) had 1 external spark,
- the small rivets for the quadruples (MS20470AD4) had 2 external sparks.

. When there was internal sparking or no sparking, the current threshold is higher than what is shown in Figure 48 and Figure 49.

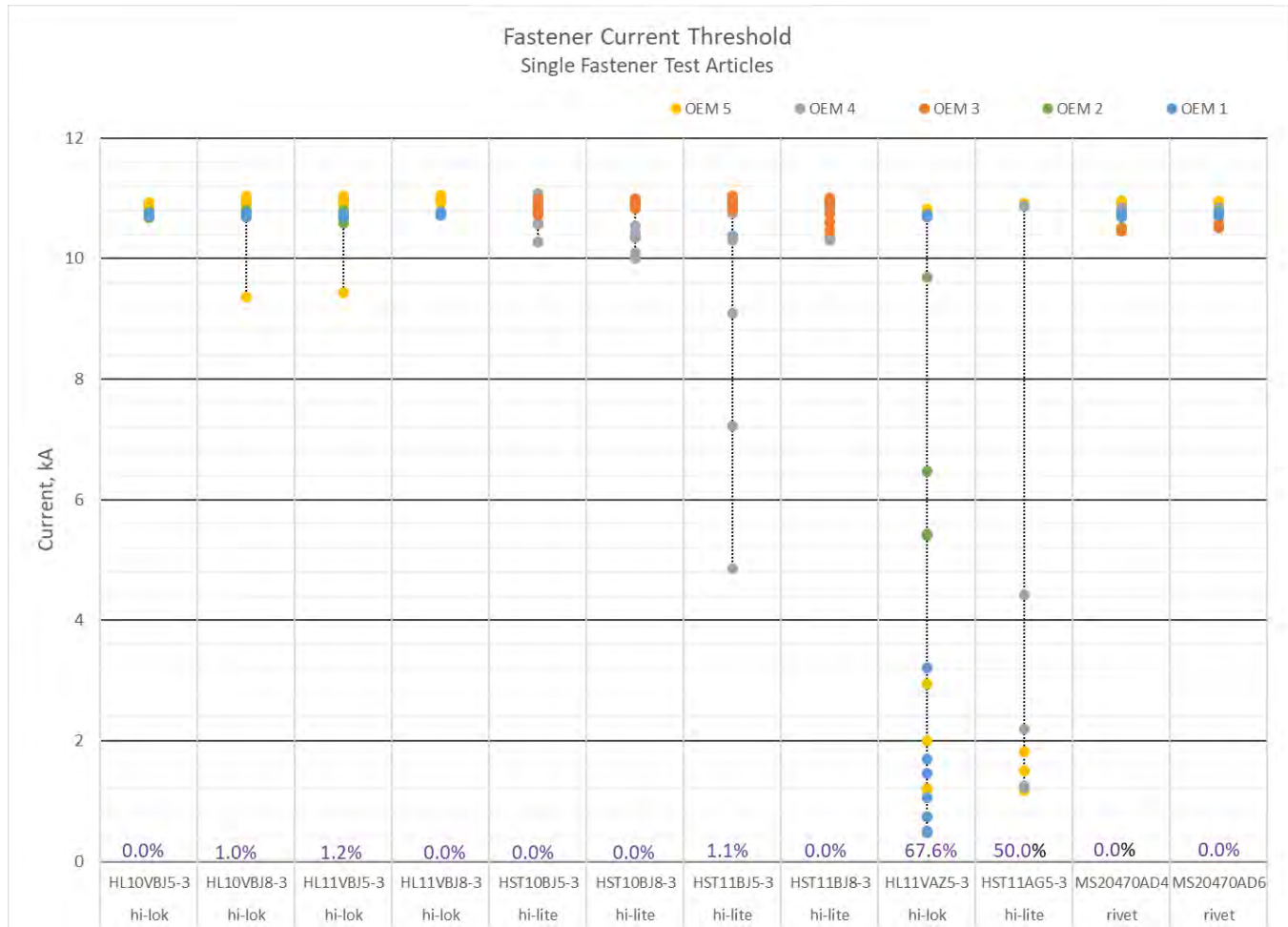


Figure 48: Nominal Single Fastener Sparking Thresholds by OEM

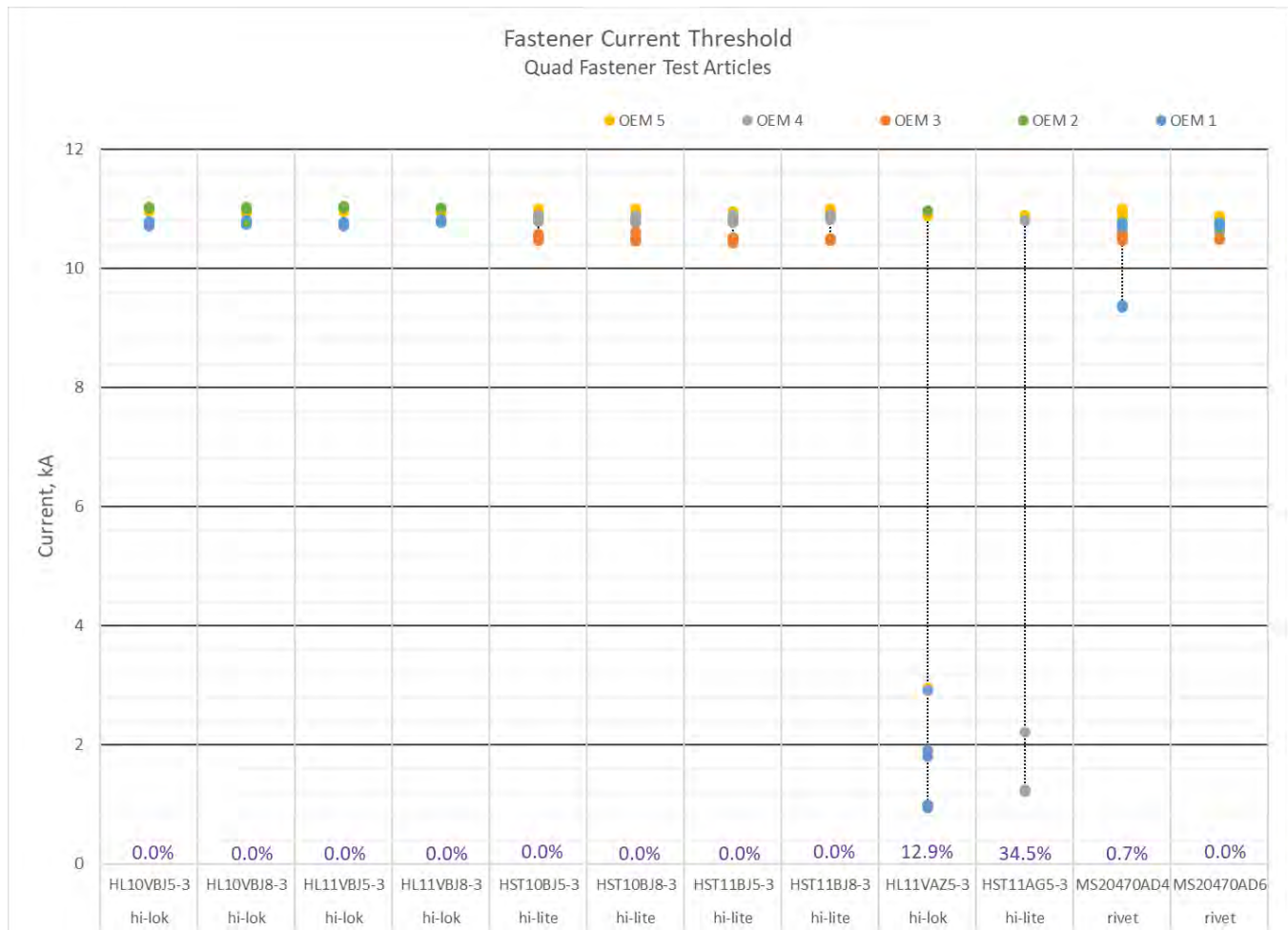


Figure 49: Nominal Quadruple Fastener Sparking Thresholds by OEM

## 7.2 Faulted Test Articles

There are 5 factors that were tested for sparking influence. By plotting the effect each of these factors had on the threshold and comparing the averages and standard deviations, we were able to determine that only 1 factor had statistically significant effects.

Shown below in Figure 50 are the nonsparking thresholds of each fastener-and-fault configuration. The conductive faulted fasteners (all of which had a small diameter) were tested to sparking however the following fault-and-fastener combinations were tested to 100kA and never sparked:

- the protruding head Hi-Loks had 5 instance of reaching 100 kA without sparking,
- the countersunk head Hi-Lok had 1 instance of reaching 100 kA without sparking,
- the protruding head Hi-Lite had 4 instances of reaching 100 kA without sparking,
- the rivets had 8 instance of reaching 100 kA without sparking.

The only nonconductive fastener that did not spark was MF1-4T11. As every other nonconductive fastener sparked, this was taken to be anomalous data and the coupon was not tested higher than 11 kA.

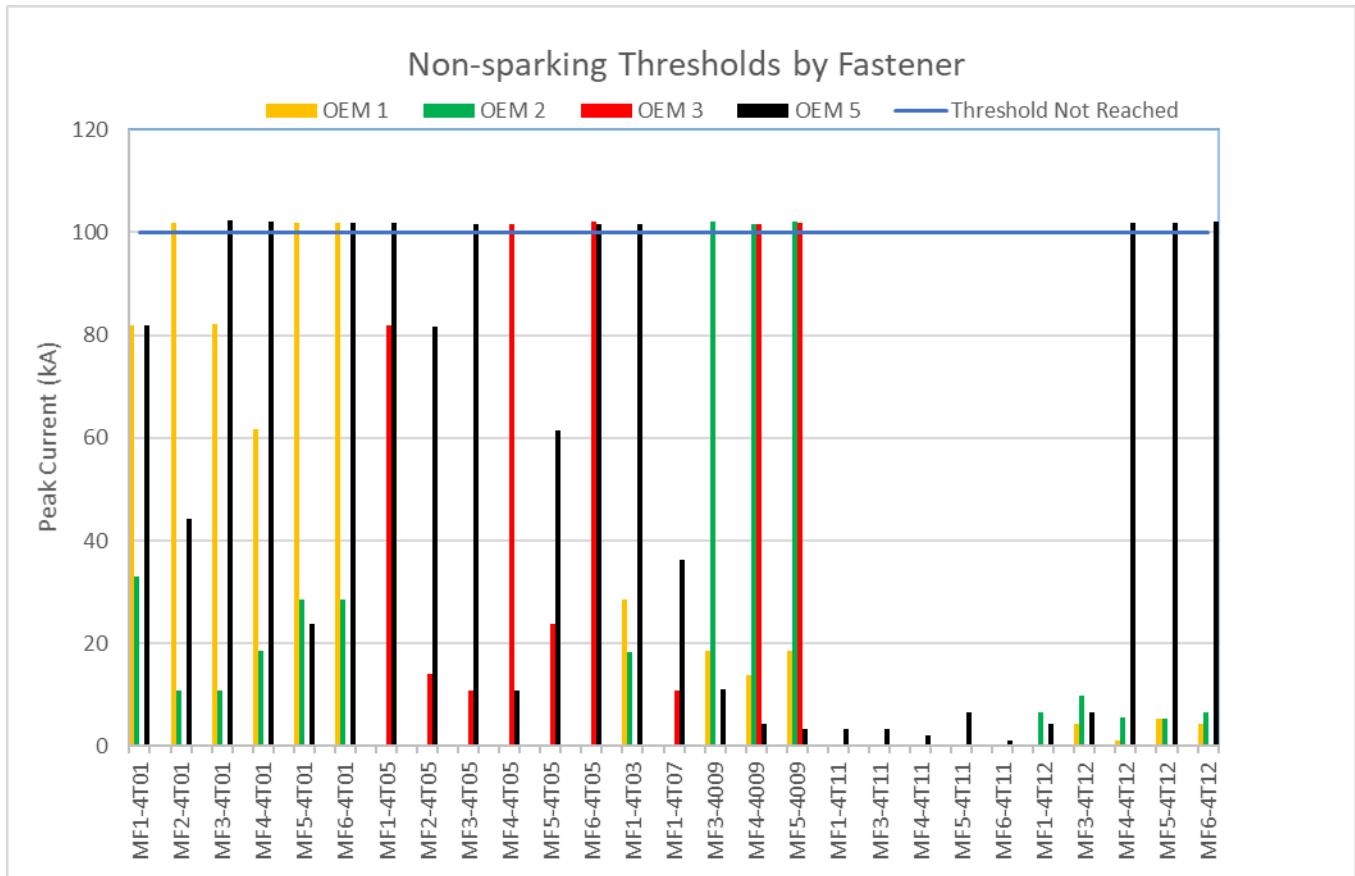


Figure 50: Nonsparking Thresholds by Fastener

### 7.3 Factor 1 - Type of Fastener

Five types of fasteners were used in this testing:

1. HI-LOK™ with a conductive coating,
2. HI-LITE™ with a conductive coating,
3. HI-LOK™ with a nonconductive coating,
4. HI-LITE™ with a nonconductive coating,
5. Rivets with a conductive coating

#### 7.3.1 Nominal Test Articles

Sparking percentages for each of the five fastener types are shown in Figure 53. It can be seen that for the nominal coupons there isn't much sparking except for the fasteners with the nonconductive coating. Therefore, the only analysis between nominal fastener types will just

be using the data from the nonconductive coating for a comparison of HI-LOK™ and HI-LITE™ fasteners.

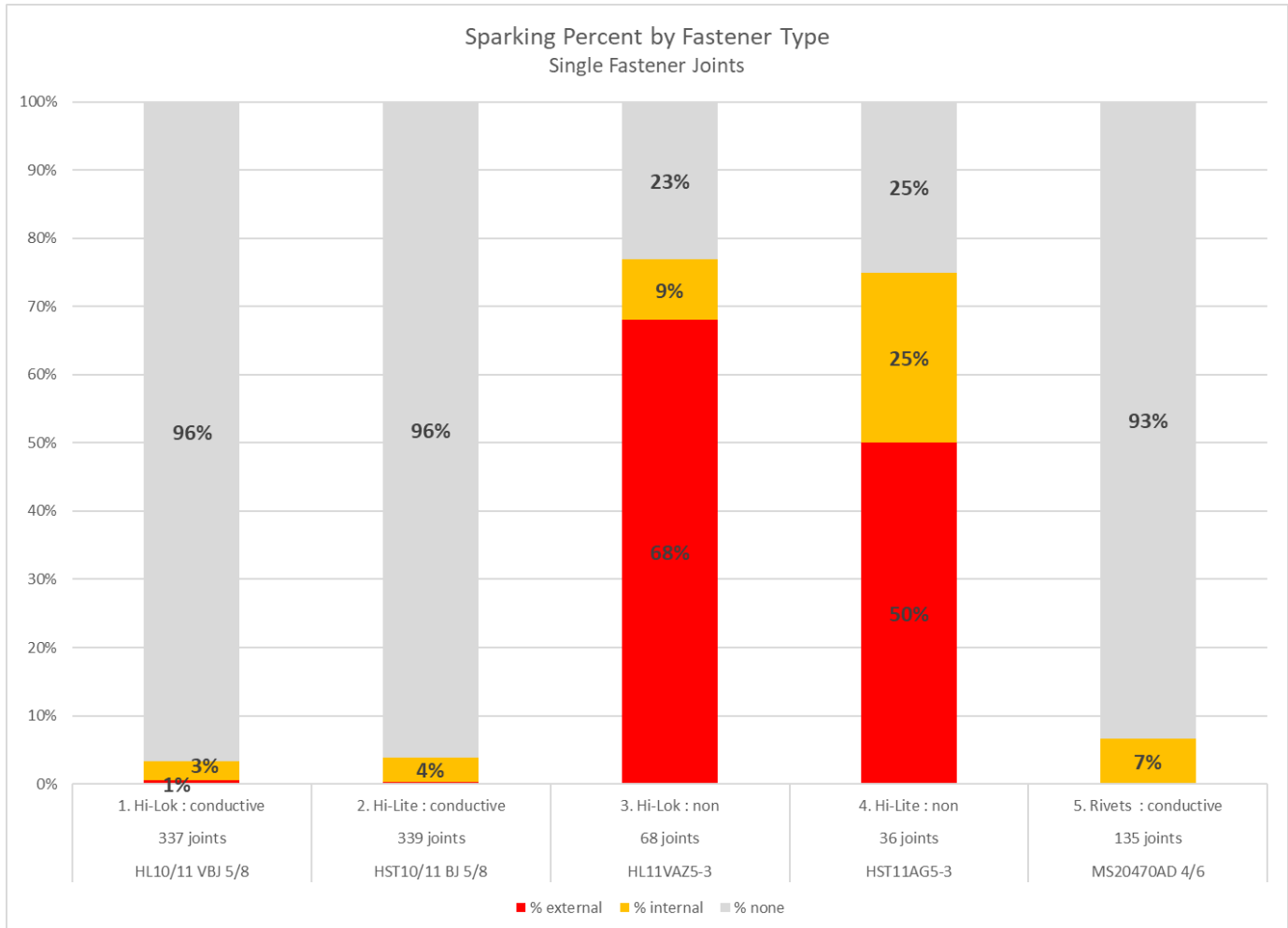


Figure 51: Sparking Percent for Fastener Types of Nominal Test Articles

In the nominal articles, the external sparking percentage for the HI-LOK™ with the nonconductive coating is 68% while the external sparking percentage for the HI-LITE™ with the nonconductive coating is 50%. Both fasteners have the same nonconductive coating - HI-KOTE™ 1. In order to tell whether this percentage difference is large enough to be significant or is just representative of variance in the data, some statistical tests were used.

A contingency table using the levels of 0, 5, and 10 for the sparking and the levels of HI-LOK™ and HI-LITE™ for the fastener type was used to compare the percent difference in sparking between the HI-LOK™ and the HI-LITE™. A general linear model using fit and fastener type for the nonconductive coating fasteners was also used to compare the fastener types. The fastener type was found to be not statistically significant so the difference in the sparking percentages was just normal variance in the data.

### 7.3.2 Faulted Test Articles

Sparking percentages for each of the five faulted fastener types are shown in Figure 52 and Figure 53. At the lower test level, the majority of the sparks came from the nonconductive fasteners, therefore only the conductive fasteners were tested at the higher test level of 100kA. At this test level, rivets sparked the least. This is likely due to the nature of rivet installation leading to a more effective transfer of current. Due to the high surface contact and good electrical bonding of rivet installations, the sparking threshold was not met for over 75% of the tested articles. Similar percentages of HI-LOK™ and HI-LITE™ fasteners sparked at 100kA. This further supports the conclusion drawn by statistical analysis for the nominal data, that HI-LOK™ and HI-LITE™ are not statistically different.

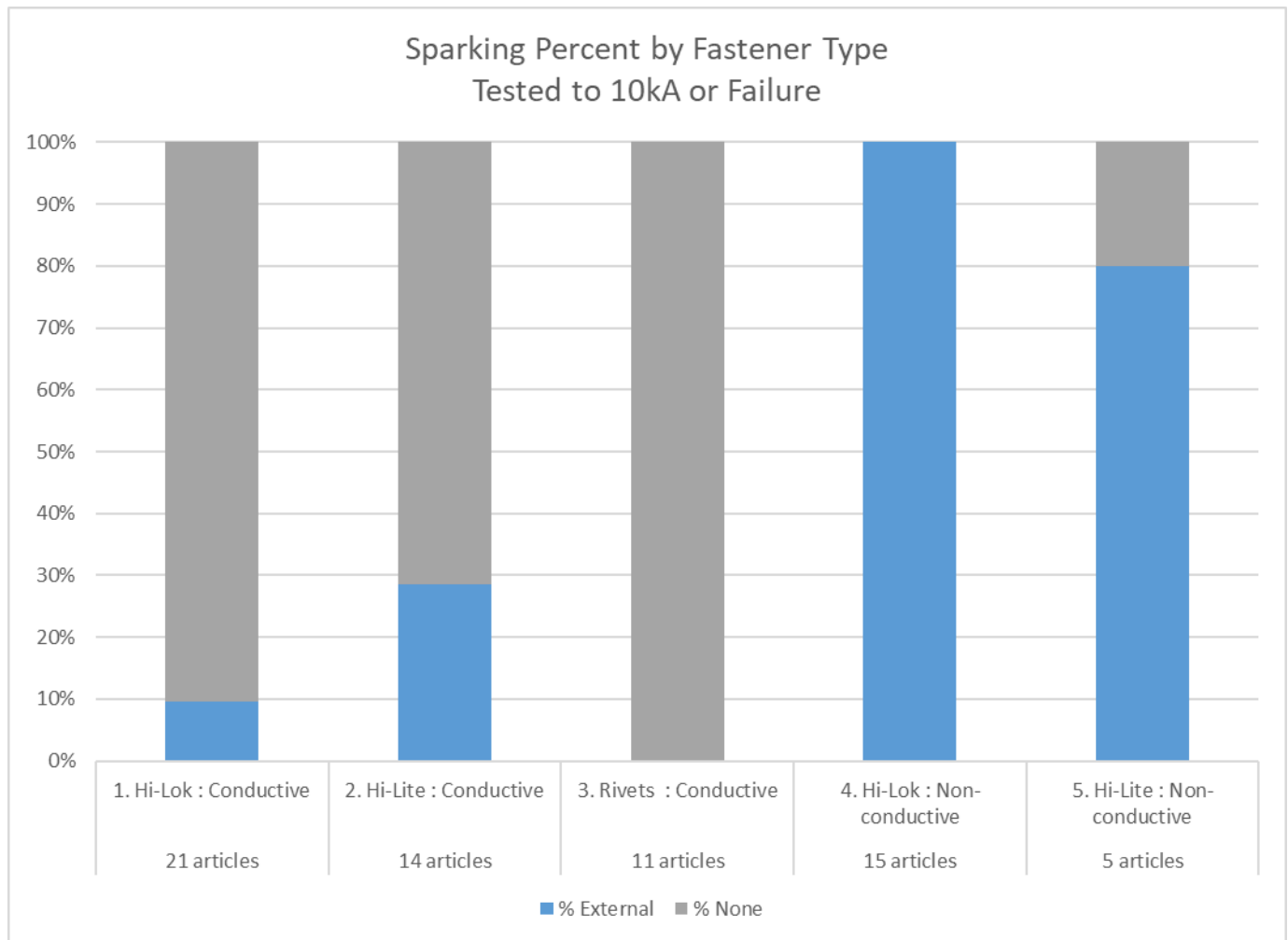


Figure 52: Sparking Percent for Fastener Types of Faulted Test Articles on 25.981 Generator

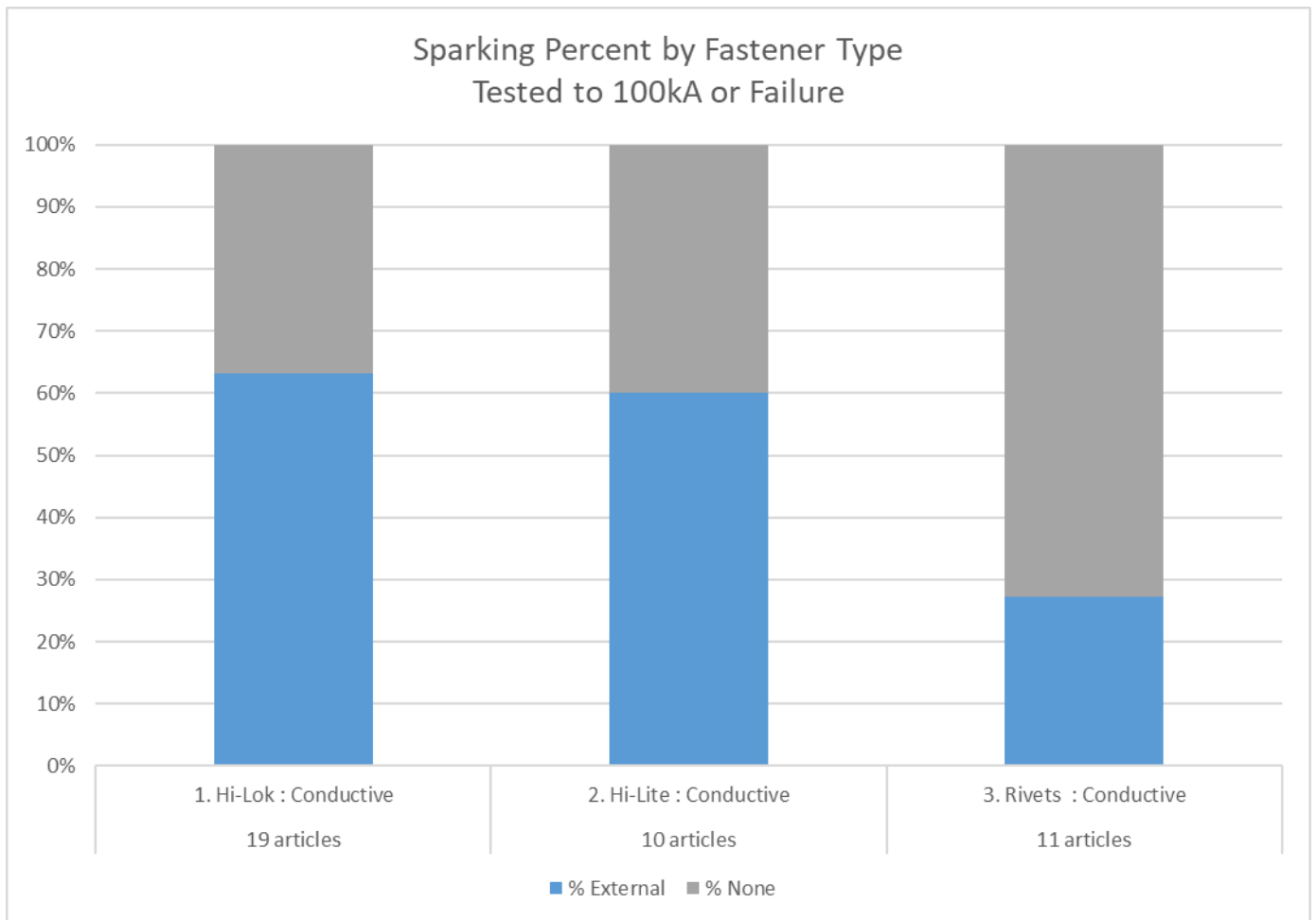


Figure 53: Sparking Percent for Fastener Types of Faulted Test Articles on DEL Generator

## 7.4 Factor 2 - Fastener Head Type

There were two different head types tested:

1. Protruding
2. Countersunk

### 7.4.1 Nominal Test Articles

The head types made no difference in the nominal test results at test levels up to 10 kA.

### 7.4.2 Faulted Test Articles



There is not enough data to show any conclusive trend from the faulted fastener test results with regard to head type.

## **7.5 Factor 3 - Diameter of Fastener**

Two different diameters tested:

1. Small
2. Large

### **7.5.1 Nominal Test Articles**

The fastener diameter made no difference in the test results at test levels up to 10 kA.

### **7.5.2 Faulted Test Articles**

All faulted fasteners were small in diameter.

## **7.6 Factor 4 - Fit Type**

There were two different fastener fit types tested:

1. Interference
2. Transition

### **7.6.1 Nominal Test Articles**

The nominal fasteners had both interference and transition fit installations. The graph shown below is the same as Figure 39 except that the data for the test articles with the nonconductive fasteners (MN-1I11 and MN-1I12), and the data for the test articles with rivets have been removed, and the divider between the interference fit and transition fit test articles has been extended.

In the graph below, it appears that fit type makes a large difference going from interference fit to transition fit because of the large change in the DC resistance. The large change in DC resistance is due to only one out of the five OEMs. None of the other OEMs show this large change so the effect is minimized when all the data is considered and the fit type is not statistically significant.

While the fit type might not have a statistical impact on the DC resistance or on external sparking, there was a difference in terms of internal sparking. It is important to note that an internal spark is not an ignition source, but it is a useful indicator of a disturbance on the differential voltage measurements and of potential manufacturing variance.

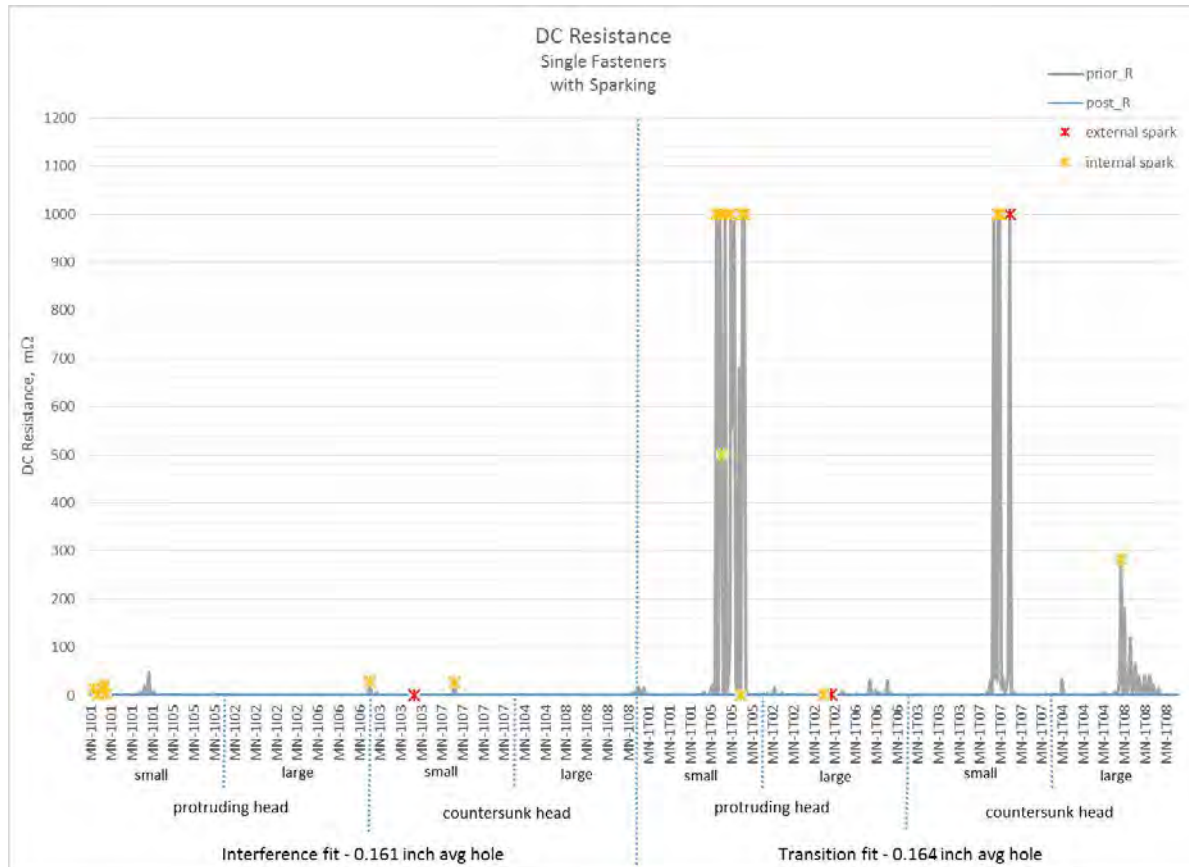


Figure 54: Effect of Fit Type Differences on DC Resistance - Nominal Single Fasteners

## 7.6.2 Faulted Test Articles

The faulted fasteners were all transition fit installations.

## 7.7 Factor 5 - Fastener Coating

There were two different types of fastener coatings tested:

1. Conductive
2. Nonconductive

Only the small, countersunk head, HI-LOK™ and HI-LITE™ fasteners were tested with the nonconductive coating. All other fastener combinations used the conductive coating. The effects of coating were the same in both nominal and faulted article testing as shown in Figure 55 and Figure 56 below. The conductive IVD coating sparked less and had a higher nonsparking threshold as compared to the nonconductive Hi-Kote coating.

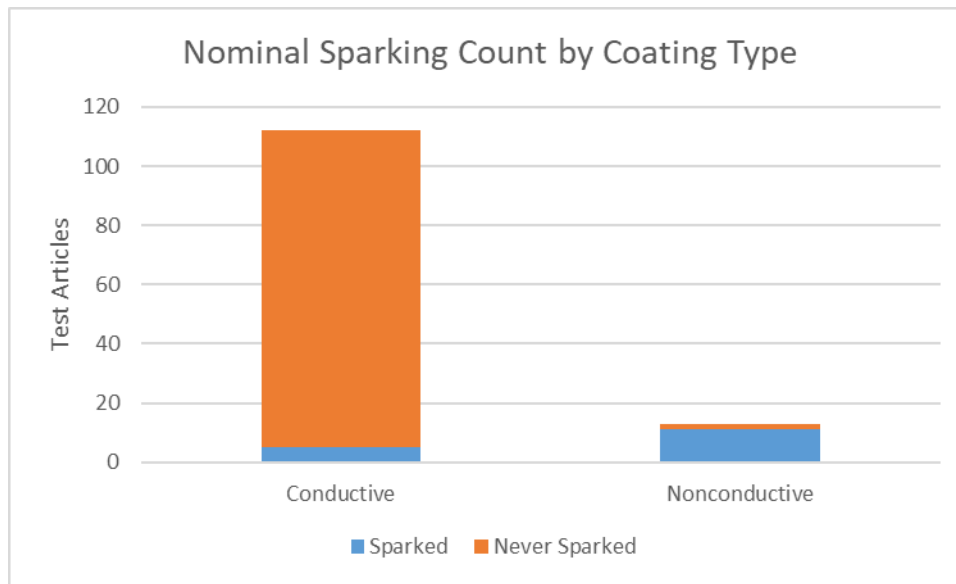


Figure 55: Nominal Sparking Count by Coating Type

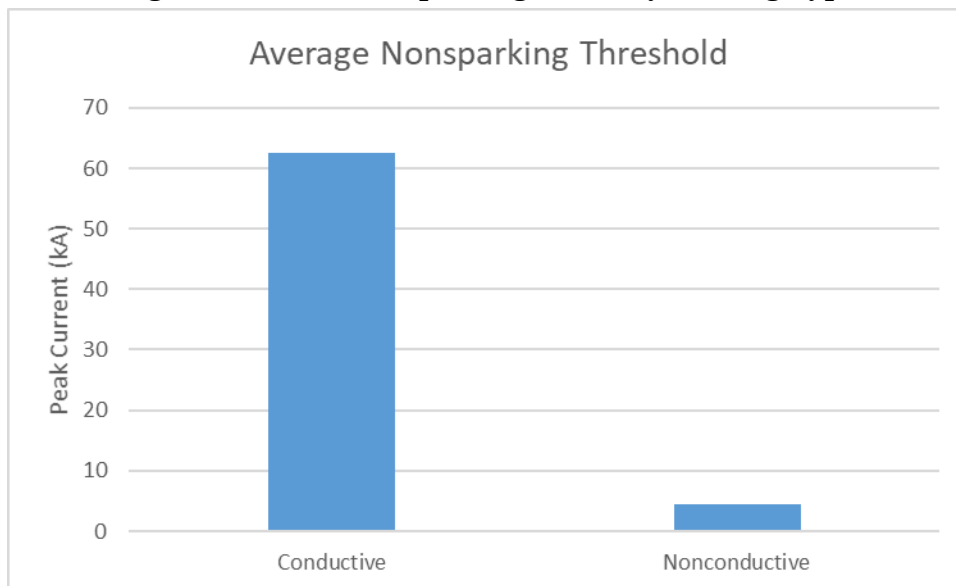


Figure 56: Faulted Average Nonsparking Threshold

#### 7.7.1 Nominal Test Articles

The nonconductive coating used on both the HI-LOK™ and HI-LITE™ fasteners is known as HI-KOTE™ 1. HI-KOTE™ 1 is a phenolic-based aluminium coating with high corrosion and temperature resistance applied by spraying and is then oven cured to fully develop its properties.

HI-KOTE™ 1 was examined more closely under a microscope. The coating was grainy and appeared to be patchy but provided an effective seal as evidenced by the data. Figure 57 shows a HI-KOTE™ 1 coated fastener. A scratch was made in the coating to better judge its depth and adhesion.



Figure 57: HI KOTE 1 coated fastener

A measurement was made from the bottom of the scratch to the top of the coating for an estimate of its thickness. This example shows that the HI KOTE 1 coating is only about 0.373 mil or about 9.5  $\mu\text{m}$  thick. Even with less than half a mil of this coating, it was still very effective in providing a nonconductive barrier and produced lower sparking thresholds. Using the nonconductive coating proved to be an extremely important factor. Almost all of the nominal sparking occurred with fasteners with the nonconductive coating and almost all of the faulted sparking at the 10 kA test level were of the nonconductive coated fasteners. This can be seen in the nominal test results by looking at Figure 51 where the HST11AG5-3 and HL11VAZ5-3 are the fasteners with the Hi-Kote coating. Looking at Figure 50, the fasteners with the Hi-Kote coating (4T11 and 4T12) had the lowest threshold values.

The conductive coating used the testing of both the nominal and faulted installations was an ion vapour deposition of aluminium (IVD-aluminum). This coating provides a conductive, corrosion prevention layer to the fasteners it is applied to.

#### 7.7.2 Faulted Test Articles

The coating had the same effect on the faulted installations as the nominal installations.

### 7.8 Factor 6 - Number of Fasteners

#### 7.8.1 Nominal Test Articles

In the nominal testing there were two different numbers of fasteners at each joint tested:

1. Single fasteners
2. Quadruple fasteners

As expected, using four fasteners per joint instead of only one fastener per joint made a big difference (see Figure 39 and Figure 42). The gray line representing the pre-test resistance measurements is much lower for the quadruple fastener test articles. The sparking percentage is lower too.

Table 7: External Sparking Percentage for Singles vs Quads (by fastener)

	All Fasteners	Hi-Lok & Hi-Lite, Nonconductive coating
Quadruple Fasteners	2% (48/2136)	21% (46/216)
Single Fasteners	7% (67/924)	62% (64/104)

Almost all the sparking for both single fastener test articles and quadruple fastener test articles was with the test articles that used the fasteners with the nonconductive coating.

### 7.8.2 Faulted Test Articles

The faulted fasteners only used the quadruple fastener installation.

## 7.9 Factor 7 - Fastener Fault Type

Fasteners may not stay in nominal condition throughout their service life. Collaboration with the SAE AE-2 committee determined how faults in the installation process and faults that may occur naturally through service and manufacturing, impact the nonsparking thresholds. See Appendix E - Faulted Fastener Designs for more details.

### 7.9.1 Nominal Test Articles

The nominal test articles had no intentional fault conditions.

### 7.9.2 Faulted Test Articles

There were 6 different types of faults:

1. Straight gap
2. Gap under head
3. Gap under collar
4. Scratch
5. Burr

## 6. Under-torqued.

See [Appendix D](#) for drawings.

To see if any particular fault had a greater effect on the nonsparking threshold, the threshold values for each fault were plotted separated by coating type (see Figure 58 and Figure 59). OEM 3 only provided conductive fasteners. The number of test articles in the analysis for each fault type is denoted by the number of TA's. It is important to note that fasteners which appear to have a nonsparking threshold value of 100 kA never sparked because the testing was capped at 100 kA. The mean nonsparking threshold across all of the conductive faulted fasteners averages to  $62.62 \text{ kA} \pm 38.9 \text{ kA}$ . The mean nonsparking threshold across all of the nonconductive faulted fasteners averages to  $4.73 \text{ kA} \pm 2.72 \text{ kA}$ . The conductive gap under head and gap under collar faults had the lowest average nonsparking thresholds at  $54 \text{ kA} \pm 45 \text{ kA}$ . The conductive under-torqued faults had the highest average threshold at  $87 \text{ kA} \pm 33 \text{ kA}$ .

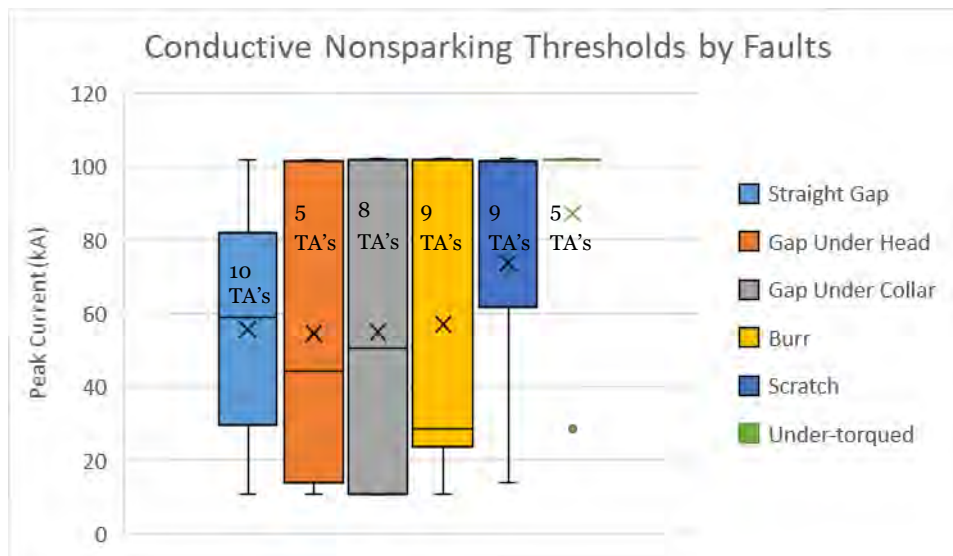


Figure 58: Conductive Nonsparking Thresholds by Faults



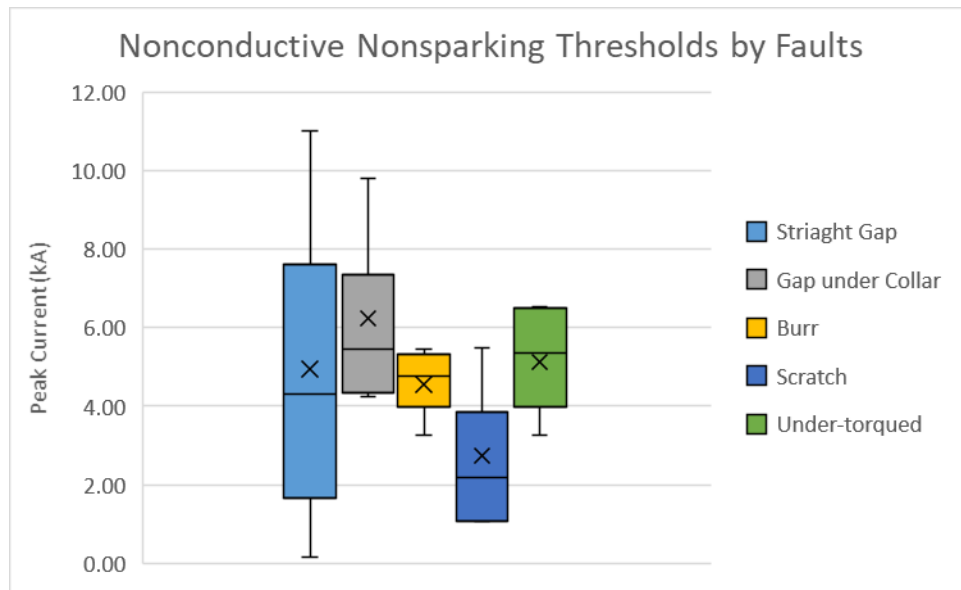


Figure 59: Nonconductive Nonsparking Thresholds by Faults

\*Note that there were 4 TA's for each nonconductive fault configuration.

To further investigate the effect of faults on sparking, every sparking incident and the specific fastener they resulted from were tallied. As only 1 fastener per joint was a faulted installation, only 25% of all fasteners tested were faulted. 35% of all sparking came from the faulted fastener installation, while the remaining 65% of sparks originated from the nominally installed fasteners on the faulted test article. Although no specific fault seemed to have a significant impact on the nonsparking threshold, individual analysis of faulted fasteners shows that the burr and gap under collar faults sparked more than any other faulted or nominal installation. The manufacturing anomalies noted earlier and in Section 7.14.2 seemed to effect the nonsparking threshold more than the type of fault present.

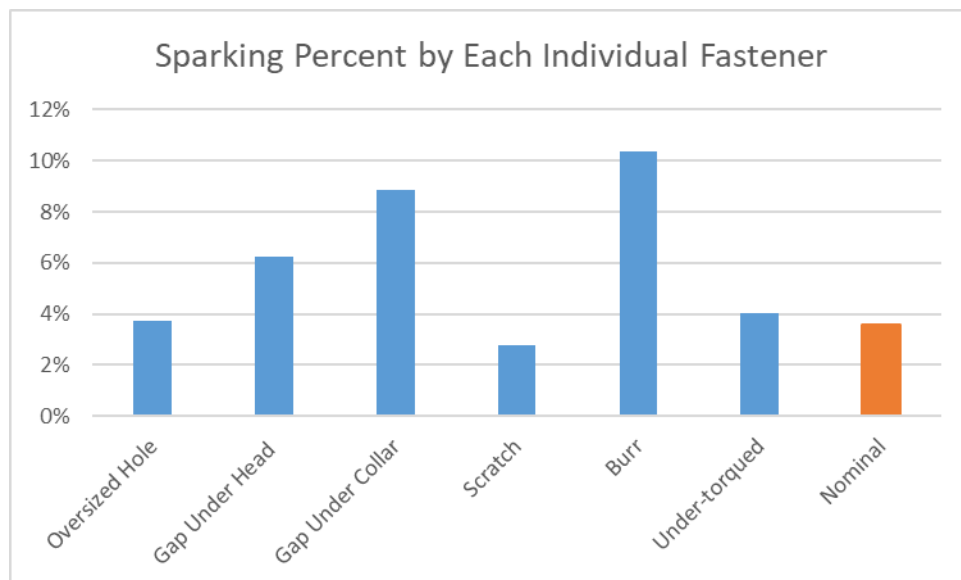


Figure 60: Sparking Percent by Each Individual Fastener

## 7.10 Factor 8 - Manufacturer

It is important to determine whether manufacturing variance between the OEMs has an effect on the sparking and nonsparking thresholds. The analysis used to determine if any OEM outperformed any other OEM is different between the nominal and faulted articles, since the approach to testing was different.

### 7.10.1 Nominal Test Articles

Table 8 was used to determine if there was any variance between the manufacturers that caused significant changes in the sparking threshold. The percentage of articles that sparked based on the number of fasteners and coating type were compared between OEMs. The results below show that no OEM consistently outperformed any other across all 4 categories in a significant manner. Thus manufacturing variance present does not significantly impact the sparking threshold.

Table 8: Sparking percentage by OEM

Fastener Type	OEM 1	OEM 2	OEM 3	OEM 4	OEM 5
Conductive Quadruple	11.11% (1/9)	0% (0/10)	0% (0/10)	0% (0/10)	0% (0/18)
Nonconductive Quadruple	100% (2/2)	0% (0/1)	N/A	100% (1/1)	50% (1/2)
Conductive Single	0% (0/8)	0% (0/9)	0% (0/10)	20% (1/5)	11.11% (1/9)
Nonconductive Single	100% (3/3)	100% (1/1)	N/A	100% (1/1)	100% (2/2)

### 7.10.2 Faulted Test Articles

To see if there was any variance between manufacturers of the faulted fastener installation, the data for each OEM was separated into conductive and nonconductive and plotted in a box-and-whisker plot seen below in Figure 61 and Figure 62. No one OEM did better or worse than the others in either plot showing that there is no significant impact on threshold based on the manufacturer.

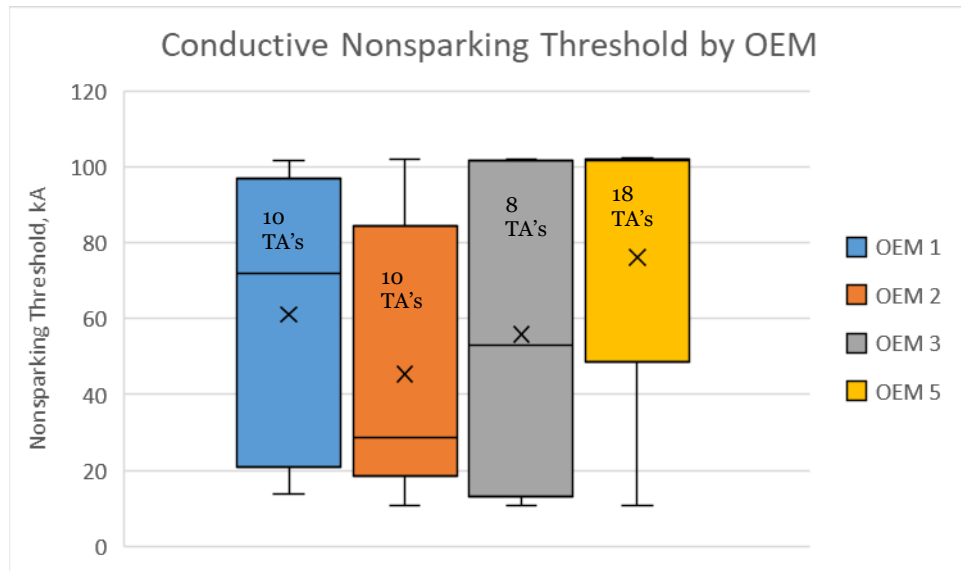


Figure 61: Conductive Fastener Nonsparking Thresholds by OEM

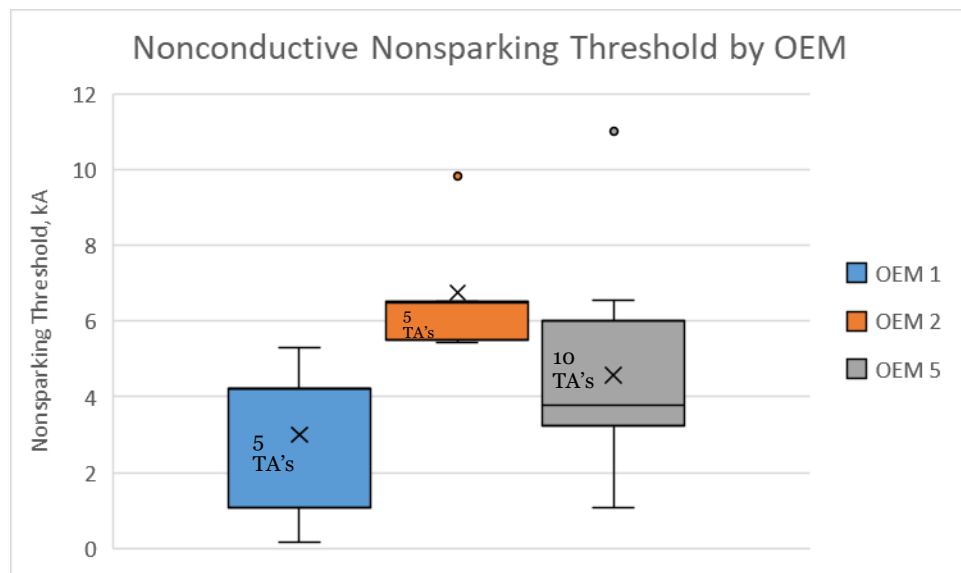


Figure 62: Nonconductive Fastener Nonsparking Thresholds by OEM

Since the test articles were built using varying manufacturing processes by 4 (faults) or 5 (nominal) OEMs, it is significant to note that the sparking thresholds were all very similar for all OEMs. This indicates that future test data by other OEM's is expected to perform similarly. Based on this observation, the data obtained through the KART Fastener Handbook project is a good baseline for future testing. It should also be noted that the determined nonsparking thresholds for all IVD conductive fastener configurations were significantly higher than the theoretical current densities that would be expected at these fastener locations.

### 7.11 Fasteners Not Coated in Sealant

It is common practice in the industry to dip fasteners in sealant before installing them over the fuel tank. This is done to eliminate leaks and protect for corrosion. A layer of non-conductive sealant would provide a lesser contact between the skin and the fastener so could be considered a worst case.

The problem is that not all OEMs use the same practices with sealant. Some dip the fasteners in sealant before installation and also fay seal around them with more sealant after installation, some dip the fasteners but don't fay seal, and some don't even dip the fasteners.

If a fastener that has been dipped in sealant is installed in a smaller hole, the sealant is pushed off the pin and is up around the head. If the fastener is dipped and then installed in a larger hole, there is no way to control how much sealant is around the fastener. Sometimes there would be a lot of sealant and sometimes there would be voids. Since the amount of sealant on/around the fastener is so difficult to control, it was eliminated from testing with the exception of the faulted test articles from OEM 1. No further analysis was done to determine the effects of sealant.

### 7.12 Pre-test DC Resistance vs Sparking Level

It seems intuitive that if a high DC resistance is measured across the joints of a test article before it is tested, there will be more sparking during testing. The data from the nominal test articles does not support that theory.

The following steps were taken when processing the DC resistance vs sparking level data:

- Only the data from the single fastener test articles was used because the quadruples required looking at the data by fastener instead of by joint. This means that only data from the nominal testing was used, as the faults only had quadruple installations.
- The data from OEM 3 was removed because they did not provide any test articles with nonconductive fasteners so their sparking percentage would be much lower.
- The data from OEM 5 was split into 5A and 5B because they provided both Hi-Loks and Hi-Lites so their sparking percentage would be artificially inflated.

Using an overall average of the pre-test measured DC resistance (values exceeding 1000 mΩ were limited to 1000 mΩ), the OEMs were ranked in order from highest to lowest. The OEMs were also ranked from highest to lowest using the number of just external sparks and the total number of internal and external sparks.

Table 9: DC Resistance vs Sparking

Pre-test Measured DC Resistance	Internal & External Sparks	External Sparks
OEM 4	OEM 1	OEM 1
OEM 1	OEM 4	OEM 5A
OEM 5A	OEM 5A	OEM 5B
OEM 5B	OEM 5B	OEM 4
OEM 2	OEM 2	OEM 2

It can be seen from the Table 9 that the order changes each time. This shows that there is not a consistent relationship between the DC resistance and sparking.

It can also be seen in Figure 63 that some of the low DC resistance values sparked while some of the high DC resistance values did not spark. The main cause of external sparks in this data was the nonconductive coating on the fasteners which disabled the conductive path. This says that sparking is a more complicated event that cannot be explained with a single variable.

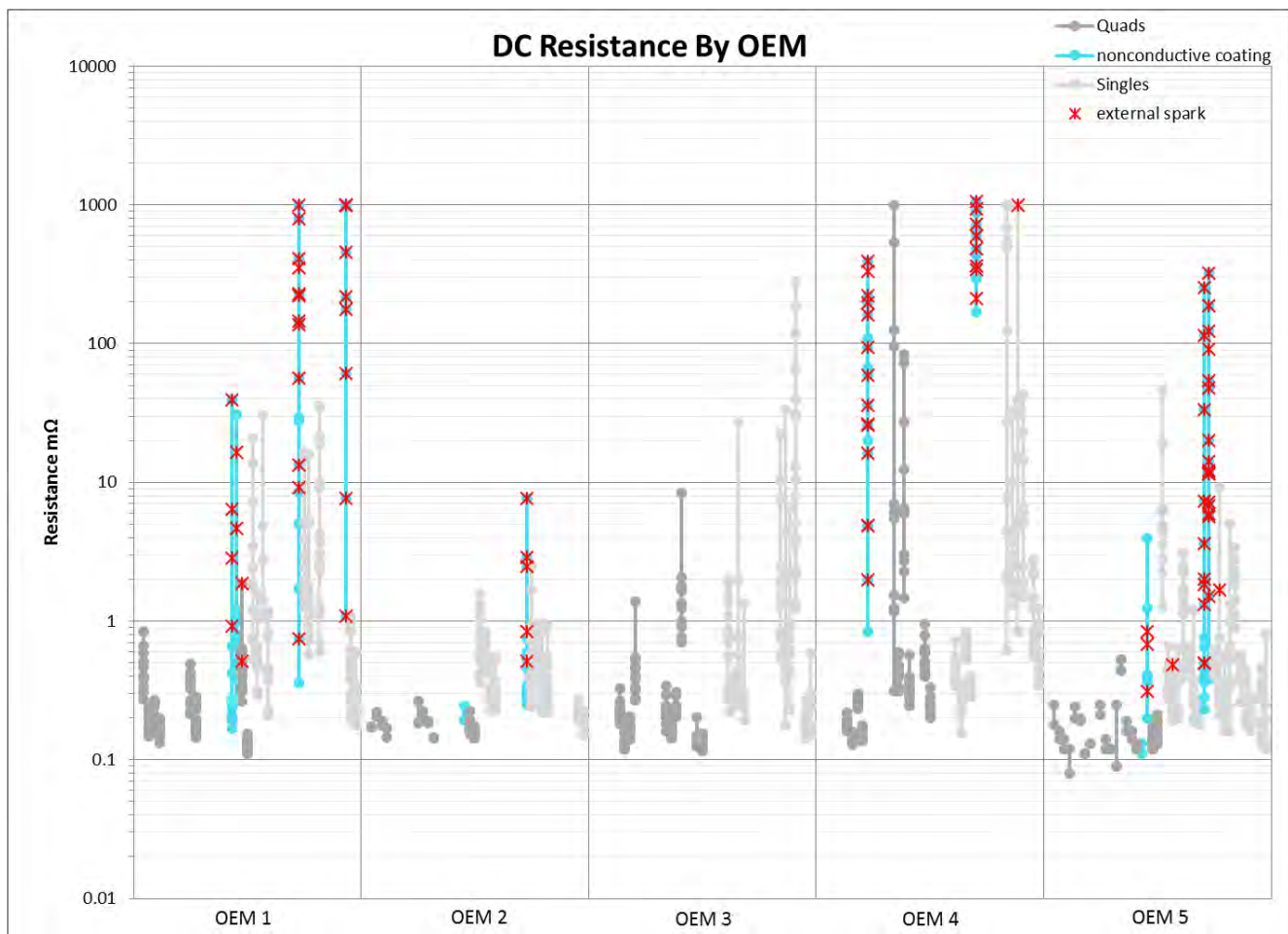


Figure 63: DC Resistance of Nominal Test Articles by OEM

This statement was also found in the referenced literature:

*“The facts of the matter are that dc resistance is a poor criterion to use for evaluating whether a joint is “good”. The ability of a joint to carry high current without sparking or burning is really determined by contact size, treatment of mating surfaces, type and number of fasteners and the contact pressure on the mating surfaces. . . .”*

[Ref.: Fisher F.A., Plumer J.A., Perala R.A. Lightning Protection of Aircraft, Lightning Technologies, Inc., Pittsfield, MA, 2004].

### **7.13 Anomalies Discovered During or After Testing**

Certain test articles were cut open after testing for further examination to determine if there were any other anomalies. Test articles were chosen due to unexpected or inconsistent sparking performance in comparison to other test results.

#### **7.13.1 Nominal Test Articles**

##### **OEM 1**

A large percentage of the rivets test articles for both singles and quadruples had sparks. This was unusual and unique to OEM 1. A couple of test articles (MN-4009-6 and MN-1010-5) were cut open and the holes were measured. It was found that the holes for MN-1010 were on the large side, elongated, and had a lot of variance.

According to the drawings, there was only supposed to be one configuration of test article using the Hi-Kote fasteners with the nonconductive coating: small, countersunk head, interference fit. Because 4To3 and 1To3 also used the Hi-Kote fasteners, it was theorized that these test articles used a transition fit sized hole. It can be seen in Figure 34 below that the data appear to support this theory because the transition fit holes have higher pre-test and post-test DC resistance values.

Several more test articles were cut open (MN-1Io3-1 and -3, MN-1To3-1 through -6, MN-4Io3-1 through -4, and MN-4To3-1 through -4) and their holes were measured to prove or disprove this theory.

The hole sizes ran large. Even the interference fit holes were mostly transition fit sized. Overall the theory holds because the interference fit holes average smaller than the transition fit holes. All the test article configurations listed above were changed to their actual configuration for data analysis. For example: all the 1To3 test articles were changed to 1T12 test articles for data analysis.

One last anomaly for OEM 1 is that the DC resistance did not decrease between the pre-test and post-test measurements as much as the other OEMs, as seen in Figure 34. For the other OEMs, the post-test DC resistance measurements were greatly reduced from the pre-test measurements due to test article conditioning during testing. From the measurements of the cut open test articles of OEM 1, it appears that this effect is due to the larger hole sizes leading to poor electrical contact.



## **OEM 2**

The hole sizes were the same for both the interference and transition fit because of the overlap in the specifications.

## **OEM 3**

As noted earlier, OEM 3 provided alternate collars for all test articles (not including rivets). The change in collar did not appear to have any effect on test results.

## **OEM 4**

There was an unusually high number of internal sparks in the single fastener test articles. It was also unusual that the DC pre-test resistance increased a lot only for the small fastener test articles with the transition fit. When four of the small fastener transition fit test articles were taken apart to have their holes examined and measured, it was discovered that the hole sizes for the top plates and the bottom plates at each joint were different. The hole size mismatch would be a good reason for the internal sparking.

## **OEM 5**

There was an unusually high number of sparks from between the plates and from the copper contacts on the sides of the black box. For the sparks at the copper contacts, there was a sticky black residue on the supposed bare metal ends of the test articles. This residue was just enough to prevent a good contact so would occasionally produce sparks. The residue may have been left from the masking before the primer was applied. For the sparks between the plates, there were gaps between the plates. Even though there were low DC resistance measurements across the joints, the gaps were enough to release the sparks. The metal coupons may have been bent before assembly or the assembly technique may produce the gaps. Neither of these types of sparks were represented in the data graphs because they wouldn't help determine the effects of the factors.

### **7.13.2 Faulted Test Articles**

#### **OEM 1**

No further anomalies were found post-test.

#### **OEM 2**

No further anomalies were found post-test.

#### **OEM 3**

As stated earlier, in the MF1-4T05 test articles, the faulted fastener was replaced with the protruding head counterpart. These articles were cut open and it was determined that the hole was not drilled countersunk so there was no gap under the head of the fastener. The loose fasteners on joint 3 of the MF2-4T05 and MF3-4T05 were the correct size and the diameters of the holes were within tolerance, so there was no obvious cause for loose fasteners.

#### **OEM 5**

The MF1-4T11 test articles from OEM 5 were the only nonconductive fasteners to not spark below 11 kA. These test articles were cut open and it was found that there was a mismatch between the hole sizes of the top and bottom plates. The smaller hole on the bottom plate may

have led to the Hi-Kote coating being scraped off, creating better conductivity. Though the hole sizes were mismatched they were still within tolerance.

## **8.0 CONCLUSIONS**

### **8.1 Nominal Test Articles**

- The two factors of “Factor 6 - Fastener Coating” and “Factor 7 - Number of Fasteners” were the only factors that tested statistically significant for the data from all the OEMs. Even with all the different manufacturing anomalies between all 5 OEMs, only the two effects of coating and number of fasteners tested significant.
- Testing of the quadruple fastener test articles showed that the lowest current level that created a spark, excluding the nonconductive Hi-Kote coated fasteners, was at 9.3 kA. This was for the small rivets, MS20470AD4.
- Testing of the single fastener test articles showed that the lowest current level that created a spark, excluding the nonconductive Hi-Kote coated fasteners, was at 4.85 kA. This was for the small countersunk Hi-Lites, HST11BJ5-3.
- Internal sparking appears to show evidence of manufacturing anomalies. Whenever test articles with a lot of internal sparking were cut open to investigate, manufacturing anomalies were found.
- It was expected to find a relationship between high pre-test DC resistance measurements and sparking levels but none was found. Sparking appears to be more complicated than to be dependent on a single variable.
- OEM 5 provided both Hi-Loks and Hi-Lites. It was interesting to see that the Hi-Lites were significantly better than the Hi-Loks for OEM 5. This effect did not hold for the overall data with all the OEMs however.
- The effects of skin thickness between 0.063” and 0.090” were not significant for this testing but may have more of an effect if a thinner skin (0.020” or 0.030”) was tested.
- Follow-on testing may be desired to investigate the effect on sparking of dipping fasteners in sealant when they are installed.

## 8.2 Faulted Test Articles

- OEM 5 provided both Hi-Loks and Hi-Lites. The Hi-Lites performed significantly better than the Hi-Loks for OEM 5 across most of the faults. For the under-torqued fault, the difference was not significant and in the case of the gap under head fault, the Hi-Lites performed better. The Hi-Lites performed better than the Hi-Loks for OEM 5, which is consistent with the results from OEM 5 nominal testing. This effect did not hold for the overall data for all OEMs.
- Only “Factor 6 - Fastener Coating” tested statistically significant for the data from all the OEMs despite all the manufacturing variance between the five OEMs.
- Testing of the quadruple fastener test articles showed that the lowest current level that created a spark, excluding the nonconductive Hi-Kote coated fasteners, was at 10.8 kA. This was for the small countersunk Hi-Lite, HST10BJ5-3/HST79CY5.
- The burr and gap under collar faults had the largest impact on the probability of an individual fastener sparking. Although, in general the faults did not have as big of an effect on the nonsparking threshold as the manufacturing variance did.
- Despite the many different manufacturers and manufacturing techniques, the nonsparking threshold did not change significantly between manufacturers.
- Sparking behavior of the nominal and faulted test articles at 10 kA was comparable, indicating that the presence of a fault does not significantly reducing the sparking threshold at test levels of 10kA or less.
- It was expected to find a relationship between high pre-test DC resistance measurements and sparking levels, but none was found. Sparking appears to be more complicated than to be dependent on a single variable.
- Follow-on testing may be desired to investigate the effect on sparking of dipping fasteners in sealant when they are installed.

## Appendix A - EMA Wing Simulation Report



7655 West Mississippi Avenue, Suite 300, Lakewood, CO 80226-4332, P.O. Box 260263, Denver, CO 80226-0263 (303) 980-0070, Fax: (303) 980-0836

### Title:

KART Wing Final Report for CEM Simulation  
Validation

Revision: Rev 0

### Document Details:

**Document No:** EMA-2019-R033

**Release Date:** 7/31/2019

### Authorship and Approval:

Author(s):	Date
Cody Weber, Principal Scientist	7/31/2019
Eric Miller, Scientist	7/31/2019

### Proprietary Statement:

All contents of this document are proprietary to EMA and The National Institute for Aviation Research Environmental Test Lab (NIAR ETL) as part of the designated project and any applicable non-disclosure agreements.

## Applicable Documents

### Standards Documents

- SAE ARP 5412 – Aircraft Lightning Environment and Related Test Waveforms
- SAE ARP 5415 -User's Manual for Certification of Aircraft Electrical/Electronic Systems for the Indirect Effects of Lightning (recommends use of EMA3D in aircraft certification)
- SAE ARP 5416 - Aircraft Lightning Test Methods
- AC 25.954 Fuel Tank Ignition Source Prevention Guidelines
- AC 20-136 B - Aircraft Electrical and Electronic System Lightning Protection

### Applicable Documents

- F. A., Plumer, J. A., Perala, R. A.: "Lightning Protection of Aircraft", Lightning Technologies, Inc., 1990.

### Abbreviations/Acronyms

3D	Three Dimensional
CAD	Computer Aided Design
CADfix	Software for CAD importing, modification and material assignment for EMA3D
CEM	Computational Electromagnetics
EM	Electromagnetic
EMA	Electro Magnetic Applications
EMA3D	FDTD software solving Maxwell's Equations for the three-dimensional EM analysis
FDTD	Finite difference time domain
FWD	Forward direction
LTA	Lightning Transient Analysis
MATLAB	A software product of Mathworks providing general plotting and analysis capabilities
MLG	Main Landing Gear
NIAR	National Institute for Aviation Research
OEM	Original Equipment Manufacturere
RCS	Return Conductor System used for test current return to generator ground
FQIS	Fuel quantity indicating system



## Table of Contents

Introduction .....	4
Select Validation Test Article .....	4
Lightning Injection Tests .....	6
Test Probes.....	8
Lightning Current Source .....	10
CEM Model Overview .....	11
Modeling Technique .....	11
Model Development .....	11
Material Property Selection .....	16
Known Metallic Properties.....	16
Parameter Measurement Activities .....	16
Model Cell Size .....	17
Model Tracking .....	17
Model Validation Simulations.....	18
Excitation Source Descriptions.....	19
Simulation Validation Results .....	19
Amplitude Validation .....	20
Waveform Validation.....	20
B-dot Probes .....	20
Current Probes .....	23
Current Density Images.....	25
Rib 12 Current Densities .....	26
Rib 7 Current Densities .....	26
Amplitude Margin Development Approach.....	27
Waveform Comparison and Reduction.....	27
Validation Conclusion .....	28
Appendix A: Simulation and Test Validation Waveform Comparisons.....	29
Configuration 1: Wing Tip to Distributed Wing Root.....	29
Configuration 2: LE Rib to TE Bracket .....	41
Configuration 3: Rib 7 Lower Skin Fastener to Upper Skin at LE Side of Wing root .....	43



## Introduction

To show compliance with CFR 14 25.981(a)(3), aircraft manufacturers must demonstrate that the lightning threat at structural and system interfaces will not create an ignition source, even when considering all foreseeable system and structural faults. It is difficult to fully assess all fuel tank interfaces in a single test program, even when grouping common design components. Furthermore, it is impossible to verify compliance with the inclusion of all fault scenarios in a full vehicle test. Therefore, many aircraft manufacturers use a combination of aircraft level characterization testing, computer simulations, and component level testing to show compliance. It is difficult if not unrealistic to evaluate current distributions throughout an entire aircraft fuel tank by testing alone. A combination of 3D CEM simulation and lightning testing can provide the most complete lightning current distribution mapping for an aircraft.

The goal of this research project is to demonstrate some the activities of model development, simulation and validation that may be used to support the fuel tank certification program. The activities presented here are not complete in the amount of testing or analysis that may be required to support a full certification program but illustrate many of the important steps. These key activities include:

1. Select a suitable representative aircraft test article
2. Perform lightning injection testing on the test article and measure EM coupling responses in and around the fuel systems regions
3. Develop a simulation model capable of characterizing the fuel systems lightning response
4. Directly compare simulation and experiment lightning coupling results to establish acceptable margins for all numerical analysis

A significant step in the process that is not covered in this effort occurs after the validation of the numerical model. This step is to perform simulations of the inflight aircraft configuration to determine all the necessary zone 3 interface levels to use with coupon testing. The model used for the inflight analysis is often similar to the validation model and can be modified appropriately to match the inflight configuration.

Each of the steps listed above is reviewed in the sections below.

## Select Validation Test Article

Fuel systems ignition prevention certification programs have utilized various test articles for numerical validation. These articles have ranged in complexity from a few rib bays of a wing box, to a production wing and all the way to a full production aircraft. The guidance material does not identify any particular test article that must be used for validation, instead, the wording indicates the article must sufficiently represent the aircraft being investigated. In general, the article should have similar components, materials, and manufacturing and installation procedures as the aircraft being certified. Any potential article should be reviewed with the cognizant ACO and justified for its representation of the aircraft being certified.

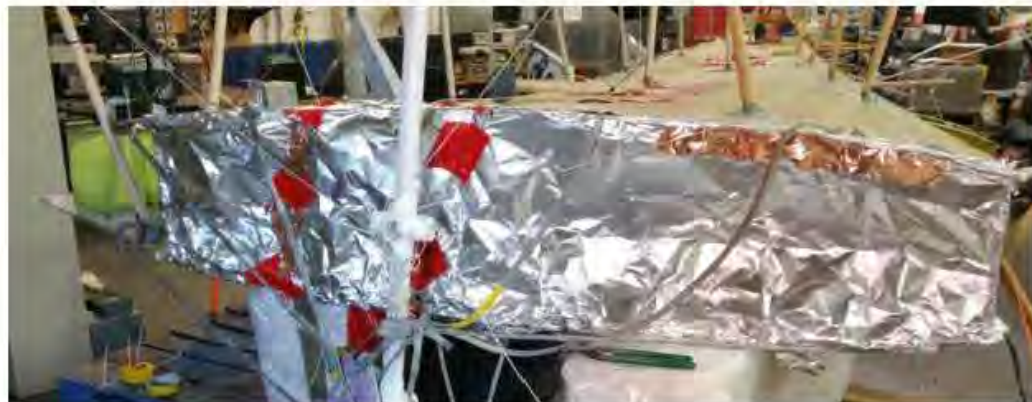
For this validation effort the test article was an aluminum wing taken from a retired business jet donated for research purposes, Figure 1. The structural aspects of this test article are highly correlated to the aircraft since the skins, spars, ribs, fasteners and installation techniques match exactly the certified aircraft configuration. However, there were some drawbacks in using this wing as a validation article. The wing had been stripped of all interior fuel system components. The exterior did not contain control surfaces, LE structure or access panels for the lower skin. The wing was cut near the root and contained an open rib bay. Part of the difficulty in characterizing zone 3 currents in aircraft fuel systems is quantifying interior transients. Since this test article did not contain interior fuel systems components, it may be difficult to

justify its use as a validation article. Nonetheless, there certainly are ways an OEM could include pipes or conductors that represent fuel system components into a test article like this one.

For example, in order to better replicate the wing's natural EM response, metal foils were applied to the lower skin access panels and exposed root rib bay. These covers are shown in Figure 2. To represent a fuel system conductor, a 4 AWG wire was rooted from near the wing root, Rib 5, to an outboard rib, Rib 15. Making these additions to the wing make it more like the inflight version of the aircraft and help to evaluate what more natural lightning response of the aircraft fuel systems might be. The wing was positioned with the lower skin facing up to provide easier access through the rib bay access panels.



*Figure 1: Retired business jet wing used as test article for this validation effort.*



*Figure 2: Example of access panel covers and root rib bay cover to seal of EM penetration into the wing bays as it would be like on the actual aircraft configurations.*



## Lightning Injection Tests

The primary objective of the lightning testing effort is to measure lightning transients, waveforms and amplitudes, in and around the fuel systems in zone 3 regions. These transients are primarily lightning currents that flow through the fuel systems components but can also be voltages that develop between components. In many ways, these tests are similar to the full vehicle lightning tests used for LTA or indirect effects testing of electrical equipment, but rather than cables being measured, transients on structural and system fuel components are measured. ARP 5416 and ARP 5415 contain guidance on performing the full vehicle tests and transient assessment and was implemented for this effort.

A test plan was developed that identified the test article, configuration, equipment, probes and procedure. An important aspect of the test configuration is the return conductor system, RCS, to provide representative current distribution on the test object and mitigate ground plane effects. The model of the test wing with RCS is shown in Figure 3.

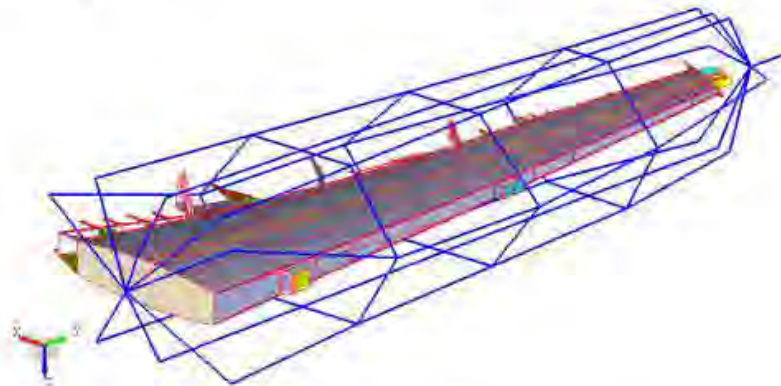


Figure 3: Return conductor configuration used on the test wing.

When evaluating lightning current distributions in aircraft, it is common to consider the possible entry and exit points determined by the aircraft zoning. Multiple entry and exit scenarios should be investigated to ensure that different current distribution cases are analyzed. The determination of most severe cases will not be elaborated here, but some effort should be dedicated to determining all of the possible lightning paths through the fuel tanks, which scenario would produce the most severe lightning environment for each design group and how the lightning environment will be determined for each design group. For this effort, three entry/exit scenarios common to fuel tank assessment were chosen:

- Configuration 1: Wing Tip – Distributed Wing Root (Figure 4)
  - This scenario will flow the full 200 kA Component A current through the wing and represents a wingtip to opposite wingtip event. Current is flowed wingtip to wing root.
- Configuration 2: Leading edge Rib – Trailing Edge Bracket (Figure 5)
  - This scenario would not necessarily apply to this business jet wing but is a common investigation for aircraft with wing mounted engines that have an engine strike. Current is flowed forward to aft across the wing.
- Configuration 3: Rib 7 upper fastener near Fwd spar – Wing Root Upper Leading Edge (Figure 6)
  - Most wings will have 2A lightning zone that extends 0.5 m from the fuselage in the wing root area. Additionally, aircraft with wing mounted engines may have Zone 2A on wing sections aft of the engine. Aircraft of a new design may have Zone 3 (A/S) attachments that

should be considered on the wing. To represent the possibility of direct attachment to a fastener in the fuel system region, current is flowed into the wing tank and concentrated on one side of the fuel systems.

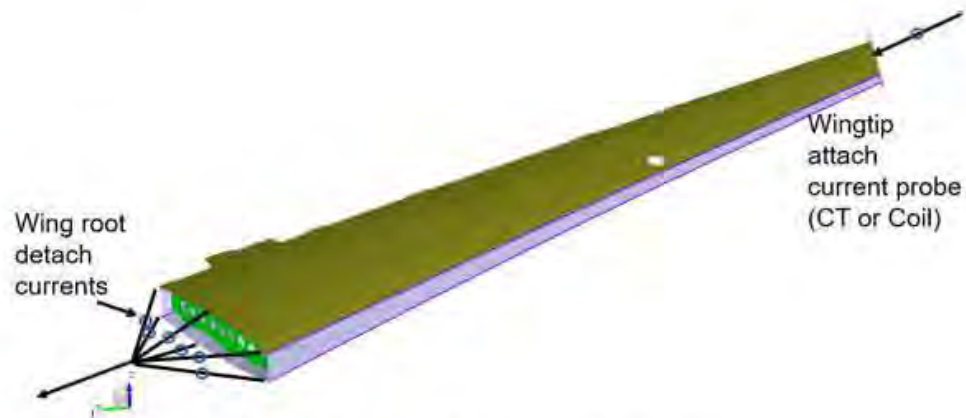


Figure 4: Test Configuration 1 - Wingtip injection, Distributed Wing Root exit.

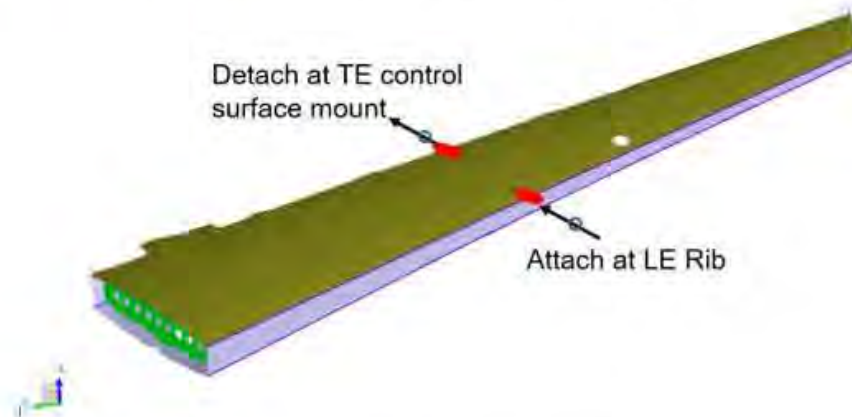


Figure 5: Test Configuration 2 - LE Rib injection, TE Bracket exit across Rib 12.



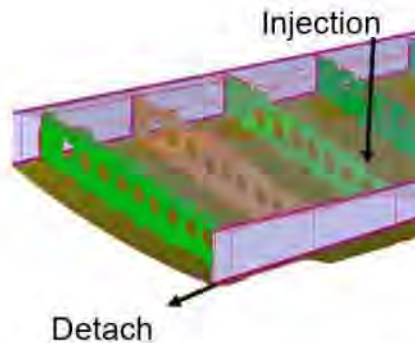


Figure 6: Test Configuration 3- Rib 7 fastener injection, Upper Wing skin TE ext.

### Test Probes

Currents are the primary input to coupon tests that detect ignition sources for components that are electrically bonded by things like fasteners, rivets or couplers. Voltages are the inputs to dielectric or potential withstand tests for components that pass through or are isolated from other components such as pipes through ribs or FQIS wires to ribs or skins. It is common to incorporate current and voltage probes into the test plan. Another way to characterize current flow is by magnetic field, or B-dot sensors. These B-dot probes capture the magnetic fields above a component which is directly related to the current flowing through the conductor via Ampere's law. The B-dot probes are especially useful for large conductors or tightly bonded components where current probes cannot be placed. It may be difficult to fully map all of the magnetic fields necessary to determine currents flowing through interfaces. However, the B-dot probes are an excellent way to correlate simulated fields to measured fields in a particular area. If the simulation and experimental results have good correlation of magnetic fields, this means the current distributions must be equivalent in those measured areas and confidence is gained in the simulation capability to reproduce accurate current distributions.

The selection of probe locations for the aircraft was concentrated on using magnetic field (b-dot) probes to review current distributions primarily on the wing exterior. The test article wing did not have any fuel systems components and therefore voltage measurements were not part of the effort. A single 4 AWG wire was routed from an inboard rib to an outboard rib to represent a long spanning fuel pipe. Some magnetic field measurements were made on a rib for the fastener injection case but minimal internal measurements were completed in this program. It may be necessary to include more internal measurements as part of an actual numerical validation effort in a certification program. Only B-dot and Pearson current probes were used for this validation effort. The test probe matrix is identified in Figure 7 below.

A total of 39 probes were included during testing for validation:

- 32 B-dot on exterior wing skins and spars
- 5 B-dot on interior rib for configuration 2
- 13 Current probes on distributed detach braids and internal 4 AWG wire
  - 5 probes represent the recorded attach and total detach currents to verify the injected current waveform. These 5 probes will not be used as part of the validation.

Test # (Configuration - Amplitude)	Waveform	Current Level (kA)	Test Wing Connections		Probe (Type)	# of Probe Locations	Description
			Injection	Return			
1-3	Comp. A (As close to 6.4 us peak as possible)	3	Wingtip (distributed through 6 braids)	Wing Root (distributed through 6 braids)	Bulk current (Pearson CT)	7	1 attach currents 6 detach currents
					Bulk current (Pearson CT)	1	1 pipe (4 AWG wire?) currents
					Magnetic fields (B-dot)	17	7 upper skin locations 6 lower skin locations 4 spar locations
2-3	Comp. A (As close to 6.4 us peak as possible)	3	LE Mount Bracket Attach	TE Mount Bracket Detach	Bulk current (Pearson CT)	2	1 attach current 1 detach current
					Magnetic fields (B-dot)	4	2 upper skin locations 2 lower skin locations
3-3	Comp. A (As close to 6.4 us peak as possible)	3	Rib 7 Fastener	Wing Root Upper TE Side	Bulk current (Pearson CT)	2	1 attach current 1 detach current
					Magnetic fields (B-dot)	11	2 upper skin locations 2 lower skin locations 2 spar locations 5 Rib 7 locations

Figure 7: Test Probe Matrix

Some sample wing skin positions of the B-dot probes are shown in figure 8. The relative positions of the internal rib B-dot probes for the configuration 2 fastener injection case are shown in Figure 9.

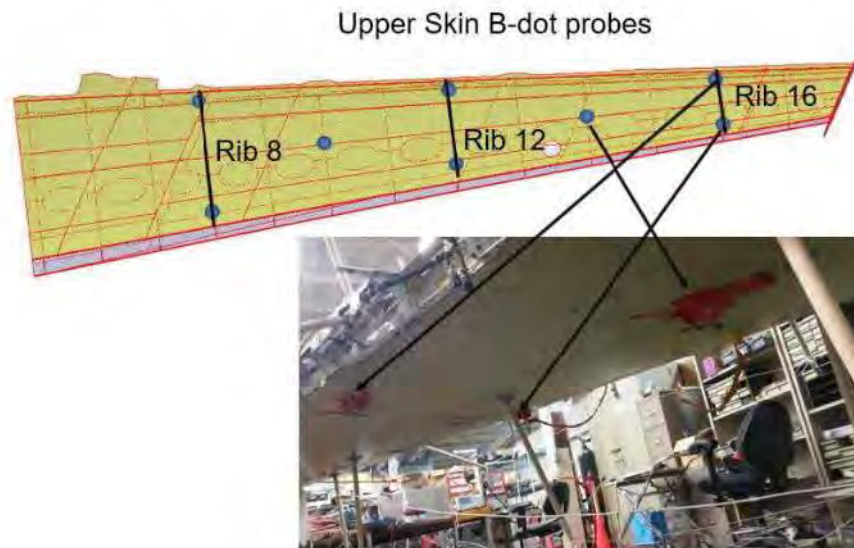


Figure 8: Upper skin B-dot probes implemented in the test configuration.



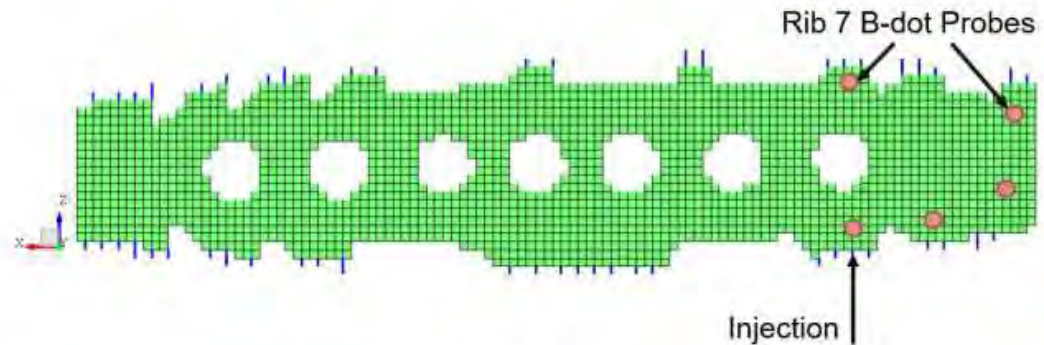


Figure 9: Rib 7 B-dot probe locations for Configuration 3.

#### Lightning Current Source

The Component A waveform with a 3 kA amplitude was used for all lightning tests. The waveform characteristics were taken from ARP 5412B as shown in Figure 10.

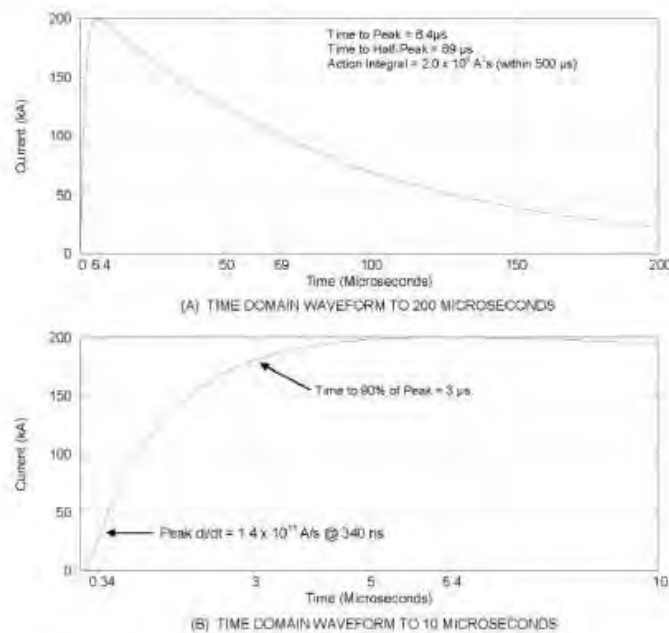


Figure 10: ARP5412B idealized lightning current waveform for Component A

## CEM Model Overview

The goal of CEM analysis is to capture the pertinent electromagnetic responses of the aircraft being simulated. The model must capture certain features of the aircraft related to resistances, inductances and capacitances. Starting with the solid body CATIA CAD ensures model components will have accurate dimensions, shapes and locations of the aircraft which relate to the inductive and capacitive EM behavior. Using appropriate material assignments within the model ensures that the resistive portion of the EM effects is captured. The development process of the CEM model involves many details to represent the EM aspects of the aircraft design. A high-level review of the model, development steps, assumptions and rationale are covered in this section.

## Modeling Technique

The model preparations are dependent on the simulation tool being used. The software users should have a keen understanding of the modeling approach and implementation of all EM parameters when performing complex vehicle analysis. All pre-analysis geometrical modifications and model preparations were performed using CADfix software. The lightning simulations for this analysis used a three-dimensional full wave finite-difference time-domain (FDTD) code. The simulation software, EMA3D, uses an analytical approach recognized in ARP5415 and the Lightning Protection of Aircraft Handbook for performing lightning simulations on aircraft. There is both a long and recent successful validation history within the aerospace and commercial aviation industry when using this analysis approach for lightning interaction problems. Aviation authorities around the world recognize EMA3D and the modeling technique described below as an acceptable technique for evaluating lightning interaction problems with aircraft. Of course, obtaining accurate simulation results requires not only a suitable simulation software tool, but adequate representation of the EM parameters of the aircraft being simulated.

## Model Development

The wing model geometry was directly imported from CATIA CAD files. The geometry was appropriately modified to have the necessary component mesh and connectivity. The final wing geometry is shown in Figures 11-13. The wing considered in this analysis was missing some very important components that should typically be considered when performing this type of validation effort. Primarily this would include system components inside the fuel region like fuel pipes, couplers, hydraulic pipes and electrical components like FQIS. Additional aircraft components outside of the fuel tanks could affect current distributions or certain interfaces that may need to be considered. Some of these additional components may include:

- Center wing or additional fuel storage areas
- Control surfaces
- Main Landing Gear (MLG)
- Fuselage
- Belly fairing
- Engines and nacelles (for wing mounted engines)

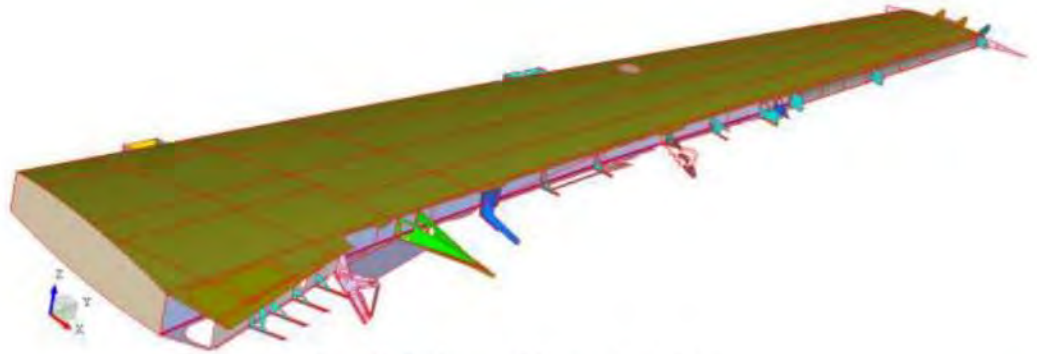


Figure 11: Final wing model geometry, top-aft view.

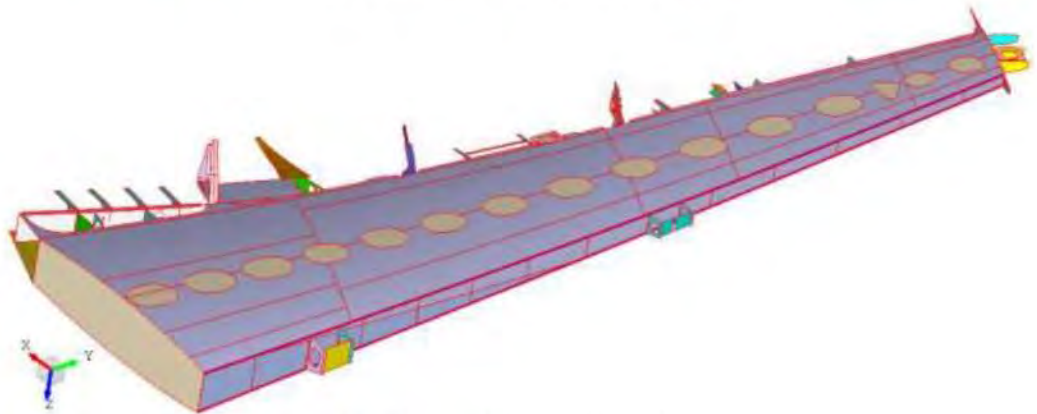


Figure 12: Final wing model geometry, bottom-forward view.

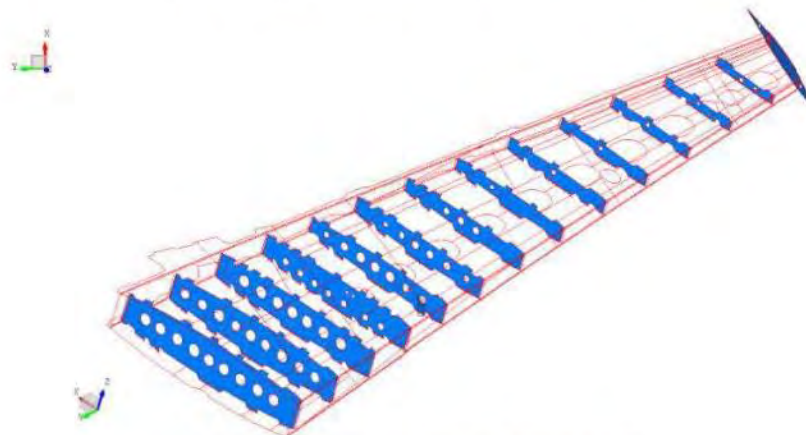


Figure 13: Final wing model geometry, interior rib view.



Although this wing model was missing some important fuel systems components, there are certain aircraft sections that may not need to be included in the validation test or simulation models because they will not impact fuel tank lightning coupling behavior. The exclusion of these components from the analysis model should be confirmed with the certifying authority but may include:

- Cockpit
- Empennage
- Nose landing gear
- Fuselage wire harnesses
- Fuselage Interior frames away from wing structure
- Fuselage and belly fairing electrical/electronic equipment

The final CAD geometry used for CEM models is derived from manufacturing CAD models but there are some very distinct differences between the two types of CAD geometries. The CEM development process requires that assumptions are made to the geometry and material properties. Some the significant differences between manufacturing CAD and CEM CAD geometries include:

- Manufacturing CAD can include all components in the design, even tiny washers, brackets and shims. -- CEM CAD geometry will exclude brackets and other small components that do not affect EM coupling and simplifications are required for nearly every component in a problem.
- Components in manufacturing CAD have very complex shapes, curvatures, cutouts, and flanged sections. -- Representations of component's shape and volume are used in the CEM model, which still result in an accurate simulation. The CEM CAD will typically use a single meshed surface or line for structures and panels while using average thickness to determine the material property definition.
- Structural joints in manufacturing CAD involve overlapping components connected by fasteners, bolts or rivets -- CEM CAD will link two jointed components with a seam that controls the impedance between structural components.

Figure 14 shows the wing ribs as originally imported from CATIA and simplified for EMA3D simulation. The EMA3D representation shown in Figure 15 maintains the appropriate shape and interfaces of the component. The resistivity of the component is maintained through the conductivity assignment in EMA3D to ensure a bulk resistivity of the component is captured in the model. Connectivity of the component is controlled through specified resistances at the barriers of the component. The FDTD mesh of the rib is illustrated in Figure 16. All of the simplification techniques listed above have been proven effective at improving modeling efficiency while capturing the pertinent EM effects for lightning interaction problems.

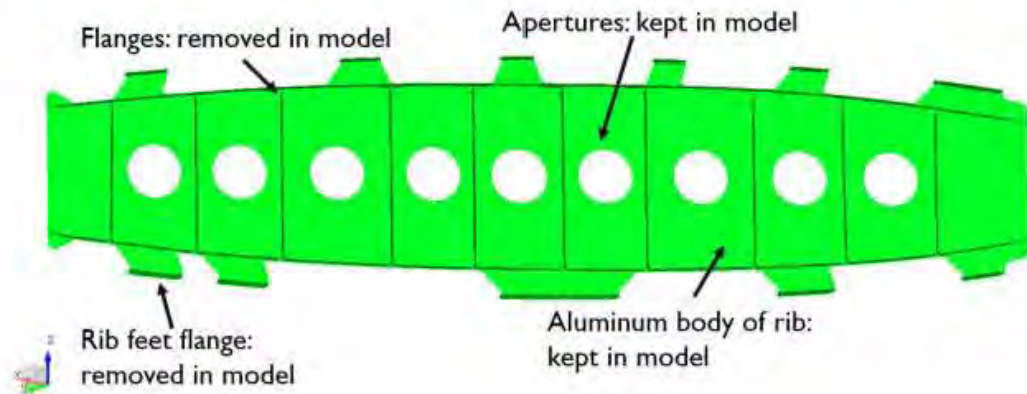


Figure 14: Rib geometry directly imported from CATIA CAD.

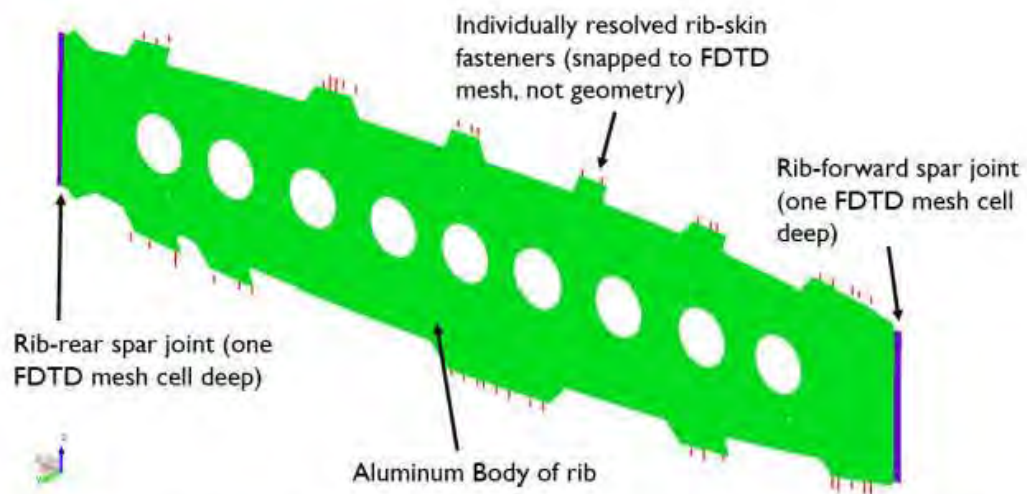


Figure 15: Sample defeaturing result of wing rib 5. The top image is the original component imported from CATIA and the bottom image is the EMA3D representation.

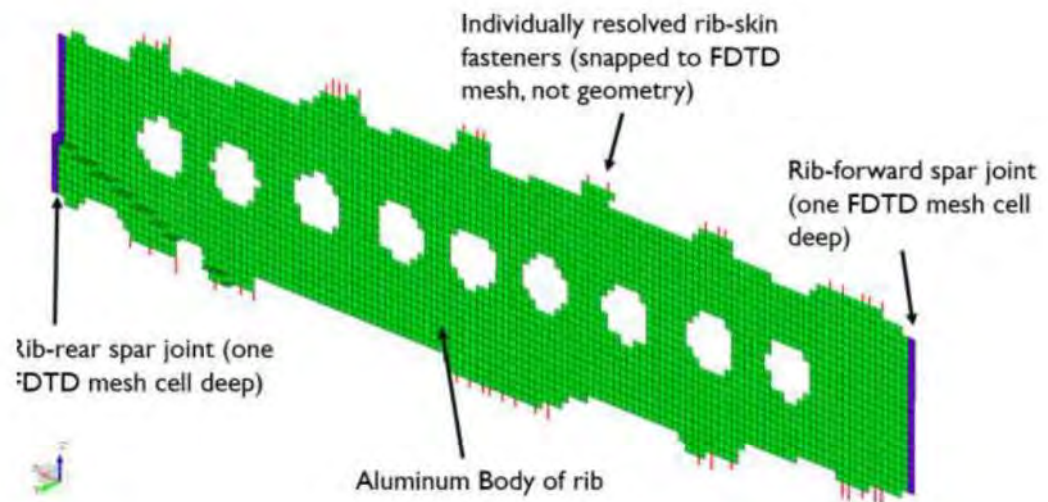


Figure 16: FDTD Mesh result for rib 5.

The final wing model with RCS is shown in Figure 17.

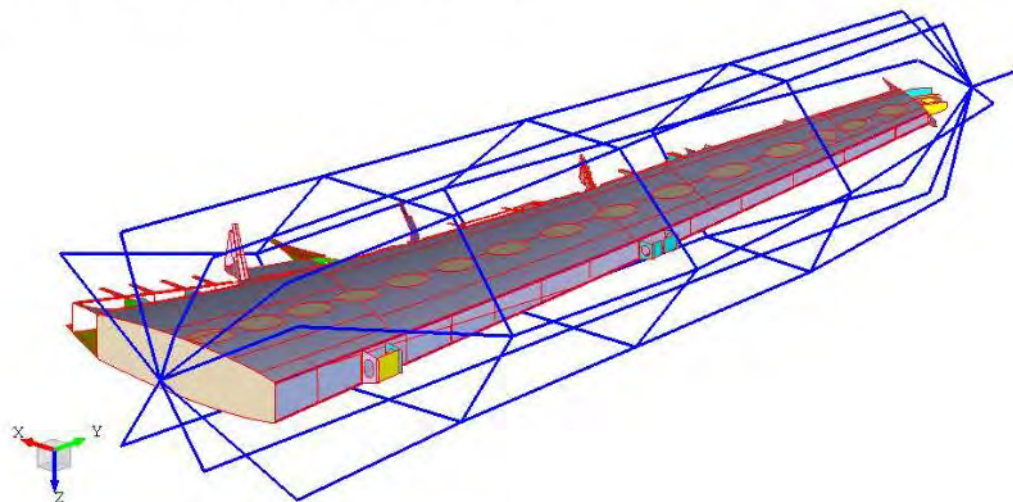


Figure 17: Final wing model with RCS.



### Material Property Selection

In CEM models, it is very important to have accurate geometrical representation, but it is equally important to have accurate material parameter assignments. Some material properties are well known, but some properties related to joint or seam impedances are less well known or installation specific. The methodology for material parameter assignment in the wing model is presented in this section.

#### *Known Metallic Properties*

Some materials, like the aluminum alloys for skins (7150-T7751 and 2024-T3) and spars (7050-T7451), have well defined properties available for lookup in engineering handbooks or specification sheets. These material parameters are simply entered in the CEM model as a conductivity which is inversely related to the resistivity of the material. All metallic components represented in the CEM model are defined in this fashion. Bulk resistivities adjustments for the component thickness relative to model cell size are accounted for in the parameter calculation.

#### *Parameter Measurement Activities*

There are many other features in the aircraft design that must be captured in the CEM model which do not have properties listed in a specification sheet. For these features, laboratory measurements or engineering estimate values are required for the material assignment process. NIAR has performed a subset of material characterization testing to determine various fastener contact DC resistance values for this wing. The samples were cut from the opposite wing of the retired aircraft and contained key joints for characterization.

Incorporating laboratory measured resistance values associated with aircraft joints is a key model input to correctly capture the lightning response. An example of measured resistances and the average value selected for model assignment is provided in Figure 18 below. For sample 7SKR1, this joint represents the forward-most Rib 7 to upper skin connection. The joint contained 4 fasteners with 0.2" diameter. The total resistance across the sample was 0.174 mΩ. This resistance value can be directly input into the model as a total joint resistance or can be converted to a resistance per fastener basis assuming each fastener has a similar contact resistance and the resistances are in parallel. If the 7SKR1 sample had a total resistance of 0.174 mΩ and 4 fasteners in parallel, the average resistance per fastener would be  $4 \times 0.174 \text{ m}\Omega = 0.7 \text{ m}\Omega/\text{fastener}$ . This resistance per fastener value can be used for other joints in the wing that have similar fasteners and connecting materials.

The contact resistance of the fastener to connecting materials depends on several factors including material type, fastener type, fastener diameter, coatings and contact force. The contact resistance measured is actually a series resistance combination of material\_1, fastener contact to material\_1, fastener, fastener contact to material\_2 and material 2. For the resistance values listed in the table, we are assuming the fastener contact to materials 1 and 2 is the highest contributor to the total resistance across the panels and represents the value to be used in the model.

Measurement #	DC Resistance (mΩ)	Side A Thickness	Side B Thickness	Coating	Fastener Count
1	0.177	0.09	0.055	Primer	4
2	0.168	0.055	0.055	Fastener ID	Unique Features
3	0.191	0.06	0.055	HST11-6	Sealant on joint
4	0.167	0.055	0.055	Fastener Diameter (Inch)	
5	0.166	0.09	0.055	.189	
Average	0.1738	0.07	0.055		

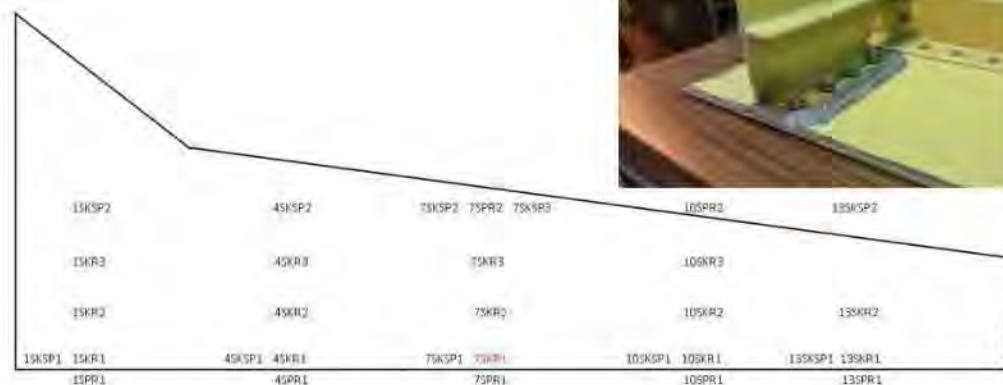


Figure 18: DC Resistance measurement results for a Rib 7 to upper skin sample.

### Model Cell Size

The FDTD simulation technique discretizes a problem in both space and time. Based on the model geometry described above, the problem space was meshed using a cubic grid of 12.5 mm. This mesh size allows for fine detail representation such that individual fasteners can be accurately represented with the model, but still allows computations to be completed efficiently. As the mesh size of a problem decreases, the computation time increases. This cell size allows for efficient computation and adequate geometry resolution.

### Model Tracking

The tracking of components and assumptions used in the CEM model is essential to verify the accuracy of the model to actual aircraft designs. A Configuration Control spreadsheet document identifying all components used in the modeling process along with their material properties has been created. A sample of the Configuration Control document for the wing structures is provided in Figure 19. This document should be referenced to identify all model components and track the following information:

- Component descriptions
- Material type and associated resistivity
- Component thickness
- Computed conductivities for parameter assignment based on model mesh size
- Set information that allows engineers to reference components in the CADfix model
- Model cell sizes used for components
- Simplifying assumptions used for this component



EMA MODEL CONFIGURATION CONTROL - Structural Surfaces							
Component Description	Material	Parameter Assignment				CAD/fix Material Type	EMA Model Modification Notes
		Actual Conductivity (S/m)	Actual Thickness (mm)	Model Cell Size (mm)	Model Conductivity (S/m)		
Lower wing skin	2124	2.38E+07	3.5	12.5	7.48E+06	Isotropic Surface	Assumed constant thickness. CATIA body didn't exist. Created from shell of surface.
Upper wing skin	7075	2.18E+07	5.5	12.5	2.13E+07	Isotropic Surface	Assumed constant thickness. Replaced body with surfaces.
Lower skin access panels	7050	2.12E+07	1.00	12.5	1.86E+06	Isotropic Surface	Assumed constant thickness. Replaced bodies with surfaces.
Leading edge spar	7050	2.12E+07	2.19	12.5	1.96E+06	Isotropic Surface	Assumed constant thickness. Replaced bodies with surfaces.
Trailing edge spar	7050	2.12E+07	3.28	12.5	6.09E+06	Isotropic Surface	Assumed constant thickness. Replaced bodies with surfaces.
Trailing edge spar	7050	2.12E+07	3.28	12.5	6.09E+06	Isotropic Surface	Assumed constant thickness. Replaced bodies with surfaces.
Trailing edge spar	7050	1.00E+04	3.28	12.5	2.62E+03	Isotropic Surface	Assumed constant thickness. Replaced bodies with surfaces.
Trailing edge spar	7050	2.12E+07	3.28	12.5	6.09E+06	Isotropic Surface	Assumed constant thickness. Replaced bodies with surfaces.
Wing box ribs (root inboard)	7075	2.58E+07	3.29	12.5	4.08E+06	Isotropic Surface	Assumed constant thickness. Replaced bodies with surfaces.
Wing box ribs	7075	2.58E+07	3.05	12.5	4.17E+06	Isotropic Surface	Assumed constant thickness. Replaced bodies with surfaces.
Wing box ribs	7075	2.58E+07	3.11	12.5	4.32E+06	Isotropic Surface	Assumed constant thickness. Replaced bodies with surfaces.

Figure 19: Configuration control spreadsheet excerpt for main aircraft skins

## Model Validation Simulations

When performing simulations for certification support, the numerical results must be validated against test results for the aircraft design in question. This validation effort gives confidence that the simulation model accurately determines the lightning response and captures the important EM behavior. Additionally, the validation effort will help to establish margins, or levels of uncertainty that may be applied to the simulation results. Validations performed on previous certification programs have shown that it may be inappropriate to apply a single margin to all lightning simulation results. This makes sense considering that currents flowing inside of metallic fuel tank may be on the order of amps while the surrounding skin currents are on the order of kiloamps; a difference of a thousand or more.

Individual probe correlation will strongly depend on the magnitude and coupling mechanism. Different coupling mechanisms (inductive, diffusion, resistive distribution) can have different levels of correlation. It has proven useful on previous certification programs to establish an upper bound, or enveloping level for all currents below a certain threshold for coupon testing. This current threshold is verified by simulation and experiment and this single waveform amplitude can more be more reasonably applied to system component tests. The simulation probes were incorporated into the model to match exactly the test configurations described above.

### Excitation Source Descriptions

For all attach/detach scenarios, the same Component A waveform used for testing was applied as the simulation source. In all cases, the lightning channel attachment is made with an electric current density source from the problem space boundary to the aircraft at the appropriate location. The injected lightning current flows through the aircraft according to the input geometry and material parameters as dictated by Maxwell's equations and the FDTD formulism. A perfectly conducting line extends from the vehicle detachment location to the RCS and then the problem space boundary as the lightning current exit channel.

### Simulation Validation Results

When comparing simulation and test results it is important not to develop an experimental bias and understand that test results can be wrong or misinterpreted. Neither testing nor simulation should be considered to provide the absolute truth in aircraft lightning response, which is why margin, or uncertainties are applied to the results. Both methods are good engineering approaches to understand complex aircraft lightning interactions. It is common in testing that if lightning results look reasonable, a standard margin value of 6 dB (factor of 2) is applied to all results. With the high-quality complex modeling options that exist today, the simulation results, once validated, may provide an appropriate electromagnetic response that can be directly referenced without the need for complex margin development.

Lightning test results can be wrong or misleading. Aircraft manufacturers and authorities should review the test results and establish a certain confidence in the results to define the aircraft lightning transient environment. If some test results are questionable, there may be a need to retest or perform some additional analysis to determine the "correct" response of the aircraft in the questionable areas. A margin level of 6 dB for test results is often accepted without significant explanation. Similarly, all simulation results should be reviewed for quality and questionable results should be further investigated. The combination of analysis and a small validation effort can reasonably be expected to be as reliable as a single lightning test program on one aircraft. It is not practical to require multiple aircraft lightning tests by multiple test houses. Rather, with the modelling ability and industry experience that exists today, analytical approaches can be viewed as favorably as full vehicle testing if the method and results are justifiable.

There is a real economic and practical justification to ease the burden of simulation validation and margin development. If reasonable justification and engineering judgement can provide evidence that simulated lightning transients are similar to those acquired from testing, simulations alone will give a legitimate answer to the actual aircraft lightning environment definition. There is no present quantitative margin development approach for lightning transient phenomena provided in industry standards. The confidence level is left up to the OEM and ACO to agree on an approach. Because there are no established criteria for simulation validation margins, each authority has a different experience, or expectation of what is required for margin development and what final margins should be. Once simulation results can qualitatively be shown to provide similar results as test methods, magnitudes on the same order and generally similar waveforms, a standard 6 dB margin should be accepted by industry.

Just as no test result should be accepted without understanding the EM coupling mechanisms involved, the sensibility of all simulation results should be evaluated. However, there are some real advantages of using simulation over testing:

- Simulation can capture the aircraft in flight configuration
- No RCS, hangar or ground effects
- No adjusting aircraft components to include test equipment
- No interference from test equipment



- No noise from test generator
- No data acquisition limits in time or scope range
- If design changes occur or a faulty test results are identified later in the program, simulation models can efficiently be updated to evaluate the effects

The above points do not necessarily imply that more simulation analysis should be performed than what is required from testing.

If the aircraft is of a new design, establishing lightning transients may be more involved than for aircraft that similar designs to previously certified aircraft. Some level of large-scale testing may be valuable. However, the systematic model development approach implemented in this program can be applied to new aircraft without the need for full scale aircraft validation. It will be necessary to quantify important material parameters for structural resistivity or joint resistance. This is especially true for new composite materials with lightning strike protection (LSP) or other materials.

#### Amplitude Validation

The simulation results were compared to the experimental results to get a quantitative margin assessment for transient amplitudes. All the simulated peak values are within 3 dB of the test peak values for all probes used. A summary scatter plot comparing all peak magnitudes for experimental and simulation data is extremely insightful when establishing margins for all ranges of results. These summary plots are provided for each probe type in sections below. By quantitatively comparing peak magnitudes and times and qualitatively comparing waveforms, an overall assessment of the simulation accuracy can be developed.

#### Waveform Validation

In addition to amplitude comparison, some evaluation about the transient waveforms is required. Whether using full vehicle testing or simulations, all the transient results are typically converted to standardized DO-160 levels and waveforms for verification testing according to Section 22. It is clear from visual inspection and comparison of peak times that the simulation and measurement results translate to nearly identical waveform specification according to DO-160. For this reason, no quantitative assessment of waveform validation is required or provided. Any issues with verification testing according to these waveforms could be explored with refined analysis as needed. Additionally, waveform reduction could be performed to quantify important waveform characteristics like peak amplitude, action integral, maximum rate of rise and total charge transfer.

#### B-dot Probes

Magnetic field probes, or B-dot probes, are indicative of the currents passing through the structure directly beneath the probe. They are very useful from a simulation validation standpoint because they can be placed on large aircraft structures that current probes cannot be placed around. For example, the current distribution on a wing skin can be mapped with B-dot probes, where it is impossible to place current probes around small sections of the structure during testing. By placing B-dot probes around various aircraft structures during testing, this provides a useful mapping of current densities that can show how well the simulation captures the current distributions in the aircraft structures. The B-dot probes are measured as voltages during testing and are integrated during post processing to get the underlying magnetic field. Surface current densities are measured as magnetic fields in EMA3D in a single FDTD cell.

The full data summary showing all B-dot probes is provided in Figure 20 below. The quality of results is viewed with a scatter plot showing the comparison of simulated to experimental results.

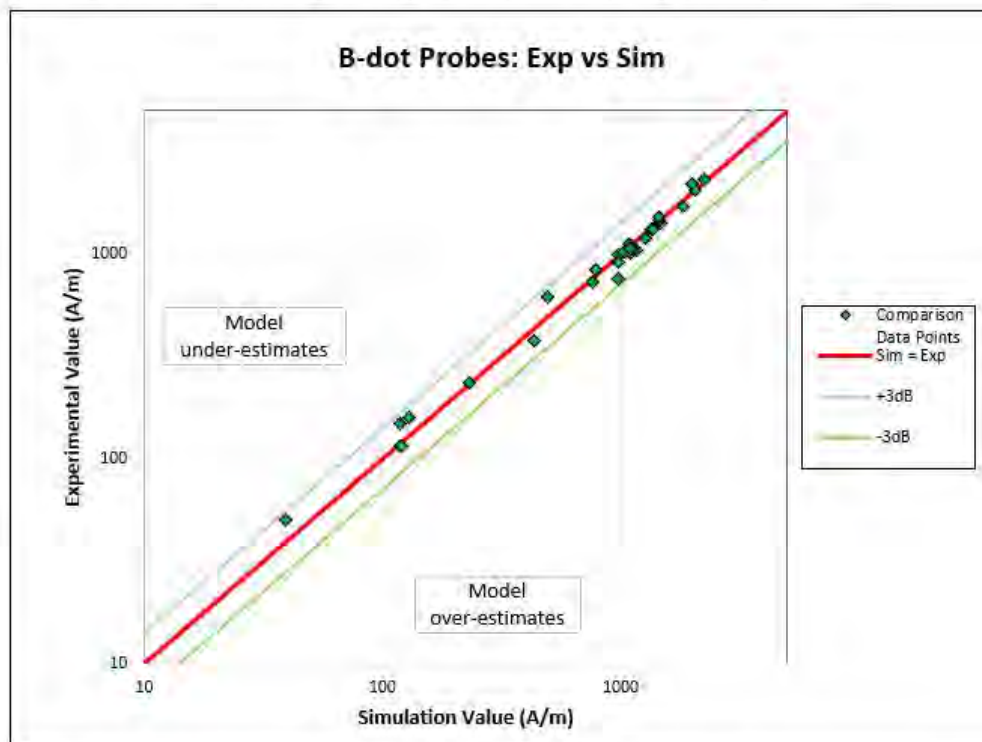


Figure 20: Full data summary scatter plot for B-dot probes. 3 dB lines added to help quantify margins.

The scatter plot correlation indicates an excellent overall correlation between experimental and simulated results. This correlation occurs for many probe locations all around and inside the fuel tank regions including:

- Upper and lower skins
- Various LE skin and TE spar regions
- Internal rib near a struck fastener

This high level of correlation across wing structure locations gives high confidence that the simulation model is capturing accurate current distributions in the aircraft structures. Some examples of extremely high correlation with B-dot probes are shown below in Figures 21 and 22. The experimental and simulation result are nearly identical in peak and wave shape for these probe locations. Figure 21 shows an external surface current near Rib 9 for configuration 1. The exterior currents on the wing match the injected Component A current. The current density measured on Rib 7 just beneath the struck fastener in configuration 3 has a much slower waveform because of the diffusion time associated with the metal wing. Both experimental and simulated waveforms peak around 200  $\mu$ s, but at a much lower amplitude than what is seen on the exterior structures. Other examples of the high-quality correlation are provided for all remaining B-dot probes in Appendix A.



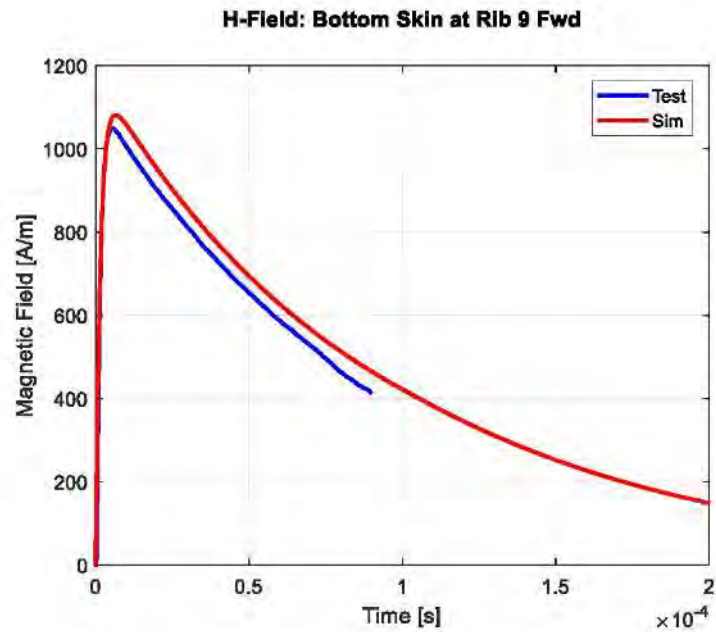


Figure 21: Surface current density on lower skin LE side near Rib 9 for configuration 1.

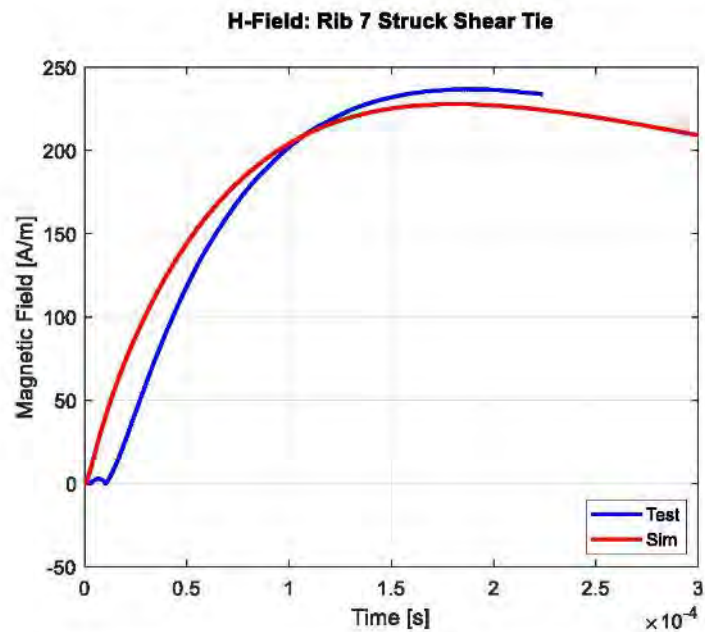


Figure 22: Surface current density on Rib 7 beneath struck fastener for configuration 3.

### Current Probes

The current distribution between structural elements such as ribs, skins, spars, stringer clips, etc. can sometimes be determined using bulk current probes. These bulk current probes are representative of current transformer probes used in testing. These probes capture all the current flowing through the material contained within the probe loop. These types of probes work very well on straight conductors like fuel tubes, hydraulics tubes, bonding jumpers and load bearing struts or links. These types of probes are not particularly well suited for structural joints that contain multiple fasteners. Although the bulk current probes can measure total structural component currents, they cannot determine how current distribution varies along the joint. In some cases, current could be flowing in one direction through some of the fasteners and in the opposite direction through neighboring fasteners. A bulk current value for these types of complex joints is very representative of the actual current pattern.

Test injection and detach location currents were verified for every experiment performed. These attach and detach currents match a 3 kA amplitude Component A waveform. The comparison of these waveforms serves only to verify that the same amount of current is injected into the aircraft and will not be considered for validation assessment. Due to the lack of systems components in this test wing, only 1 current probe was implemented for a 4 AWG wire that was strung between rib 6 and rib 15 as shown in Figure 24. The other current probes were for the distributed currents at root wing detach for configuration 1. All the current probes had an excellent correlation as shown in the scatter plot summary in Figure 23.

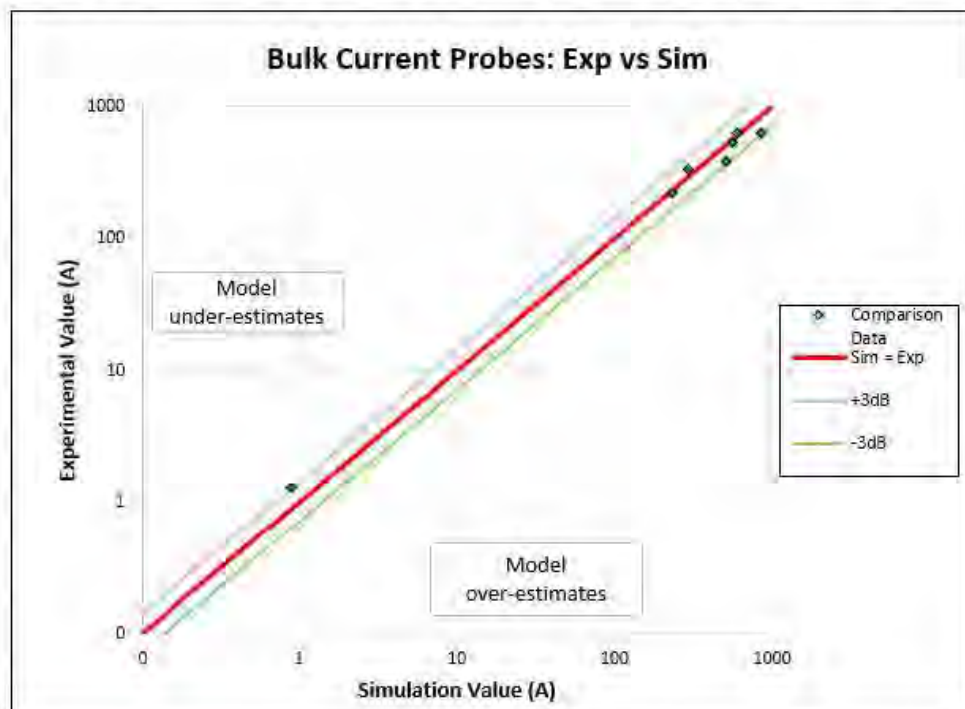


Figure 23: Bulk Current Probe Scatter Plot

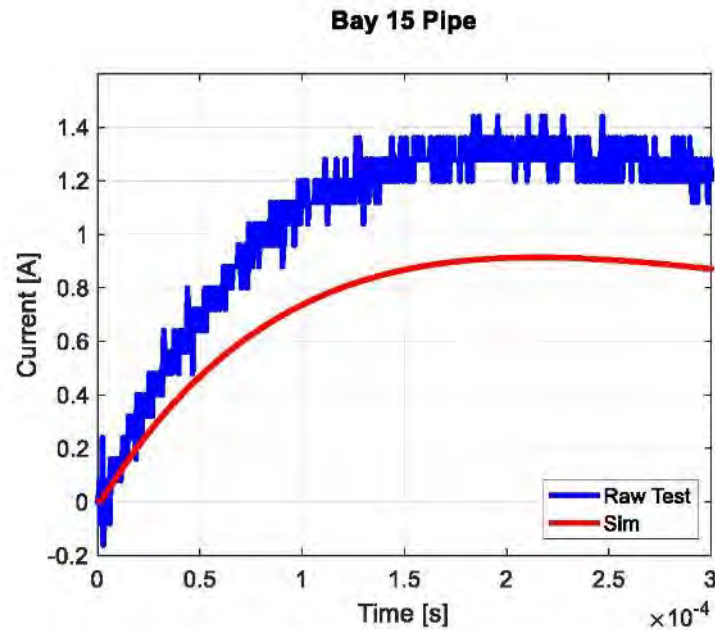


Figure 24: Wire current spanning Ribs 6 to 15 in configuration 1.

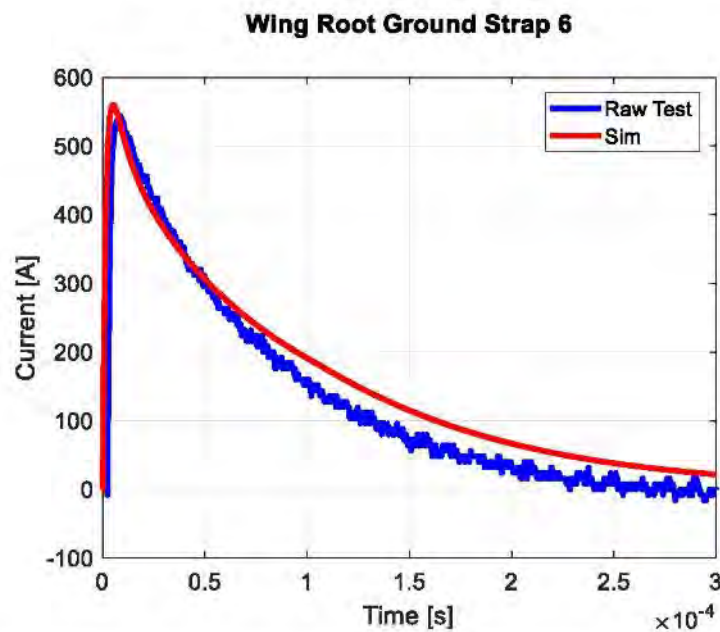


Figure 25: Ground strap current for one of the root wing distributed detach currents in configuration 1.



### Current Density Images

The currents that transfer inside the fuel tank regions are of the primary interest when considering ignition prevention. It is critical to get current distributions correct throughout the model, but it is often difficult to characterize currents inside the fuel regions. Probes can be added around system pipes and tubes but those were not available in this test article. Some successful characterization of magnetic fields on ribs was discussed above and is directly related to the currents flowing in materials. Rib connections to skins and spars may not be available to loop coil probes around. Even if flexible probes may fit into these crowded areas, there may be sensitivity issues with low signals and the active probe elements. Furthermore, the currents flowing through these loop probes may not be uniform throughout the structural joint and could provide misleading current values if bulk measurements are made.

The current densities associated with internal wing components is often complex in nature due to the many interfacing fasteners. Characterizing interface current levels can be quite difficult for connections that span multiple fasteners. For rib shear tie or rib post connections that contain multiple fasteners, the current distribution can vary significantly across the length of the joint. Using a bulk current probe to measure all the current flowing down the shear tie component cannot capture the complex current distribution across the connection and may underestimate the amount of current that flows down a struck fastener. When fasteners penetrating the fuel tank are directly struck, the attached lightning current will mostly spread to the skins. Some portion of current will flow down the struck fastener to the underlying rib or spar. Although current is flowing down through the struck fastener, current can circulate and flow up neighboring fasteners or shear ties back to the skin. The upward flowing currents in the shear tie connection may oppose some of the currents flowing down the struck fastener and complicate the bulk current measurement of a structural joint.

One of the significant advantages of simulation is the ability to characterize currents anywhere in the model, especially where physical probes cannot be placed in aircraft configurations. For configurations 2 and 3, current density images were taken of the ribs nears the current injection location. Arrows are added within the rib cells to indicate current flow direction around that particular cell. Figure 26 shows the Rib 12 current density evolution at 6, 30 and 270  $\mu$ s. Although the component A injected current peaks near 6  $\mu$ s, the current density on the rib does not significantly develop until much later in time, once the lightning current has had time to diffuse through the metallic wing skins. In the 270  $\mu$ s capture of Rib 7 in Figure 27, the current patterns are quite complex around the neighboring shear ties and both rib posts. These types of current patterns on internal structures can also be beneficial to explore when systems components are mounted to the ribs.

*Rib 12 Current Densities*

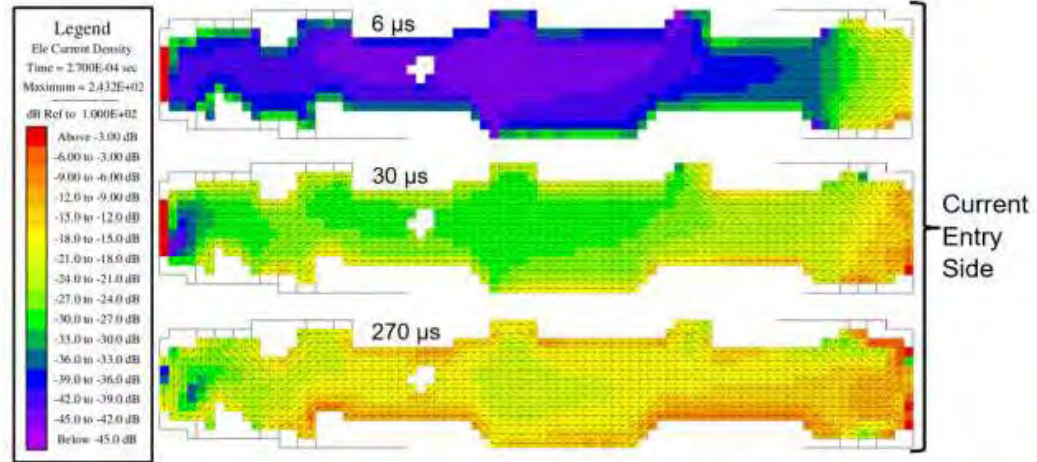


Figure 26: Rib 12 Current Density at 6, 30 and 270  $\mu$ s for Configuration 2.

*Rib 7 Current Densities*

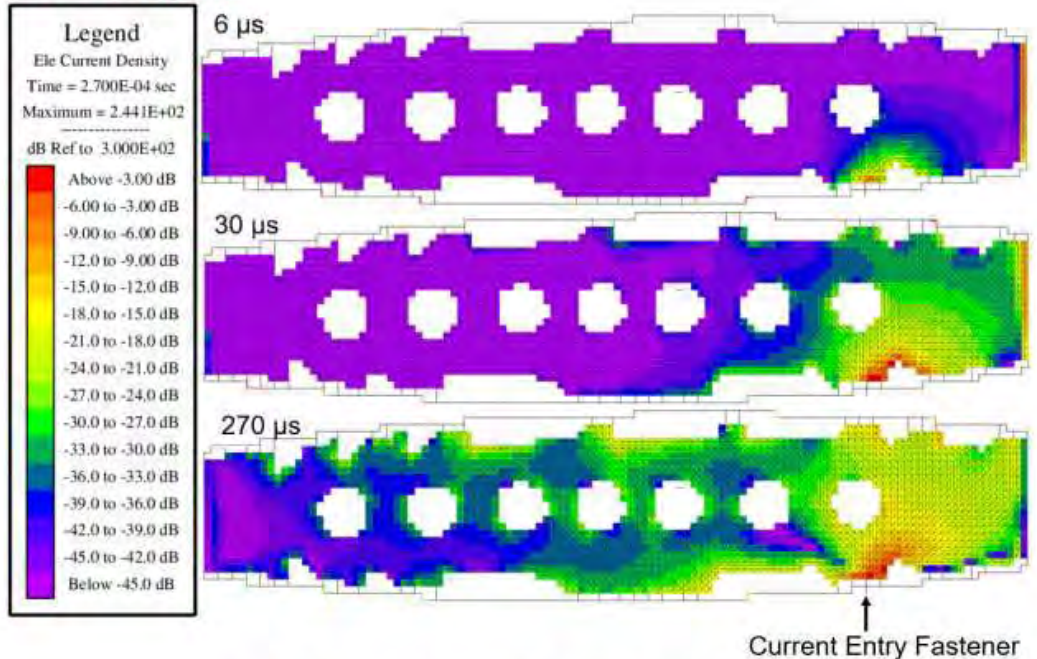


Figure 27: Rib 7 Current Density at 6, 30 and 270  $\mu$ s for Configuration 3.



#### Amplitude Margin Development Approach

A review of simulation and test results indicates that both methods give highly comparable transient amplitudes for all measurement locations. Peak value comparison plots were created, and it is shown in the comparative scatter plots that the simulation results are within 3 dB of experimental results for all measurements.

Some reviewers of simulation margin development believe multiple aspects of uncertainty should be included in the development process. One of the typical margins is a validation margin,  $M_{VAL}$ , that quantifies how well the analysis technique and specific model can match test results. Another margin may be expected to capture other uncertainties that aren't quantifiable from the validation effort. This second margin is related to the standard uncertainty that is typically applied to test results and will be referred to as  $M_{UNC}$ . A reasonable way to combine these types of uncertainty is to establish an overall margin that considers both aspects of uncertainty. The total margin,  $M_{TOT}$ , may be computed in a quadrature fashion as shown in equation 1. The values for uncertainty and validation margin should be computed using real factors and not the logarithmic ratios.

$$(1) \quad M_{TOT} = \sqrt{M_{VAL}^2 + M_{UNC}^2}$$

AC 20-136B paragraph (8)(i), Verify Compliance to the Requirements, discusses how margins account for uncertainties in the verification method. It also suggests that as confidence in the verification method increases, the margin can decrease. In this validation process, two methods for establishing aircraft lightning transients were used, one by full wing testing and one by full wing numerical simulation. The results of the validation effort provide greater confidence that each method provides an accurate response, and thereby lowers the standard uncertainty associated with each approach by itself. Therefore, it is reasonable to consider a margin that is lower than the standard uncertainty,  $M_{UNC}$ , value of 6 dB.

To consider how this proposed margin might be developed, let's assume a validation margin of 3 dB (factor of 1.4) is acceptable based on the correlation of simulation and experimental amplitudes. Since two techniques, simulation and testing, were used to validate each other and improve the confidence that both techniques capture the lightning response of the wing, let's assume the uncertainty margin is lowered to 3.5 dB (factor of 1.5) instead of the normal factor of 2 (6 dB). If the proposed values,  $M_{VAL} = 1.4$  and  $M_{UNC} = 1.5$ , are used and plugged into equation 1, this gives a total margin of  $M_{TOT} = 2$  (or 6 dB).

This final margin level is the same as the typical margin of 6 dB applied to test results but may carry less uncertainty than a result determined by testing alone since the results were determined using two techniques that validate each other.

If different levels of validation margin were determined based on probe amplitude or coupling technique, in a sliding scale fashion, then this same approach could be applied to determine total margins for the various correlation groups.

#### Waveform Comparison and Reduction

The above discussion on margins applies only to the peak amplitude quantification. It is also necessary to determine the waveform of the transient and understand the energy or action integral associated with each transient. It is clear from visual inspection alone that all comparisons have the same transient shape. Therefore, no detailed quantification of waveform is necessary as part of the validation. The transient waveforms in this effort are validated by visual inspection. In production aircraft, there are many different waveforms or combinations of waveforms that exist inside the aircraft during a lightning event and



validation by visual inspection alone may not be possible. In these cases, a more quantitative approach to peak time or action integral may be required.

Test houses should not be responsible for generating all possible waveforms that occur in a lightning event. However, lightning test houses and generators can typically produce the standardized lightning waveforms as identified in ARP 5412B. A reasonable approach to this problem is to convert all transient results (with appropriate applied margins) to standardized waveforms that are typically created by the test house. An important consideration of this waveform conversion is the rise time and action integral associated with the waveform. It would be reasonable to perform a waveform reduction to find equivalent waveforms for test houses to inject on the coupon samples. ARP 5415B contains explanations of how to perform waveform reduction and this exercise is not included as part of this project.

### Validation Conclusion

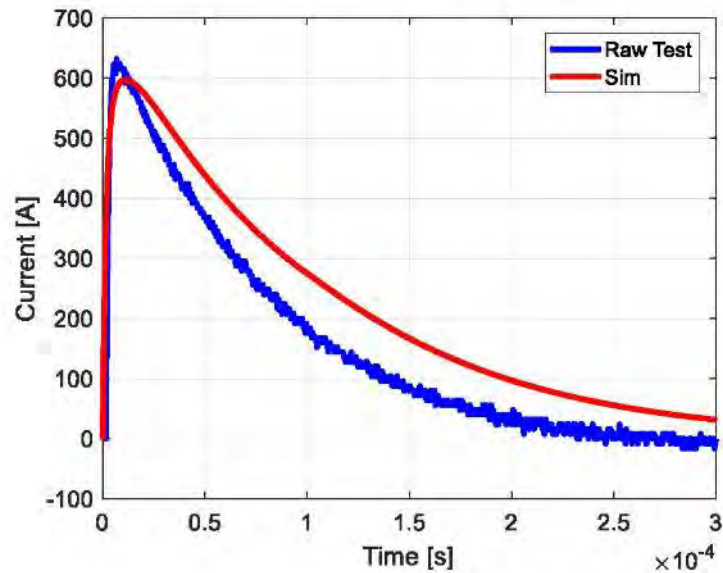
This paper demonstrates how complex CEM simulation models can be developed and simulated to determine high fidelity transient lightning responses in aircraft. The simulation results were compared to full wing test results to validate the model. Some discussions were provided about margin development. The modeling and validation techniques described in this paper can be used to support a certification program and to evaluate the lightning response of a complex aircraft in zone 3 fuel systems regions. The simulation approach described in paper is recognized in the guidance material as acceptable analysis method can be applied to many different aircraft and lightning attachment scenarios. Whenever using simulations to support a certification program it is critical that an analysis approach be discussed with the appropriate certifying authorities.

It is critical during the validation effort that both types of results, simulation and testing, are used to augment each other and help the designers achieve the full lightning coupling response needed for certification. A validation effort comparing simulation and experimental results is traditionally used to establish acceptable margins for all simulation results. There is not one single accepted approach and no standard or specific recommended practice exists to quantify CEM model validation for lightning transient phenomena. A correlation between experimental and simulated results has been accepted by aviation authorities using peak value and visual waveform comparisons, which is the method utilized in this program. An excellent correlation of simulation and experimental values is observed for all probes with peak value correlations within 3 dB. Furthermore, a method to combine a validation margin and overall uncertainty is presented. Detailed margin development is possible and often required. However, it is also reasonable to consider that once the simulation results are validated to a level agreed upon by the certifying authority, the simulation results can be used with a typical margin of 6 dB applied, just like what is done from testing.

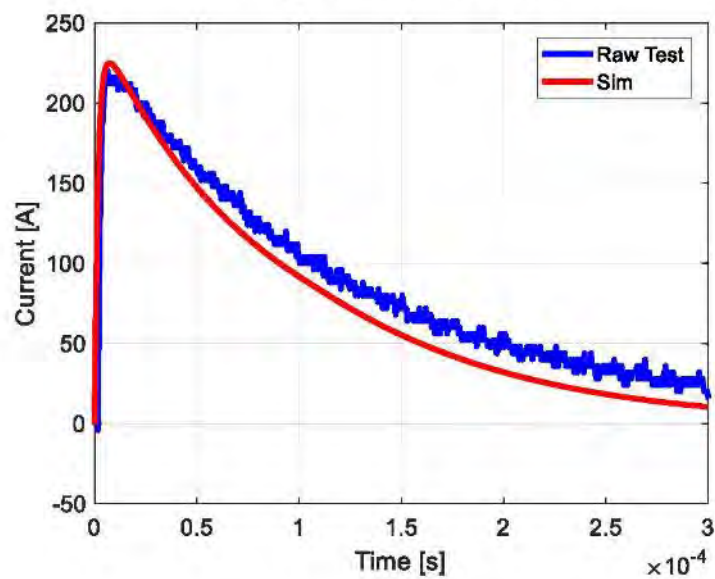
Using simulations for certification support is an attractive possibility to reduce full aircraft lightning testing. Full aircraft LTA tests are expensive to perform and tie up valuable aircraft availability during certification phases when the aircraft could be addressing valuable flight time or other certification activities. Another significant advantage of using simulations for the transient determination is the aircraft can be considered in its natural in-flight configuration that would occur during a lightning event. Whenever LTA tests are performed on aircraft, they are completed with return networks, equipment and test configurations that can alter the natural lightning coupling response of the cables. Simulations can produce transient results that are, in many ways, less perturbed than the test results.

Appendix A: Simulation and Test Validation Waveform Comparisons  
Configuration 1: Wing Tip to Distributed Wing Root

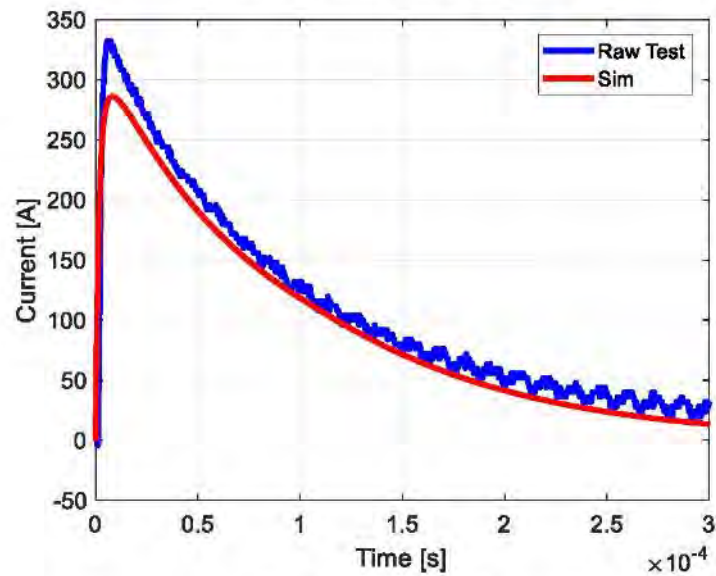
**Wing Root Ground Strap 1**



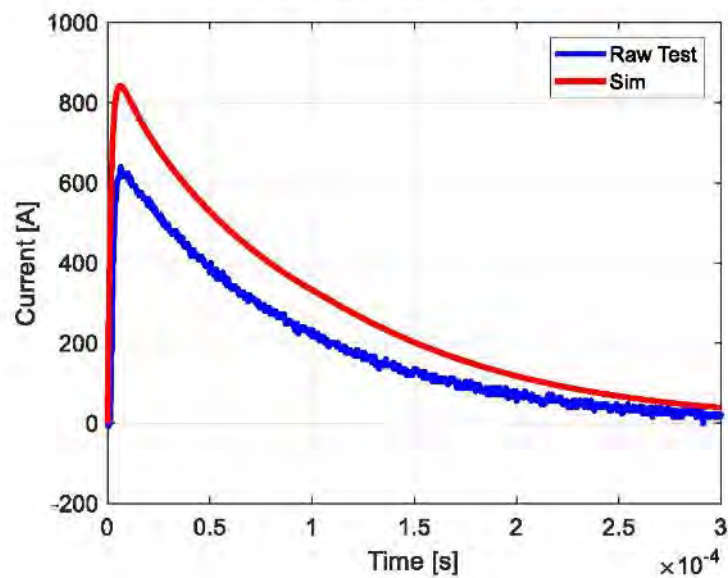
**Wing Root Ground Strap 2**



**Wing Root Ground Strap 3**

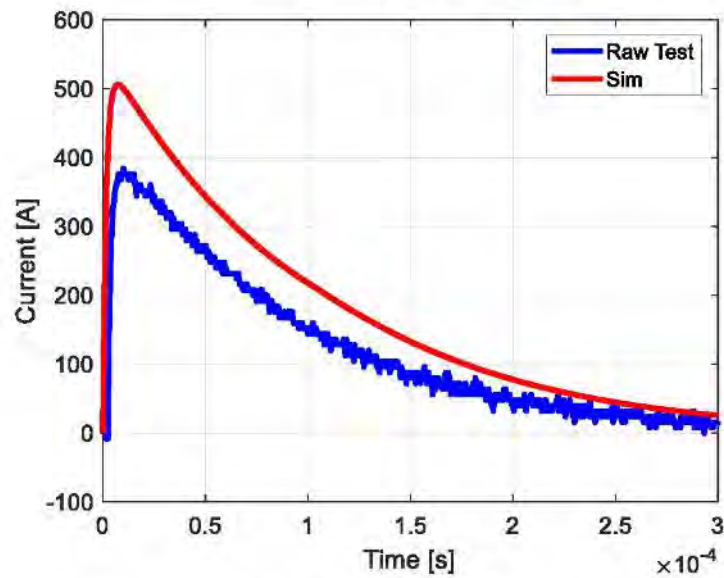


**Wing Root Ground Strap 4**

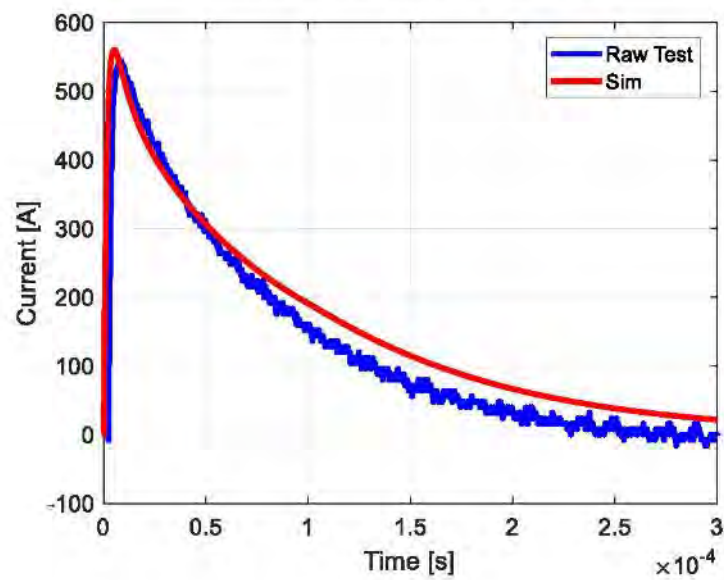




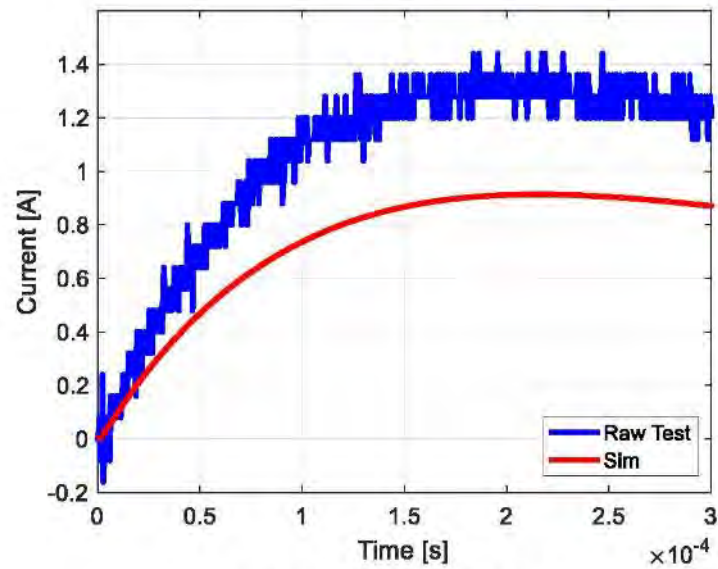
**Wing Root Ground Strap 5**



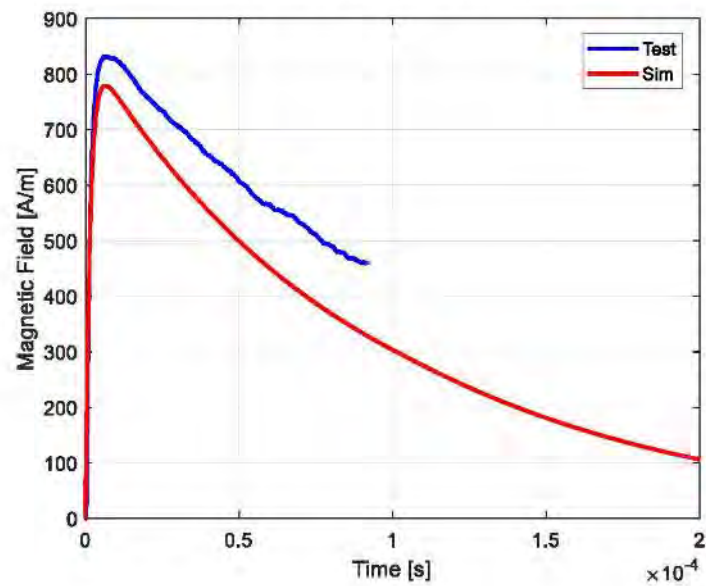
**Wing Root Ground Strap 6**



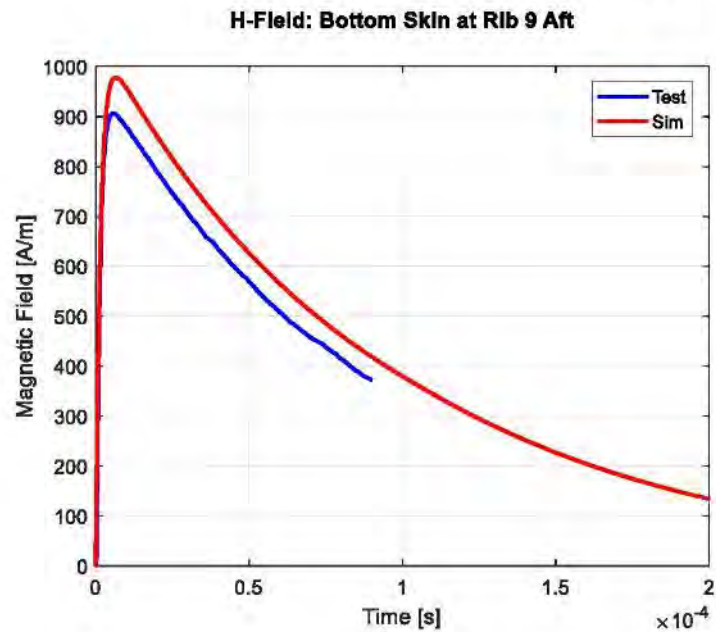
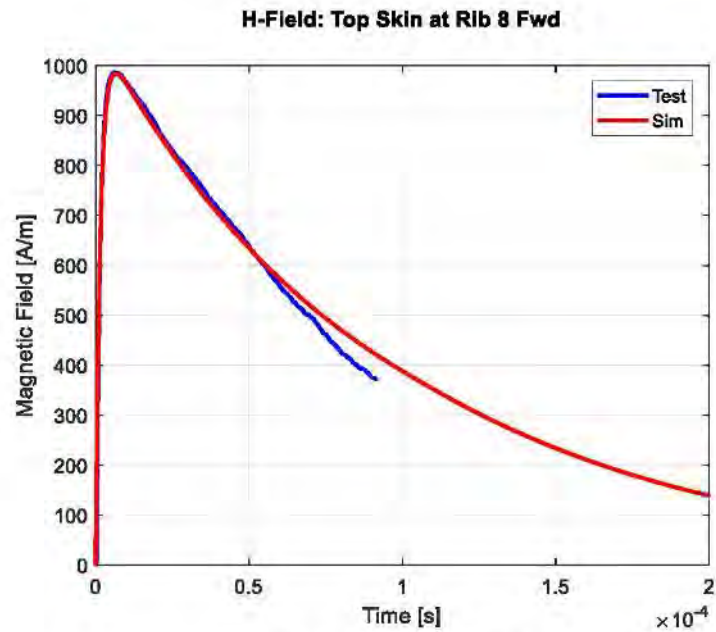
**Bay 15 Pipe**

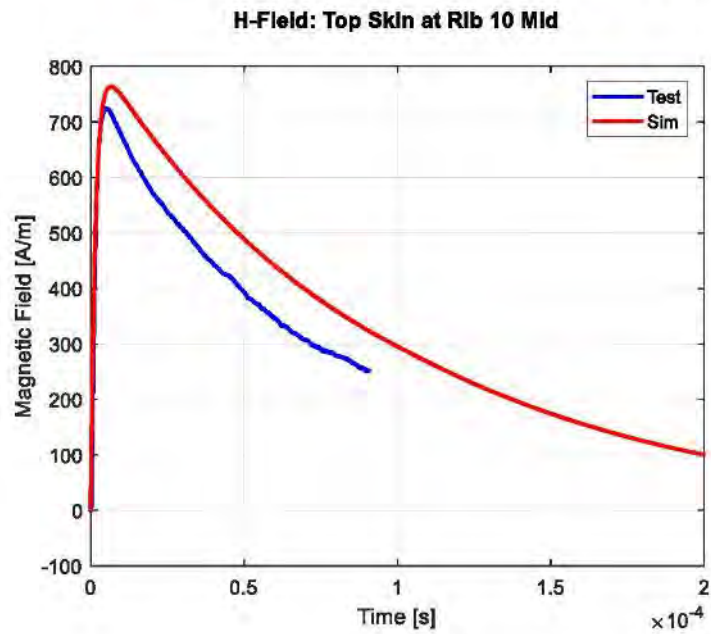
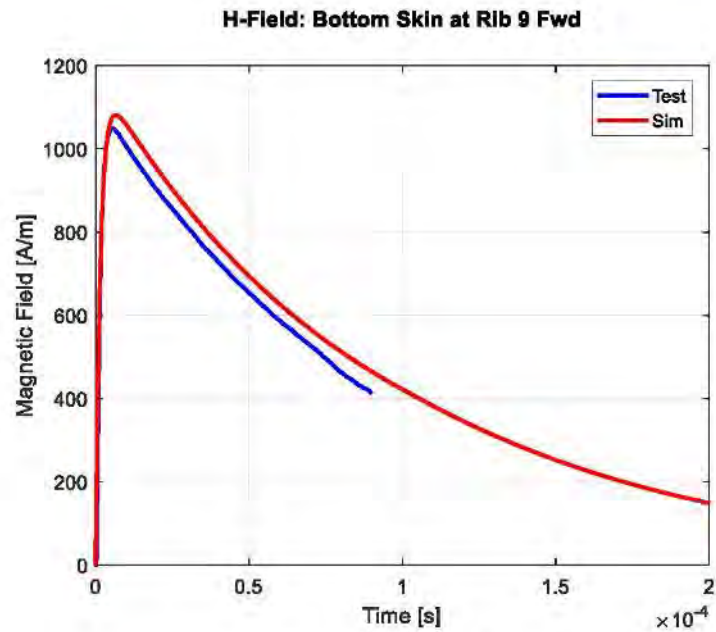


**H-Field: Top Skin at Rib 8 Aft**

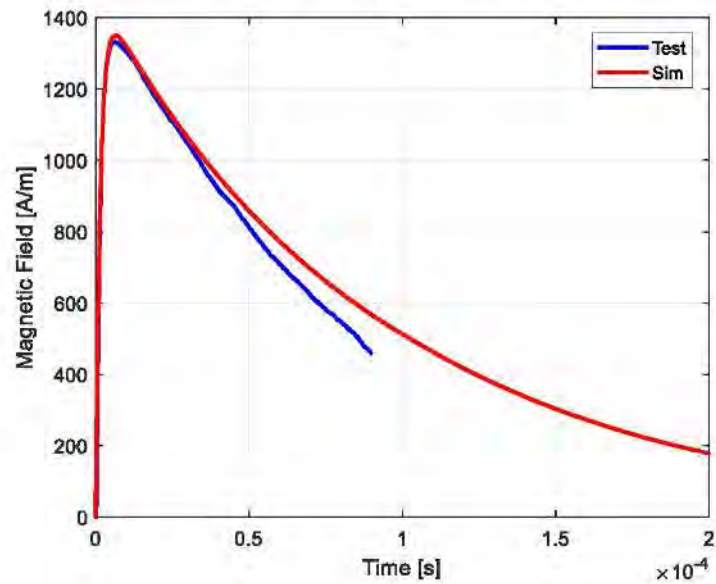




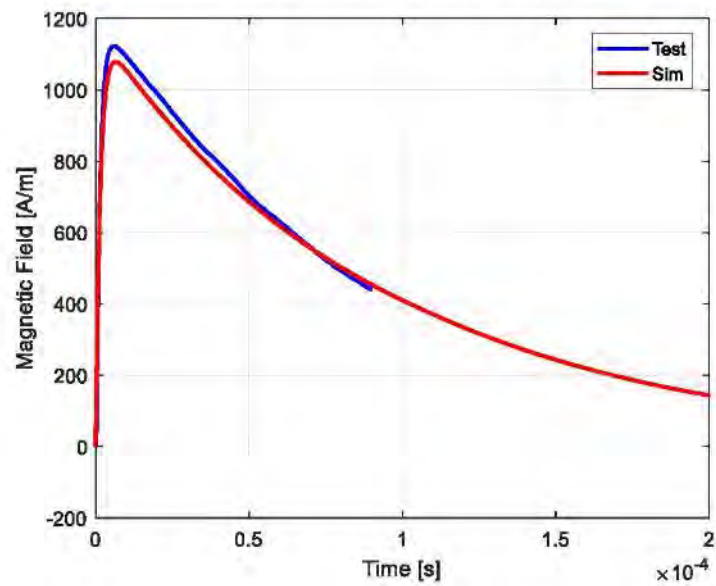


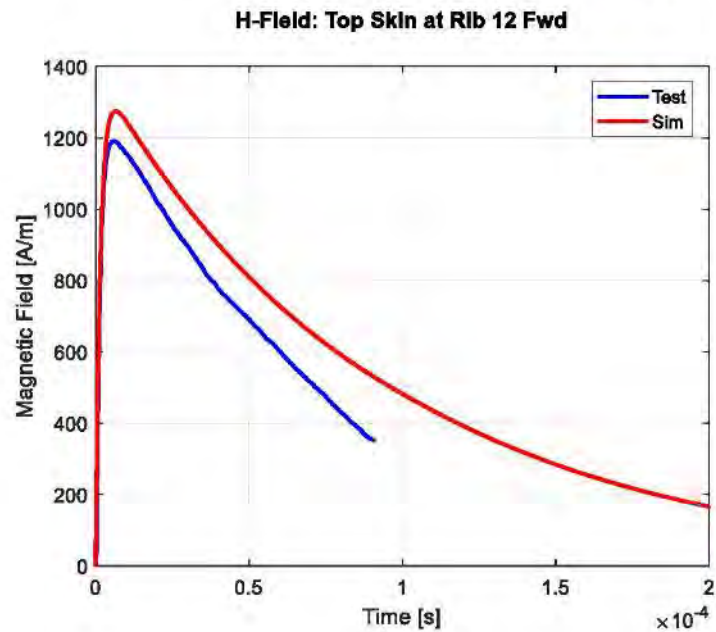
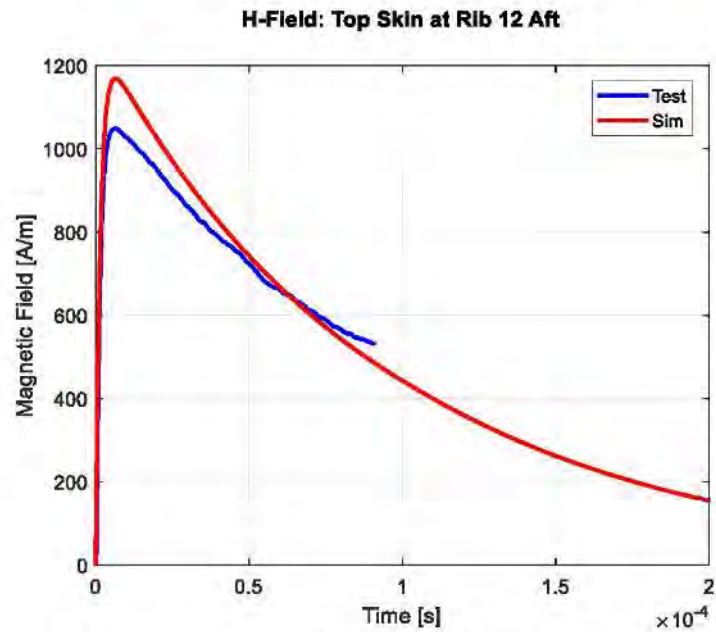


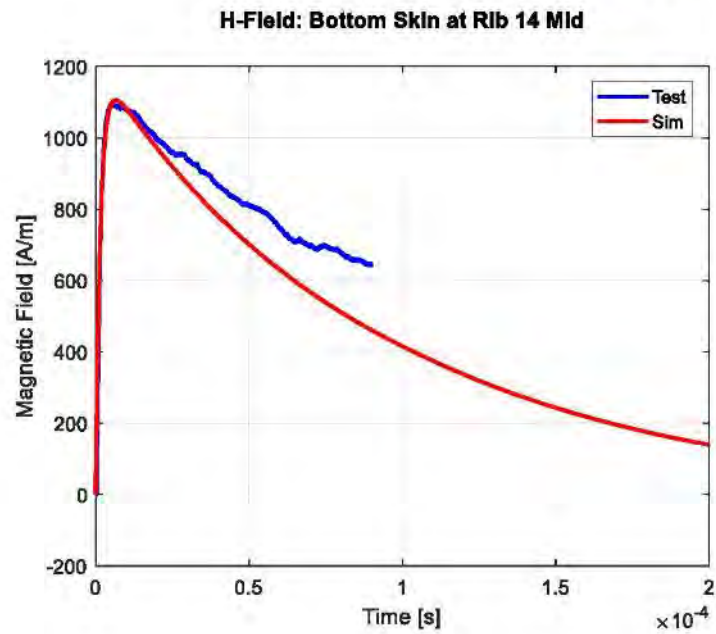
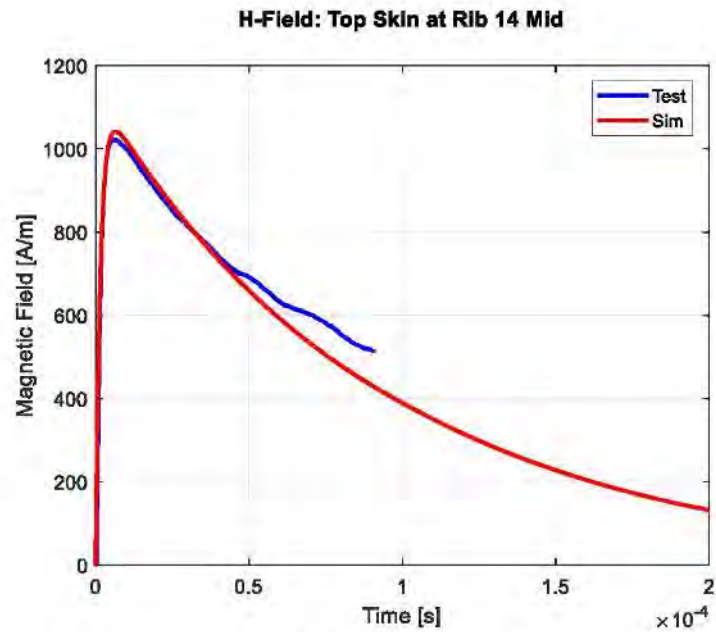
**H-Field: Bottom Skin at Rib 12 Fwd**



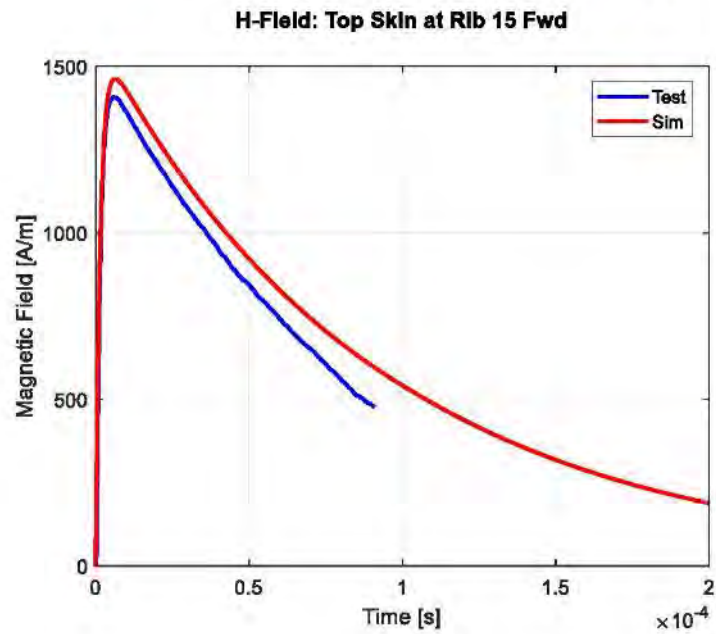
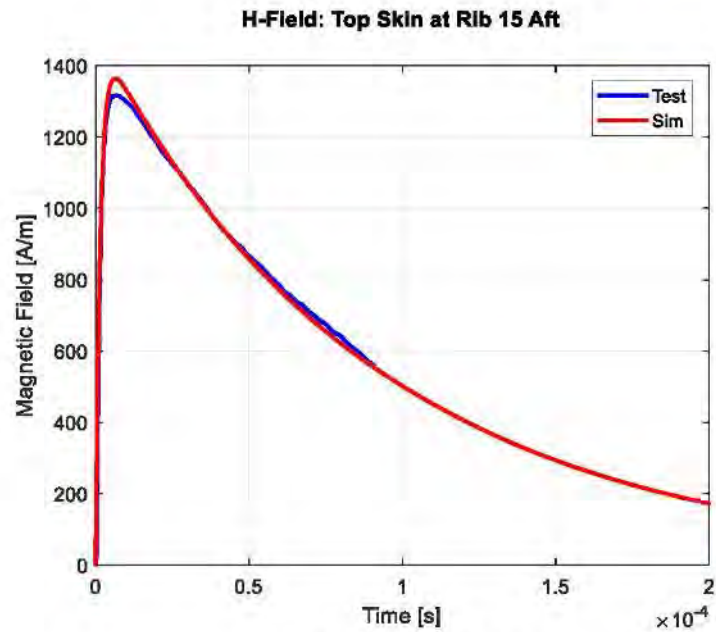
**H-Field: Bottom Skin at Rib 12 Aft**

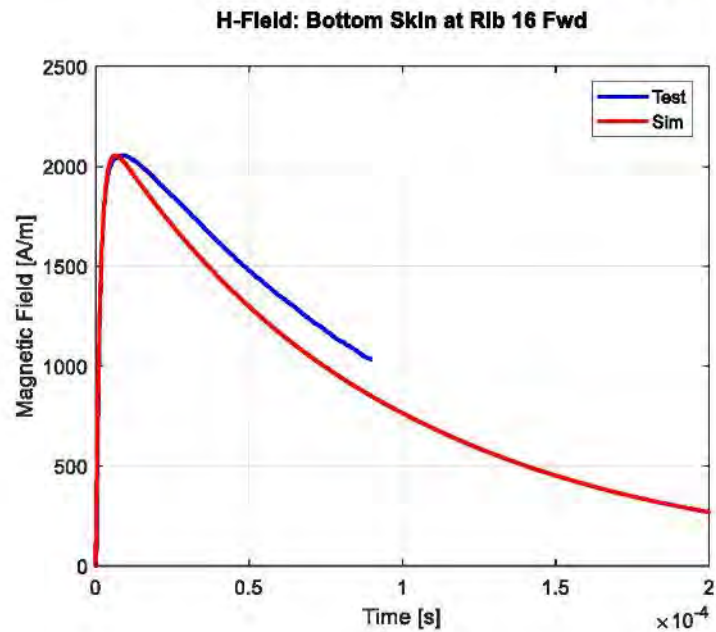
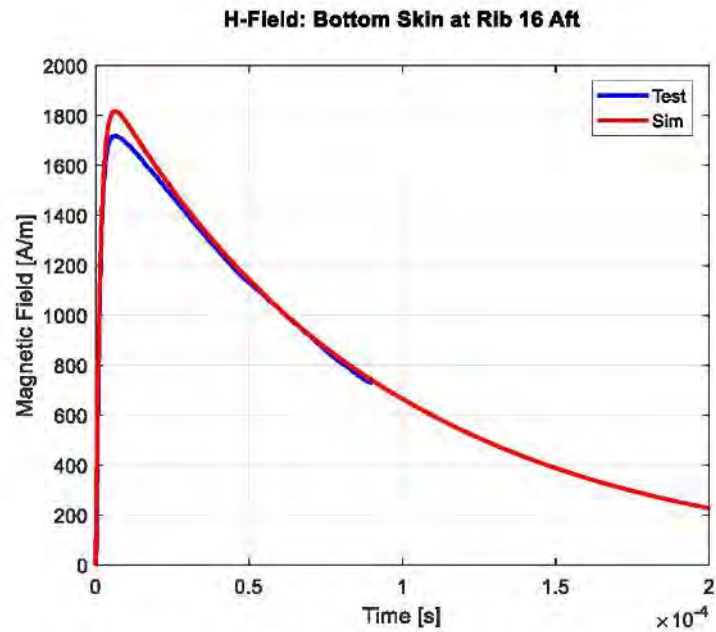


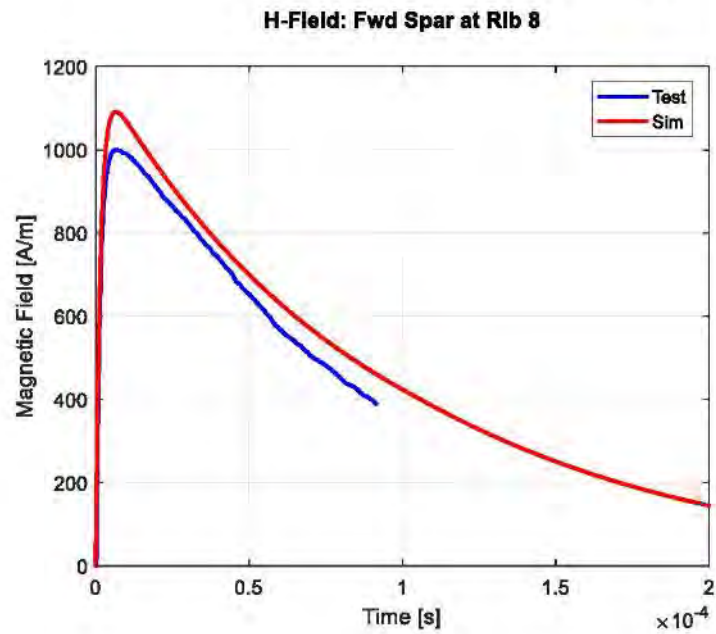
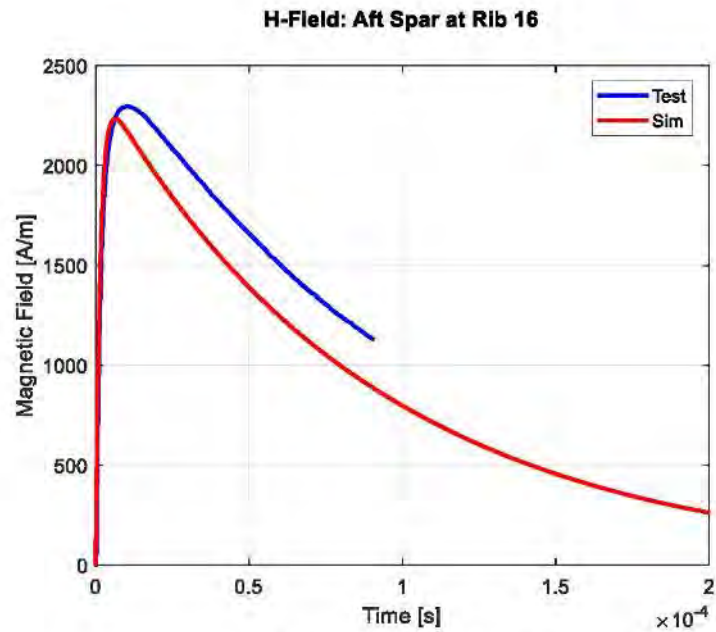






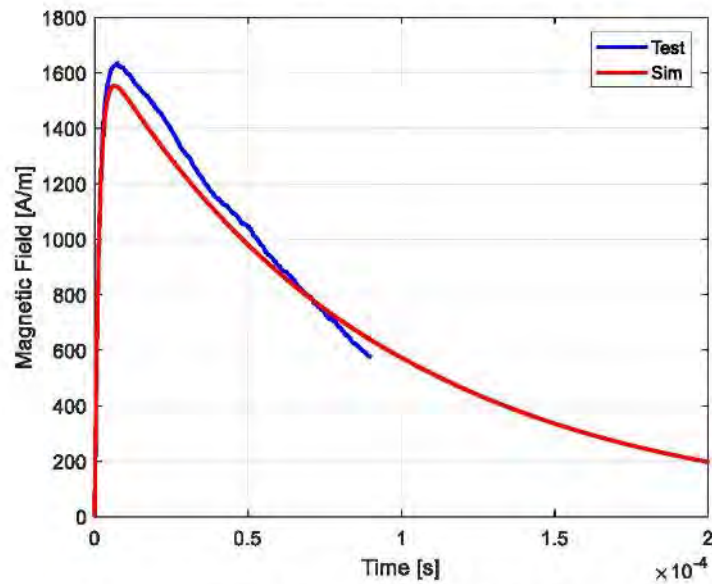




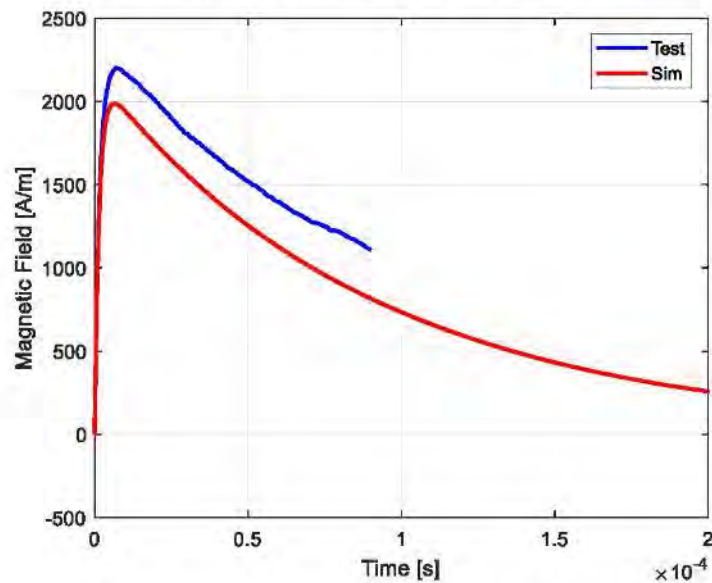


Configuration 2: LE Rib to TE Bracket

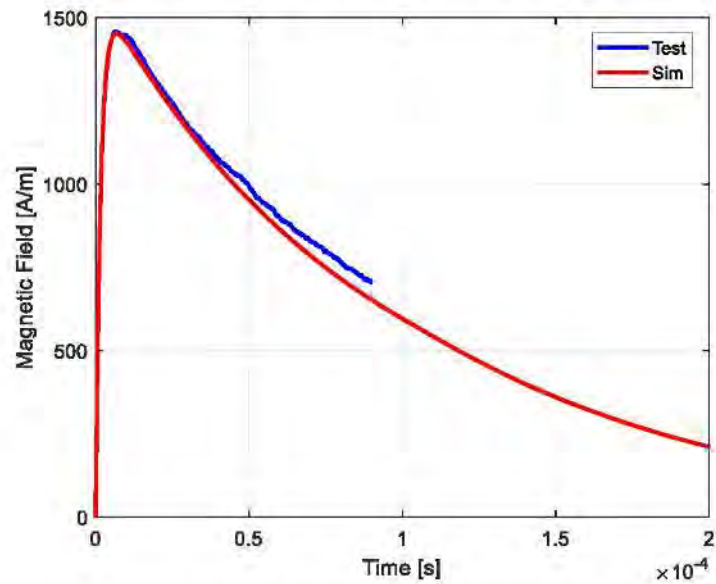
**H-Field: Upper Skin at Fwd Rib 12 Perp**



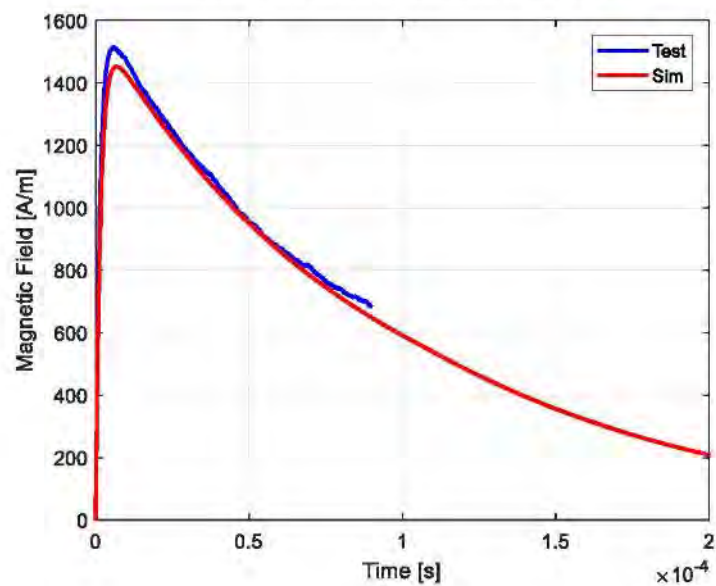
**H-Field: Bottom Skin at Fwd Rib 12 Per**



**H-Field: Upper Skin at Aft Rib 12 Perp**



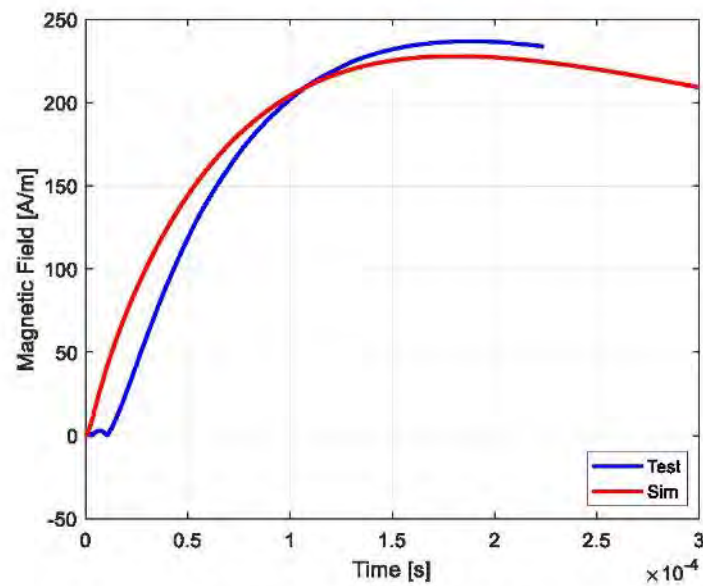
**H-Field: Bottom Skin at Aft Rib 12 Perp**



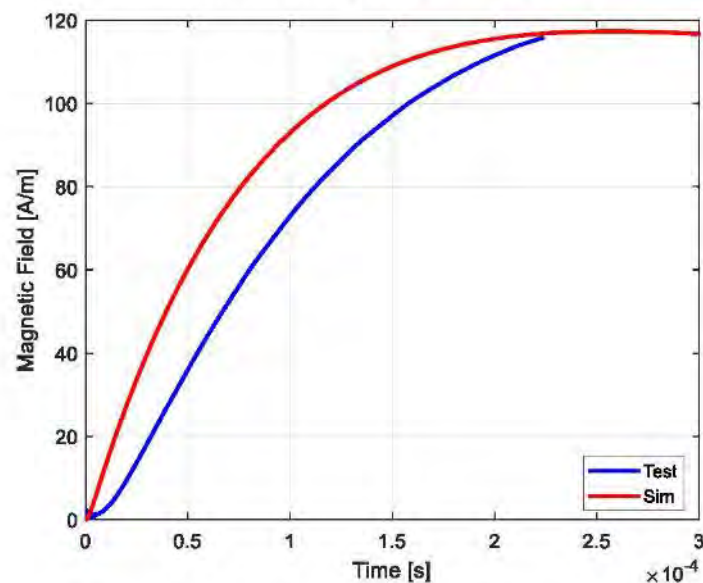


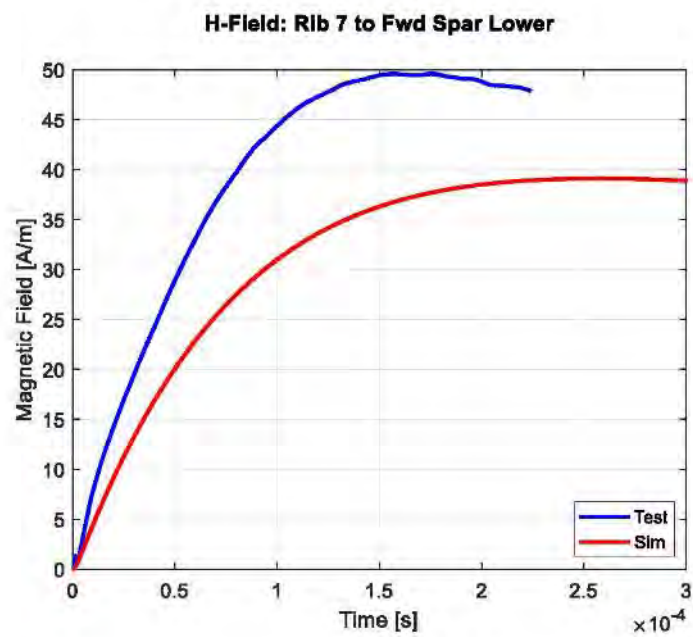
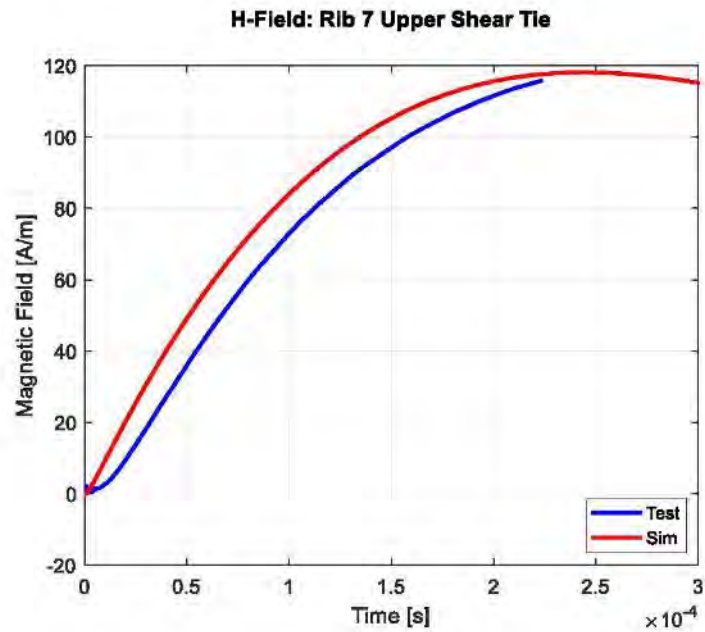
Configuration 3: Rib 7 Lower Skin Fastener to Upper Skin at LE Side of Wing root

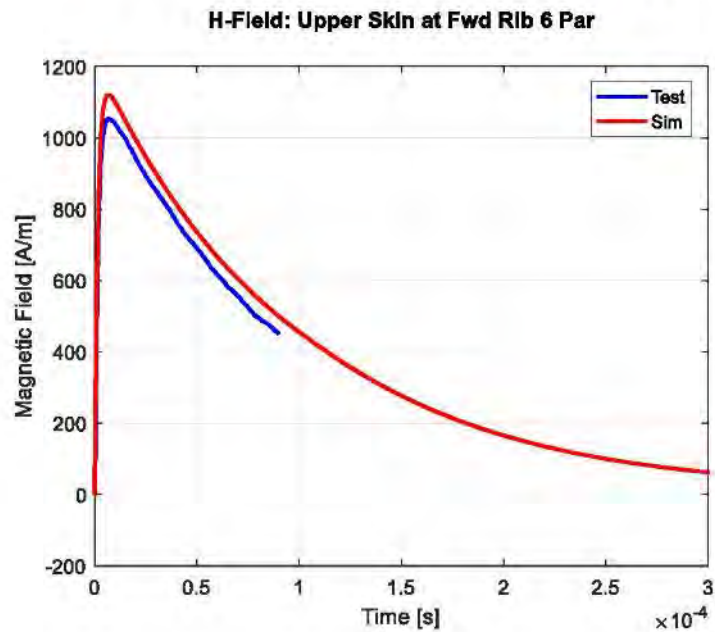
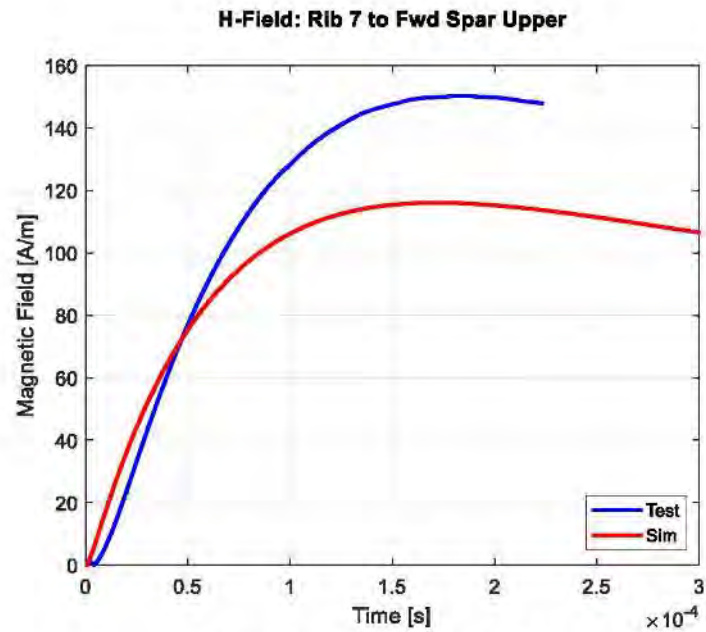
**H-Field: Rib 7 Struck Shear Tie**

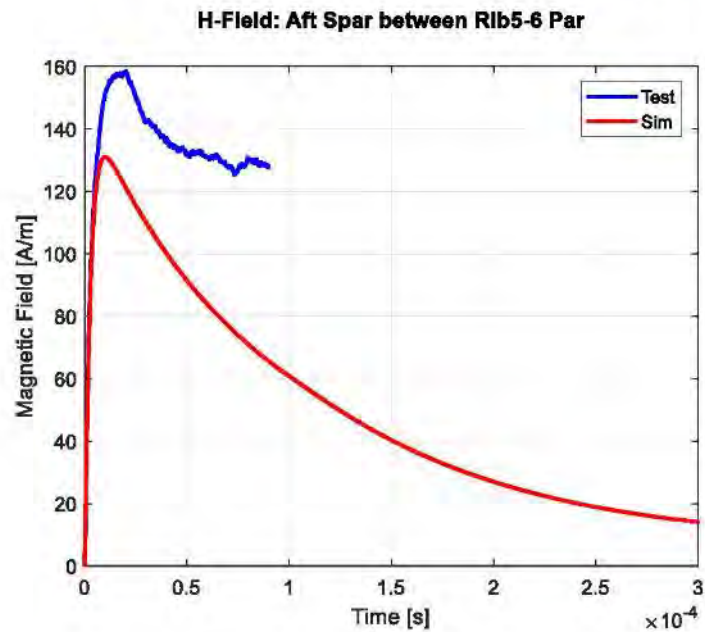
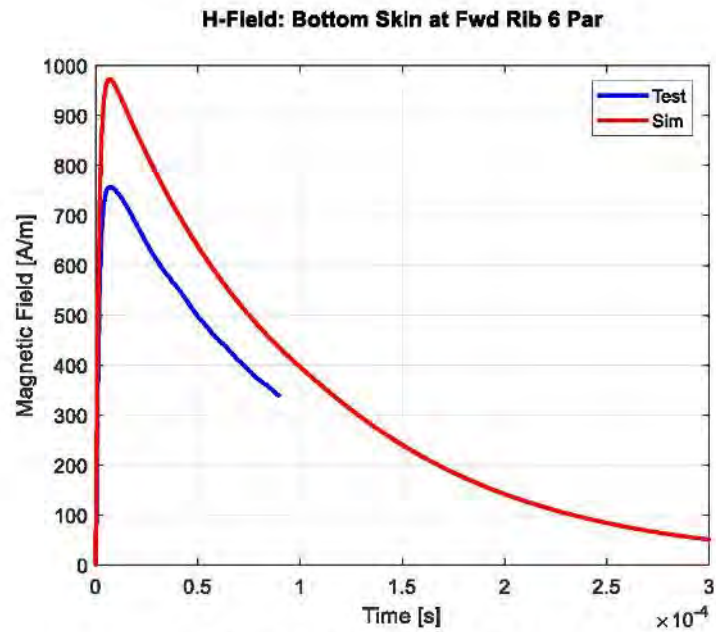


**H-Field: Rib 7 Lower Shear Tie Fwd**

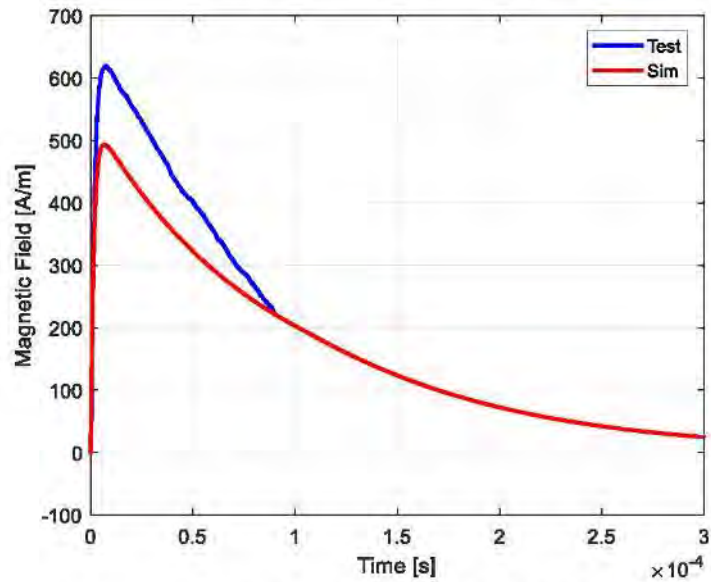




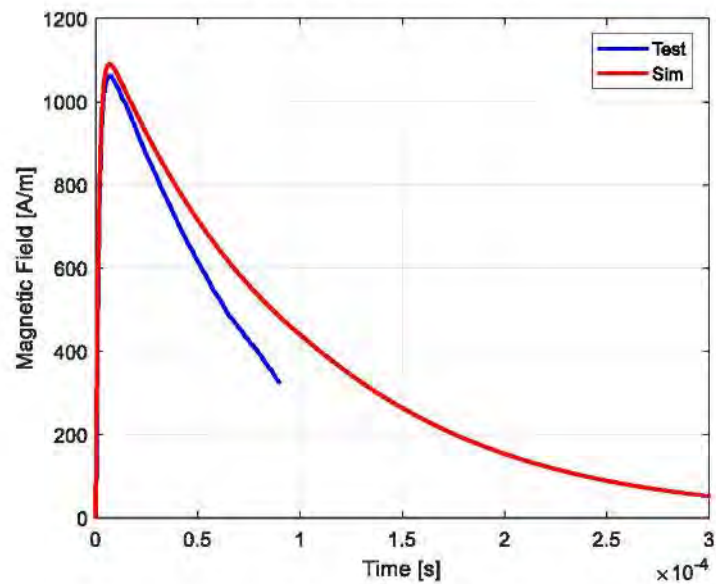




**H-Field: Upper Skin at Aft Rib 7 Par**



**H-Field: Fwd Spar between Rib5-6 Par**





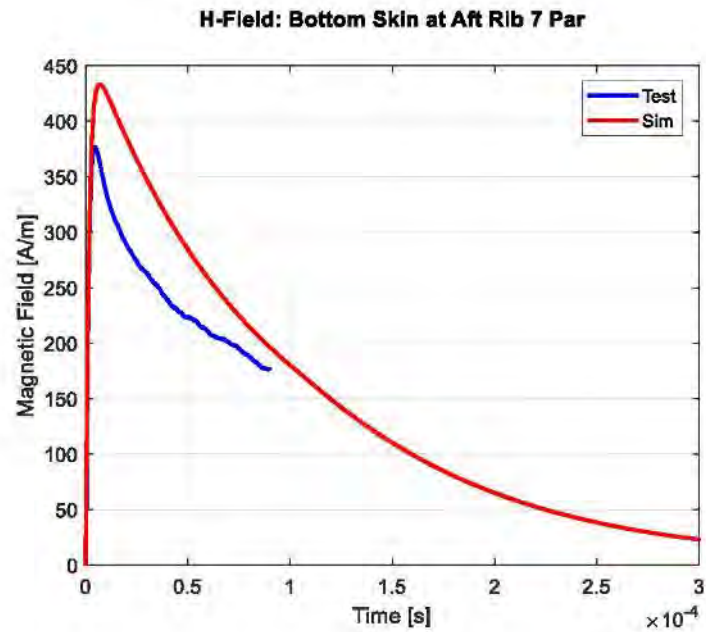


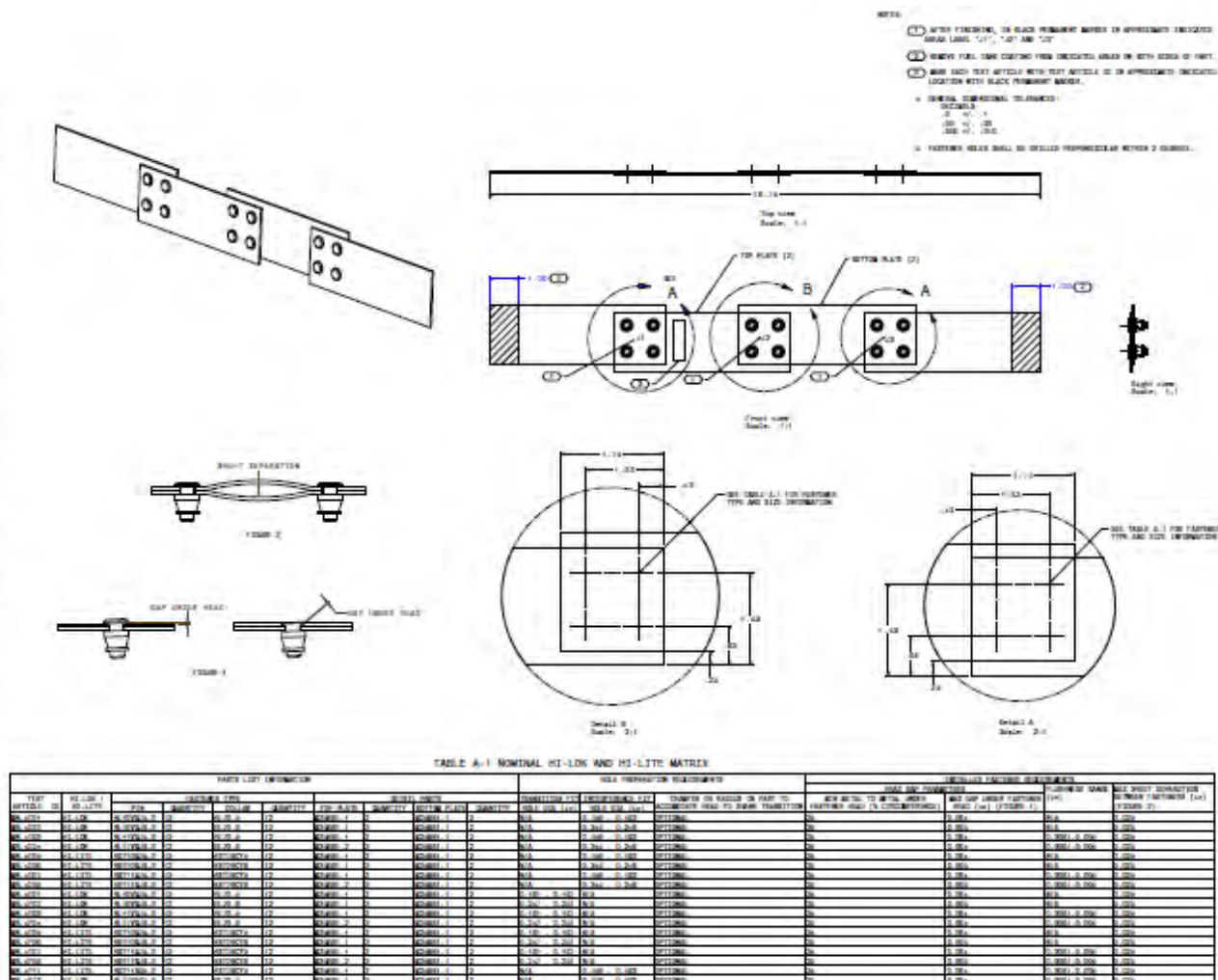
Figure 3-1: Assembly drawing of a three-bladed propeller. The drawing includes a perspective view at the top left, a top view at the top right, a front view at the bottom left, and a right side view at the bottom right. Dimensions are provided for various parts: blade length (1.125), blade width (0.875), hub diameter (0.875), and blade thickness (0.125). Section lines are used to indicate cross-sections. Notes specify that the blades are to be made of aluminum and that the hub is to be made of steel. The drawing is labeled 'Figure 3-1' and 'Sheet 1 of 1'.

TABLE A-2 NOMINAL HI-LOK AND HI-LITE MATRIX

[illegible]

## Appendix C - Quad-Fastener Joint Drawing

Appendix A: Engineering Drawings, Part List, and Test Article Count for Nominal Installations (continued)



## Appendix D - Faulted Fastener Joint Drawings

### Straight Gap

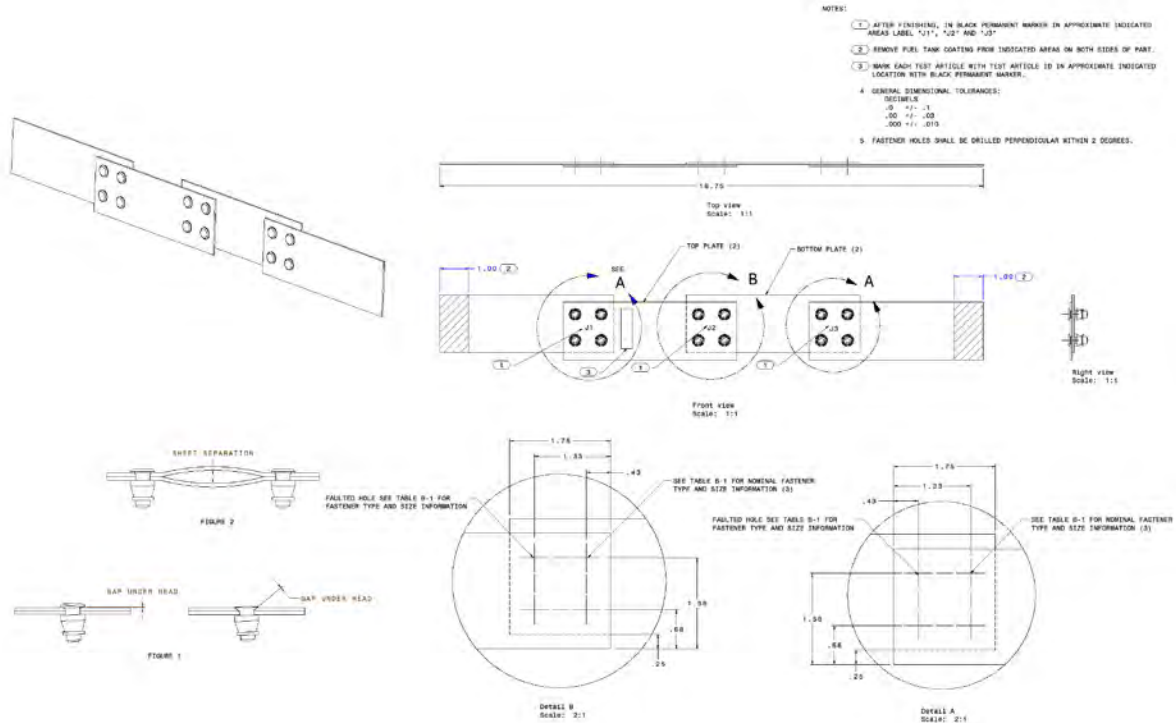


TABLE B-1 STRAIGHT GAP HI-LOK AND HI-LITE MATRIX

PARTS LIST INFORMATION										HOLE PREPARATION REQUIREMENTS					DETAILED FASTENER REQUIREMENTS				
TEST ARTICLE	ARTICLE QTY	HI-LOK / HI-LITE	FASTENER TYPE		QUANTITY	COLLAR	QUANTITY	TOP PLATE	DETAIL PARTS		QUANTITY	NOMINAL HOLE	FAULTED HOLE	CHAMFER OR RADIUS IN PART TO ACCOMMODATE HEAD TO SHANK TRANSITION	HEAD GAP PARAMETERS		MIN METAL TO METAL UNDER FASTENER HEAD (X CIRCUMFERENCE)	MAX GAP UNDER FASTENER HEAD (1X) (FIGURE 1)	FLANGES RANGE MAX SHEET SEPARATION BETWEEN FASTENERS (1X) (FIGURE 2)
			QUANTITY	COLLAR					QUANTITY	QUANTITY		QUANTITY	HOLE DIA (IN)		HOLE DIA (IN)	MIN GAP (IN)			
WP1-4100	5	HI-LOK	AL7086B-3 1/2	HI-LOK-3 1/2	12	NI4000-1 1/2	2	NI4000-1 1/2	2	NI4000-1 1/2	2	0.181 - 0.187	0.187 - 0.191	OPTIONAL	25	0.004	N/A	0.005	
WP1-4100	5	HI-LITE	AL7086B-3 1/2	HI-LITE-3 1/2	12	NI4000-1 1/2	2	NI4000-1 1/2	2	NI4000-1 1/2	2	0.181 - 0.187	0.187 - 0.191	OPTIONAL	25	0.004	0.008/0.005	0.005	
WP1-4100	5	HI-LOK	AL7086B-3 1/2	HI-LOK-3 1/2	12	NI4000-1 1/2	2	NI4000-1 1/2	2	NI4000-1 1/2	2	0.181 - 0.187	0.187 - 0.191	OPTIONAL	25	0.004	N/A	0.005	
WP1-4100	5	HI-LITE	AL7086B-3 1/2	HI-LITE-3 1/2	12	NI4000-1 1/2	2	NI4000-1 1/2	2	NI4000-1 1/2	2	0.181 - 0.187	0.187 - 0.191	OPTIONAL	25	0.004	0.008/0.005	0.005	
WP1-4111	5	HI-LITE	AL7086B-3 1/2	HI-LITE-3 1/2	12	NI4000-1 1/2	2	NI4000-1 1/2	2	NI4000-1 1/2	2	0.181 - 0.187	0.187 - 0.191	OPTIONAL	25	0.004	0.008/0.005	0.005	
WP1-4111	5	HI-LOK	AL7086B-3 1/2	HI-LOK-3 1/2	12	NI4000-1 1/2	2	NI4000-1 1/2	2	NI4000-1 1/2	2	0.181 - 0.187	0.187 - 0.191	OPTIONAL	25	0.004	0.008/0.005	0.005	

### Gap Under Head

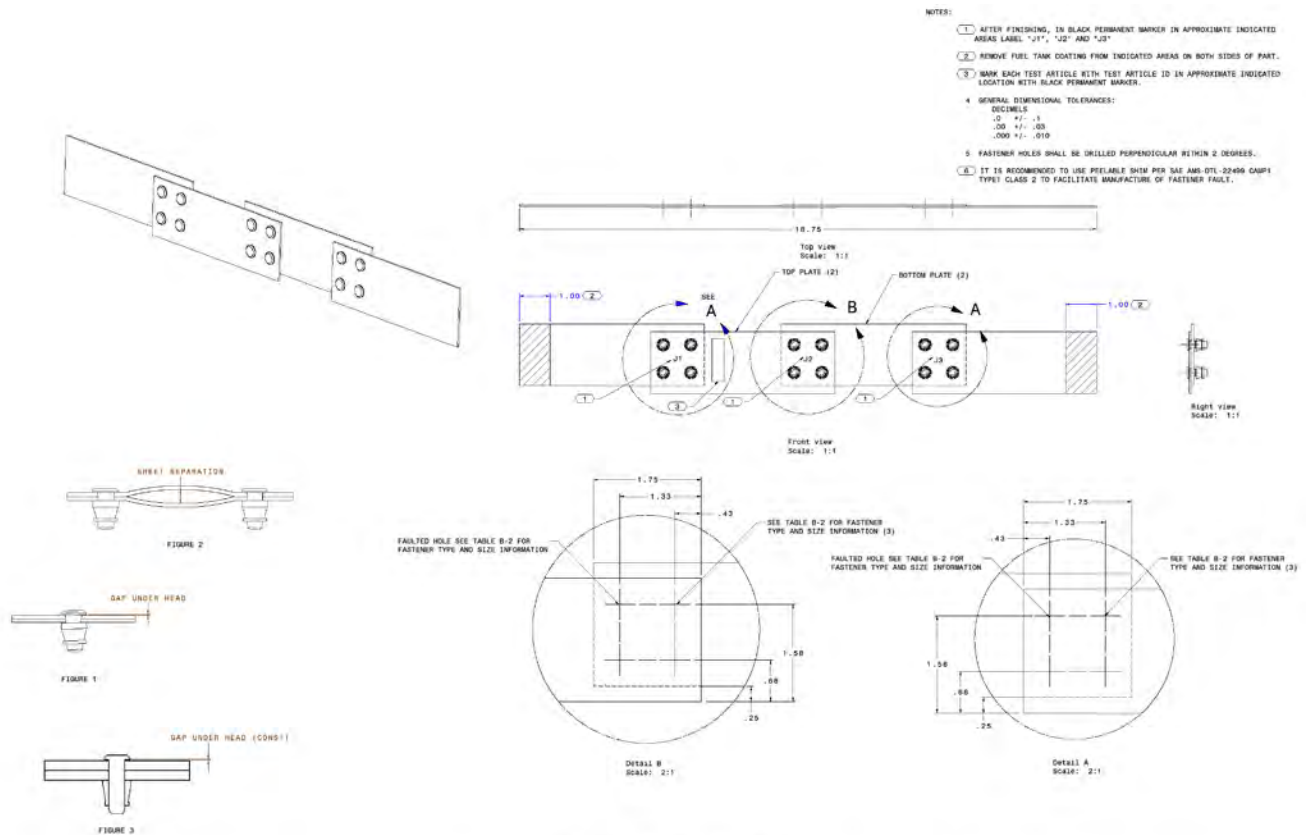


TABLE B-2 GAP UNDER HEAD HI-LOK AND HI-LITE MATRIX

PARTS LIST INFORMATION										HOLE PREPARATION REQUIREMENTS				INSTALLED FASTENER REQUIREMENTS						
TEST ARTICLE ID	ARTICLE QTY	HI-LOK / HI-LITE	FASTENER		DETAIL PARTS				NOMINAL HOLE DIA. (IN)		CHAMFER OR RADIUS IN PART TO ACCOMMODATE HOLE TO SHANK TRANSITION		MIN METAL TO METAL UNDER FASTENER HEAD (X CIRCUMFERENCE)		NOMINAL MIN/EL MAX GAP UNDER FASTENER HEAD (IN) (FIGURE 1)		FAILED FASTENER INSTALLED UNDER FASTENER HEAD (IN) (FIGURE 3) (E)		FLUIDNESS RANGE MAX SHEET SEPARATION (FIGURE 2)	BETWEEN FASTENERS (IN) (FIGURE 2)
			PIN	QUANTITY	COLOR	QUANTITY	TOP PLATE	QUANTITY	BOTTOM PLATE	QUANTITY										
WP-4751	8	HI-LOK	HS100HS-8-12	12		HS08B-1-2	2	HS08B-1-2	2	0.161 - 0.167	OPTIONAL		25	9.004	0.006		N/A	0.025		
WP-4752	8	HI-LOK	HS100HS-8-12	12		HS08B-1-2	2	HS08B-1-2	2	0.161 - 0.167	OPTIONAL		25	9.004	0.006		N/A	0.025		
WP-4753	8	HI-LITE	HS100HS-8-12	12		HS08B-1-2	2	HS08B-1-2	2	0.161 - 0.167	OPTIONAL		25	9.004	0.006		N/A	0.025		



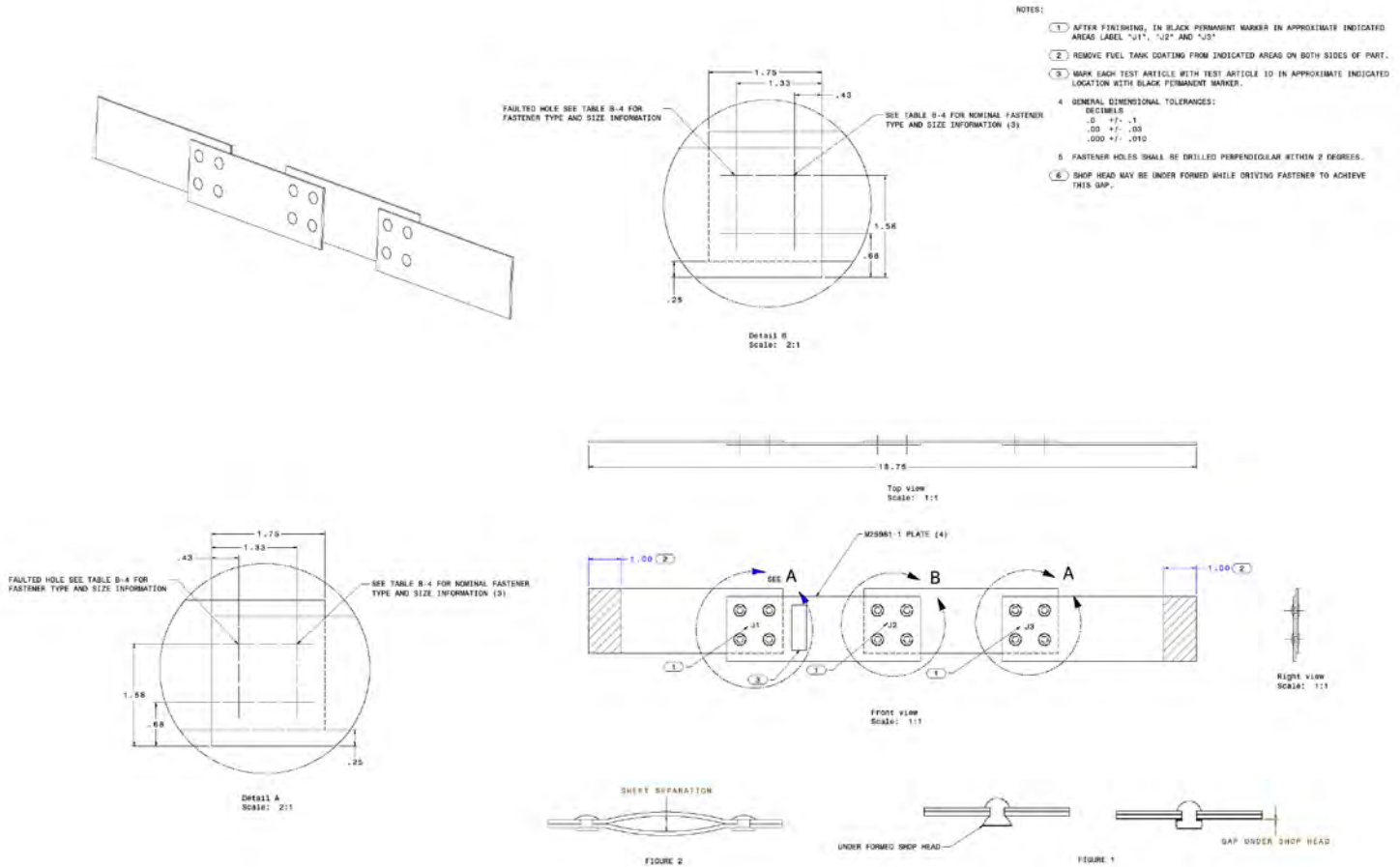
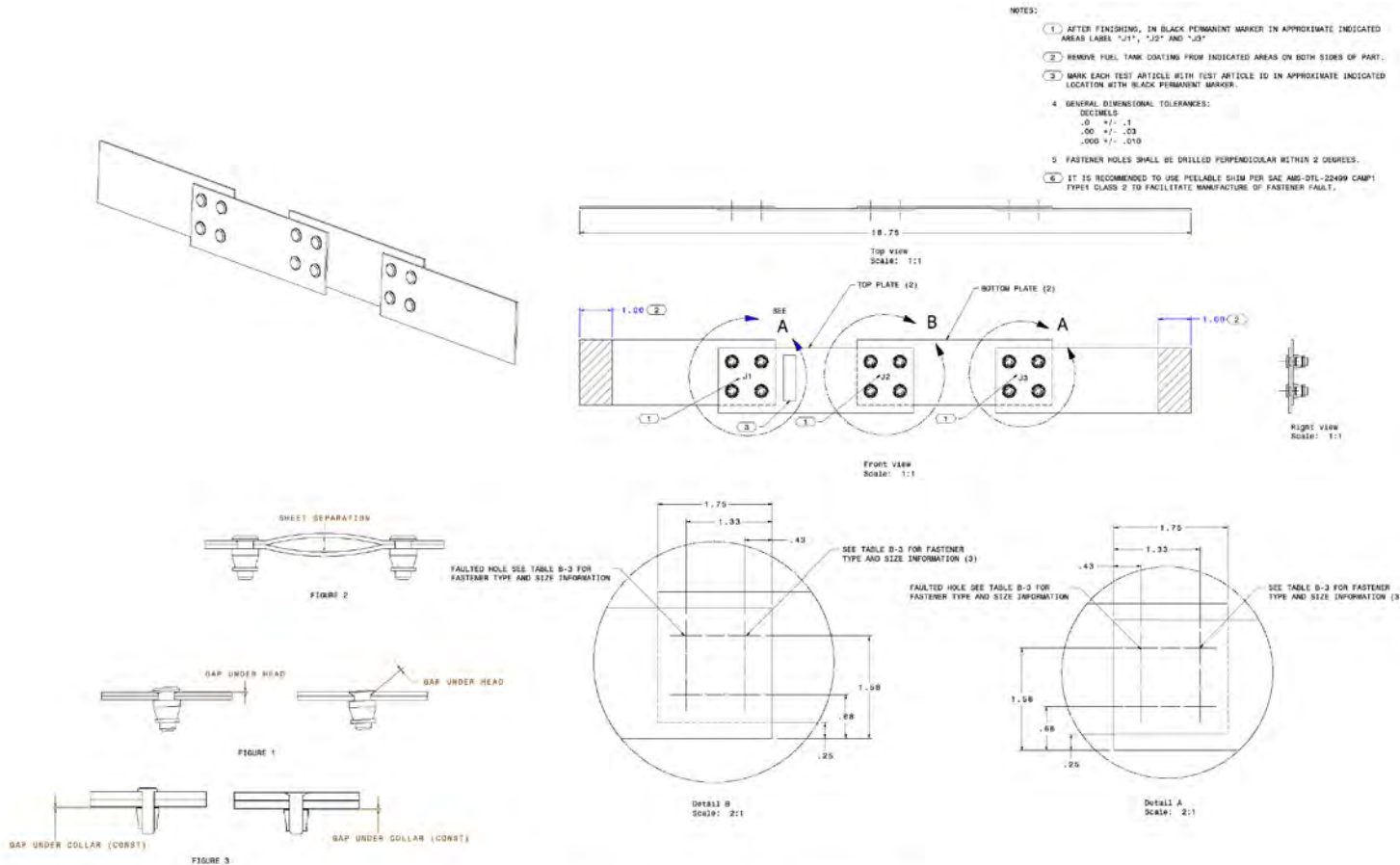


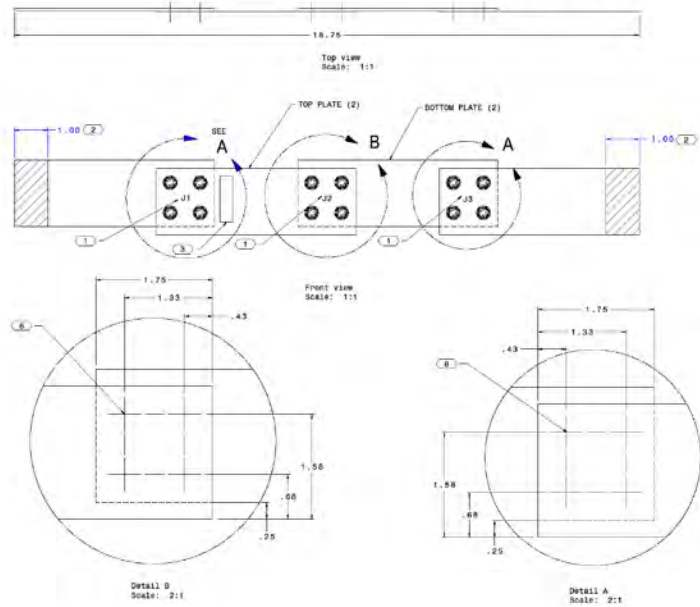
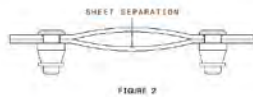
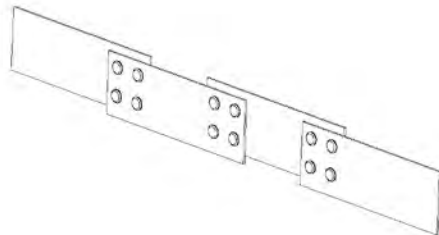
TABLE B-4 GAP UNDER SHOP HEAD

PARTS LIST INFORMATION					HOLE PREPARATION REQUIREMENTS		INSTALLED FASTENER REQUIREMENTS					MAX SHEET SEPARATION BETWEEN	
TEST ARTICLE ID	QUANTITY	FASTENER TYPE	DETAIL PART	QUANTITY	HOLE DIA (IN)	MAX CHAMFER IN PART TO ACCOMMODATE HEAD TO SHANK TRANSITION (deg/in)	SHOP HEAD HEIGHT (IN)	SHOP HEAD WIDTH (IN)	HEAD HEIGHT (IN)	NOMINAL FASTENER DIA, MAX GAP UNDER SHOP HEAD (IN) (FIG. 1)	FASTENED FASTENER DIA, GAP UNDER SHOP HEAD (IN) (FIG. 2)	MAX SHEET SEPARATION BETWEEN	
MP3-4009	5	M20470AD4	M20981-1	4	0.128 - 0.136	OPTIONAL	0.037 - 0.100	0.163 - 0.240	0.042 MIN	0.004	0.006 (FIG. 1) (FIG. 2)	0.005	

## Gap Under Collar



## Scratch



- NOTES:
- (1) AFTER FINISHING, IN BLACK PERMANENT MARKER IN APPROXIMATE INDICATED AREAS LABEL "J1", "J2" AND "J3"
  - (2) REMOVE FUEL TANK COATING FROM INDICATED AREAS ON BOTH SIDES OF PART.
  - (3) MARK EACH TEST ARTICLE WITH TEST ARTICLE ID IN APPROXIMATE INDICATED LOCATION WITH BLACK PERMANENT MARKER.
  - (4) GENERAL DIMENSIONAL TOLERANCES:  
DECIMALS:  
.00  $\pm$  .01  
.00  $\pm$  .02  
.00  $\pm$  .03
  - (5) FASTENER HOLES SHALL BE DRILLED PERPENDICULAR WITHIN 2 DEGREES.
  - (6) AT INDICATED FASTENER LOCATIONS, CREATE A SCRATCH IN THE COLLAR-SIDE PLATE PRIOR TO FASTENER INSTALLATION. SCRATCH SHALL BE 0.5" LONG, 0.005" WIDE AND 0.005" DEEP AND SHALL START AT THE EDGE OF THE FASTENER HOLE. IT IS RECOMMENDED TO USE ELOMETER 1006 DIN SCRATCHING TOOL OR SIMILAR TO CREATE THIS SCRATCH.

TABLE B-5 FUEL TANK COATING SCRATCH HI-LOK AND HI-LITE MATRIX

PARTS LIST INFORMATION										HOLE PREPARATION REQUIREMENTS				INSTALLED FASTENER REQUIREMENTS			
TEST ARTICLE ID	ARTICLE QTY	HI-LOK / HI-LITE	FASTENER TYPE			DETAIL PARTS			NOMINAL HOLE HOLE DIA (IN)	CHAMFER OR RADIUS IN PART TO ACCOMMODATE HEAD TO SHANK TRANSITION	MIN METAL TO METAL UNDER FASTENER HEAD (% CIRCUMFERENCE)	MAX GAP UNDER FASTENER HEAD (IN) (FIGURE 1)	FLUIDNESS RANGE (IN)	MAX SHEET SEPARATION BETWEEN FASTENERS (IN) (FIGURE 2)			
			PIN	QUANTITY	COLLAR	QUANTITY	TOP PLATE	QUANTITY							BOTTOM PLATE		
MP4-4T01	5	HI-LOK	NL10VBL-3	12	NL70-S	12	N25901-1	2	N25901-1	2	0.161 - 0.187	OPTIONAL	25	0.004	N/A	0.025	
MP4-4T05	5	HI-LITE	NL11VBL-3	12	NL70VCL-12	12	N25901-1	2	N25901-1	2	0.161 - 0.187	OPTIONAL	25	0.004	N/A	0.025	
MP4-4T11	5	HI-LITE	NL11VBL-3	12	NL70VCL-12	12	N25901-1	2	N25901-1	2	0.161 - 0.187	OPTIONAL	25	0.004	0.006/-0.005	0.025	
MP4-4T12	5	HI-LOK	NL11VBL-3	12	NL70-S	12	N25901-1	2	N25901-1	2	0.161 - 0.187	OPTIONAL	25	0.004	0.006/-0.005	0.025	

## Burr

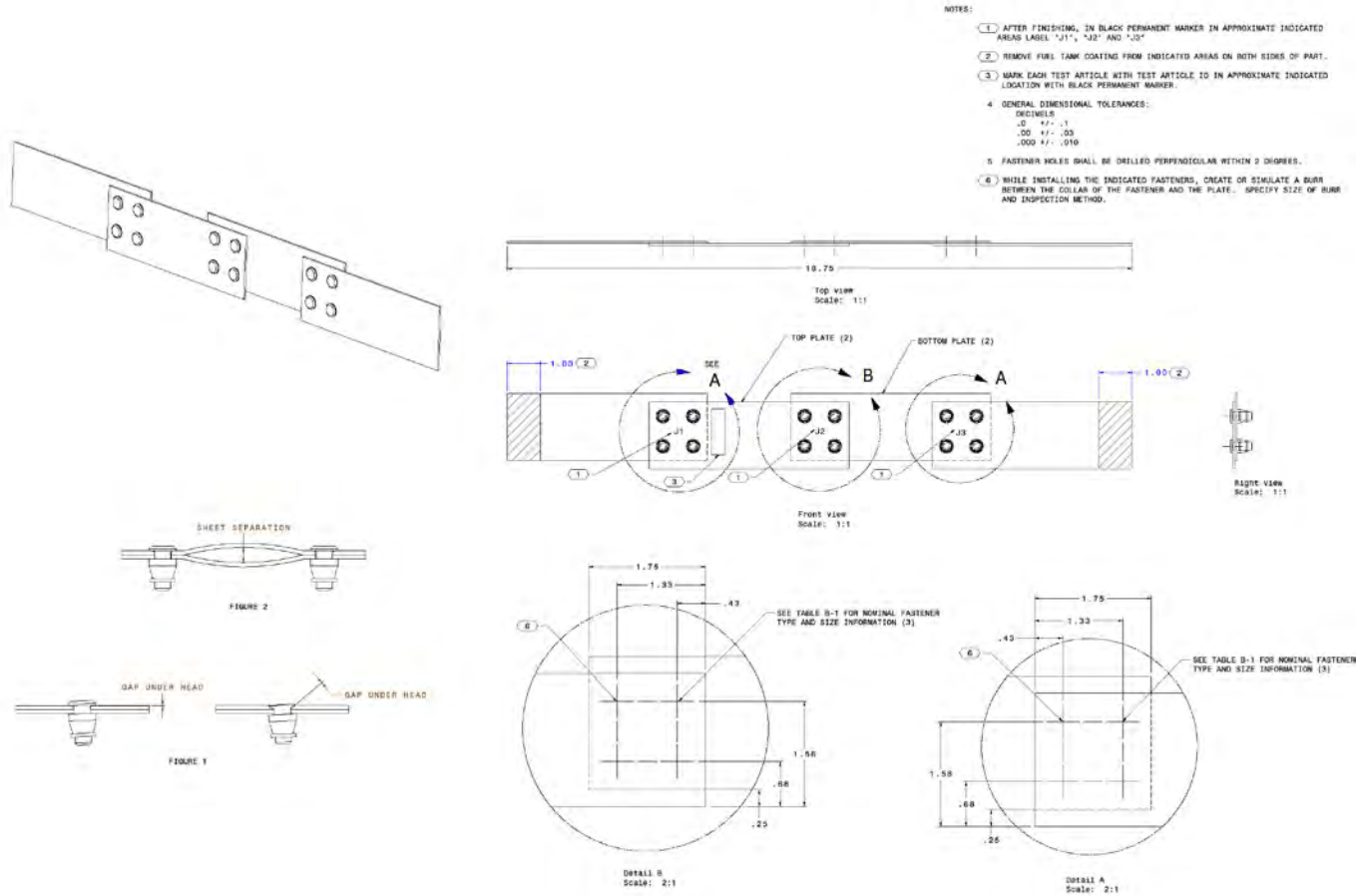


TABLE B-8 BURR HI-LOK AND HI-LITE MATRIX

PARTS LIST INFORMATION										HOLE PREPARATION REQUIREMENTS			INSTALLED FASTENER REQUIREMENTS					
TEST ARTICLE ID	ARTICLE QTY	HI-LOK / HI-LITE	FASTENER TYPE			DETAIL PARTS			NOMINAL HOLE		CHAMFER OR RADIUS IN PART TO ACCOMMODATE HEAD TO SHANK TRANSITION	HEAD GAP PARAMETERS		FLUORESCENCE RANGE (IN) (FIGURE 2)	MAX SHEET SEPARATION BETWEEN FASTENERS (IN) (FIGURE 3)			
			PIN	QUANTITY	COLLAR	QUANTITY	TOP PLATE	QUANTITY	BOTTOM PLATE	QUANTITY		HOLE DIA (IN)	FAULTED HOLE HOLE DIA (IN)			MIN METAL TO METAL UNDER FASTENER HEAD (% CIRCUMFERENCE)	MAX GAP UNDER FASTENER HEAD (IN) (FIGURE 1)	
WFS-4701	5	HI-LOK	HL10VRS-3	12		HL70-S	12	MS5881-1	2	MS5881-1	2	0.161 - 0.167	0.167 - 0.171	OPTIONAL	25	0.004	N/A	0.025
WFS-4709	5	HI-LITE	HL10BJS-3	12		HL70CYS	12	MS5881-1	2	MS5881-1	2	0.161 - 0.167	0.167 - 0.171	OPTIONAL	25	0.004	N/A	0.025
WFS-4711	5	HI-LITE	HL11VRS-3	12		HL70CYS	12	MS5881-1	2	MS5881-1	2	0.161 - 0.167	0.167 - 0.171	OPTIONAL	25	0.004	0.0067-0.008	0.025
WFS-4712	5	HI-LOK	HL11VRS-3	12		HL70-S	12	MS5881-1	2	MS5881-1	2	0.161 - 0.167	0.167 - 0.171	OPTIONAL	25	0.004	0.0067-0.008	0.025

## Under-torqued

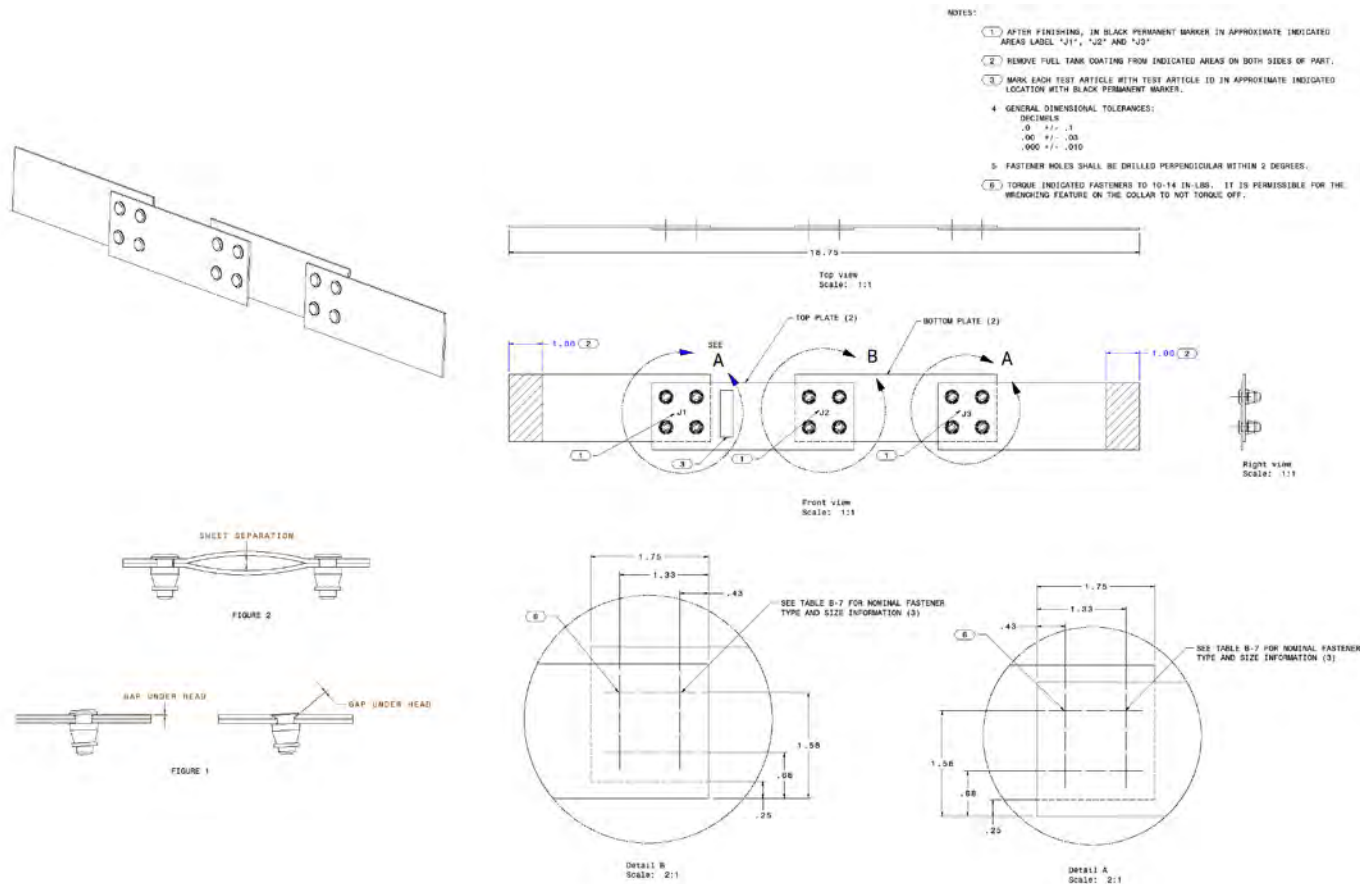


TABLE B-7 UNDER TORQUED HI-LOK AND HI-LITE MATRIX

PARTS LIST INFORMATION										HOLE PREPARATION REQUIREMENTS		INSTALLED FASTENER REQUIREMENTS					
TEST ARTICLE ID	ARTICLE QTY	HI-LOK / HI-LITE	FASTENER TYPE				DETAIL PARTS				NOMINAL HOLE DIA. (IN)	CHAMFER OR RADIUS IN PART TO ACCOMMODATE HEAD TO SHANK TRANSITION	WIN METAL TO METAL UNDER FASTENER HEAD (% CIRCUMFERENCE)		MAX GAP UNDER FASTENER HEAD (IN) (FIGURE 1)	FLUSHNESS RANGE (IN)	MAX SHEET SEPARATION BETWEEN FASTENERS (IN) (FIGURE 2)
			PIN	QUANTITY	COLLAR	QUANTITY	TOP PLATE	QUANTITY	BOTTOM PLATE	QUANTITY							
MF6-4101	5	HI-LOK	HL10VBL-3	12	HL20-5	12	M25981-1	2	M25981-1	2	0.181 - 0.187	OPTIONAL	25	0.004	N/A	0.025	
MF6-4105	5	HI-LITE	HL10VBL-3	12	HL20-5	12	M25981-1	2	M25981-1	2	0.181 - 0.187	OPTIONAL	25	0.004	N/A	0.025	
MF6-4111	5	HI-LITE	HL11VBL-3	12	HL20-5	12	M25981-1	2	M25981-1	2	0.181 - 0.187	OPTIONAL	25	0.004	0.005/-0.005	0.025	
MF6-4112	5	HI-LOK	HL11VBL-3	12	HL20-5	12	M25981-1	2	M25981-1	2	0.181 - 0.187	OPTIONAL	25	0.004	0.005/-0.005	0.025	



## Appendix E - Faulted Fastener Designs

Table 10: Description of Faults

Groups	Description
1.	<b>Oversized Hole at Pin-Part Interface</b> This group utilizes an oversized hole with round circumference having the fastener installation fit exceeding the designated one—such an assembly will result in the next larger fit type, e.g. interference to transition, transition to clearance. This fault-installation group is well defined by the tolerances for nominal installations.
2.	<b>Gap Under Head Around Circumference</b> This group utilizes an induced gap around the entire circumference in the interference and clearance fit types, the thickness of which exceeds tolerance defined in the nominal installations.
3.	<b>Gap Under Collar Around Circumference</b> The same approach is used to produce this gap as in group 2.
4.	<b>Fuel-Tank Coating Scratch under Collar</b> This type utilizes a 0.005” deep, 0.005” wide, and 0.5” long scratch inflicted under the collar on the part. A scratch tool (e.g. elcometer 1538) is recommended to be used to produce a scratch with repeatable dimensions. Alternatively, a computer numerical control (CNC) engraving tooling is also recommended to obtain best repeatability and the exact dimensions and depth on all specimens.
5.	<b>Burr</b> This group utilizes a burr created or shaving placed at the circumference of the hole under the collar. As one of the recommendations, it is feasible to create burrs as a result of pushing the metal out of the hole while not using a backing while drillings. The size of the burrs could be adjustable depending on the feed and speed of the cutting drill. Selection of burrs must be most representative of those that may result during the OEM’s installation process. Example of varying degrees of the burrs is shown below: <div data-bbox="462 1417 1364 1591" data-label="Image"> </div>
6.	<b>Under-Torque 30%</b> This fault type does not produce a gap as in groups 2 and 3, but a weaker contact results at the fastener-part interface.

## Appendix F - Test Photographs

### LIST OF FIGURES

Figure 1: MN-1I03-1, before testing .....	132
Figure 2: MN-1I03-1, during test, external sparks on all 3 joints .....	132
Figure 3: MN-1I03-3, before test .....	132
Figure 4: MN-1I03-3, during test, external sparks on all 3 joints.....	132
Figure 5: MN-1I12-1, before test .....	132
Figure 6: MN-1I12-1, during test, external sparks on all 3 joints.....	132
Figure 7: MN-1I12-2, before test .....	133
Figure 8: MN-1I12-2, during test, external sparks on J1 & J3 .....	133
Figure 9: MN-1I12-3, before test.....	133
Figure 10: MN-1I12-3, during test, external spark on J2 .....	133
Figure 11: MN-1I12-4, before test.....	133
Figure 12: MN-1I12-4, during test, external spark on J2 .....	133
Figure 14: MN-1T03-1, during test, external sparks on all 3 joints.....	134
Figure 13: MN-1T03-1, before test .....	134
Figure 15: MN-1T03-2, before test.....	134
Figure 16: MN-1T03-2, during test, external sparks on all 3 joints .....	134
Figure 17: MN-1T03-3, before test.....	134
Figure 18: MN-1T03-3, during test, external sparks on all 3 joints .....	134
Figure 19: MN-1T03-4, before test.....	135
Figure 20: MN-1T03-4, during test, external sparks on all 3 joints.....	135
Figure 21: MN-1T03-5, before test.....	135
Figure22: MN-1T03-5, during test, external spark on J1 .....	135
Figure 23: MN-1T12-1, before test .....	135
Figure 24: MN-1T12-1, during test, external spark on J1, internal on J2 .....	135
Figure 25: MN-1T12-2, before test .....	136
Figure 26: MN-1T12-2, during test, external spark on J1 & J2 .....	136
Figure 27: MN-1T12-3, before test .....	136
Figure 28: MN-1T12-3, during test, external spark on J1 .....	136
Figure 29: MN-1T12-6, before test.....	136
Figure 30: MN-1T12-6, during test, external spark on J1 .....	136
Figure 31: MN-1T07-6, before test.....	137
Figure 32: MN-1T07-6, during test, external spark on J2.....	137
Figure 33: MN-1I11-1, before test.....	137
Figure 34: MN-1I11-1, during test, external sparks on all 3 joints .....	137
Figure 35: MN-1I11-2, before test .....	138
Figure 36: MN-1I11-2, during test, internal spark on J1, external sparks on J2 & J3 .....	138

Figure 37: MN-1I11-3, before test .....	138
Figure 38: MN-1I11-3, during test, internal sparks on J1 & J3, external spark on J2 .....	138
Figure 39: MN-1I11-4, before test .....	138
Figure 40: MN-1I11-4, during test, external spark on J1, internal spark on J3 .....	138
Figure 41: MN-1I11-6, before test.....	139
Figure 42: MN-1I11-6, during test, internal sparks on J1 & J2, external spark on J3 .....	139
Figure 43: MN-1I03-2, before test .....	139
Figure 44: MN-1I03-2, during test, external spark on J3 .....	139
Figure 45: MN-1I12-1, shot 1, before test.....	140
Figure 46: MN-1I12-1, shot 1, during test, external sparks on all 3 joints .....	140
Figure 48: MN-1I12-2, during test, external sparks on all 3 joints .....	140
Figure 47: MN-1I12-2, before test.....	140
Figure 50: MN-1I12-3, during test, external sparks on all 3 joints .....	140
Figure 49: MN-1I12-3, before test.....	140
Figure 52: MN-1I12-4, during test, external sparks on all 3 joints .....	141
Figure 53: MN-1I12-4, before test.....	141
Figure 53: MN-1I12-5, before test.....	141
Figure 54: MN-1I12-5, during test, external sparks on J1 & J3.....	141
Figure 56: MN-1I12-6, during test, external sparks on J1 & J2 .....	141
Figure 57: MN-1I12-6, before test .....	141
Figure 58: MN-1T02-3, during test, external spark on J1.....	142
Figure 59: MN-1T02-3, before test .....	142
Figure 60: MN-1I11-1, shot 1, during test, external sparks on all 3 joints.....	142
Figure 61: MN-1I11-1, shot 1, before test.....	142
Figure 62: MN-1I11-1, shot 2, during test, external spark on J2 .....	142
Figure 63: MN-1I11-1, shot 2, before test.....	142
Figure 64: MN-1I11-2, during test, external sparks on J2 & J3 .....	143
Figure 65: MN-1I11-2, before test .....	143
Figure 66: MN-1I11-3, during test, external spark on J3 .....	143
Figure 67: MN-1I11-3, before test .....	143
Figure 68: MN-1I11-5, during test, external sparks on J2 & J3 .....	143
Figure 69: MN-1I11-5, before test .....	143
Figure 70: MN-1I11-6, during test, external sparks on J2 & J3 .....	144
Figure 71: MN-1I11-6, before test.....	144
Figure 71: MN-4I03-1, before test.....	145
Figure 72: MN-4I03-1, during test, external sparks on J1 & J2 .....	145
Figure 73: MN-4I03-3, before test.....	145
Figure 74: MN-4I03-3, during test, external spark on J1 .....	145
Figure 75; MN-4I03-4, before test.....	145
Figure 76: MN-4I03-4, during test, external spark on J2 .....	145

Figure 77: MN-4To3-2, before test .....	146
Figure 78: MN-4To3-2, during test, external spark on J3 .....	146
Figure 79: MN-4To3-3, before test .....	146
Figure 80: MN-4To3-3, during test, external spark on J2.....	146
Figure 81: MN-4009-1, before test .....	146
Figure 82: MN-4009-1, during test, external spark on J2 .....	146
Figure 83: MN-4009-6, before test.....	147
Figure 84: MN-4009-6, during test, external spark on J2.....	147
Figure 85: MN-4I11, shot 1, before test.....	147
Figure 86: MN-4I11, shot 1, during test, external sparks on all 3 joints .....	147
Figure 87: MN-4I11-2, shot 1, before test .....	148
Figure 88: MN-4I11-2, shot 1, during test, external sparks on J2 & J3 .....	148
Figure 89: MN-4I11-3, before test.....	148
Figure 90: MN-4I11-3, during test, external sparks on all 3 joints .....	148
Figure 91: MN-4I11-4, before test .....	148
Figure 92: MN-4I11-4, during test, external sparks on J1 & J2, internal spark on J3.....	148
Figure 93: MN-4I11-5, before test.....	149
Figure 94: MN-4I11-5, during test, external sparks on J1 & J2, internal spark on J3.....	149
Figure 95: MN-4I11-6, before test.....	149
Figure 96: MN-4I11-6, during test, internal spark on J1, external sparks on J2 & J3.....	149
Figure 97: MN-4T12, before test .....	149
Figure 98; MN-4T12, during test, external sparks on all 3 joints .....	149
Figure 99: MF1-4To1-3, before test, front .....	150
Figure 100: MF1-4To1-3, 100kA, J1, during test, front.....	150
Figure 101: MF1-4To3-1, before test, front.....	150
Figure 102: MF1-4To3-1, 35kA, J1, during test, front .....	150
Figure 103: MF1-4T12-2, before test, front.....	150
Figure 104: MF1-4T12-2, 0.5kA, J1, during test, front.....	150
Figure 105: MF3-4To1-3, before test, front .....	151
Figure 106: MF3-4To1-3, 100kA, J2, during test, front.....	151
Figure 107: MF3-4T12-1, before test, front.....	151
Figure 108: MF3-4T12-1, 15kA, J2 & J3, during test, front.....	151
Figure 109: MF3-4009-2, before test, front .....	151
Figure 110: MF3-4009-2, 45kA, J2 & J3, during test, front.....	151
Figure 111: MF3-4009-2, before test, rear .....	152
Figure 112: MF3-4009-2, 45kA, J2, during test, rear.....	152
Figure 113: MF4-4To1-3, before test, front.....	152
Figure 114: MF4-4To1-3, 80kA, J1, during test, front.....	152
Figure 115: MF4-4T12-1, before test, front .....	152
Figure 116: MF4-4T12-1, 5kA, J1, during test, front.....	152

Figure 117: MF4-4009-2, before test, front .....	153
Figure 118: MF4-4009-2-20kA-J1 & J3, during test, front.....	153
Figure 119: MF4-4009-2, before test, rear .....	153
Figure 120: MF4-4009-2, 20kA, J1, during test, rear .....	153
Figure 121: MF5-4T12-1, before test, front .....	153
Figure 122: MF5-4T12-1, 6kA, J3, during test, front .....	153
Figure 123: MF5-4009-3, before test, front.....	154
Figure 124: MF5-4009-3, 30kA, J1 & J2, during test, front.....	154
Figure 125: MF5-4009-3, before test, rear .....	154
Figure 126: MF5-4009-3, 30kA, J2 & J3-during test-rear.....	154
Figure 127: MF6-4T12-3, before test, front .....	154
Figure 128: MF6-4T12-3, 5kA, J1 & J3, during test, front .....	154
Figure 129: MF1-4T01-2, before test, front .....	155
Figure 130: MF1-4T01-2, 45kA, J3, during test, front.....	155
Figure 131: MF1-4T01-2, before test, rear .....	155
Figure 132: MF1-4T01-2, 45kA, J1 & J3, during test, rear .....	155
Figure 133: MF1-4T03-2, before test, front .....	155
Figure 134: MF1-4T03-2, 30kA, J1, during test, front .....	155
Figure 135: MF1-4T12-2, before test, front .....	156
Figure 136: MF1-4T12-2, 7kA, J3, during test, front .....	156
Figure 137: MF2-4T0-3, before test, front.....	156
Figure 138: MF2-4T01-3, 35kA, J2, during test, front .....	156
Figure 139: MF3-4T01-3, before test, front .....	156
Figure 140: MF3-4T01-3, 13kA, J3, during test, front .....	156
Figure 141: MF3-4T12-2, before test, front.....	157
Figure 142: MF3-4T12-2, 10kA, J2 & J3, during test, front .....	157
Figure 143: MF3-4T12-2, before test, rear.....	157
Figure 144: MF3-4T12-2, 10kA, J2 & J3, during test, rear.....	157
Figure 145: MF4-4T01-1, before test, front.....	157
Figure 146: MF4-4T01-1, 25kA, J3, during test, front.....	157
Figure 147: MF4-4T12-1, before test, front .....	158
Figure 148: MF4-4T12-1, 7kA, J21, during test, front .....	158
Figure 149: MF5-4T01-1, before test, rear .....	158
Figure 150: MF5-4T01-1, 35kA, J1, during test, rear.....	158
Figure 151: MF5-4T12-2, before test, front .....	158
Figure 152: MF5-4T12-2, 7kA, J2, during test, front.....	158
Figure 153: MF6-4T01-1, before test, front.....	159
Figure 154: MF6-4T01-1, 35kA, J2, during test, front.....	159
Figure 155: MF6-4T01-1, before test, rear .....	159
Figure 156: MF6-4T01-1, 35kA, J2, during test, rea.....	159



Figure 157: MF6-4T12-3, before test, front.....	159
Figure 158: MF6-4T12-3-5kA-J1,J3, during test, front .....	159
Figure 159: MF1-4T05-3, before test, front .....	160
Figure 160: MF1-4T05-3, 100kA, J1-during test, front .....	160
Figure 161: MF1-4T07-1, before test, rear .....	160
Figure 162: MF1-4T07-3, 45kA, J1, during test, rear .....	160
Figure 163: MF2-4T05-2, before test, rear .....	160
Figure 164: MF2-4T05-2-25kA, J3, during test, rear .....	160
Figure 165: MF3-4T05-2, before test, front.....	161
Figure 166: MF3-4T05-2, 15kA, J2, during test, front .....	161
Figure 167: MF5-4T05-1, before test, rear .....	161
Figure 168: MF5-4T05-1-35kA-J1, during test, front.....	161
Figure 169: MF1-4T01-3, before test, rear .....	161
Figure 170: MF1-4T01-3, 100kA, J3, during test, rear .....	161
Figure 171: MF1-4T05-1, before test, rear .....	162
Figure 172: MF1-4T05-1, 35kA, J1, during test, rear .....	162
Figure 173: MF1-4T07-2, before test, front .....	162
Figure 174: MF1-4T07-2, 60kA, J2, during test, front .....	162
Figure 175: MF1-4T12-2, before test, front .....	162
Figure 176: MF1-4T121, 3kA, J2 & J3, during test, front.....	162
Figure 177: MF2-4T01-1, before test, rear .....	163
Figure 178: MF2-4T01-1, 60kA, J2, during test, rear .....	163
Figure 179: MF3-4T05-2, before test, rear .....	163
Figure 180: MF3-4T05-2, 60kA, J1, during test, rear .....	163
Figure 181: MF3-4T11-2, 4kA, J3, during test, front .....	163
Figure 182: MF3-4T11-2, before test, front.....	163
Figure 183: MF3-4T12-2, before test, front .....	164
Figure 184: MF3-4T12-2, 8kA, J2 & J3, during test, front.....	164
Figure 185: MF4-4T05-2, before test, rear .....	164
Figure 186: MF4-4T05-2, 80kA, J3, during test, rear.....	164
Figure 187: MF4-4T11-1, before test, front .....	164
Figure 188: MF4-4T11-1, 4kA, J1, during test, front .....	164
Figure 189: MF4-4T12-3, before test, front .....	165
Figure 190: MF4-4T12-3, 3kA, J1, J2, & J3, during test, front .....	165
Figure 191: MF5-4T01-1, before test, rear.....	165
Figure 192: MF5-4T01-1, 35kA, J2, during test, rea.....	165
Figure 193: MF5-4T05-3, before test, rear .....	165
Figure 194: MF5-4T05-3, 35kA, J2, during test, rear .....	165
Figure 195: MF5-4T11-1, before test, rea .....	166
Figure 196: MF5-4T11-1, 4kA, J2, during test, rear .....	166

---

Figure 197: MF5-4T12-2, before test, rear .....	166
Figure 198: MF5-4T12-2, 5kA, J2, during test, rear .....	166
Figure 199: MF6-4T11-1, before test, rear.....	166
Figure 200: MF6-4T11-1, 5kA, J2, during test, rear .....	166
Figure 201: MF6-4T12-3, before test, rear.....	167
Figure 202: MF6-4T12-3, 7kA, J2, during test, rear .....	167
Figure 1: Calibration Photographs for Camera 1.....	168
Figure 2: Calibration Photographs for Camera 2.....	169
Figure 3: Camera Calibration Test Setup at DNB Engineering, Inc.....	170

## **Nominal Single Fastener Test Articles**

### **OEM 1**

Note: this photo was extremely bright and whited out the camera shot.



Figure 1: MN-1I03-1, before testing

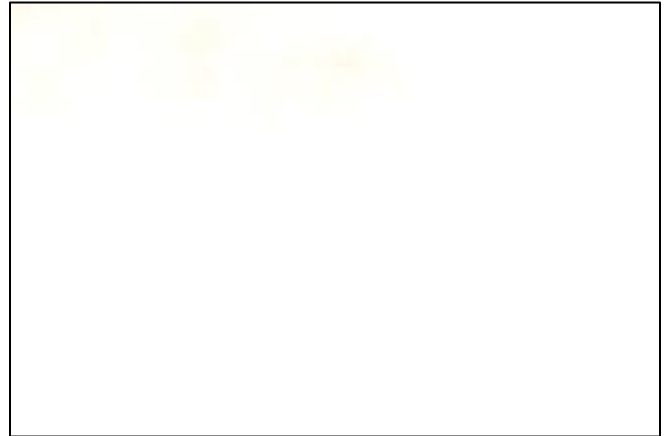


Figure 2: MN-1I03-1, during test, external sparks on all 3 joints

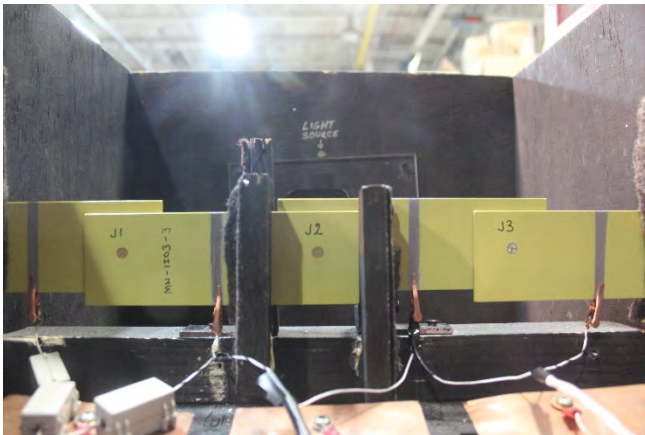


Figure 3: MN-1I03-3, before test



Figure 4: MN-1I03-3, during test, external sparks on all 3 joints

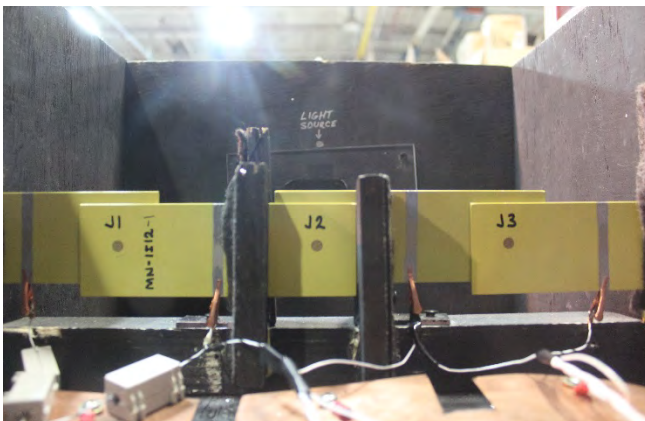


Figure 5: MN-1I12-1, before test



Figure 6: MN-1I12-1, during test, external sparks on all 3 joints

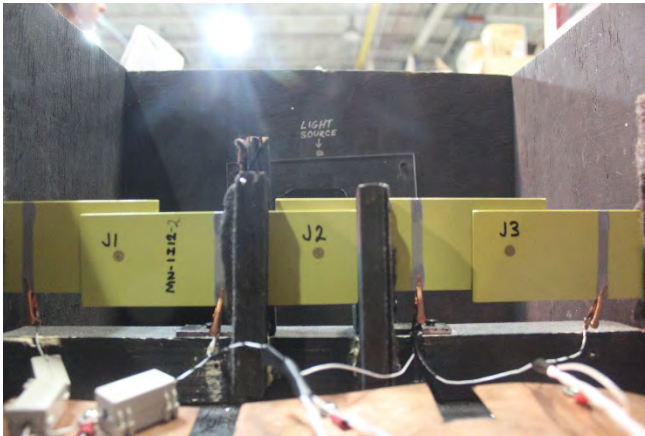


Figure 7: MN-1I12-2, before test



Figure 8: MN-1I12-2, during test, external sparks on J1 & J3

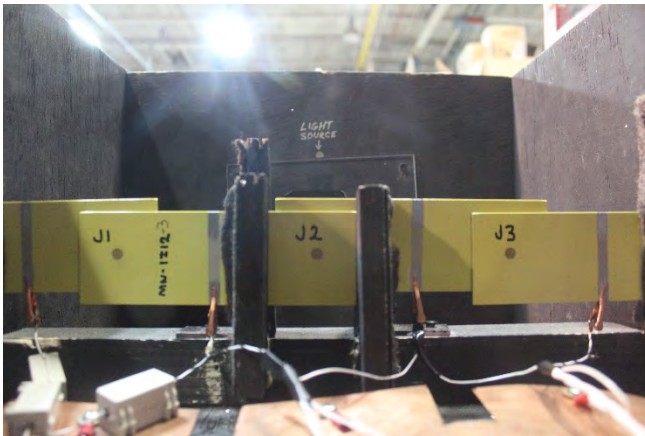


Figure 9: MN-1I12-3, before test



Figure 10: MN-1I12-3, during test, external spark on J2

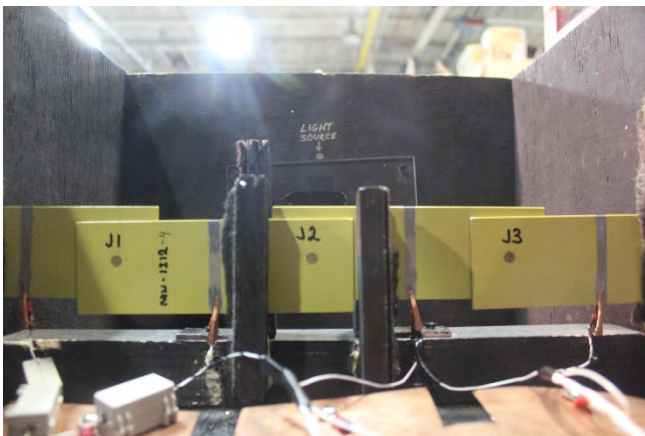


Figure 11: MN-1I12-4, before test

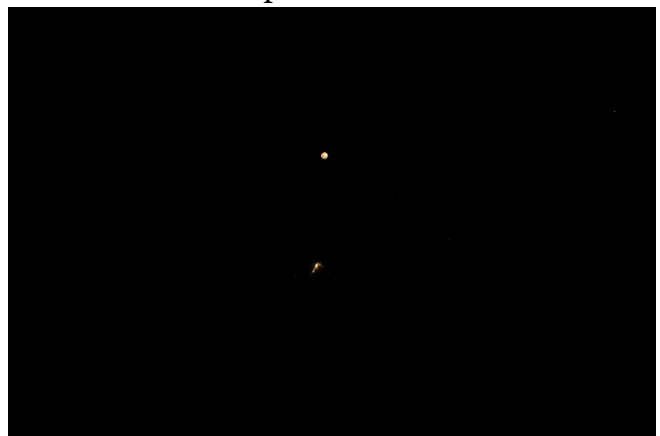


Figure 12: MN-1I12-4, during test, external spark on J2



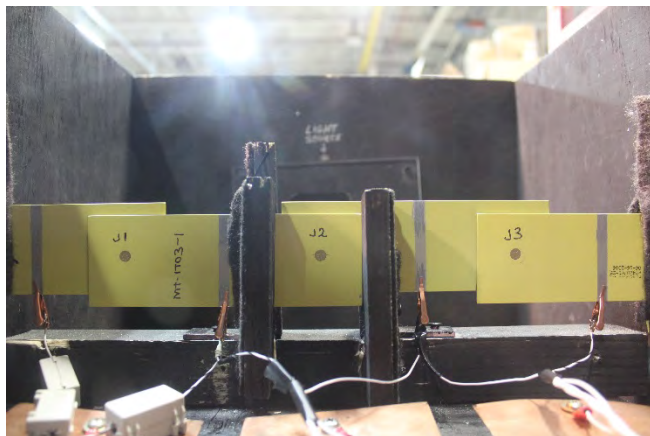


Figure 13: MN-1To3-1, before test



Figure 14: MN-1To3-1, during test, external sparks on all 3 joints

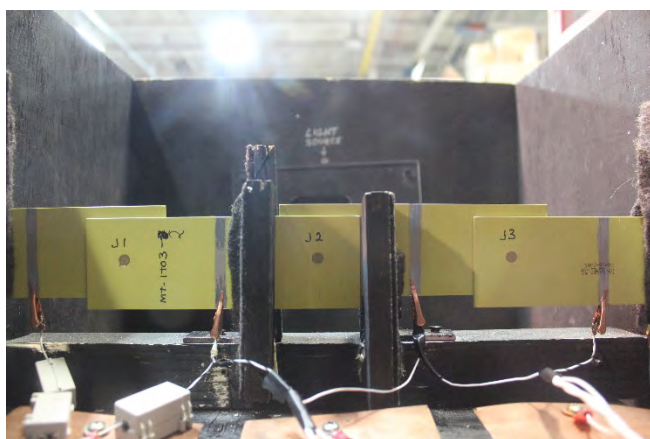


Figure 15: MN-1To3-2, before test

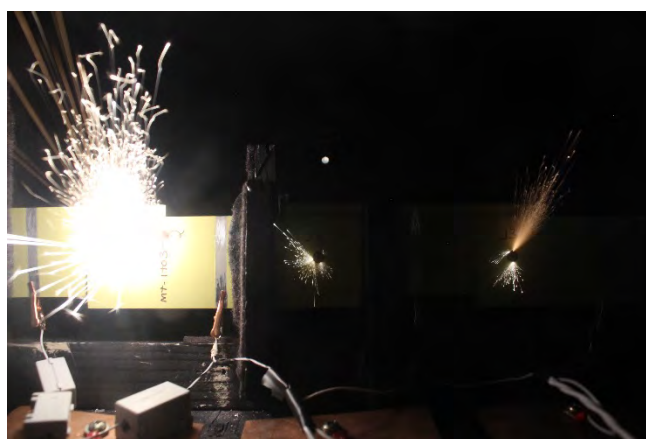


Figure 16: MN-1To3-2, during test, external sparks on all 3 joints

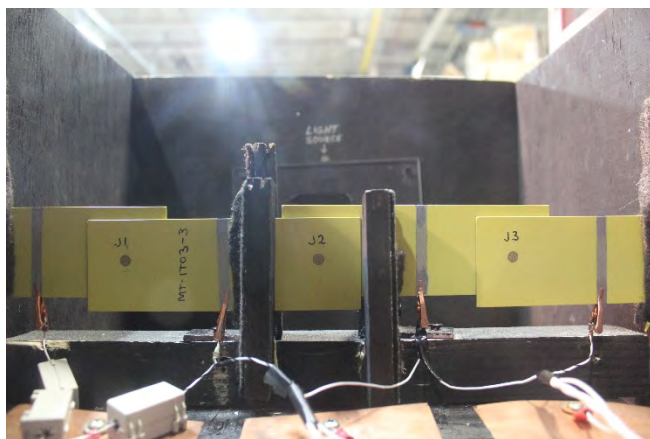


Figure 17: MN-1To3-3, before test

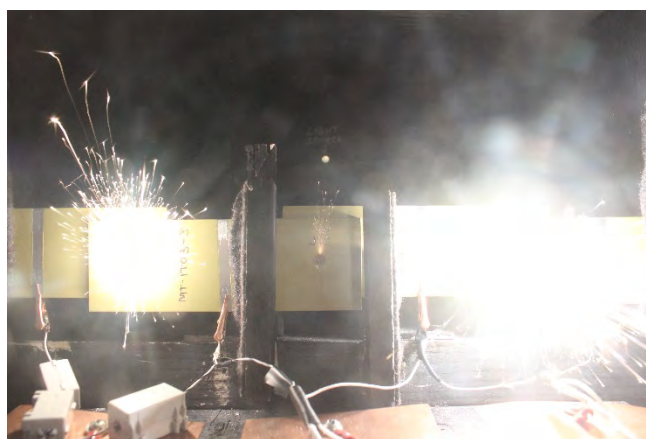


Figure 18: MN-1To3-3, during test, external sparks on all 3 joints



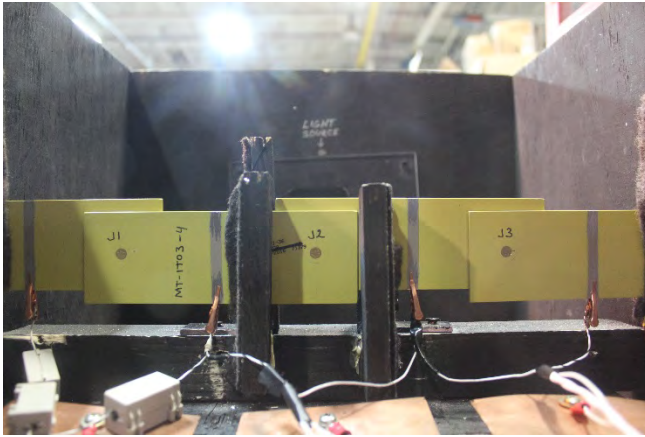


Figure 19: MN-1To3-4, before test



Figure 20: MN-1To3-4, during test, external sparks on all 3 joints

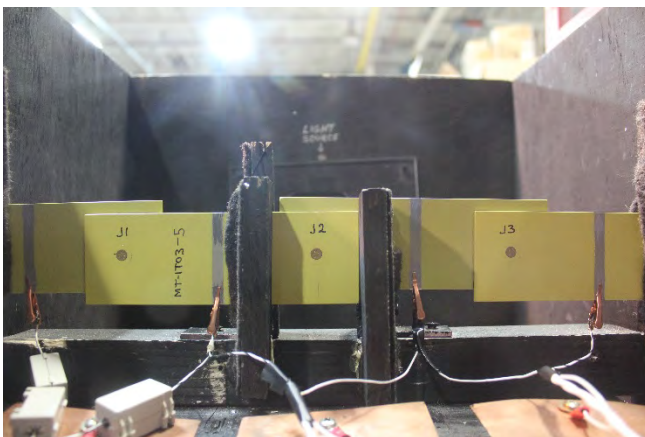


Figure 21: MN-1To3-5, before test  
**OEM 2**

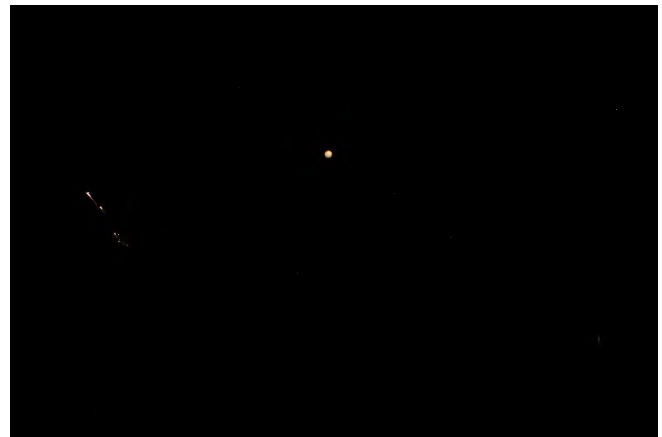


Figure 22: MN-1To3-5, during test, external spark on J1



Figure 23: MN-1T12-1, before test

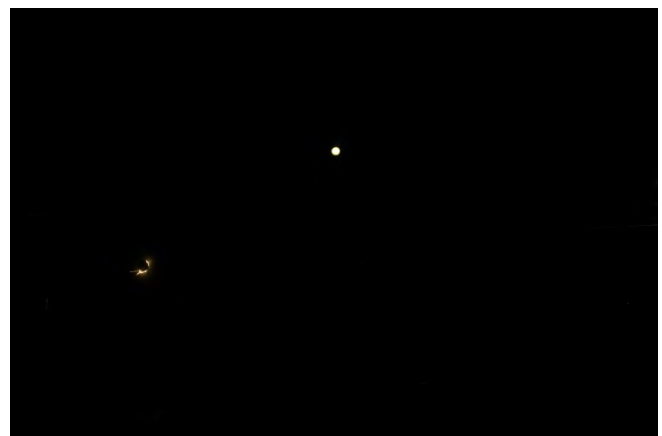


Figure 24: MN-1T12-1, during test, external spark on J1, internal on J2



Figure 25: MN-1T12-2, before test



Figure 26: MN-1T12-2, during test, external spark on J1 & J2



Figure 27: MN-1T12-3, before test

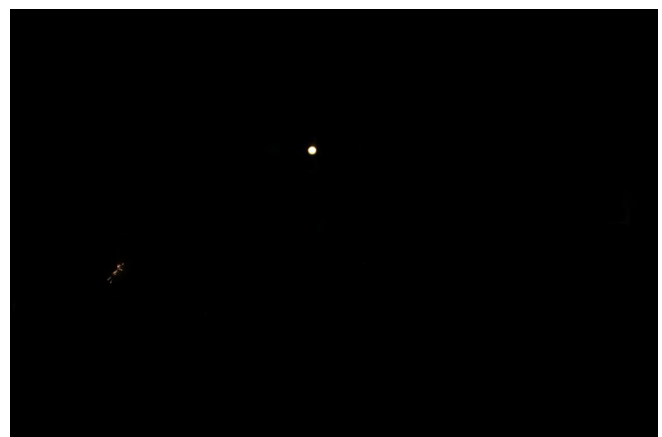


Figure 28: MN-1T12-3, during test, external spark on J1



Figure 29: MN-1T12-6, before test

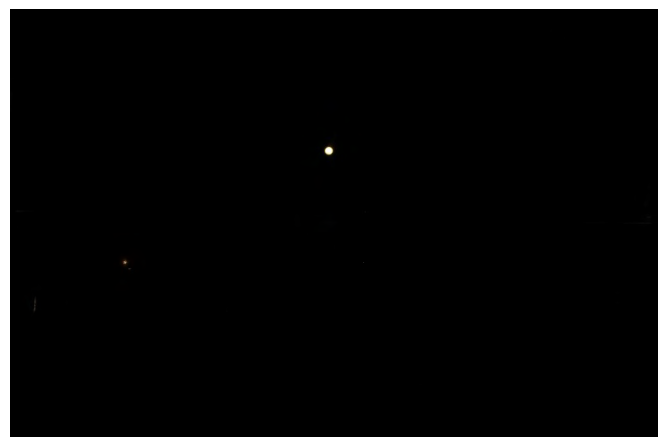


Figure 30: MN-1T12-6, during test, external spark on J1

**OEM 3** – no external sparking in Single fastener test articles

**OEM 4**

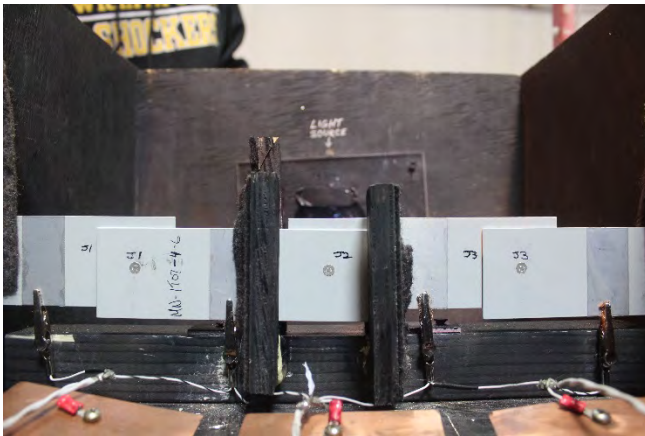


Figure 31: MN-1To7-6, before test

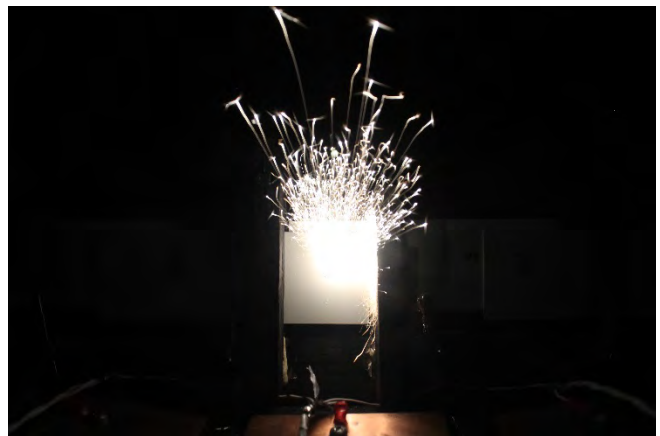


Figure 32: MN-1To7-6, during test, external spark on J2



Figure 33: MN-1I11-1, before test

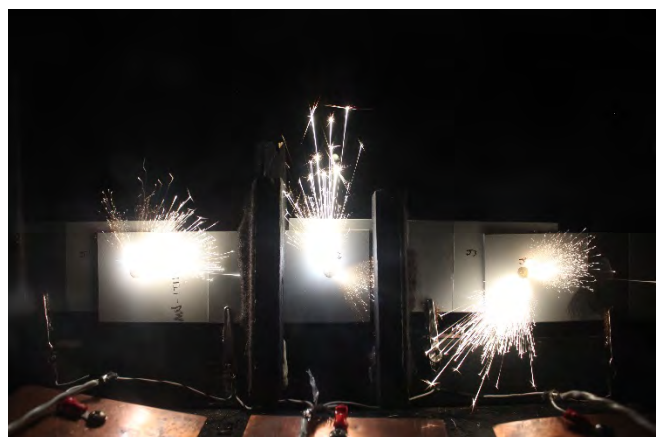


Figure 34: MN-1I11-1, during test, external sparks on all 3 joints





Figure 35: MN-1I11-2, before test

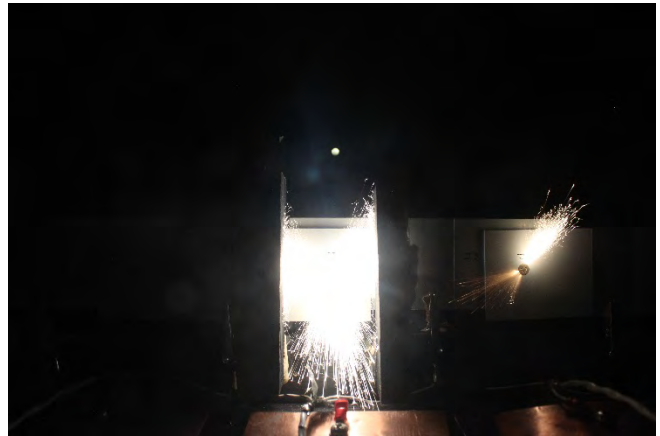


Figure 36: MN-1I11-2, during test, internal spark on J1, external sparks on J2 & J3

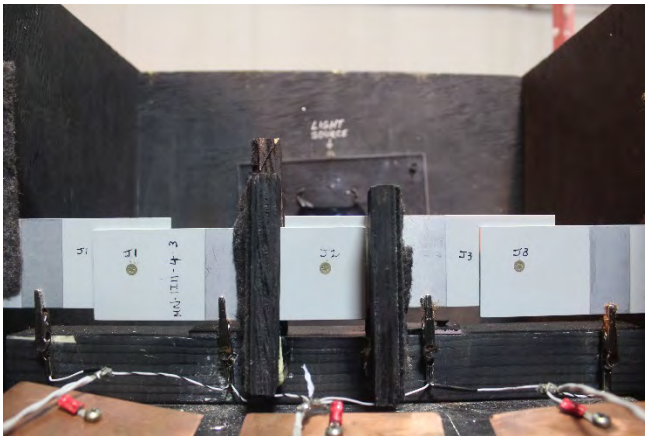


Figure 37: MN-1I11-3, before test

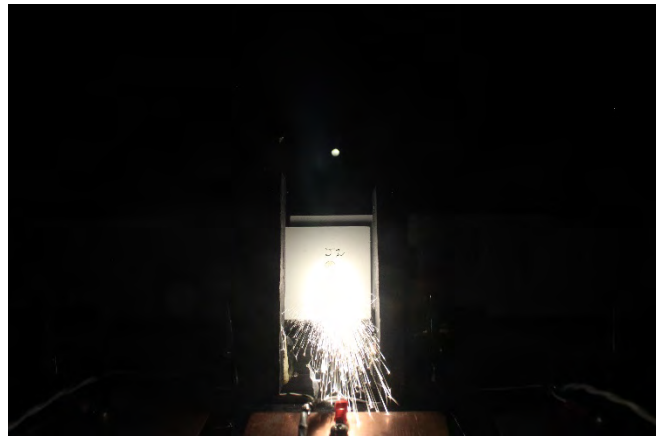


Figure 38: MN-1I11-3, during test, internal sparks on J1 & J3, external spark on J2



Figure 39: MN-1I11-4, before test



Figure 40: MN-1I11-4, during test, external spark on J1, internal spark on J3



Figure 41: MN-1I11-6, before test



Figure 42: MN-1I11-6, during test, internal sparks on J1 & J2, external spark on J3

## OEM 5



Figure 43: MN-1IO3-2, before test

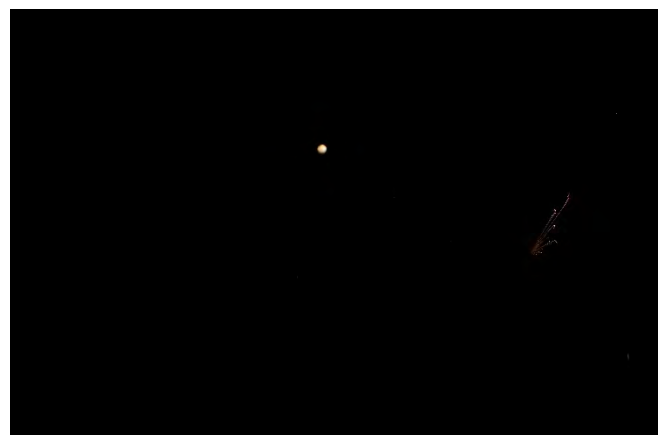


Figure 44: MN-1IO3-2, during test, external spark on J3





Figure 45: MN-1I12-1, shot 1, before test



Figure 46: MN-1I12-1, shot 1, during test, external sparks on all 3 joints

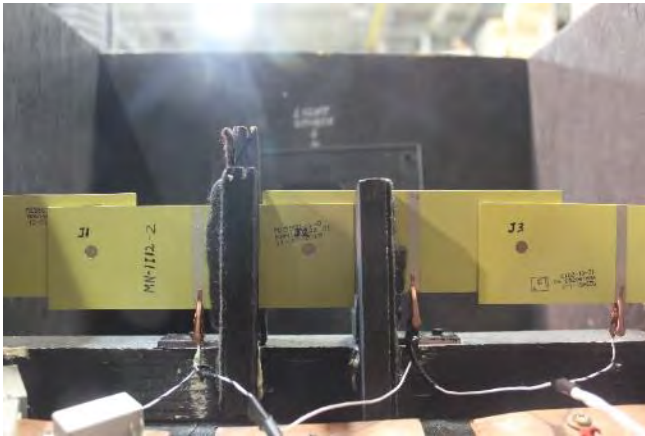


Figure 47: MN-1I12-2, before test



Figure 48: MN-1I12-2, during test, external sparks on all 3 joints

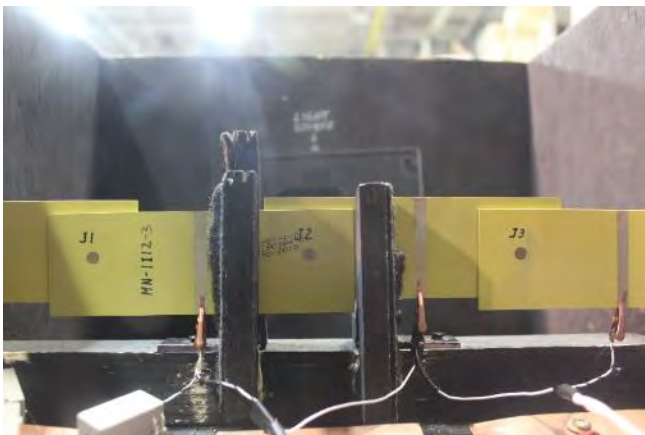


Figure 49: MN-1I12-3, before test

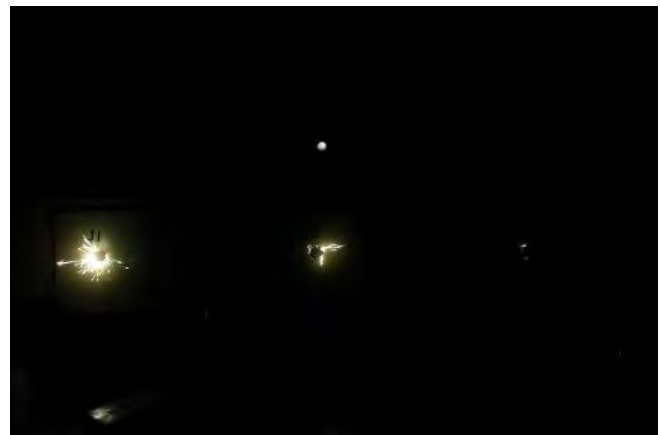


Figure 50: MN-1I12-3, during test, external sparks on all 3 joints

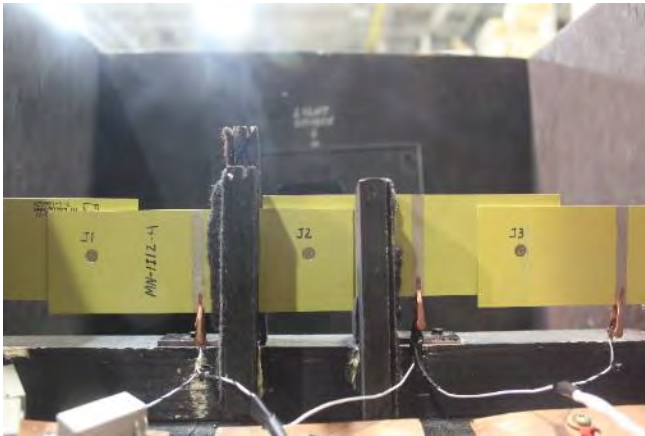


Figure 53: MN-1I12-4, before test



Figure 52: MN-1I12-4, during test, external sparks on all 3 joints

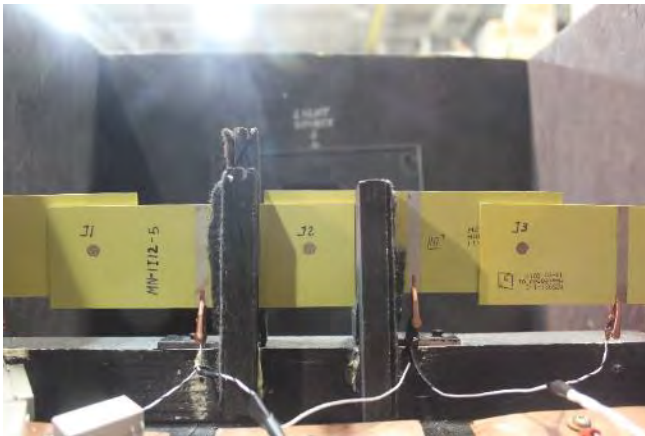


Figure 53: MN-1I12-5, before test

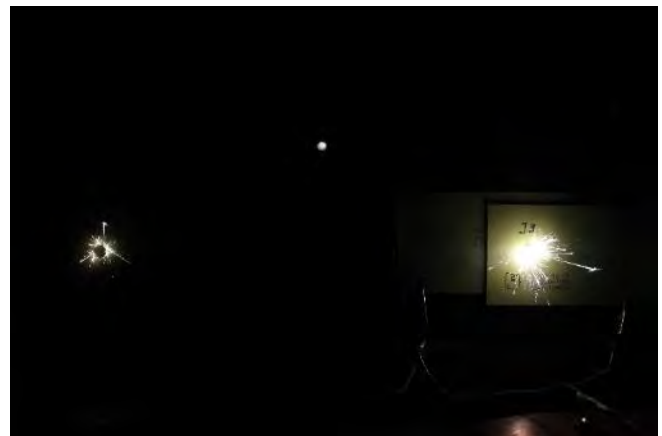


Figure 54: MN-1I12-5, during test, external sparks on J1 & J3

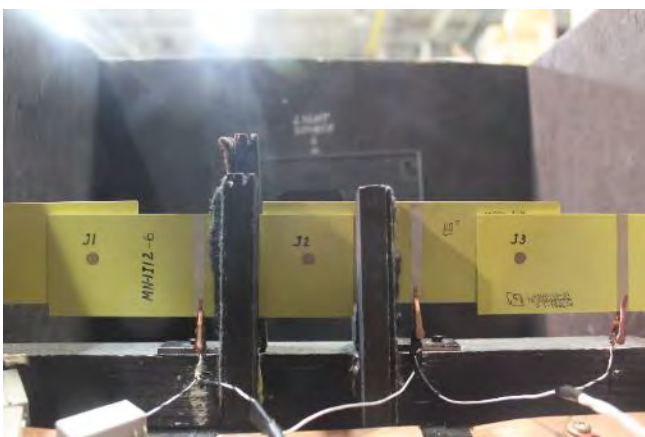


Figure 57: MN-1I12-6, before test



Figure 56: MN-1I12-6, during test, external sparks on J1 & J2

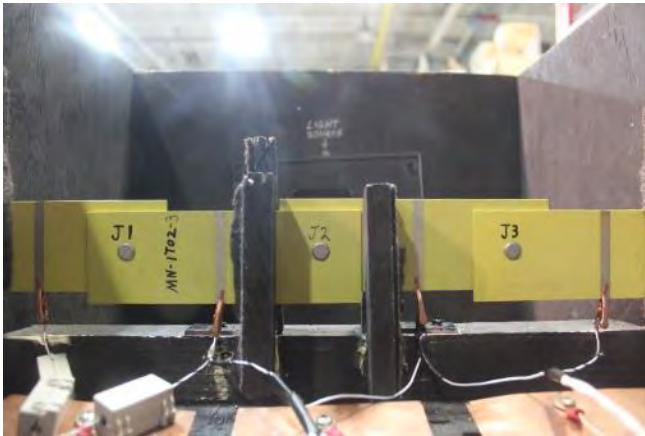


Figure 59: MN-1T02-3, before test



Figure 58: MN-1T02-3, during test, external spark on J1

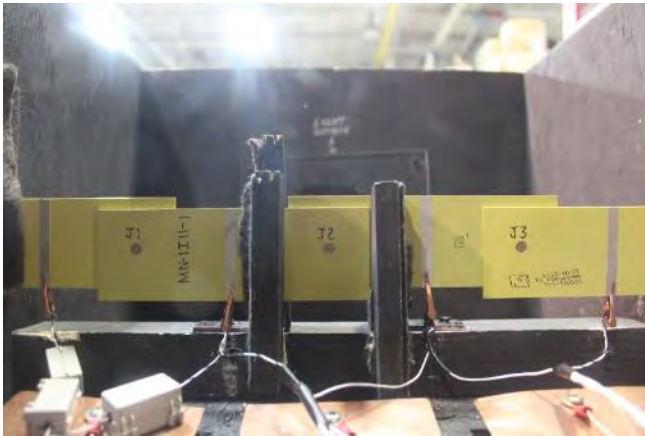


Figure 61: MN-1I11-1, shot 1, before test

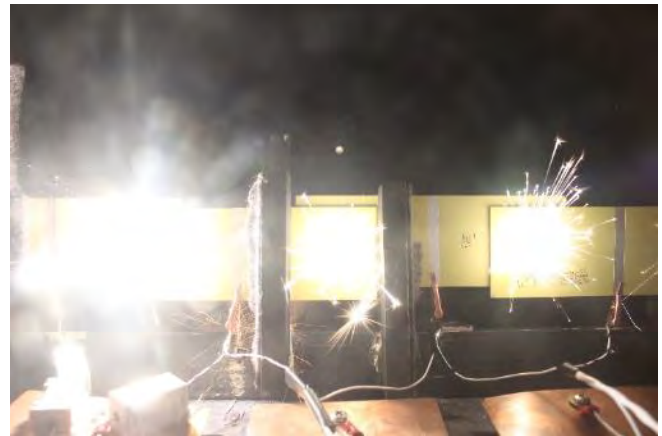


Figure 60: MN-1I11-1, shot 1, during test, external sparks on all 3 joints

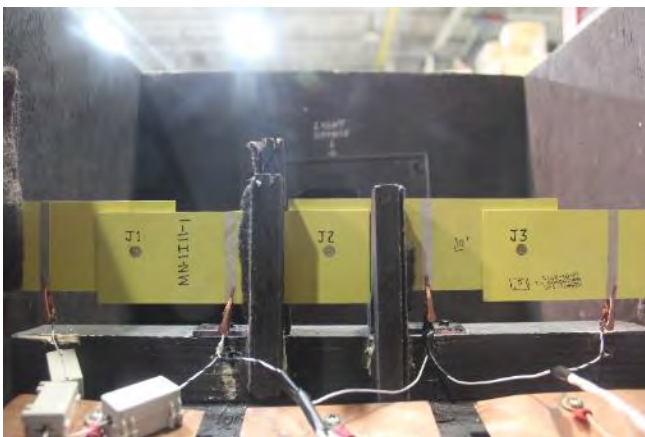


Figure 63: MN-1I11-1, shot 2, before test



Figure 62: MN-1I11-1, shot 2, during test, external spark on J2





Figure 65: MN-1I11-2, before test



Figure 64: MN-1I11-2, during test, external sparks on J2 & J3



Figure 67: MN-1I11-3, before test



Figure 66: MN-1I11-3, during test, external spark on J3



Figure 69: MN-1I11-5, before test

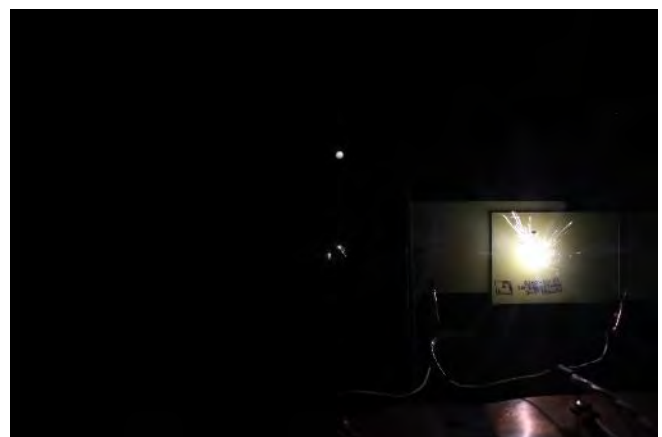


Figure 68: MN-1I11-5, during test, external sparks on J2 & J3

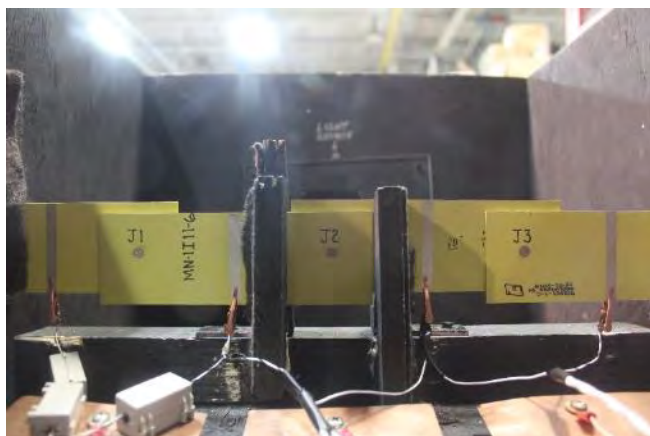


Figure 71: MN-1I11-6, before test

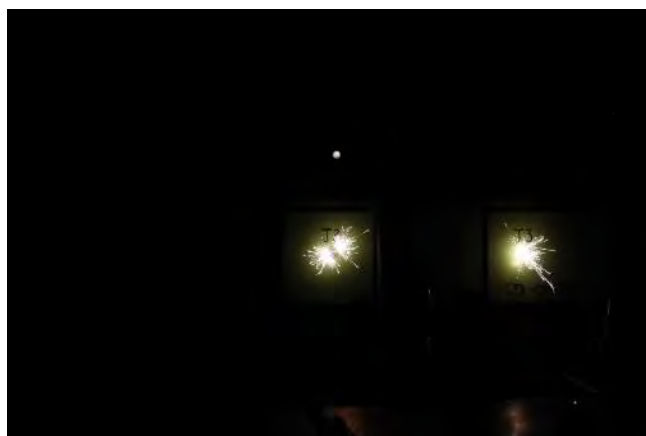


Figure 70: MN-1I11-6, during test, external sparks on J2 & J3



## **Nominal Quadruple Fastener Test Articles**

### **OEM 1**

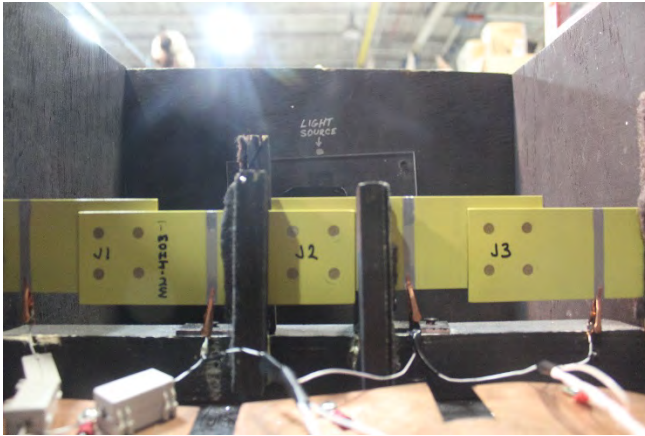


Figure 71: MN-4IO3-1, before test



Figure 72: MN-4IO3-1, during test, external sparks on J1 & J2

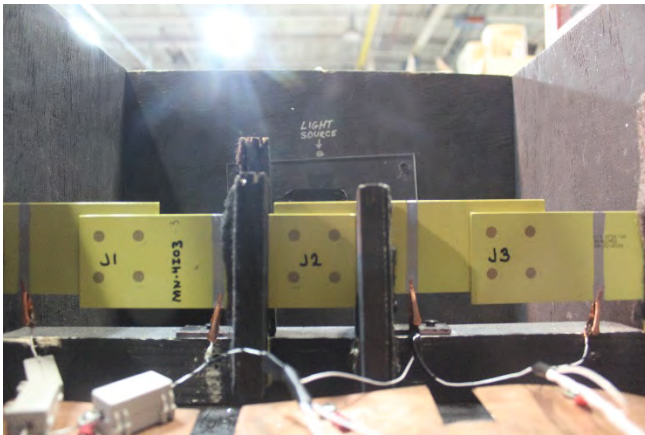


Figure 73: MN-4IO3-3, before test



Figure 74: MN-4IO3-3, during test, external spark on J1

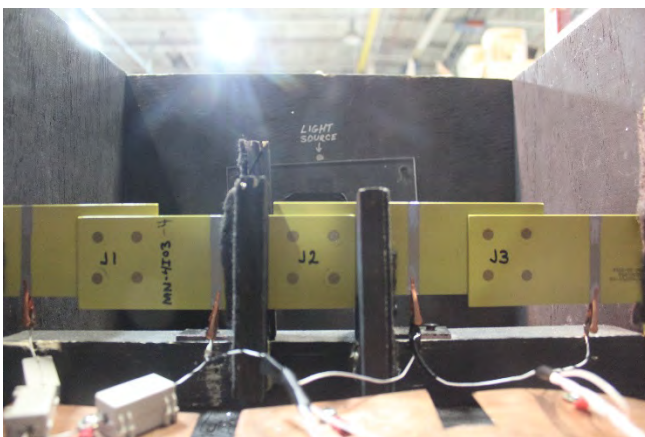


Figure 75: MN-4IO3-4, before test

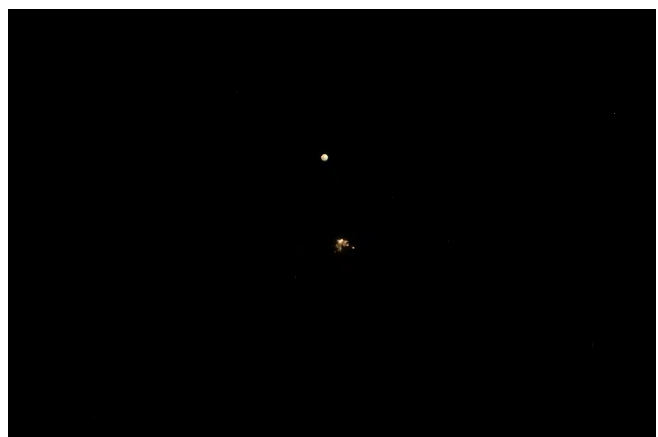


Figure 76: MN-4IO3-4, during test, external spark on J2

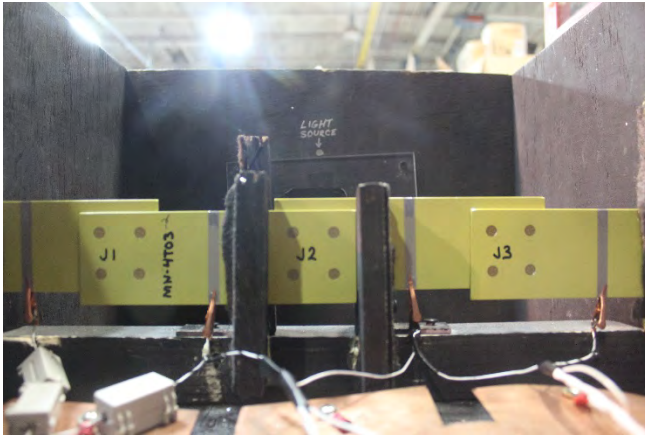


Figure 77: MN-4To3-2, before test

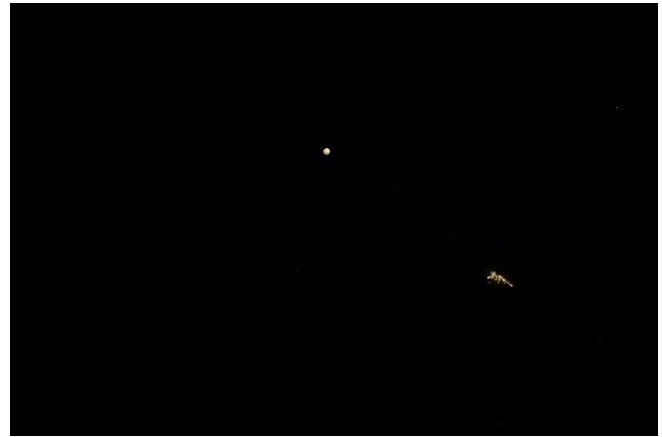


Figure 78: MN-4To3-2, during test, external spark on J3

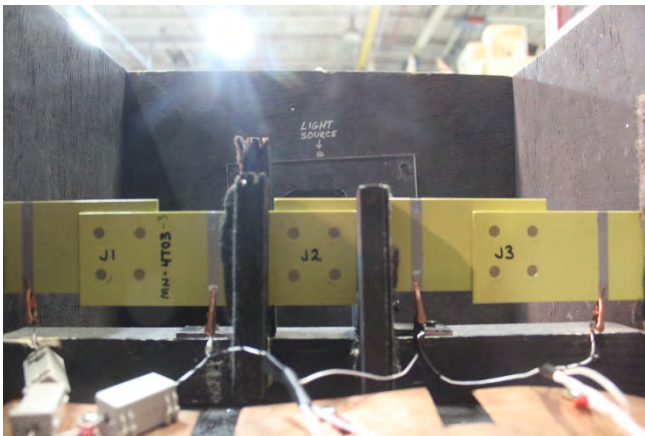


Figure 79: MN-4To3-3, before test

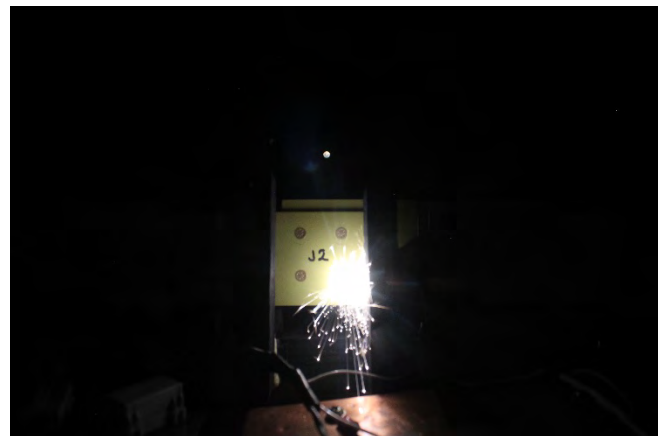


Figure 80: MN-4To3-3, during test, external spark on J2

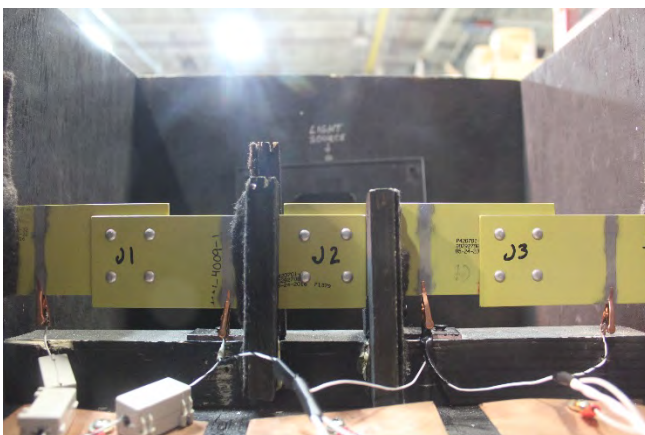


Figure 81: MN-4009-1, before test

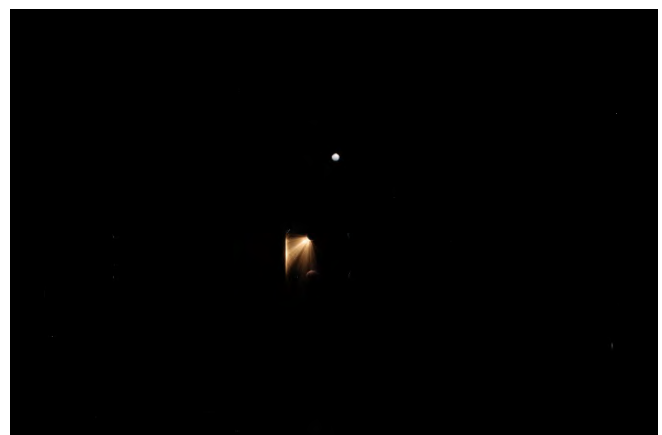


Figure 82: MN-4009-1, during test, external spark on J2

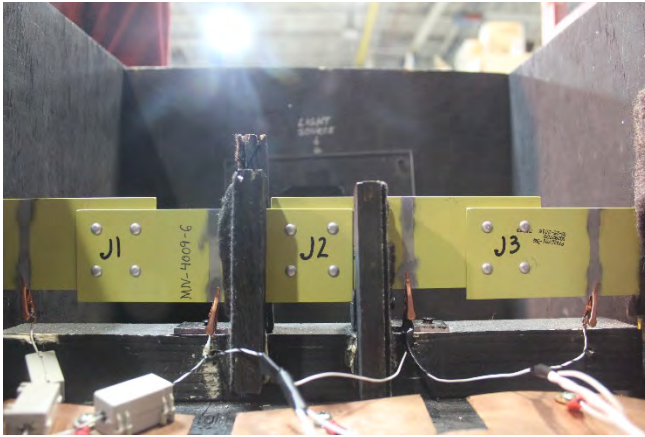


Figure 83: MN-4009-6, before test



Figure 84: MN-4009-6, during test, external spark on J2

**OEM 2 – no external sparking in Quadruple fastener test articles**

**OEM 3 – no external sparking in Quadruple fastener test articles**

**OEM 4**

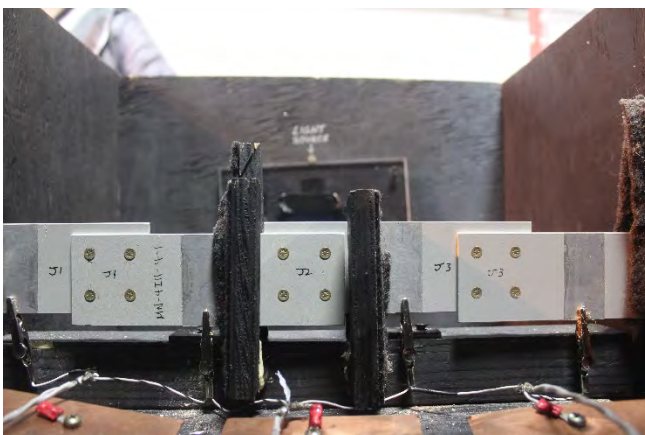


Figure 85: MN-4I11, shot 1, before test

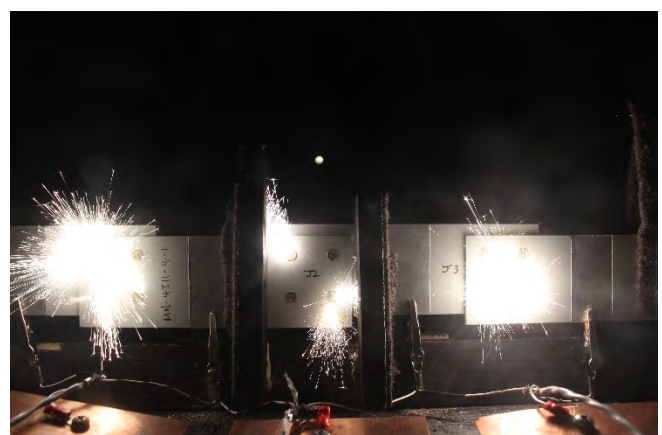


Figure 86: MN-4I11, shot 1, during test, external sparks on all 3 joints



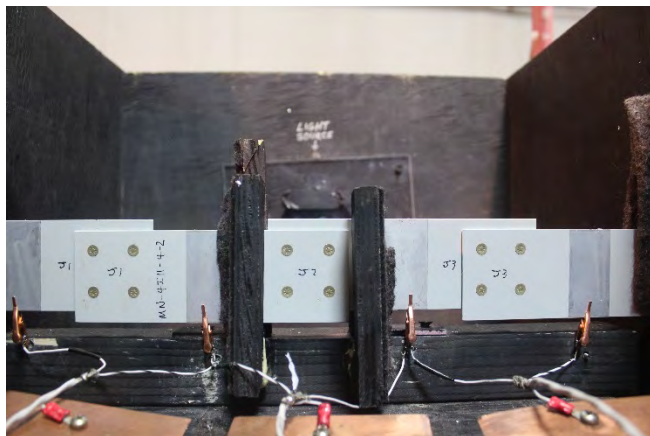


Figure 87: MN-4I11-2, shot 1, before test

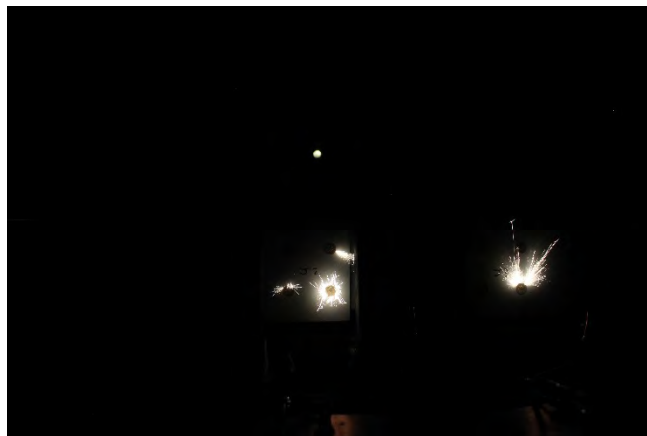


Figure 88: MN-4I11-2, shot 1, during test, external sparks on J2 & J3

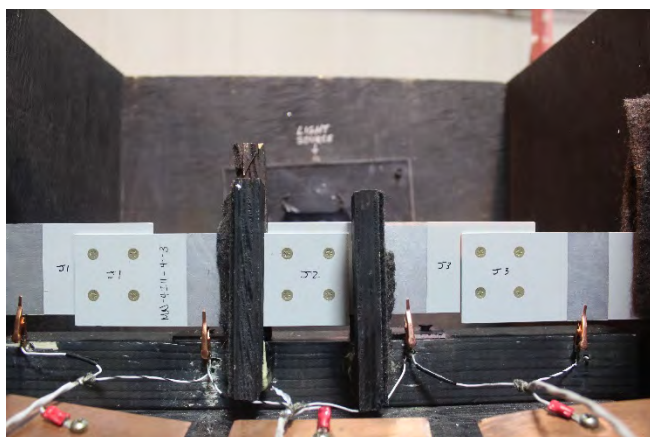


Figure 89: MN-4I11-3, before test

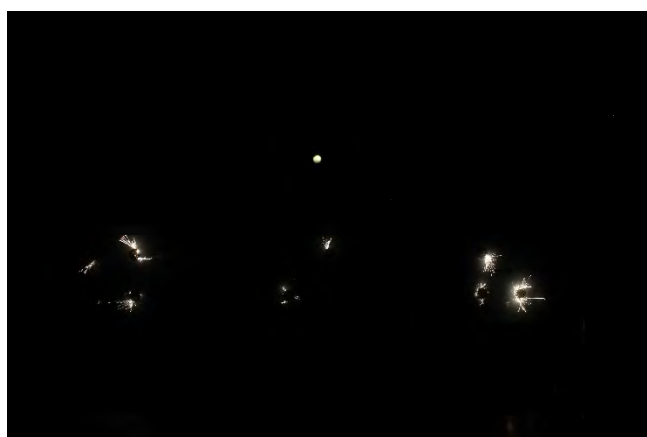


Figure 90: MN-4I11-3, during test, external sparks on all 3 joints

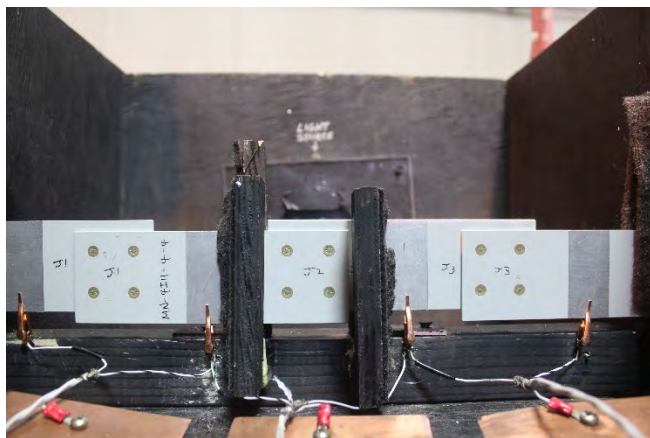


Figure 91: MN-4I11-4, before test

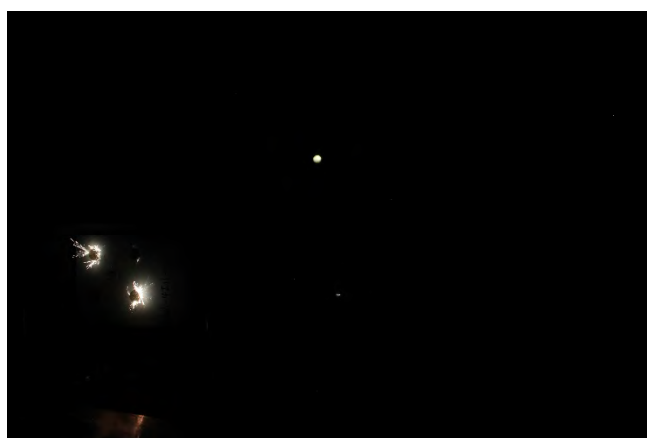


Figure 92: MN-4I11-4, during test, external sparks on J1 & J2, internal spark on J3

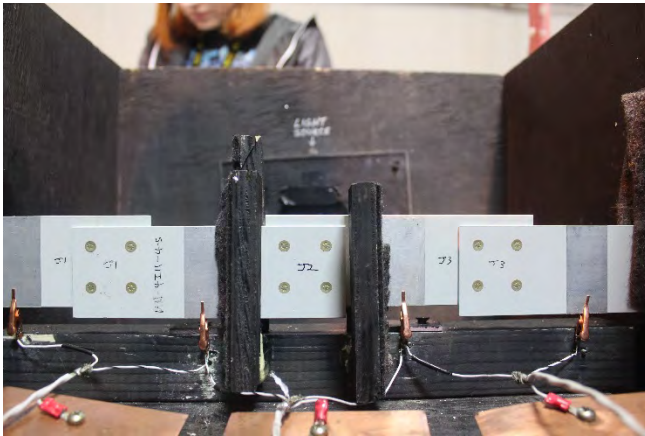


Figure 93: MN-4I11-5, before test



Figure 94: MN-4I11-5, during test, external sparks on J1 & J2, internal spark on J3



Figure 95: MN-4I11-6, before test

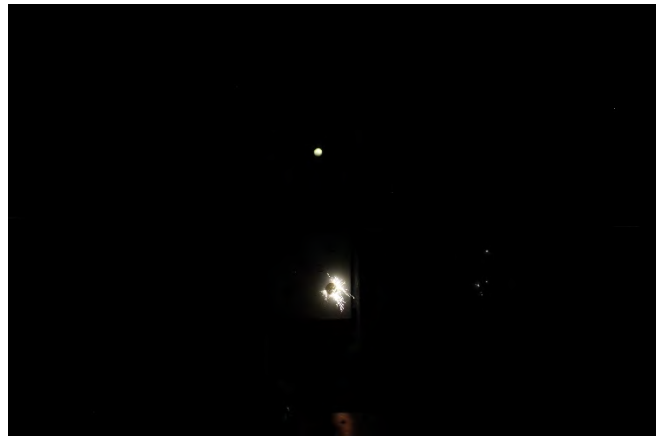


Figure 96: MN-4I11-6, during test, internal spark on J1, external sparks on J2 & J3

## **OEM 5**

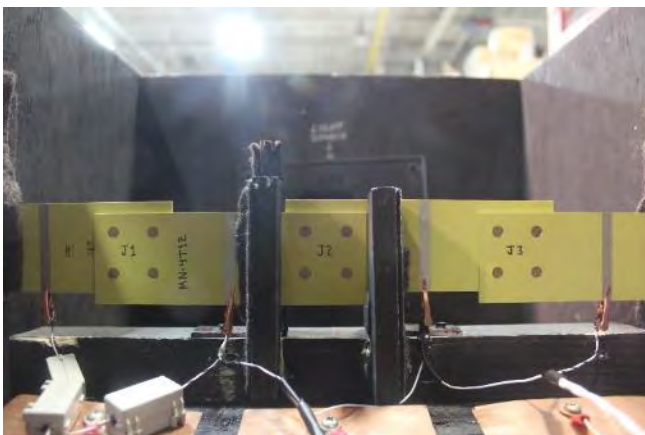


Figure 97: MN-4T12, before test

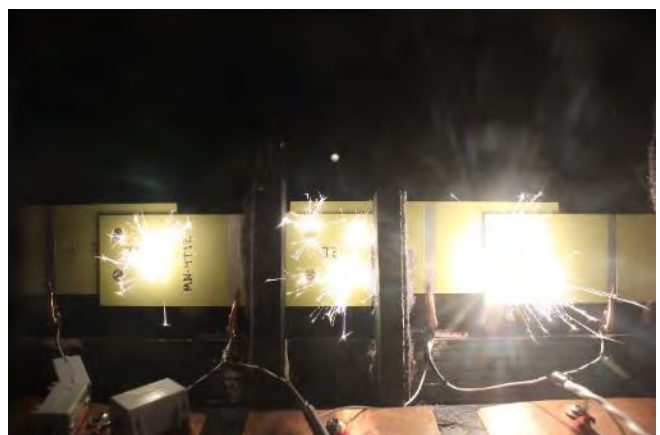


Figure 98; MN-4T12, during test, external sparks on all 3 joints



**Faulted Fastener Test Articles**  
**OEM 1**

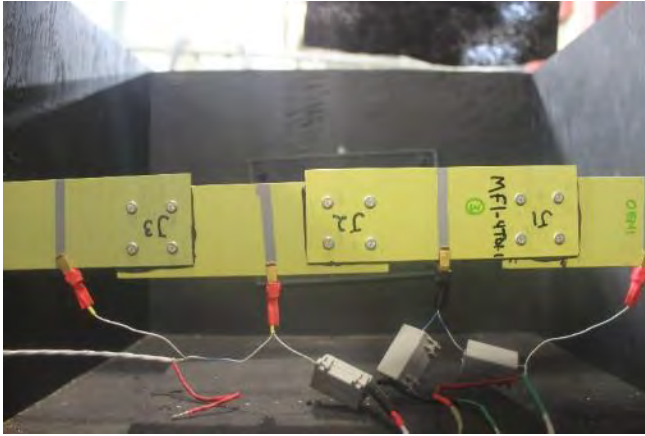


Figure 99: MF1-4T01-3, before test, front



Figure 100: MF1-4T01-3, 100kA, J1, during test, front

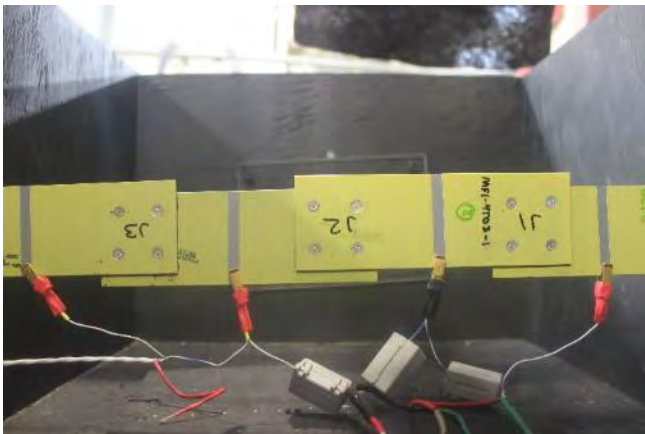


Figure 101: MF1-4T03-1, before test, front

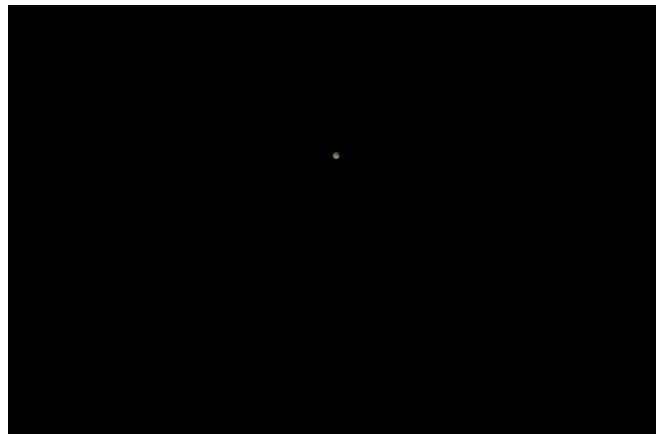


Figure 102: MF1-4T03-1, 35kA, J1, during test, front



Figure 103: MF1-4T12-2, before test, front



Figure 104: MF1-4T12-2, 0.5kA, J1, during test, front

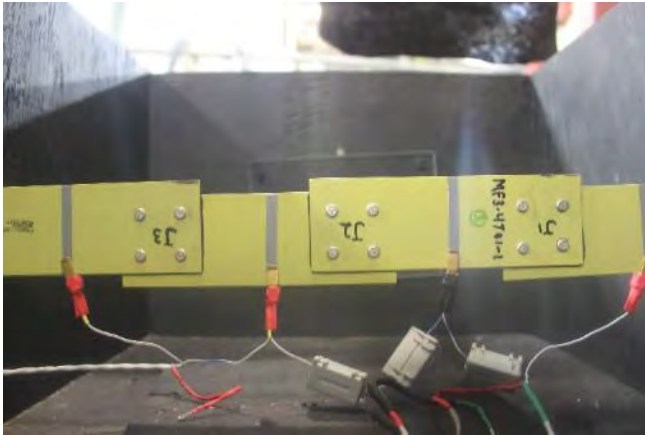


Figure 105: MF3-4To1-3, before test, front



Figure 106: MF3-4To1-3, 100kA, J2, during test, front



Figure 107: MF3-4T12-1, before test, front



Figure 108: MF3-4T12-1, 15kA, J2 & J3, during test, front

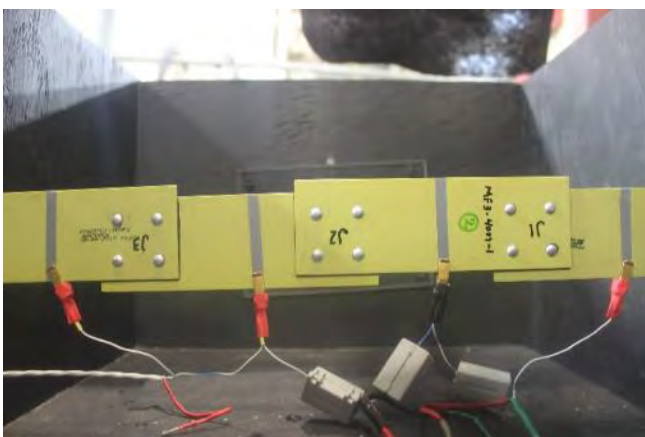


Figure 109: MF3-4009-2, before test, front

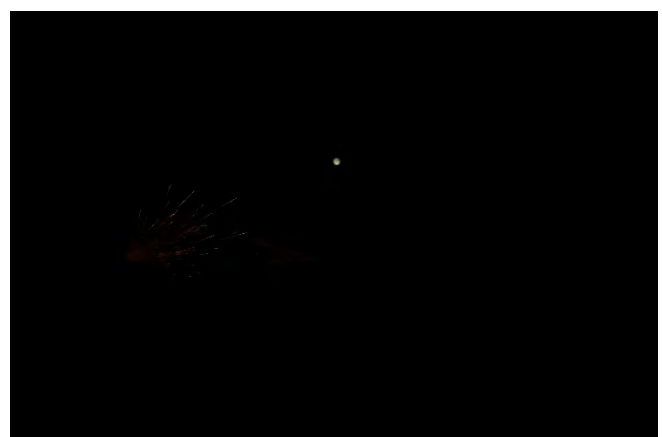


Figure 110: MF3-4009-2, 45kA, J2 & J3, during test, front

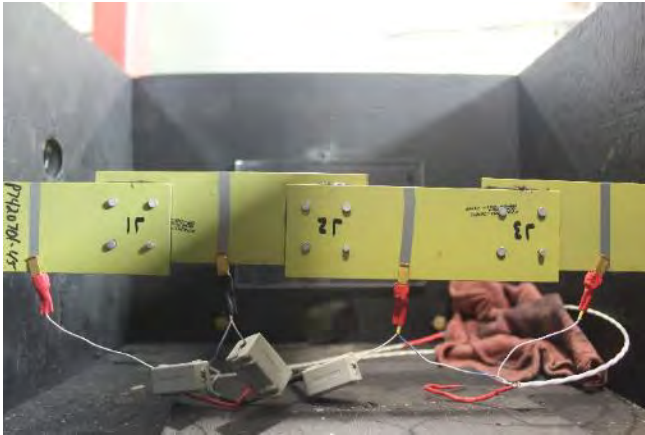


Figure 111: MF3-4009-2, before test, rear



Figure 112: MF3-4009-2, 45kA, J2, during test, rear

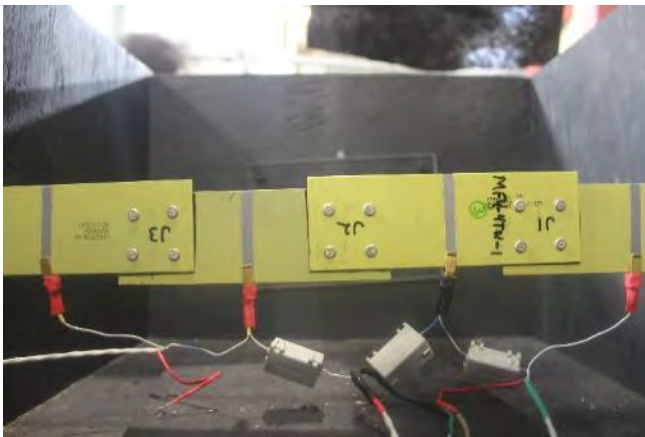


Figure 113: MF4-4T01-3, before test, front

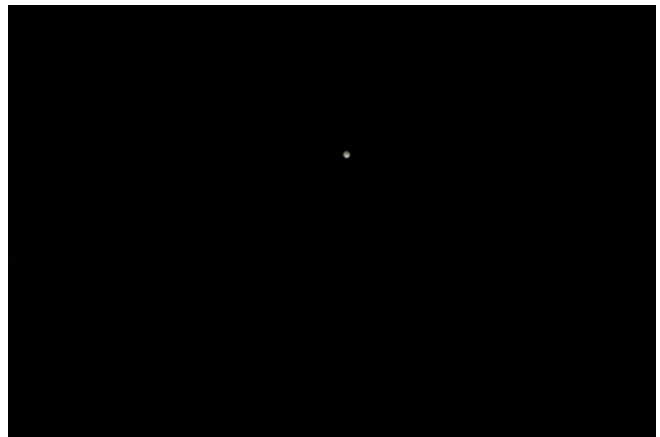


Figure 114: MF4-4T01-3, 80kA, J1, during test, front

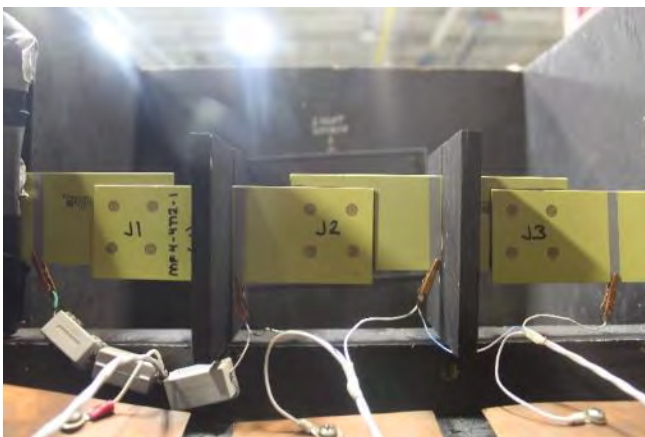


Figure 115: MF4-4T12-1, before test, front

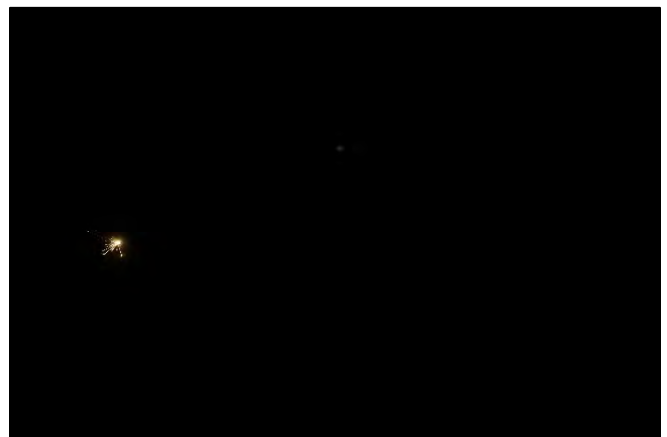


Figure 116: MF4-4T12-1, 5kA, J1, during test, front



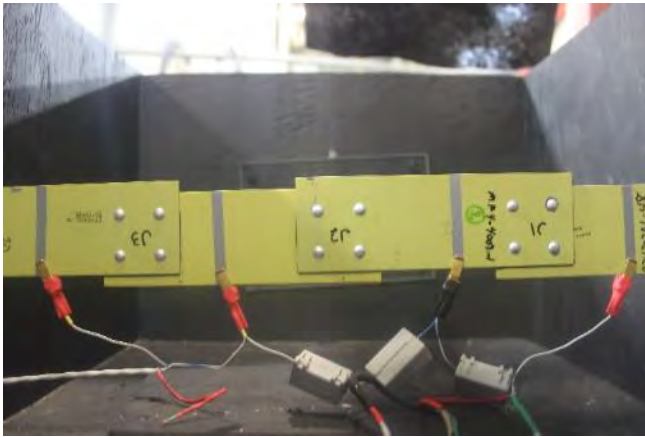


Figure 117: MF4-4009-2, before test, front



Figure 118: MF4-4009-2-20kA-J1 & J3,  
during test, front

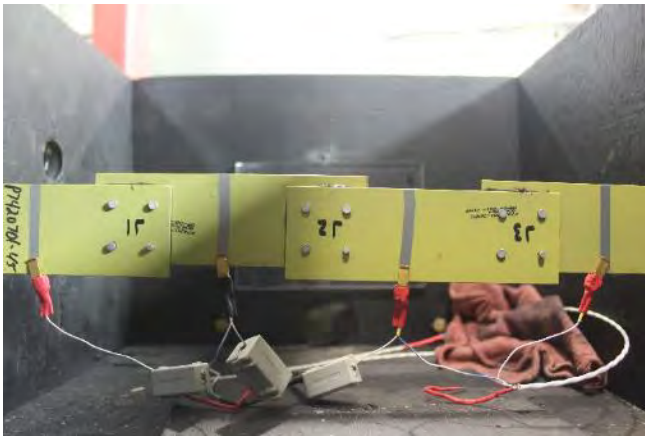


Figure 119: MF4-4009-2, before test, rear

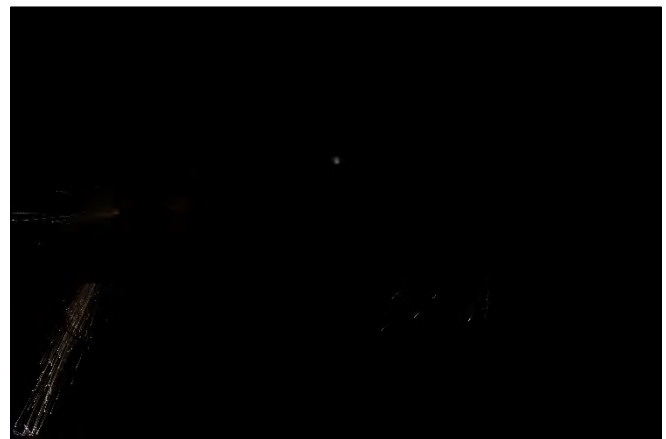


Figure 120: MF4-4009-2, 20kA, J1, during  
test, rear



Figure 121: MF5-4T12-1, before test, front

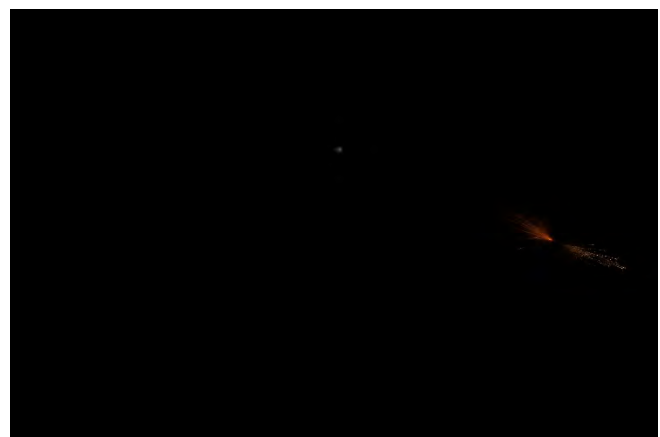


Figure 122: MF5-4T12-1, 6kA, J3, during test,  
front



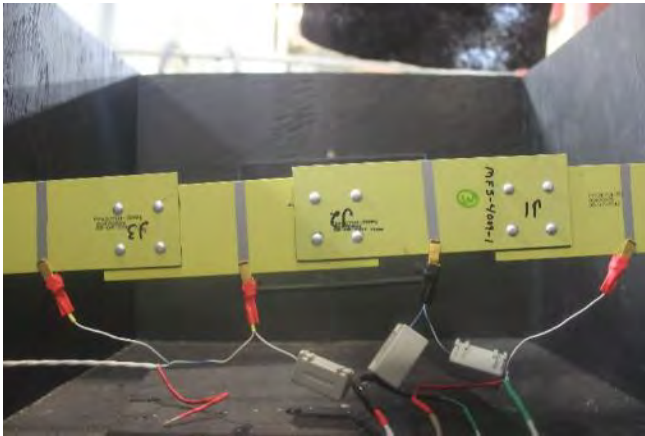


Figure 123: MF5-4009-3, before test, front



Figure 124: MF5-4009-3, 30kA, J1 & J2, during test, front

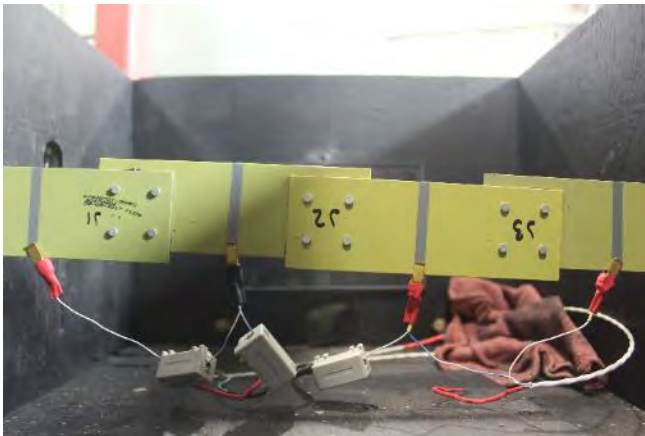


Figure 125: MF5-4009-3, before test, rear



Figure 126: MF5-4009-3, 30kA, J2 & J3, during test, rear



Figure 127: MF6-4T12-3, before test, front

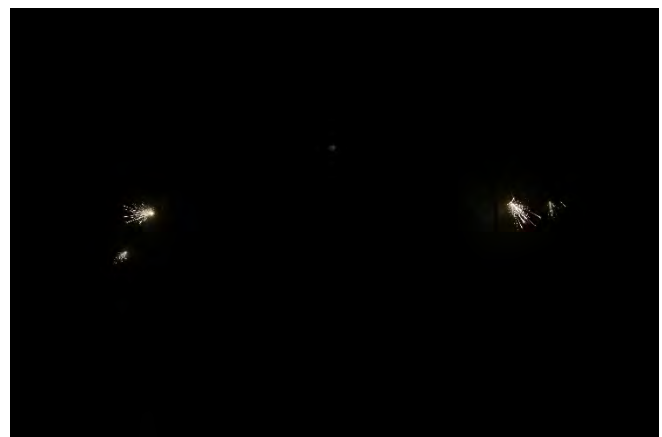


Figure 128: MF6-4T12-3, 5kA, J1 & J3, during test, front

## OEM 2

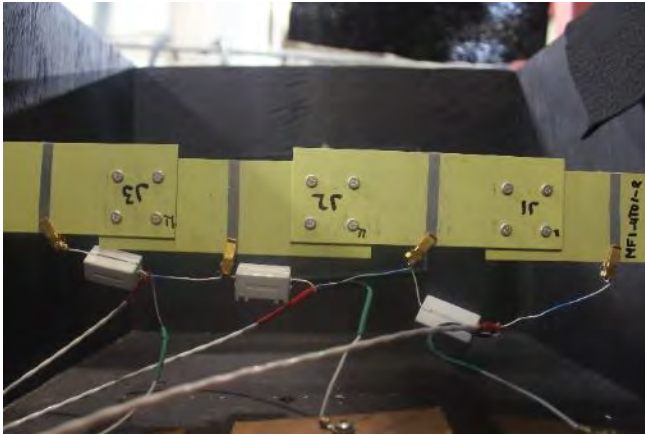


Figure 129: MF1-4TO1-2, before test, front



Figure 130: MF1-4TO1-2, 45kA, J3, during test, front

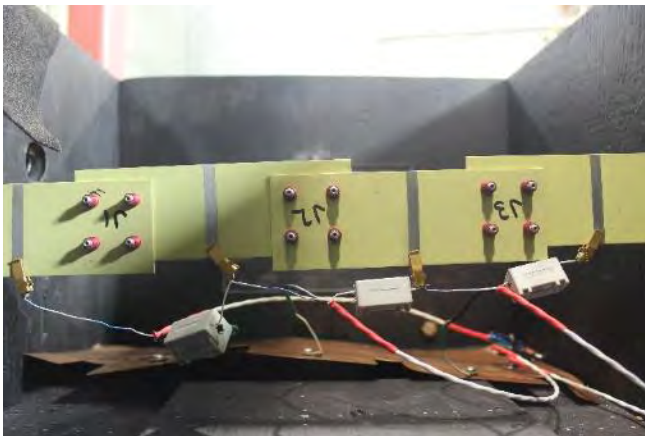


Figure 131: MF1-4TO1-2, before test, rear

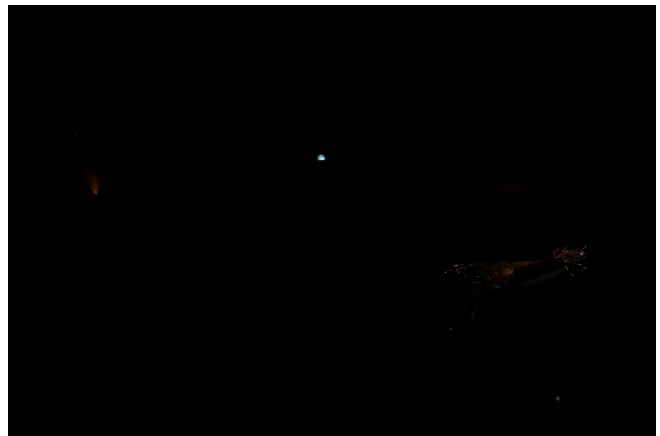


Figure 132: MF1-4TO1-2, 45kA, J1 & J3, during test, rear

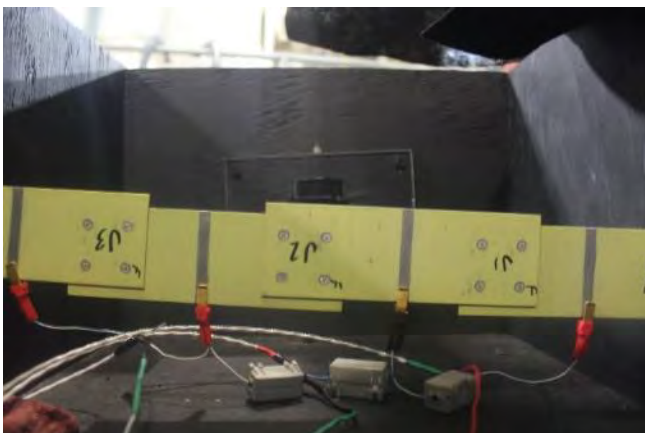


Figure 133: MF1-4TO3-2, before test, front



Figure 134: MF1-4TO3-2, 30kA, J1, during test, front

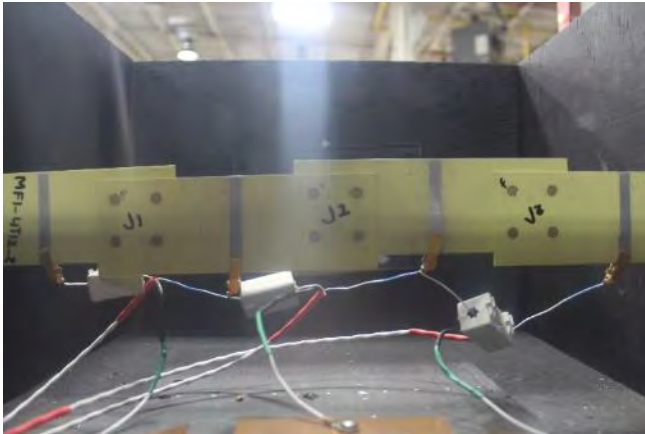


Figure 135: MF1-4T12-2, before test, front



Figure 136: MF1-4T12-2, 7kA, J3, during test, front

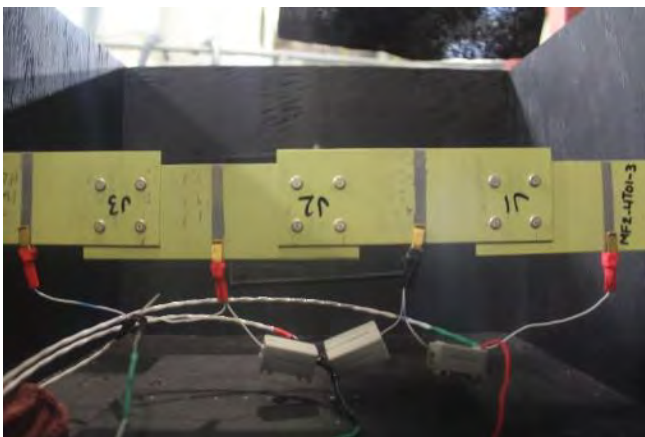


Figure 137: MF2-4To-3, before test, front

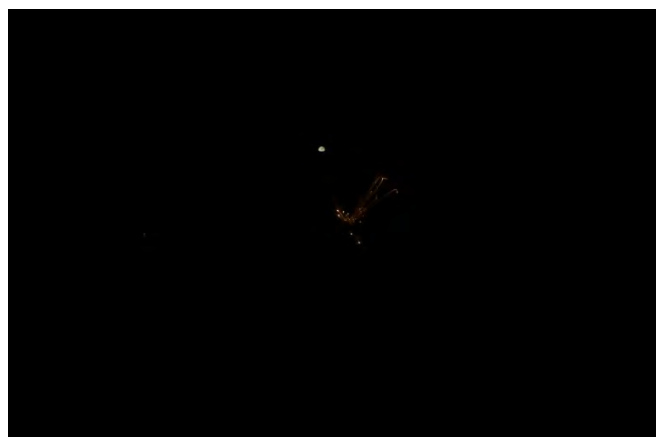


Figure 138: MF2-4To1-3, 35kA, J2, during test, front

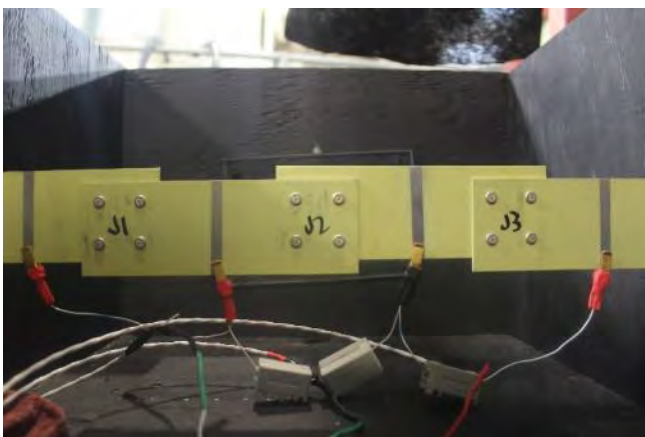


Figure 139: MF3-4To1-3, before test, front

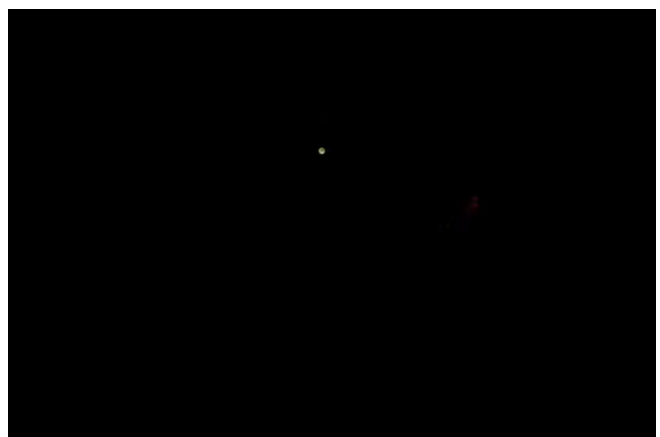


Figure 140: MF3-4To1-3, 13kA, J3, during test, front



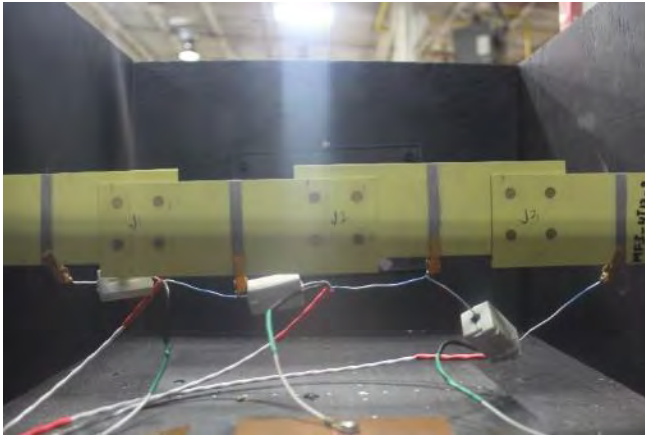


Figure 141: MF3-4T12-2, before test, front



Figure 142: MF3-4T12-2, 10kA, J2 & J3, during test, front

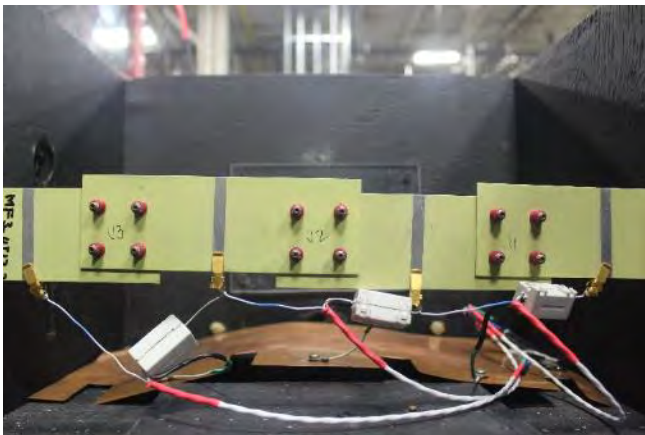


Figure 143: MF3-4T12-2, before test, rear



Figure 144: MF3-4T12-2, 10kA, J2 & J3, during test, rear

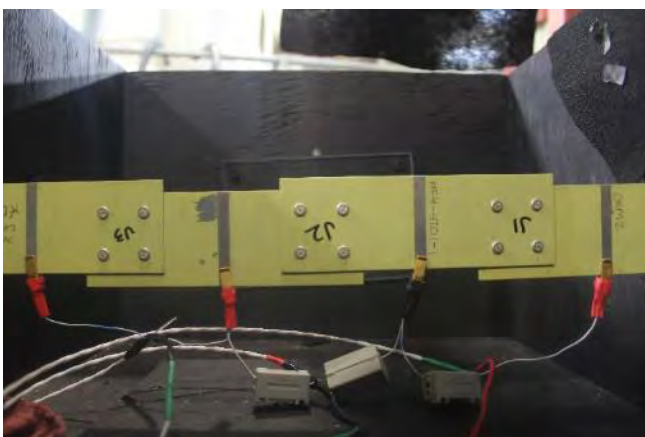


Figure 145: MF4-4T01-1, before test, front

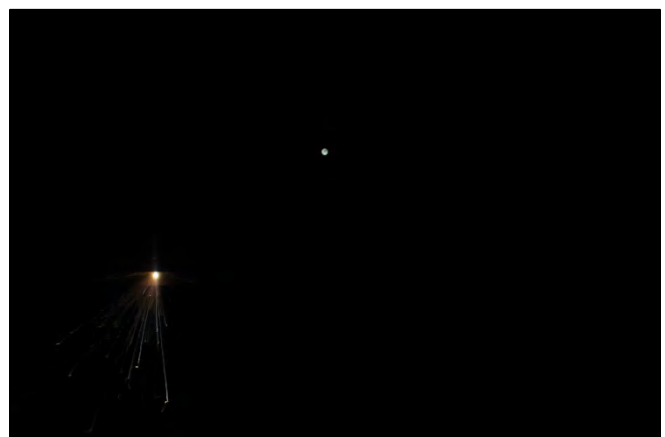


Figure 146: MF4-4T01-1, 25kA, J3, during test, front



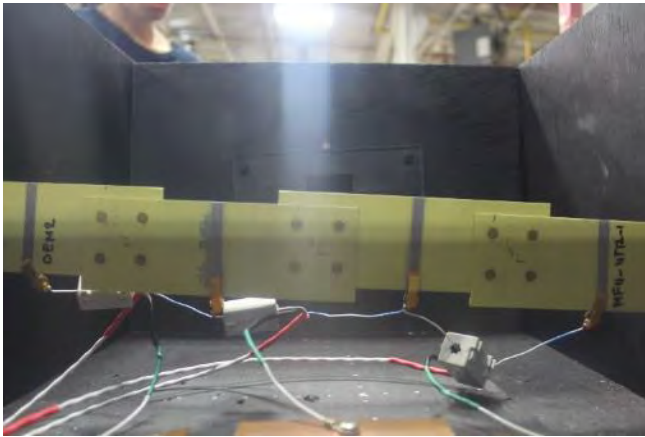


Figure 147: MF4-4T12-1, before test, front



Figure 148: MF4-4T12-1, 7kA, J21, during test, front

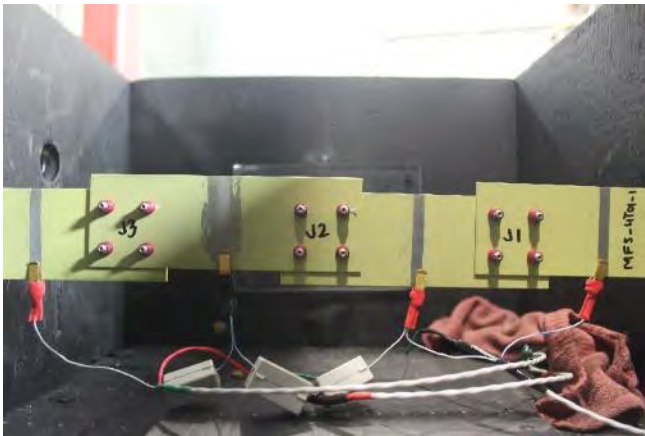


Figure 149: MF5-4T01-1, before test, rear

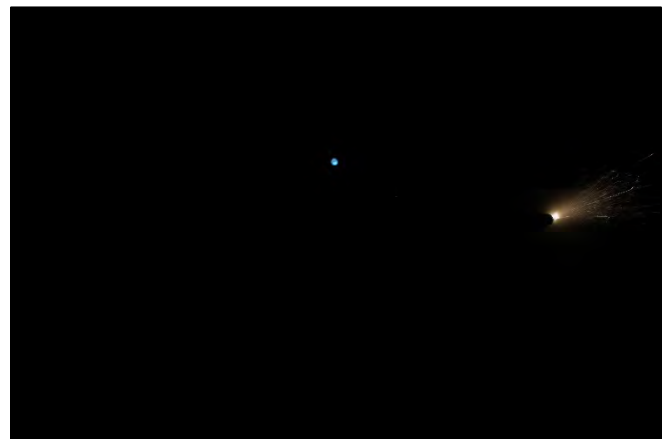


Figure 150: MF5-4T01-1, 35kA, J1, during test, rear

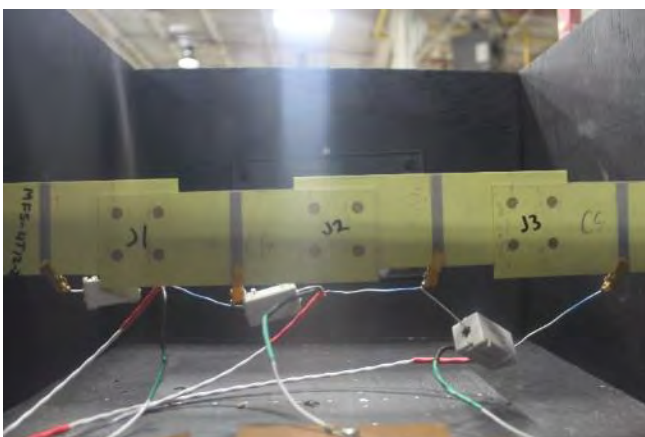


Figure 151: MF5-4T12-2, before test, front

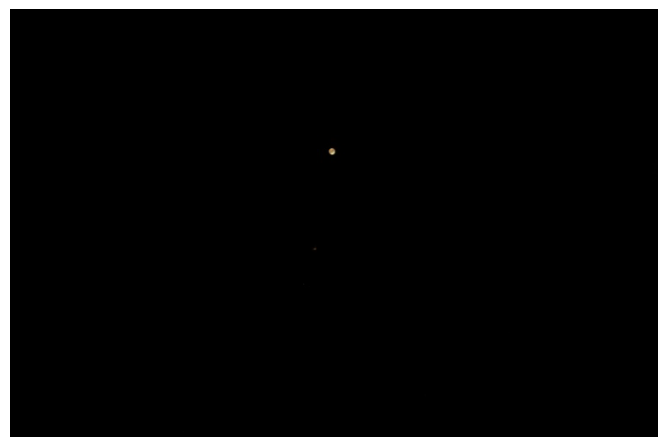


Figure 152: MF5-4T12-2, 7kA, J2, during test, front

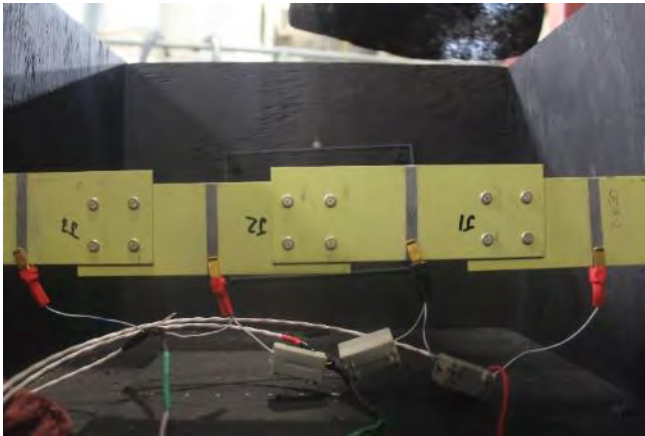


Figure 153: MF6-4To1-1, before test, front

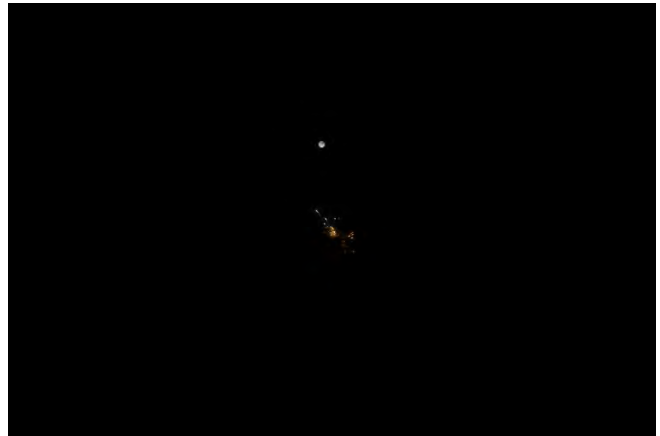


Figure 154: MF6-4To1-1, 35kA, J2, during test, front

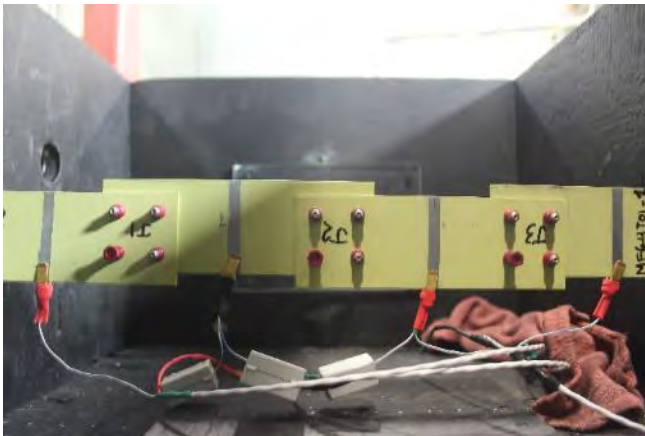


Figure 155: MF6-4To1-1, before test, rear

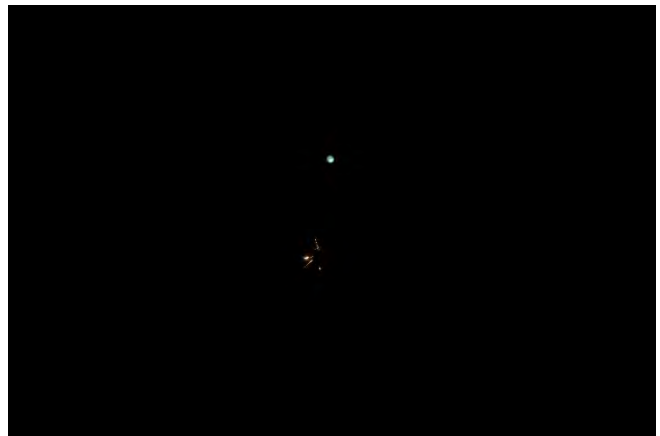


Figure 156: MF6-4To1-1, 35kA, J2, during test, rear

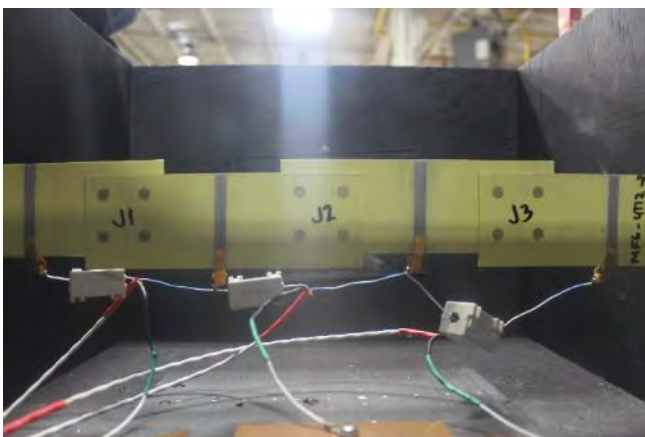


Figure 157: MF6-4T12-3, before test, front

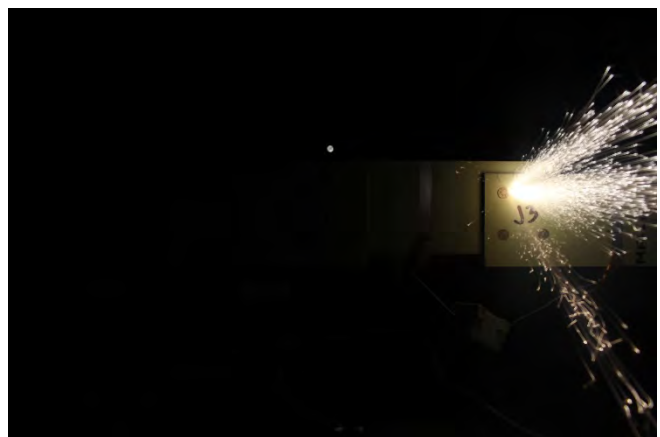


Figure 158: MF6-4T12-3-5kA-J1,J3, during test, front

### OEM 3

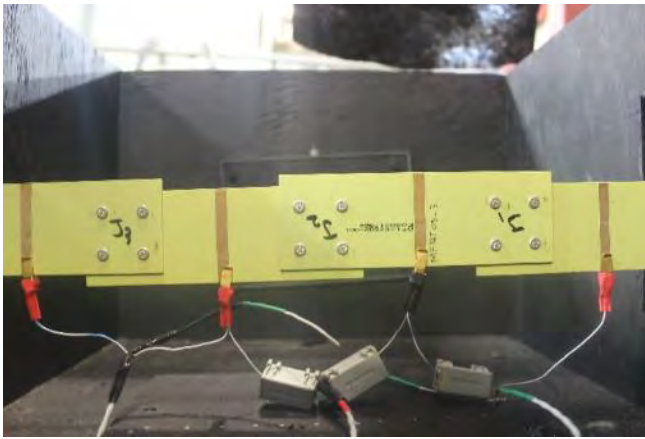


Figure 159: MF1-4T05-3, before test, front



Figure 160: MF1-4T05-3, 100kA, J1-during test, front



Figure 161: MF1-4T07-1, before test, rear

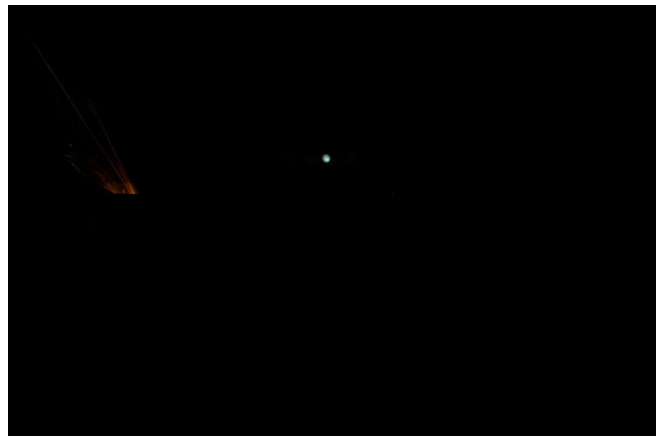


Figure 162: MF1-4T07-3, 45kA, J1, during test, rear



Figure 163: MF2-4T05-2, before test, rear

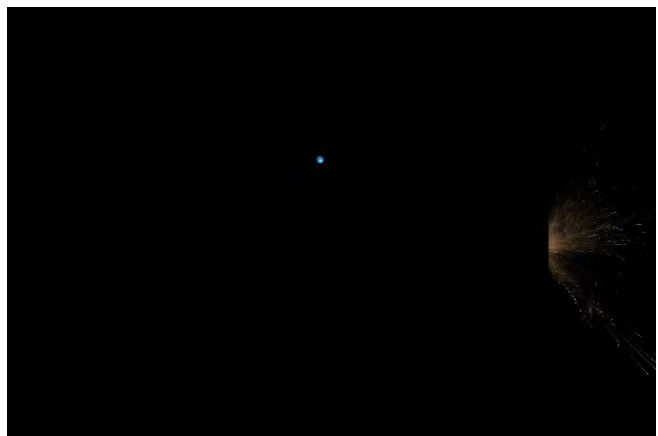


Figure 164: MF2-4T05-2-25kA, J3, during test, rear



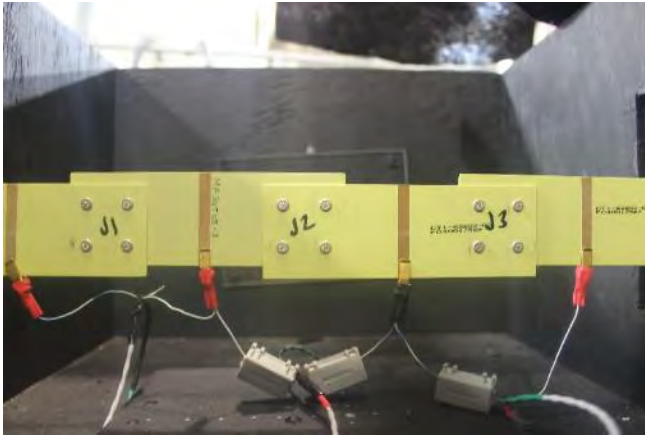


Figure 165: MF3-4T05-2, before test, front



Figure 166: MF3-4T05-2, 15kA, J2, during test, front



Figure 167: MF5-4T05-1, before test, rear

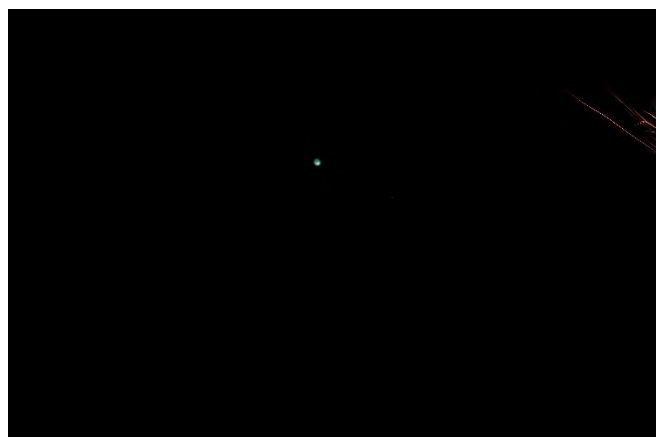


Figure 168: MF5-4T05-1-35kA-J1, during test, front

## **OEM 5**



Figure 169: MF1-4T01-3, before test, rear

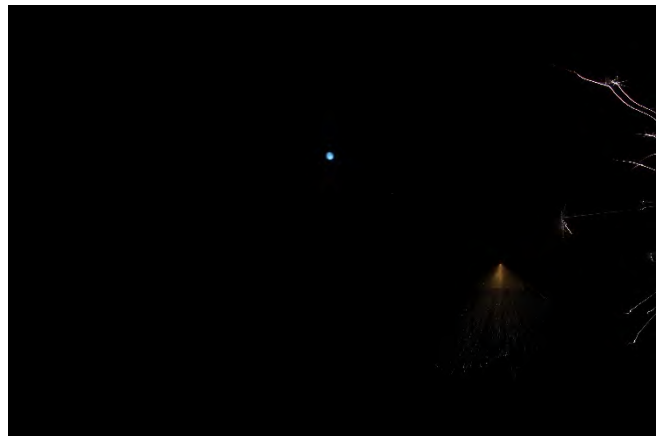


Figure 170: MF1-4T01-3, 100kA, J3, during test, rear





Figure 171: MF1-4To5-1, before test, rear

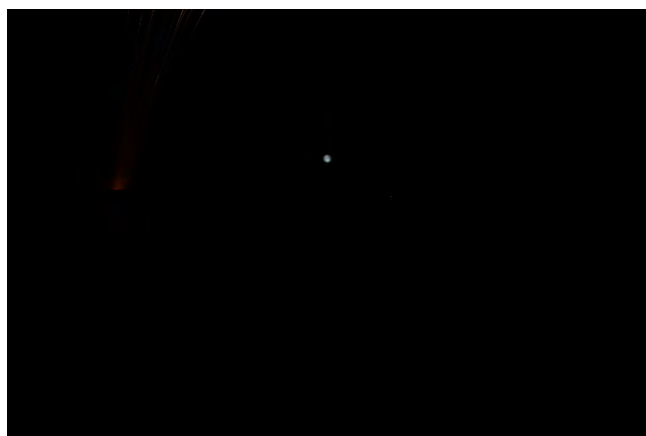


Figure 172: MF1-4To5-1, 35kA, J1, during test, rear

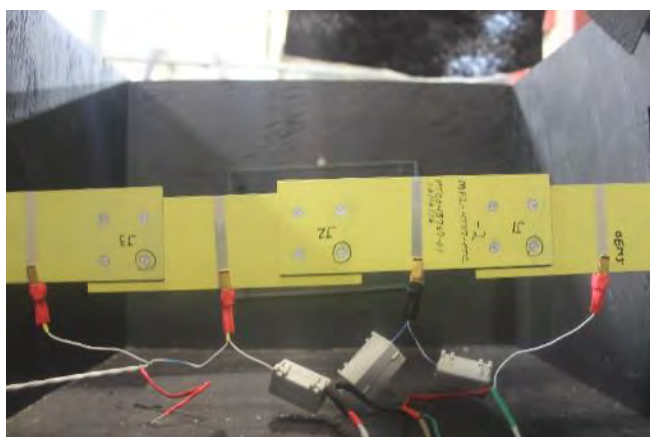


Figure 173: MF1-4To7-2, before test, front

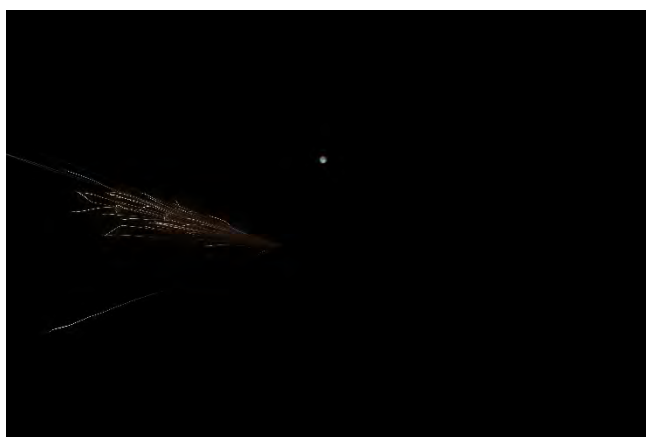


Figure 174: MF1-4To7-2, 60kA, J2, during test, front

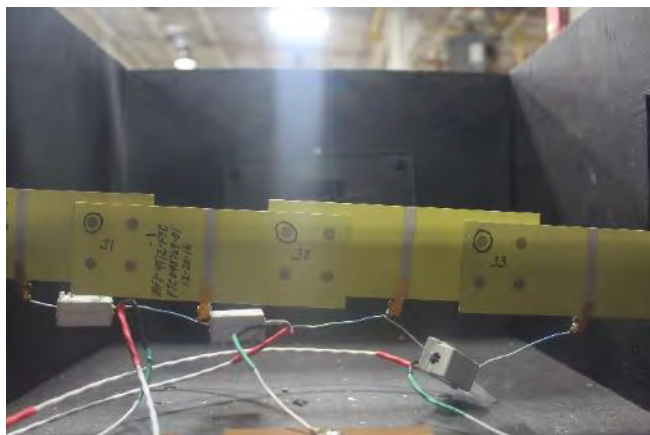


Figure 175: MF1-4T12-2, before test, front

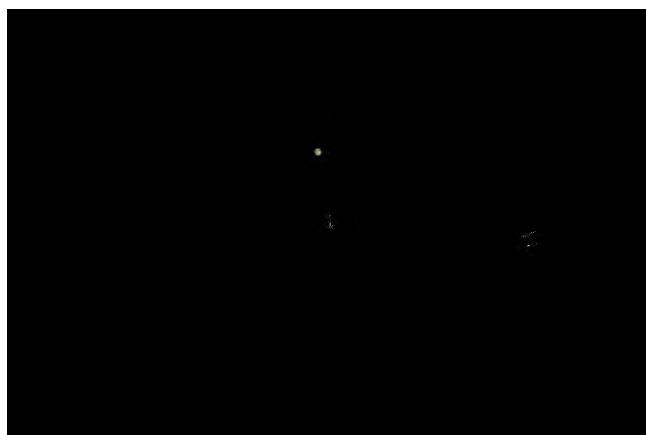


Figure 176: MF1-4T121, 3kA, J2 & J3, during test, front

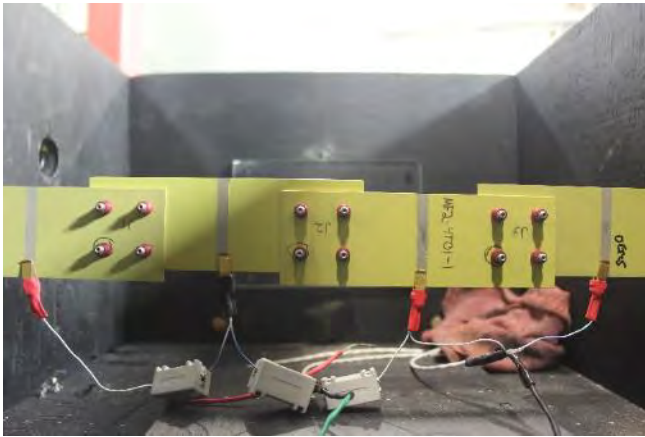


Figure 177: MF2-4T01-1, before test, rear

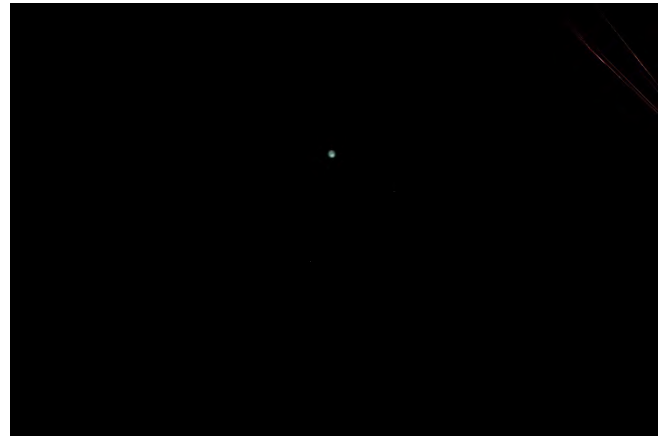


Figure 178: MF2-4T01-1, 60kA, J2, during test, rear

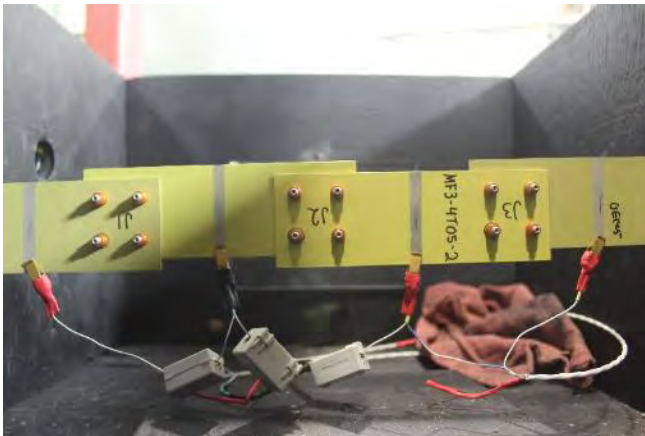


Figure 179: MF3-4T05-2, before test, rear

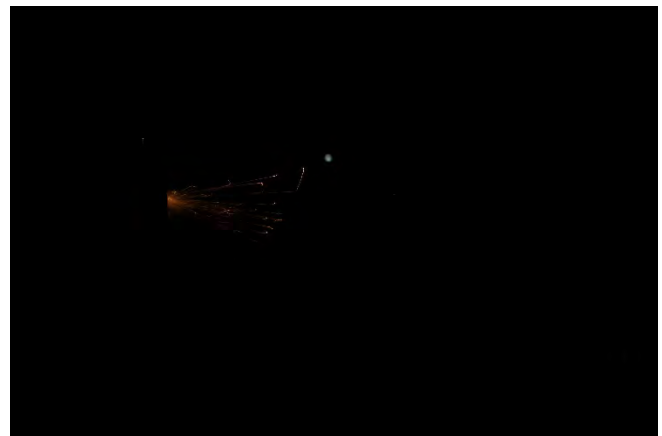


Figure 180: MF3-4T05-2, 60kA, J1, during test, rear

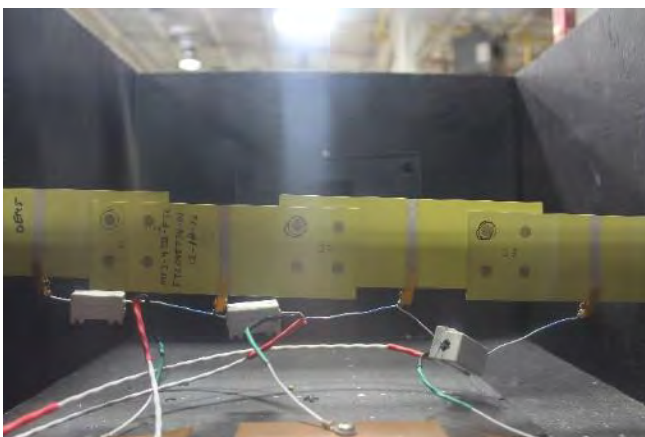


Figure 182: MF3-4T11-2, before test, front



Figure 181: MF3-4T11-2, 4kA, J3, during test, front

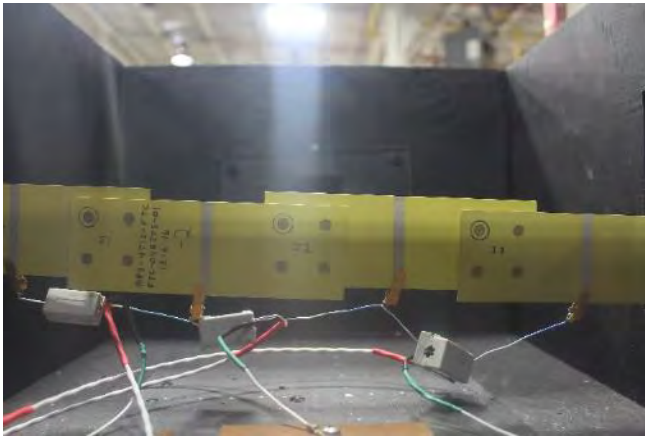


Figure 183: MF3-4T12-2, before test, front



Figure 184: MF3-4T12-2, 8kA, J2 & J3, during test, front

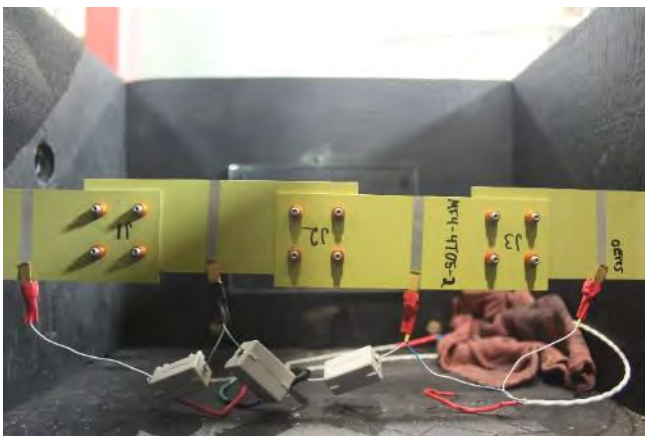


Figure 185: MF4-4T05-2, before test, rear

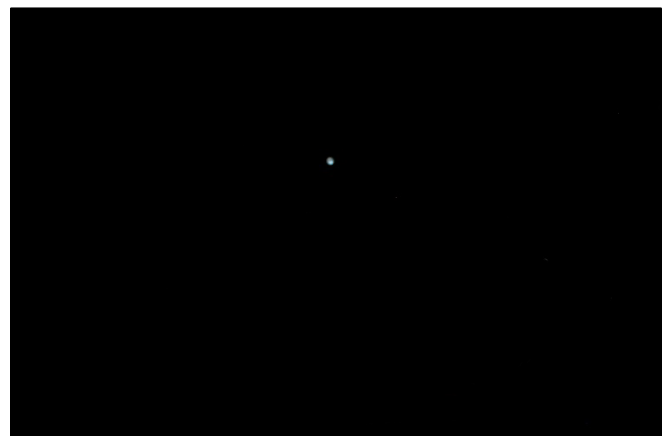


Figure 186: MF4-4T05-2, 80kA, J3, during test, rear

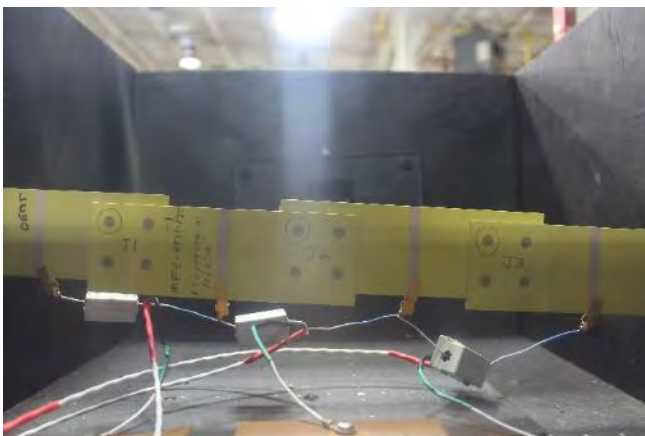


Figure 187: MF4-4T11-1, before test, front



Figure 188: MF4-4T11-1, 4kA, J1, during test, front

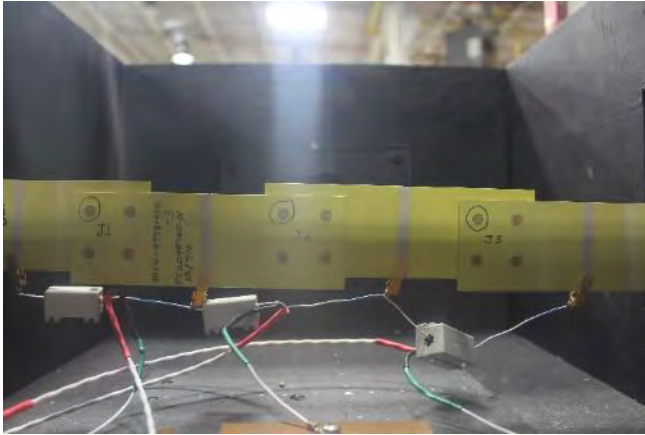


Figure 189: MF4-4T12-3, before test, front

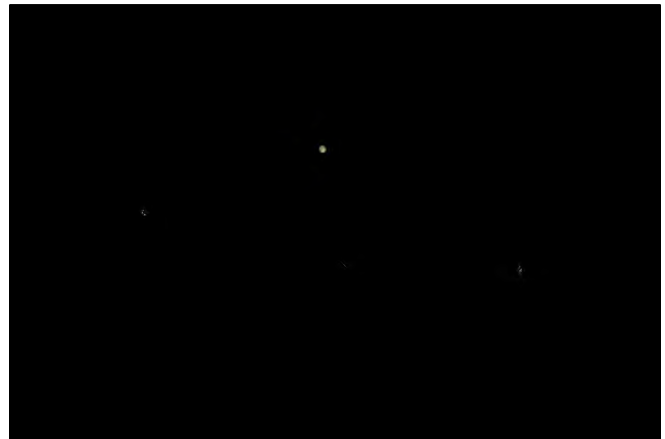


Figure 190: MF4-4T12-3, 3kA, J1, J2, & J3, during test, front



Figure 191: MF5-4T01-1, before test, rear

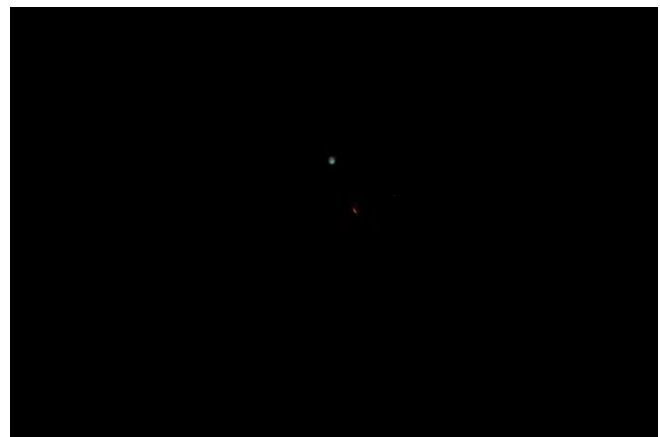


Figure 192: MF5-4T01-1, 35kA, J2, during test, rear



Figure 193: MF5-4T05-3, before test, rear

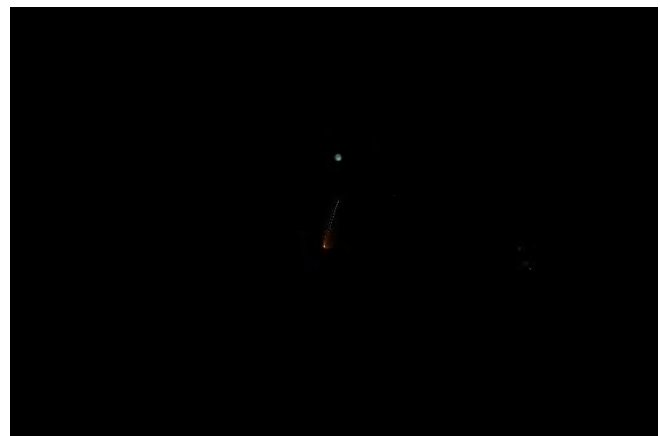


Figure 194: MF5-4T05-3, 35kA, J2, during test, rear



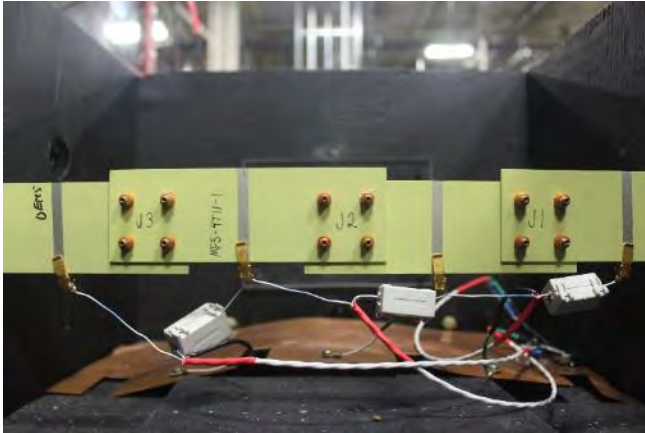


Figure 195: MF5-4T11-1, before test, rear



Figure 196: MF5-4T11-1, 4kA, J2, during test, rear

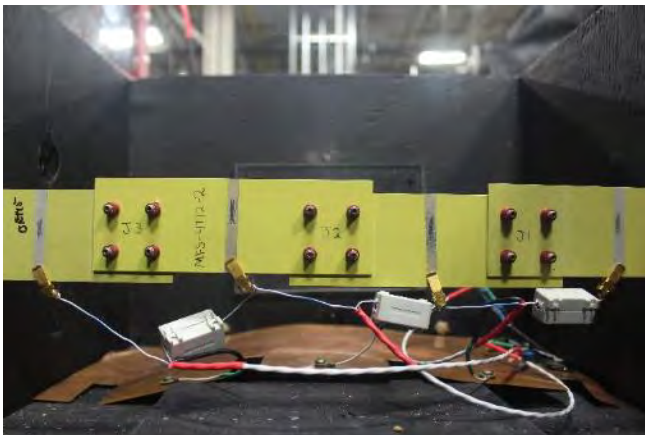


Figure 197: MF5-4T12-2, before test, rear

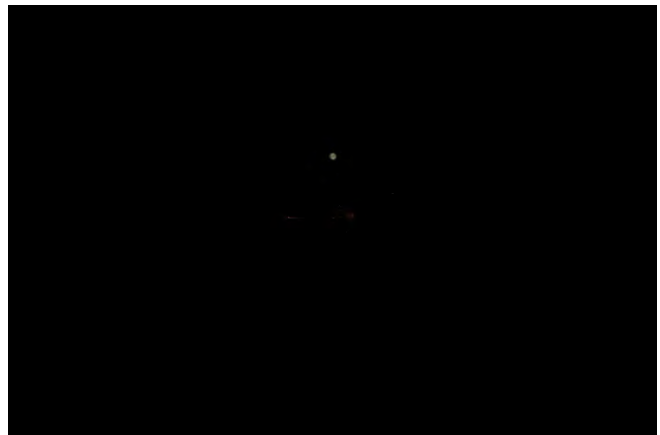


Figure 198: MF5-4T12-2, 5kA, J2, during test, rear

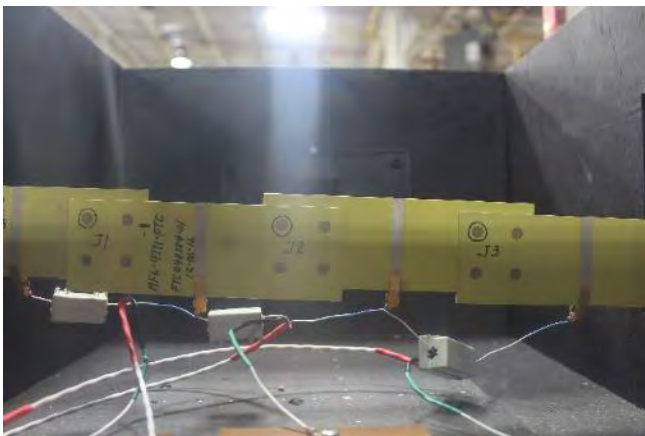


Figure 199: MF6-4T11-1, before test, rear

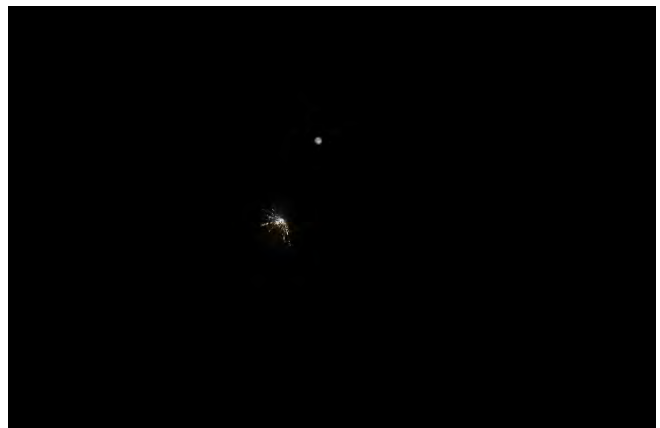


Figure 200: MF6-4T11-1, 5kA, J2, during test, rear

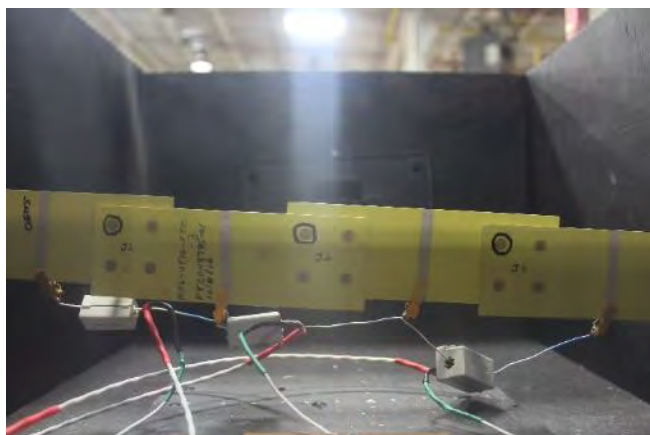


Figure 201: MF6-4T12-3, before test, rear

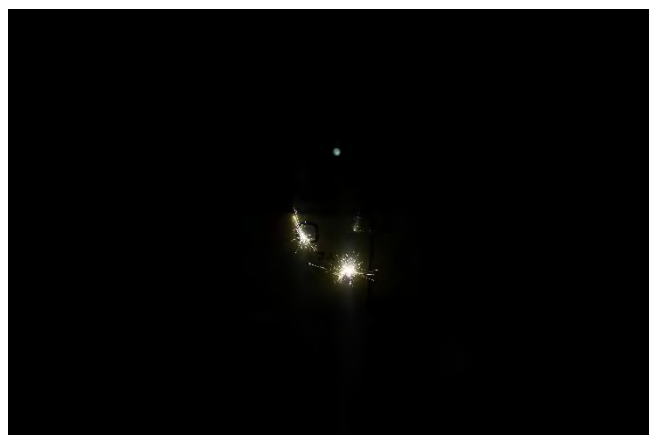


Figure 202: MF6-4T12-3, 7kA, J2, during test, rear

## Appendix G - 200 $\mu$ J Camera Calibration

### Nominal Test Articles

Table 11 and Figure 1 -Figure 3 present the camera calibration parameters and the photographs of the camera 200  $\mu$ J-based calibration procedure conducted by DNB Engineering, Inc., Fullerton, California used for testing the nominal fasteners. The photographs of the calibration setup and 200  $\mu$ J voltage spark generation and detection with the cameras to be calibrated are shown for camera 1 (S/N 142073019286) and camera 2 (S/N 122073012940) having the focal length of 18mm. In order to assist viewing of the 200  $\mu$ J spark in the photographs below, brightness and contrast settings were increased by 93% and 40%, respectively, in the Picture Corrections of Microsoft Word.

Table 11: Camera Calibration Parameters

CAMERA	TEST CONDITIONS (Temp.; Humidity; Pressure)		ISO	f Stop	IGNITION ENERGY (pF; KV; $\mu$ J)
<b>Cam 1 (Front)</b>	72.7; 35.4%; 29.87	S/N 142073019286	1600	5.6	9.0; 6.6; 196
<b>Cam 2 (Back)</b>	74.3; 35.3%; 29.89	S/N 122073012940	1600	5.6	9.0; 6.6; 196

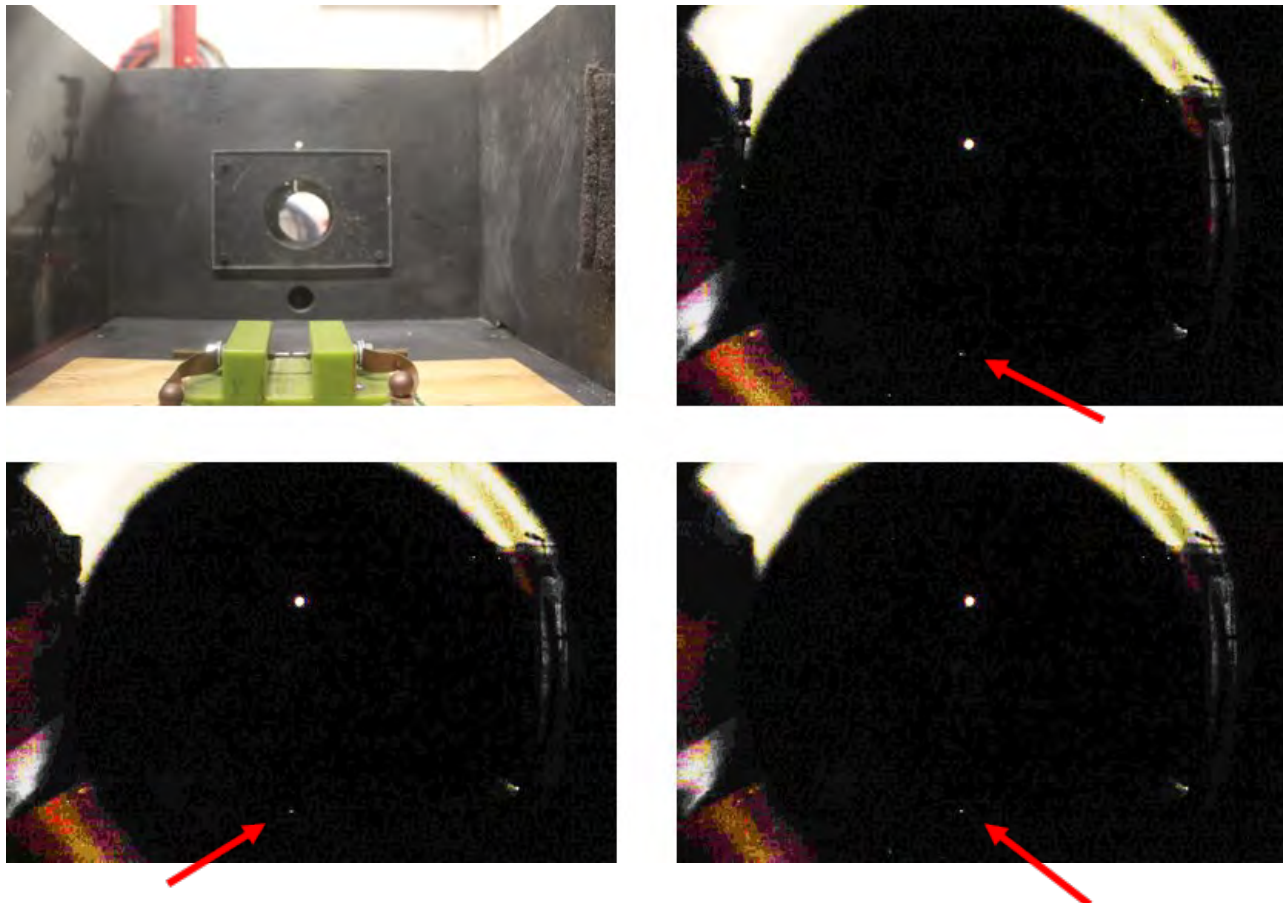


Figure 1: Calibration Photographs for Camera 1

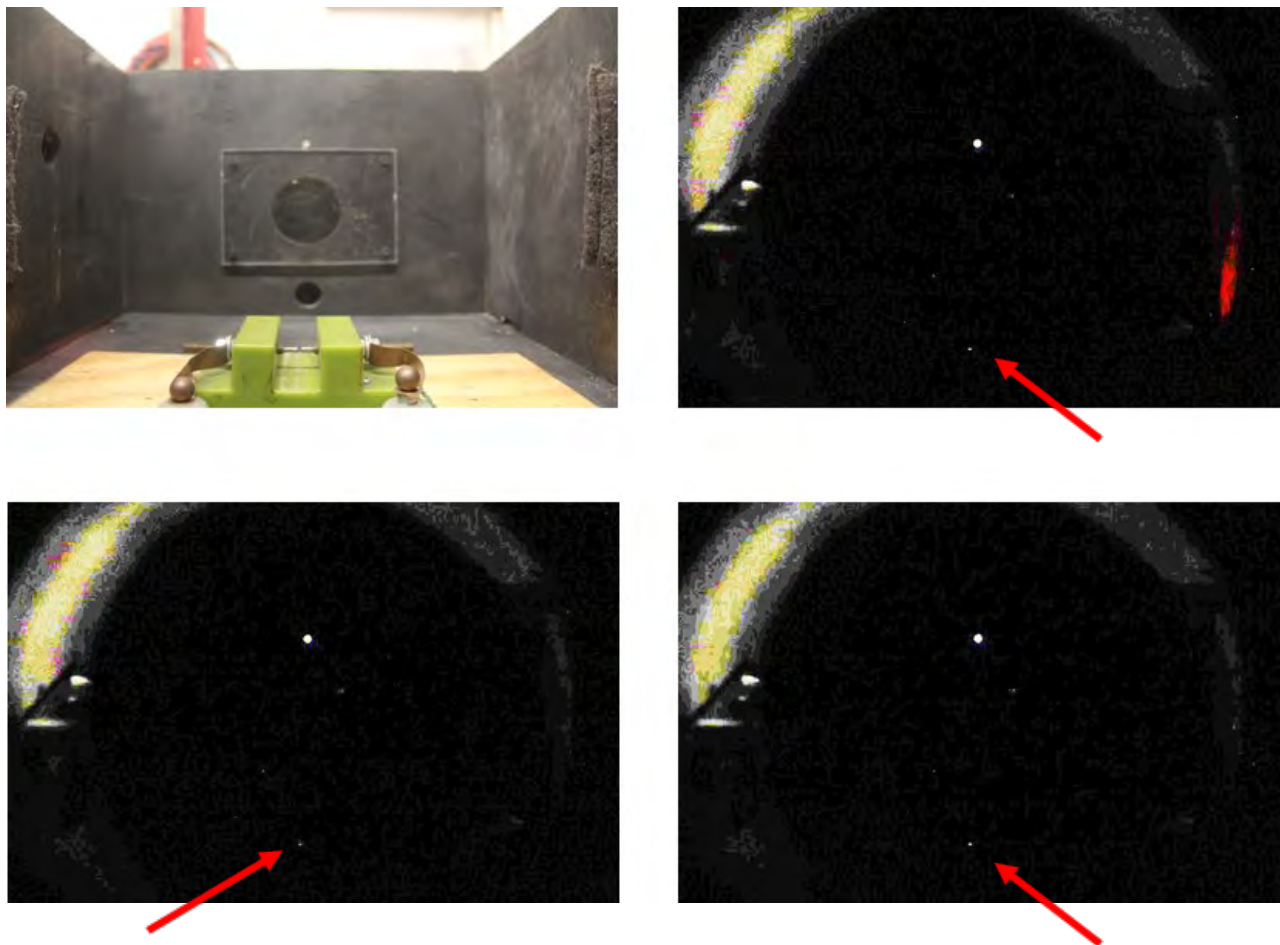


Figure 2: Calibration Photographs for Camera 2





Figure 3: Camera Calibration Test Setup at DNB Engineering, Inc.

### **Faulted Test Articles**

The camera calibration procedure underwent some changes between testing of the nominal and faulted articles. Detailed in the document below is the camera calibration procedure used during the faulted testing.

**National Institute for Aviation Research  
Wichita State University  
1845 N. Fairmount  
Wichita, Kansas 67260-0093**

**NIAR Camera Verification Procedure  
Certification Testing**

**EXPORT CONTROLLED DATA.**

This document may contain technical data whose export is restricted by the International Traffic in Arms Regulations (ITAR) or the Export Administration Regulations (EAR). Violations of these export laws are subject to severe criminal penalties.

**TABLE OF CONTENTS**

<b><u>SECTION</u></b>	<b><u>TITLE</u></b>	<b><u>PAGE</u></b>
1.0	Scope .....	4
1.1	Introduction .....	4
2.0	Test Setup .....	5
2.1	Cameras .....	5
2.2	Voltage Spark Circuit .....	5
3.0	Equipment List .....	6
4.0	Applicable Documents .....	6
5.0	Procedure for Verification .....	6
5.1	Procedure for Testing: .....	9
Appendix A	.....	11

### **List of Abbreviations, Acronyms, and Symbols**

AC	Advisory Circular, Alternating Current
AES	Avionics and Electrical Systems
A, Amp	Amperes
AOR	Axis of Rotation
APSD	Average Power Spectral Density
APU	Auxiliary Power Unit
ARINC	Aeronautical Radio Incorporation
ARP	Aerospace Recommended Practice
AUX	Auxiliary
C	Celsius
CFR	Code of Federal Regulations
DC, dc	Direct Current
DWG	Drawing
EME	Electromagnetic Effects
ESD	Electro Static Discharge
ETL	Environmental Test Laboratory
EUT	Equipment Under Test
FAA	Federal Aviation Administration
Ft.	Feet
HIRF	High Intensity Radiated Field
Hz	Hertz (measure of Frequency)
IEL	Indirect Effects of Lightning
IO	Input / Output
kHz	Kilohertz
LISN	Line Impedance Stabilization Network
LI-ION	Lithium ion
m	Meter(s)
MEE	Mechanical Environmental Effects
MHz	Megahertz
NIAR	National Institute for Aviation Research
ODA	Organization Designation Authorization
PCB	Printed Circuit Board
PC	Printed Circuit
PWR	Power
QTP	Qualification Test Plan
QTR	Qualification Test Results
RF	Radio Frequency
RMS	Root Mean Square
RTCA	Radio Technical Commission for Aeronautics
Temp.	Temperature
UM	Unit Member
VDC	Volts Direct Current
°	Degrees
Ω	Ohms



## **1.0 Scope**

The purpose of this document is to serve as the procedure for the verification of cameras to be used with the photographic method of ignition source detection. The resulting peak pixel value thresholds in Appendix A serve as the verification data for each cameras, valid for one year after the verification procedure is performed.

### **1.1 Introduction**

SAE ARP 5416A section 7.7.1.1 allows for cameras to be used to detect ignition sources of electrical sparks or thermal sparks. The guidance states that digital cameras can be used, but that they must be capable of detecting a 200  $\mu$ J  $\pm$ 0/-10% electrical spark. There is much variation on how bright a picture of a 200  $\mu$ J spark in a dark box appears from different cameras, even when the cameras are both of the same make and model. To use digital cameras to detect an ignition source, a quantitative method must be used to determine if the possible ignition source detected during testing is above the 200  $\mu$ J threshold. The allowable false pass rate for 200  $\mu$ J photos is set at 10%, in correlation with the flammable gas mixture test method, which in section 7.7.2.3 step 1 requires the verification of the mixture calibration in nine out of ten successive tests using 200  $\mu$ J sparks. The pass/fail threshold is derived from the peak pixel values present in multiple images of the 200  $\mu$ J spark. The threshold is then verified by proving that all of the photos taken of 300  $\mu$ J sparks fall above the threshold. Peak pixel value is obtained during post-test image analysis using an open source image processing software, ImageJ, or equivalent. During analysis, peak pixel values are obtained when the image is scaled to 8 bits, resulting in a brightness scale ranging from 0-255.

## **2.0 Test Setup**

### **2.1 Cameras**

The quantitative output of the camera verification is the peak pixel value obtained from the image using image analysis software. The camera, lens, and camera settings should be treated as a set of calibrated equipment, which should be calibrated every 12 months. The changing of lenses or camera settings falls outside the verification and will require reverification of the cameras.

### **2.2 Voltage Spark Circuit**

The spark circuit should be operated in relatively dry air. 1.6 mm tungsten electrodes with a 0.8 mm radius hemispherical tip are recommended, with a gap of 1.5 to 2.0 mm between them. A calibrated capacitance bridge should be used to verify the capacitance of the circuit. The spark circuit should be charged with a high voltage power supply, and the breakdown voltage between the electrodes should be recorded with a calibrated meter. The energy (Joules) in the spark can be found by the following formula for energy in a capacitor:  $J = \frac{1}{2} C \cdot V^2$ .

### 3.0 Equipment List

Description	Manufacturer	Model	Serial Number	Last Cal	Cal Due
Electrostatic Volt Meter	Trek	341	073	1/12/2018	1/12/2019
Oscilloscope	Rigol	DS1104	DS1ZA181305414	9/26/2017	9/30/2018
RLC Meter	GenRad	1689	8243454004	3/26/2018	3/31/2019
200 $\mu$ J Spark circuit	NIAR	SS001	001	N/A	N/A

### 4.0 Applicable Documents

Document Number	Description
SAE Aerospace ARP 5416A Revised 2013	Aircraft Lightning Test Methods

### 5.0 Procedure for Verification

1. Condition the spark electrode with approximately 10,000 discharges to achieve a consistent level of oxidation on the electrodes. Tungsten electrodes are recommended.
2. Record camera manufacturer, model number or name, and serial number. If the camera uses removable parts such as lenses, camera backs, etc., record the manufacturer, model number or name, and serial number for each of these items. The verification only applies to the recorded camera system.



3. Determine breakdown voltage and set the capacitance of the spark circuit accordingly to ensure spark energies are 200  $\mu\text{J}$   $\pm 10\%$ . Verify capacitance with calibrated meter.
4. Set up the voltage spark source in black-out-box in order to eliminate any extraneous light sources.
5. Place both cameras (front and rear) at the same distance from the spark gap. Camera centerline of sight should be perpendicular to the electrode gap. The distance from camera to electrodes should be the same or slightly farther than the distance between the camera and the test articles that will be tested with the calibrated cameras.
6. Record the distance from camera to electrodes, environmental conditions, and any mirrors used.
7. Take open box photo of the spark source electrodes with the camera's "auto" mode to verify the location of the spark gap, that the electrodes are in focus, and that the spark gap is at least 5 pixels across.
8. Set up camera and record camera and lens settings. The camera and lens settings should be manual and all internal image processing and filters should be disabled. The aperture setting (f-number) should be based on the required depth of field so that the distance range for expected test articles is in focus.
9. Close the box and take a pre-test dark box photo to verify that there are no light leaks. This dark box photo will later be used for background subtraction with the spark photos.



10. In the black out box, take several photos of  $200 \mu\text{J} \pm 10\%$  sparks. Analyze the photos and determine the peak pixel value of the spark. Adjust and record the ISO and camera aperture settings so that the measured peak pixel value is well above the random noise in the photo, and falls near the middle of the camera's dynamic range.
11. Capture 100 photos of  $200 \mu\text{J} \pm 10\%$  spark events. Verify that all recorded sparks fall within the required energy range. Save an unedited copy of the original photo data file.
12. Analyze images using ImageJ 1.48v software or equivalent as follows.
  - a. Perform a background subtraction of each spark photo minus the pre-test dark box photo to remove noise/hot pixels.
  - b. Measure peak pixel values for the 100 background subtracted photos, save the results from each image in a spreadsheet.
  - c. Set the threshold level  $T_w$  of the analysis method so that 10% of the photos have peak pixel values of the spark that fall below the threshold and the remaining 90% of the photos have peak pixel values of the spark above the threshold.
  - d. Multiply  $T_w$  by 0.8 to get  $T_{P/F}$ .  $T_{P/F}$  is the threshold that test photos will be compared against. Record pass/fail threshold  $T_{P/F}$ .
13. Adjust capacitance of the spark circuit to produce  $300 \mu\text{J} \pm 10\%$  sparks. Verify capacitance with calibrated meter.

14. Take an open box photo of sparker to verify the location of the spark gap, that the spark gap is in focus, and that the spark gap is at least 5 pixels across.
15. Close the box and take a pre-test dark box photo to verify that there are no light leaks. This dark box photo will be used for background subtraction with the spark photos.
16. Capture 100 photos of 300 uJ  $\pm 10\%$  spark events
17. Analyze images using ImageJ 1.48v software or equivalent as follows.
  - a. Perform a background subtraction of each spark photo minus the pre-test dark box photo to remove noise/hot pixels.
  - b. Measure peak pixel values for the 100 photos, save the results for each image in a spreadsheet.
  - c. Ensure that all of the max pixel values for the 300 uJ sparks fall above the threshold  $T_w$ .

#### **5.1 Procedure for Testing:**

1. Set up cameras and test article so that the distance between them is no farther than the calibrated distance. There should be a clear, unobstructed, in focus view of the entire test article.
2. Perform test and capture test images.
3. Analyze the images and determine the peak pixel value of the image in the region of interest. The same software used for the verification must be used for the test itself.

- a. Perform a background subtraction of the test photo minus the dark box photo to remove noise/hot pixels.
  - b. Cropping around the test article to remove false light artifacts is permitted as long as the region of interest for analysis includes the entire test article area that is being evaluated for potential ignition sources.
4. Measure the peak pixel value of the test image and evaluate it against the pass/fail threshold  $T_{P/F}$  and identify any potential ignition sources.
5. Verify that the identified potential ignition sources can be correlated to the test article and eliminate possible camera defects or test artifacts. The use of two or three calibrated digital cameras will help eliminate possible camera defects that may otherwise be confused as ignition sources.
6. If the peak pixel value falls above the pass/fail threshold  $T_{P/F}$  the test should be considered a failure. If all peak pixel values in regions of potential ignition sources fall below the pass/fail threshold  $T_{P/F}$  the test should be considered a pass.

## Appendix A

### Results of Verification



Figure 1: Camera 1 Verification Data, 100 instances each of 200 and 300 $\mu$ J sparks. Threshold = 39.2 .....	14
Figure 2: Camera 2 Verification Data, 100 instances each of 200 and 300 $\mu$ J sparks. Threshold = 36.8 .....	14
Figure 3: Camera 3 Verification Data, 100 instances each of 200 and 300 $\mu$ J sparks. Threshold = 36 .....	15
Figure 4: Camera 5 Verification Data, 100 instances each of 200 and 300 $\mu$ J sparks. Threshold = 78.4 .....	15
Figure 5: Camera 6 Verification Data, 100 instances each of 200 and 300 $\mu$ J sparks. Threshold = 82.4 .....	16
Figure 6: Camera 7 Verification Data, 100 instances each of 200 and 300 $\mu$ J sparks. Threshold = 80 .....	16

Data charts display the resulting peak pixel values from 100 images of 200  $\mu\text{J}$   $\pm 10\%$  spark events, the pass/fail threshold  $T_{P/F}$ , and the resulting peak pixel values from 100 images of 300  $\mu\text{J}$   $\pm 10\%$  spark events. The pass/fail threshold  $T_{P/F}$  is the threshold value that test photos will be compared against.

Material of electrodes: Tungsten

Electrode gap: 1.5 - 2 mm

Distance from camera to electrode: 10"

F-stop: f/5.6

ISO speed: ISO-200

Exposure Time: 3.2 sec.

Exposure Bias: 0 step

Focal Length: 18 mm

File type: Fine quality JPEG

Description	Manufacturer	Model	Serial Number	Last Cal	Cal Due
Camera 1	Canon	EOS Rebel T5 DS126491	Body: 142073019286 Lens: 2566055831	4/18/2018	4/18/2019
Camera 2	Canon	EOS Rebel T5 DS126491	Body: 122073012940 Lens: 2466060995	4/18/2018	4/18/2019
Camera 3	Canon	EOS Rebel T3i DS126311	Body: 402077002849 Lens: 1446092416	4/18/2018	4/18/2019
Camera 5	Canon	EOS Rebel T6i DS126571	Body: 352072015527 Lens: 610204005413	4/18/2018	4/18/2019
Camera 6	Canon	EOS Rebel T6i DS126571	Body: 352072015432 Lens: 610204005366	4/18/2018	4/18/2019
Camera 7	Canon	EOS Rebel T6i DS126571	Body: 352072015496 Lens: 610204005502	4/18/2018	4/18/2019

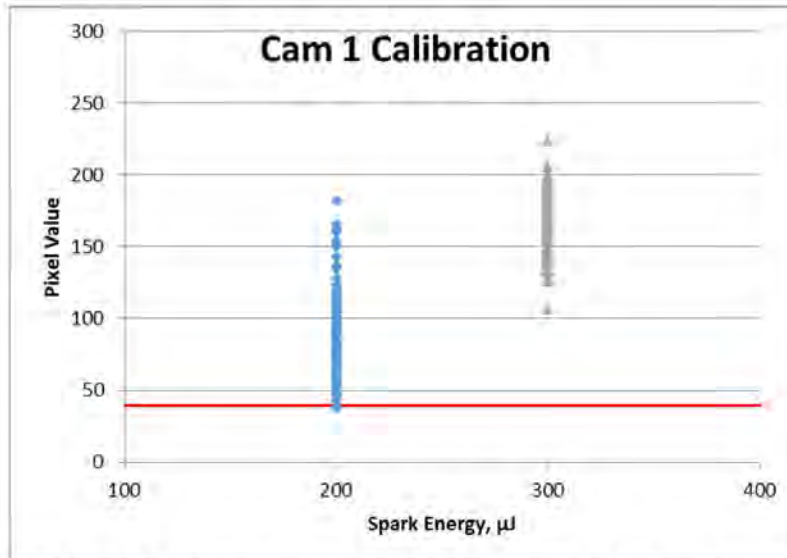


Figure 1: Camera 1 Verification Data, 100 instances each of 200 and 300  $\mu\text{J}$  sparks.  
Threshold,  $T_{PT} = 39.2$

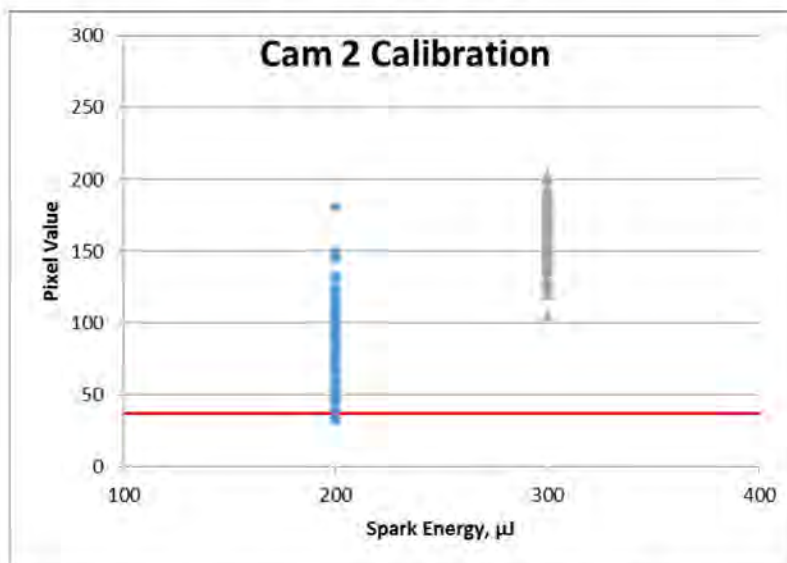


Figure 2: Camera 2 Verification Data, 100 instances each of 200 and 300  $\mu\text{J}$  sparks.  
Threshold,  $T_{PT} = 36.8$

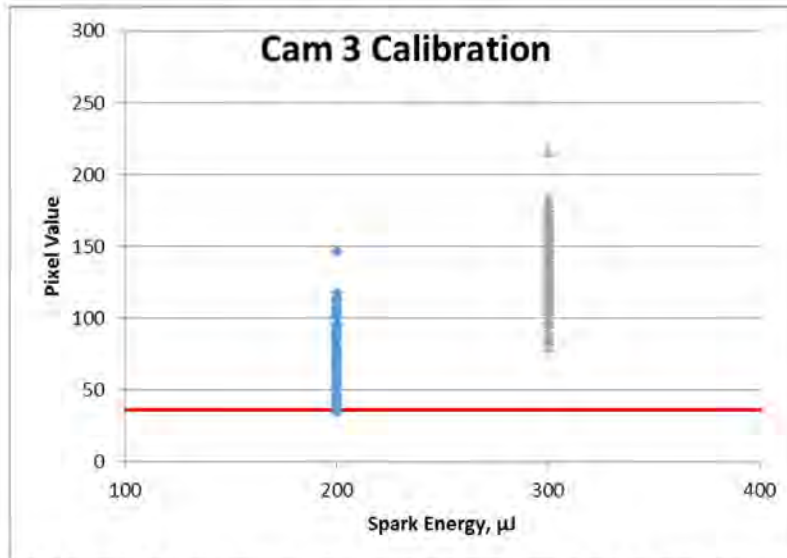


Figure 3: Camera 3 Verification Data, 100 instances each of 200 and 300 μJ sparks.  
Threshold,  $T_{P/F} = 36$

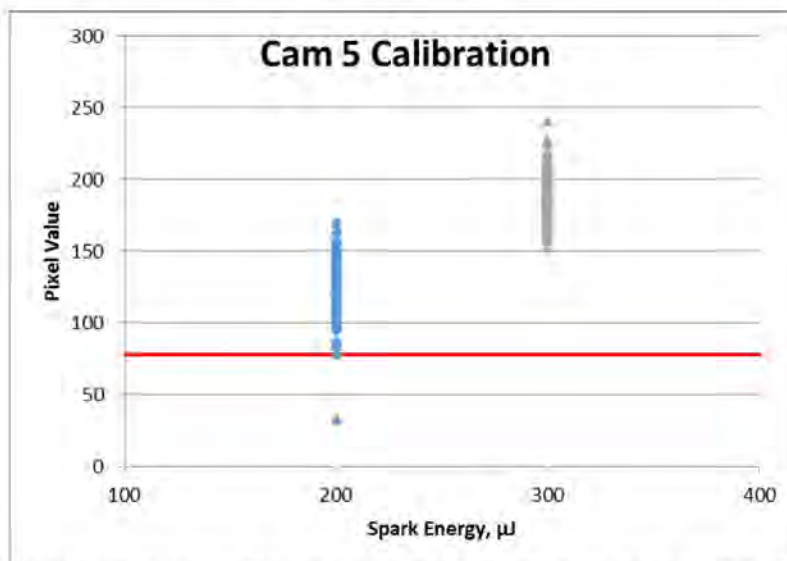


Figure 4: Camera 5 Verification Data, 100 instances each of 200 and 300 μJ sparks.  
Threshold,  $T_{P/F} = 78.4$



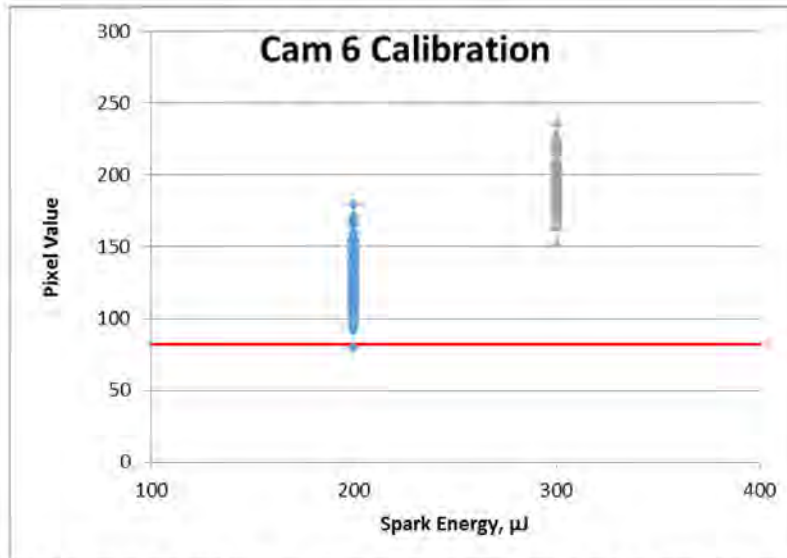


Figure 5: Camera 6 Verification Data, 100 instances each of 200 and 300  $\mu\text{J}$  sparks.  
Threshold,  $T_{PF} = 82.4$

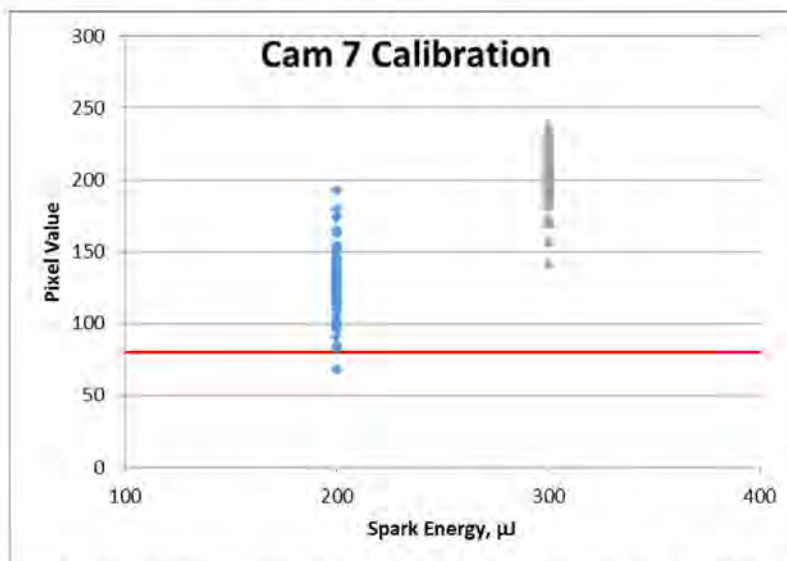


Figure 6: Camera 7 Verification Data, 100 instances each of 200 and 300  $\mu\text{J}$  sparks.  
Threshold,  $T_{PF} = 80$

## Appendix H – Test Article Data

### Nominal Test Articles

Table 12: Nominal Test Article Data

TA ID	Fastener Type	Diameter	Sparking Threshold (kA)
MN-1I03-5	HL11VBJ5-3/HL70-5	5	10.940
MN-1I11-4	HST11AG5-3/HST79CY5	5	1.240
MN-1I11-5	HST11AG5-3/HST79CY5	5	1.190
MN-1I12-1	HL11VAZ5-3/HL70-5	5	10.700
MN-1I12-2	HL11VAZ5-3/HL70-5	5	5.430
MN-1I12-5	HL11VAZ5-3/HL70-5	5	1.190
MN-1T12-1	HL11VAZ5-3/HL70-5	5	0.742
MN-1T02-5	HL10VBJ8-3/HL70-8	8	10.950
MN-1T07-4	HL11BJ5-3/HST79CY5	5	10.760
MN-4I11-4	HST11AG5-3/HST79CY5	5	1.235
MN-4I12-1	HL11VAZ5-3/HL70-5	5	1.909
MN-4T12-1	HL11VAZ5-3/HL70-5	5	0.981
MN-4009-1	MS2047AD4	4	10.750

### Faulted Test Articles

Table 13: Faulted Test Article Data

TA ID	Fastener Type	Diameter	Fault	Non-Sparking Threshold (kA)
MF1-4T05-5	HL10BJ5-3/HST79CY5	5	Straight Gap	81.7
MF1-4T05-3	HL10BJ5-3/HST79CY5	5	Straight Gap	82
MF2-4T05-5	HL10BJ5-3/HST79CY5	5	Gap Under Head	101.57
MF2-4T05-3	HL10BJ5-3/HST79CY5	5	Gap Under Head	13.97
MF3-4T05-5	HL10BJ5-3/HST79CY5	5	Gap Under Collar	10.82
MF3-4T05-3	HL10BJ5-3/HST79CY5	5	Gap Under Collar	10.8
MF4-4T05-5	HL10BJ5-3/HST79CY5	5	Scratch	61.53
MF4-4T05-3	HL10BJ5-3/HST79CY5	5	Scratch	101.57
MF5-4T05-5	HL10BJ5-3/HST79CY5	5	Burr	10.8
MF5-4T05-3	HL10BJ5-3/HST79CY5	5	Burr	23.73
MF6-4T05-5	HL10BJ5-3/HST79CY5	5	Under-Torque	101.63
MF6-4T05-3	HL10BJ5-3/HST79CY5	5	Under-Torque	101.97
MF1-4T01-5	HL10VBJ5-3/HL70-5	5	Straight Gap	81.83
MF1-4T01-2	HL10VBJ5-3/HL70-5	5	Straight Gap	32.97
MF1-4T01-1	HL10VBJ5-3/HL70-5	5	Straight Gap	81.93
MF2-4T01-5	HL10VBJ5-3/HL70-5	5	Gap Under Head	44.13
MF2-4T01-2	HL10VBJ5-3/HL70-5	5	Gap Under Head	10.82
MF2-4T01-1	HL10VBJ5-3/HL70-5	5	Gap Under Head	101.7
MF3-4T01-5	HL10VBJ5-3/HL70-5	5	Gap Under Collar	102.3
MF3-4T01-2	HL10VBJ5-3/HL70-5	5	Gap Under Collar	10.84
MF3-4T01-1	HL10VBJ5-3/HL70-5	5	Gap Under Collar	82.17

TA ID	Fastener Type	Diameter	Fault	Non-Sparking Threshold (kA)
MF4-4T01-5	HL10VBJ5-3/HL70-5	5	Scratch	101.97
MF4-4T01-2	HL10VBJ5-3/HL70-5	5	Scratch	18.47
MF4-4T01-1	HL10VBJ5-3/HL70-5	5	Scratch	61.67
MF5-4T01-5	HL10VBJ5-3/HL70-5	5	Burr	23.8
MF5-4T01-2	HL10VBJ5-3/HL70-5	5	Burr	28.5
MF5-4T01-1	HL10VBJ5-3/HL70-5	5	Burr	101.83
MF6-4T01-5	HL10VBJ5-3/HL70-5	5	Under-Torque	101.87
MF6-4T01-2	HL10VBJ5-3/HL70-5	5	Under-Torque	28.5
MF6-4T01-1	HL10VBJ5-3/HL70-5	5	Under-Torque	101.8
MF1-4T07-5	HL11BJ5-3/HST79CY5	5	Straight Gap	36.233
MF1-4T07-3	HL11BJ5-3/HST79CY5	5	Straight Gap	10.83
MF1-4T12-5	HL11VAZ5-3/HL70-5	5	Straight Gap	2.159
MF1-4T12-2	HL11VAZ5-3/HL70-5	5	Straight Gap	6.482
MF1-4T12-1	HL11VAZ5-3/HL70-5	5	Straight Gap	0.16
MF3-4T12-5	HL11VAZ5-3/HL70-5	5	Gap Under Collar	6.541
MF3-4T12-2	HL11VAZ5-3/HL70-5	5	Gap Under Collar	9.817
MF3-4T12-1	HL11VAZ5-3/HL70-5	5	Gap Under Collar	4.23
MF4-4T12-5	HL11VAZ5-3/HL70-5	5	Scratch	1.09
MF4-4T12-2	HL11VAZ5-3/HL70-5	5	Scratch	5.503
MF4-4T12-1	HL11VAZ5-3/HL70-5	5	Scratch	1.08
MF5-4T12-5	HL11VAZ5-3/HL70-5	5	Burr	4.239
MF5-4T12-2	HL11VAZ5-3/HL70-5	5	Burr	5.45
MF5-4T12-1	HL11VAZ5-3/HL70-5	5	Burr	5.29
MF6-4T12-5	HL11VAZ5-3/HL70-5	5	Under-Torque	6.541
MF6-4T12-2	HL11VAZ5-3/HL70-5	5	Under-Torque	6.5
MF6-4T12-1	HL11VAZ5-3/HL70-5	5	Under-Torque	4.23
MF1-4T03-5	HL11VBJ5-3/HL70-5	5	Straight Gap	101.93
MF1-4T03-2	HL11VBJ5-3/HL70-5	5	Straight Gap	18.4
MF1-4T03-1	HL11VBJ5-3/HL70-5	5	Straight Gap	28.53
MF1-4T11-5	HST11AG5-3/HST79CY5	5	Straight Gap	11.02
MF3-4T11-5	HST11AG5-3/HST79CY5	5	Gap Under Collar	4.39
MF4-4T11-5	HST11AG5-3/HST79CY5	5	Scratch	3.29
MF5-4T11-5	HST11AG5-3/HST79CY5	5	Burr	3.25
MF6-4T11-5	HST11AG5-3/HST79CY5	5	Under-Torque	3.26
MF3-4009-5	MS2047AD4	4	Gap Under Collar	101.8
MF3-4009-2	MS2047AD4	4	Gap Under Collar	102.17
MF3-4009-1	MS2047AD4	4	Gap Under Collar	18.53
MF4-4009-5	MS2047AD4	4	Scratch	101.93
MF4-4009-3	MS2047AD4	4	Scratch	101.6
MF4-4009-2	MS2047AD4	4	Scratch	101.5
MF4-4009-1	MS2047AD4	4	Scratch	13.73
MF5-4009-5	MS2047AD4	4	Burr	102.07
MF5-4009-3	MS2047AD4	4	Burr	101.7
MF5-4009-2	MS2047AD4	4	Burr	102.07
MF5-4009-1	MS2047AD4	4	Burr	18.5